A role for EFR3A during insulin stimulated dispersal of GLUT4 at the plasma membrane.

Kamilla Margrethe Ebbesen Laidlaw

BSc (Hons)

Thesis submitted in fulfilment of the requirements for the Degree of Doctor of Philosophy

Institute of Molecular, Cell and Systems Biology

College of Medical, Veterinary and Life Sciences

University of Glasgow

ABSTRACT

The regulation of blood glucose levels post-prandial relies on insulin-stimulated glucose uptake within adipocytes and striated muscle. The insulin effect in these tissues is a result of the translocation of the facilitative glucose transporter type IV (GLUT4) from intracellular storage vesicles to the plasma membrane. GLUT4 translocation results in the majority of glucose uptake in the body post-prandial. A major contribution to developing Type-2 diabetes is insulin-resistance, which is a result of ineffective insulin signalling, and glucose uptake.

GLUT4 is found in insulin sensitive tissue, such as adipose and striated muscle, it is sequestered and stored intracellularly in specialised GLUT4 storage vesicles (GSV) in the absence of insulin. GSVs are a dynamic vesicle which translocate in response to insulin stimulation to the plasma membrane. In the absence of insulin stimulation GSVs which arrive at the PM show reduced fusion to the membrane and are quickly re-endocytosed. Upon insulin stimulation there is an increase in GSVs translocation to the plasma membrane and upon arrival fusion with retention at the plasma membrane is increased.

At the plasma membrane GLUT4 arrives within in a cluster. Within this cluster GLUT4 is dynamic but corralled within in the cluster. In the absence of insulin GLUT4 is quickly re-endocytosed in a “kiss-and-run” type event. In the insulin-stimulated cell GLUT4 arrives in clusters which have been observed to disperse from the original site of fusion. In response to insulin stimulation GLUT4 mobility at the plasma membrane is increased with increased dispersal. This indicates that insulin stimulation has an effect on the behaviour of GLUT4 at the plasma membrane. This dispersal is hypothesised to increase GLUT4 dwell time at the plasma membrane increasing the effect of insulin signalling for a greater period of time. The dispersal of GLUT4 at the plasma membrane is an insulin mediated response which has no known molecular mechanism.

A genetic screen conducted in *S. cerevisiae* indicate a role for a mutant allele, *fgy1-1,* of the protein Efr3. This protein has two homologous mammalian orthologues EFR3A and EFR3B. The mammalian EFR3 is a palymitoylated protein responsible for membrane localisation and as a result the activity of the phosphoinositide kinase,

PI4K type IIIα. PI4KIIIα activity is required for generation of phosphoinositide 4-phosphate (PI4P) at the plasma membrane inner leaflet.

The phospho-identity of the membrane phosphoinositide has been shown to affect a variety of cellular functions. Mobility of plasma membrane inserted proteins is dictated by the composition of the membrane and cytoskeletal network below the membrane. Single molecule tracking of GLUT4 at the plasma membrane shows increased mobility in the insulin-stimulated cell. Increased mobility and increased dispersal of GLUT4 in response to insulin stimulation has no known molecular mechanism which made EFR3 a promising candidate for further investigation.

This thesis aims to investigate EFR3A and of PI4P during insulin stimulated GLUT4 dispersal.

The results from these experiments showed that EFR3A is the expressed homolog within adipocyte cell types used in this investigation. Results indicating that in mice with impaired glucose tolerance EFR3A and PI4KIIIα protein levels are increased in insulin responsive striated muscle samples. This indicates a compensatory effect as insulin resistance occurs in these animals. Results showed that increased expression of EFR3A led to increasing the plasma membrane GLUT4 in the absence of insulin stimulation signifying GLUT4 is enriched in the plasma membrane instead of intracellularly within GSVs when EFR3A is over expressed. Inhibition of EFR3A plasma membrane localisation through expression of a cytosolic mutant leads to inhibition of the insulin stimulated increase of GLUT4 at the plasma membrane. This indicates that EFR3A at the plasma membrane is important for insulin stimulated GLUT4 increase. In concurrence with these data inhibition of EFR3A and PI4KIIIα through siRNA depletion resulted in inhibited insulin stimulated glucose uptake. Increased glucose uptake is the end result of insulin stimulation, and inhibition of EFR3A machinery inhibits this activity.

Taken together these findings indicate that EFR3A has a positive effect on plasma membrane GLUT4 and insulin stimulated glucose uptake. A role for the generation of PI4P at the plasma membrane is proposed to be behind this positive effect, which future work could aim to elucidate.

1 TABLE OF CONTENTS

TABLE OF FIGURES

ACKNOWLEDGEMENTS

I would like to extend my gratitude to both my supervisors Gwyn and Nia whose knowledge, positivity and belief in me allowed for this body of work to come to fruition. This work could not have been completed without the generous support provided by Diabetes UK studentship scholarship fund.

Thanks to the entirety of Lab 241, past and present, your help keeping the focus, our lunch time chats, made for an enjoyable time in lab 241. I also want to extend a thank you to the Bryant group at the University of York for welcoming me for visits and especially Dr Hannah Black for guiding me through FACS.

Everyone has their village of friends that keep them sane and together. My village is scattered near and far throughout the world. Distance and time zones never stopped your much-needed support getting through to me. You have spent hours on facetime; given me a place to stay when I needed it; made sure I enjoyed myself even when I didn't want to; helped me carry furniture up 2 flights of stairs late at night; and made many a memorable getaway.

Family is forever the foundation for my every achievement

Til min Bedstemor og Bedstefar, din støtte udvidet gennem generationer, og dit eksempel til mig og alle dine børnebørn har givet os mulighed for at blive de personer, vi er i dag. Jeg elsker jer begge. Granny I am grateful for the copious amounts of your amazing shortbread and support you continuously offer. Papa, I wish you could still be here to see a Laidlaw become a PhD, it was close.

Mor og Daddy, you have raised three women who all think the world of you. Your continued love, support and example to me has made starting and finishing a PhD a possibility I am beyond grateful for. Thanks for your proof reads and patience. Katrina and Nikoline, the little sisters, I am lucky to have you through our shared life experiences, you're the best.

Laidlaw Clan till the end.

Problems worthy
of attack
Prove their worth
by fighting back.

- Piet Hein

AUTHOR'S DECLARATION

I declare that the work presented in this thesis is my own, unless otherwise cited or acknowledged. It is entirely of my own composition and has not, in whole or in part, been submitted for any other degree.

DEFINITIONS AND ABBREVIATIONS

EFR3	PHO eighty five requiring
PM	plasma membrane
GLUT4	glucose transporter type IV
GSV	insulin -sensitive pool of GLUT4
cAMP	Cyclic adenosine monophosphate
GPCR	G-protein coupled receptor
GAPDH	Glyceraldehyde 3-phosphate dehydrogenase
IR	Insulin receptor
IRS	Insulin receptor substrate
APS	Adaptor protein with pleckstrin homology and Src homology domains
CAP	c-CBL associated protein
CIP4	Cdc42-interacting protein 4
GEF	guanine nucleotide exchange factor
PI3K	phosphatidylinositol 3-kinase
PI-3,4,5P_3	phosphatidylinositol 3,4,5 triphosphate
PDK1	phosphoinositide dependant kinase 1
PH	pleckstin homology
GAP	GTPase activating protein
SGLT	sodium glucose co-transporters
PI4KIIIα	Phosphatidylinositol 4 – Kinase type III α
PI	Phosphatidylinositol
PI4P	Phosphatidylinositol 4-phosphate
PI4,5P_2	Phosphatidylinositol 4,5-bisphosphate
PJ	Pseudojanin
T2D	Type-2 diabetes
T1D	Type-1 diabetes
w/v	Units weight per unit volume
v/v	Units volume per unit volume
PTB	phosphotyrosine binding

Akt	Protein Kinase B (PKB)
AS160	Akt substrate of 160kDa
LDM	Low density membrane
HDM	High density membrane
TGN	*trans*-Golgi network
SNARE	soluble *N*-ethlmaleimide-sensitive factor activating protein receptor
NSF	*N*-ethylmaleimide-sensitive factor
FPALM	fluorescence photo-activation localization microscopy
TIRF	Total internal reflection fluorescence microscope
EM	Electron microscopy
TfR	Transmembrane transferrin receptor
DOPE	L-α-dioleoylphosphatidylethanolamine
μOR	μ-opioid receptor
SPT	Single particle tracking
3D	Three-dimensional
Δhxt	Deficient in hexose transporter
FGY	functional expression of Glut4 in yeast
PAO	Phenylarsine oxide
HCV	Hepatitis C virus
DAG	diacyglycerol
IP_3	inositol 1,4,5 tri-phosphate

2 INTRODUCTION

2.1 DIABETES

Diabetes is a disease of un-regulated blood glucose; a characteristic component of the diabetes mellitus disease is high glucose blood concentrations caused by defects in insulin secretion and, or action (Genuth *et al.*, 2003; The Expert Committee on the Diagnosis and Classification of Diabetes Mellitus, 2003; American Diabetes Association, 2010). A result of un-managed diabetes is chronic hyperglycaemia, the long-term consequences of which marks a variety of organs, in particular the kidneys, nerves at the extremities, eyes, blood vessels and the heart are adversely affected by this condition (Diabetes and American Diabetes Association, 2010). Diabetes can largely be classed as two forms, Type-1 and Type-2. Type-1 diabetes (T1D) is defined by a total lack of insulin production, commonly a result of an autoimmune response to the insulin producing ß-islet cells (The Expert Committee on the Diagnosis and Classification of Diabetes Mellitus, 2003). Type-2 diabetes (T2D) is defined by insulin-resistance, when insulin is produced but the response no longer results in a decrease of blood glucose concentration (Weyer *et al.*, 1999; Kahn *et al.*, 2014; Diabetes UK, 2016). The cause of insulin resistance is associated with obesity but ultimately unknown, and there are multiple processes during insulin signalling which could be affected (Perley and Kipnis, 1966; Weyer *et al.*, 1999; Kahn *et al.*, 2006). As of 2015 global estimates indicated that 415 million adults live with the disease, with a predicted rise to over 600 million by 2040, this makes diabetes a growing problem for society. Currently in the UK 3.5 million people are diagnosed with diabetes, with a further estimated 1.1 million undiagnosed persons (Diabetes UK, 2016). T1D accounts for 10% of patients with diabetes in the UK and the other 90% live with T2D (Diabetes UK, 2016).

Currently it is estimated that up to 10% of the NHS budget is spent on diabetes associated treatments, which is equivalent to £10 billion, a number predicted to rise in the future (Hex *et al.*, 2012). The discovery of insulin was one of the most powerful treatments in modern times, its delivery reversed the severe symptoms related to T1D (Abel, 1926). However, despite insulin's capability as a therapeutic treatment it is not a simple solution as the body's ability to self-regulate glucose

levels is unparalleled. Complications related to hyperglycaemia are common for many T1D patients and life expectancy is significantly reduced (Livingstone *et al.*, 2015). The treatment of T2D, however, has been a far more complex issue, with no silver bullet treatment like insulin for this disease. Similarly to T1D patients with T2D have reduced life expectancy, those diagnosed in their 50s on average live 6 years less (Seshasai *et al.*, 2014).

2.2 BLOOD GLUCOSE REGULATION

In healthy humans, blood glucose is usually kept within fairly narrow limits between 4 and 6mM, and a range of complex mechanisms achieves this. Blood glucose levels spike considerably after meals, it is essential that post-prandial blood glucose is lowered to avoid the effects of chronic hyperglycaemia. Glucose homeostasis is the process whereby a constant sugar is available in the blood for the maintenance of muscle activity and glucose hungry synaptic activity in the brain. The lowering of blood glucose post-prandial not only provides a mechanism to store the excess glucose but also serves to ensure proper osmotic pressure of the blood vessels (Tups *et al.*, 2011). The regulation of glucose is therefore vital for a variety of cellular processes.

Glucose homeostasis can be regarded as being primarily regulated by two opposing hormones: glucagon and insulin, both produced in respective specialised cells within the islet of Langerhans of the pancreas (Herman & Kahn 2006; Tirone & Brunicardi 2001). During the fasting state hypoglycaemia is sensed by the α-cells of the islet of Langerhans which release glucagon (Brelje *et al.*, 1989; Brissova, 2005). A schematic diagram of glucose homeostasis is shown in Figure 1.

The action of these two opposing hormones has been widely investigated, this thesis will focus on the effect of insulin stimulation at the plasma membrane in adipocytes. Glucagon primarily acts in the liver through a G-protein coupled receptor (GPCR), a G_{α} coupled receptor which signals through cAMP and protein kinase A pathway. This signalling pathway stimulates gluconeogenesis and glycogenolysis resulting in an increase in glucose release from stores. Therefore increasing and stabilising the blood glucose to normal levels (Quesada *et al.*, 2008).

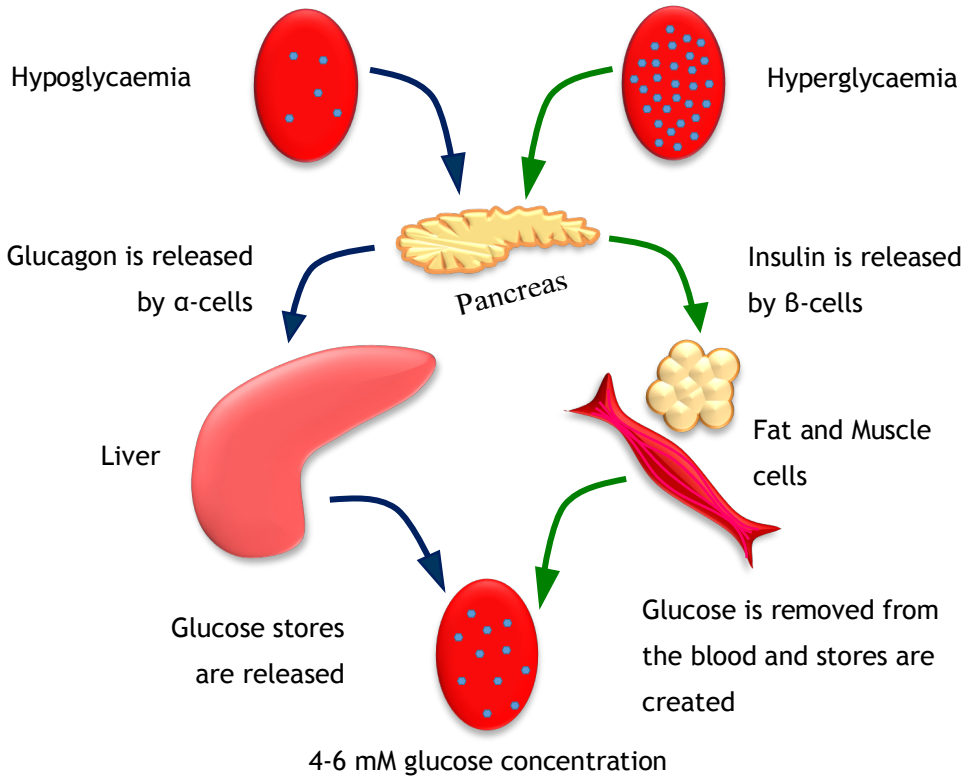

Figure 1: Schematic of glucose homeostasis.

The islet of Langerhans α-cell and ß-cell produce the opposing hormones glucagon and insulin respectively. Glucagon is released in response to hypoglycaemia and works to release stores of glucose from the liver. Insulin is released in response to hyperglycaemia and lowers glucose concentration by promoting the storing of excess glucose.

ß-cells of the islet of Langerhans are responsible for the sensing of glucose in response to hypo/hyperglycaemia. Insulin is produced and released from the ß-cells in response to raised ATP levels in the cell when an abundance of glucose is present (Brelje *et al.*, 1989; Brissova, 2005). The primary function of insulin is to signal to peripheral tissue the requirement to store the excess glucose, and therefore lower the blood glucose levels to within the normal range (Park and Johnson, 1955; Levine and Goldstein, 1958). Insulin signals through the insulin receptor (IR), a tyrosine kinase receptor which is located at the PM dimerised. The IR is predominantly found in; striated muscle, adipose tissue, and the liver (Shia and Pilch, 1983; Gammeltoft and Van Obberghen, 1986; Rowland *et al.*, 2011). In the liver and muscle insulin stimulates glycogen synthesis and in adipose tissue insulin stimulates triacylglycerol

synthesis (Dimitriadis *et al.*, 2011). Both of these tissues react to insulin by storing glucose for later use as glycogen or triacylglycerides respectively.

In both muscle and adipose tissue the rate of glucose uptake is increased during insulin signalling. The glucose transporter type IV (GLUT4) has been identified as the signalling target within this system (Cushman and Wardzala, 1980; Suzuki and Kono, 1980; Fukumoto *et al.*, 1989; James *et al.*, 1989; Wieczorke *et al.*, 2003). Insulin induced glucose uptake in this tissue is due to the translocation of GLUT4 from internal stores to the plasma membrane. The translocation of GLUT4 acts as a molecular dam system increasing the ability for glucose to enter the cell in times of plenty (Marette *et al.*, 1992; Bryant *et al.*, 2002; Bradley *et al.*, 2015). GLUT4 is a member of the facilitative glucose transporter family, covered below in 2.2.1, and is predominantly found in striated muscle, adipose tissue and the brain (Kobayashi *et al.*, 1996). GLUT4 is responsible for the majority of insulin stimulated glucose uptake, and the predominantly expressed isoform in insulin sensitive tissue.

As previously covered in 2.1 Diabetes is a disease of glucose homeostasis, of which there are two predominant classifications, type 1 and Type 2. T1D is the result of pancreatic ß-cell destruction or inability to produce insulin. T2D is associated with a lack of an appropriate insulin response, insulin is produced but cells are resistant to insulin signalling.

2.2.1 Overview of Glucose Transport

The 12-member glucose transporter (GLUT) protein family orchestrate the transport of sugars throughout the body. GLUT transporters were initially identified as 12 transmembrane proteins from hydrophobicity plots, which has later been confirmed by modelling of crystal structures (Mohan *et al.*, 2009, 2010; Deng *et al.*, 2014). GLUT transporters are glucose, fructose or dual specific channels with varying tissue specificity (Wieczorke *et al.*, 2003; Zhao and Keating, 2007). GLUT transporters transport sugar through facilitative transport down its concentration gradient; by comparison the sodium glucose co-transporters (SGLT) family transport glucose using the coupled movement of NA^{+} ions (Gould and Holman, 1993; Zhao and Keating, 2007). The affinity for glucose and other saccharides vary between transporters. This allows for sugar sensing and the absorption of sugar in specialised cells (Zhao and Keating, 2007).

The ubiquitously expressed GLUT1 is responsible for the glucose distribution in most cell types in the absence of insulin signalling (Zhao and Keating, 2007). After a meal glucose is absorbed through the intestinal lumen (Turner *et al.*, 1997). Initially the Na^+ coupled SGLT1 transports glucose against the concentration gradient into the lumen epithelial cells (Hediger *et al.*, 1987; Takata, 1996; Röder *et al.*, 2014). SGLT1 localisation is confined to the apical plasma membrane insuring an influx from the intestinal lumen into the cell (Suzuki *et al.*, 2001). The transport of increased intracellular glucose concentration out of the epithelial cells into the interstitial space is coordinated through GLUT2 (Thorens, 1993; Röder *et al.*, 2014). GLUT2 is a facilitative glucose transporter with a high capacity and low affinity which is localised basolaterally ensuring a flow through the epithelial cell postprandial (Mueckler, 1994; Uldry *et al.*, 2002). Glucose is further absorbed into the microvasculature and carried around the body. In response to increased postprandial blood glucose concentration insulin is released by islet ß-cells. GLUT2 has a low affinity for glucose and is localised to ß-cells, which allows for glucose to influx into the cells in response to increased glucose (Thorens, 2001). The release of insulin results in the uptake of glucose by adipose, skeletal, cardiac and brain tissue (Leney and Tavaré, 2009; Ashrafi *et al.*, 2017). This is mediated through insulin mediated GLUT4 translocation (Gibbs *et al.*, 1988; Zaid *et al.*, 2008; Rowland *et al.*, 2011). This thesis will focus mainly on GLUT4, and consequently subsequent sections emphasise the role and regulation of this protein during glucose regulation.

2.3 INSULIN SIGNALLING

Insulin is a 5kDa peptide hormone originally discovered in 1921 by Banting and Best which is composed of an A chain and B chain linked by disulphide bonds (Dodson and Steiner, 1998; Mayer et al., 2007). Insulin is synthesised in the ß-cells of the islet of Langerhans and is processed through the Golgi apparatus which generated the precursor called proinsulin (Howel *et al.*, 1978; Huang and Arvan, 1995). Proinsulin is cleaved during the formation of storage vesicles for exocytosis by membrane associated endopeptidase PC2, leaving the A and B chain linked and kept in a crystalline state (Abel, 1926; Bennett *et al.*, 1992). Insulin is released by exocytosis into the blood in proportion to blood glucose concentration.

When Insulin signals through binding to the α subunit of the dimerised insulin receptor (IR), the tyrosine kinase activity of the ß subunit is activated via auto phosphorylation (Kasuga et al., 1982; Shia and Pilch, 1983). Activation of the IR results in a cascade of tyrosine kinase signalling through insulin receptor substrate (IRS) and adaptor protein with pleckstrin homology and Src homology domains (APS) activation, depicted in Figure 3. The variety of effects caused by insulin signalling are summarised in Figure 2.

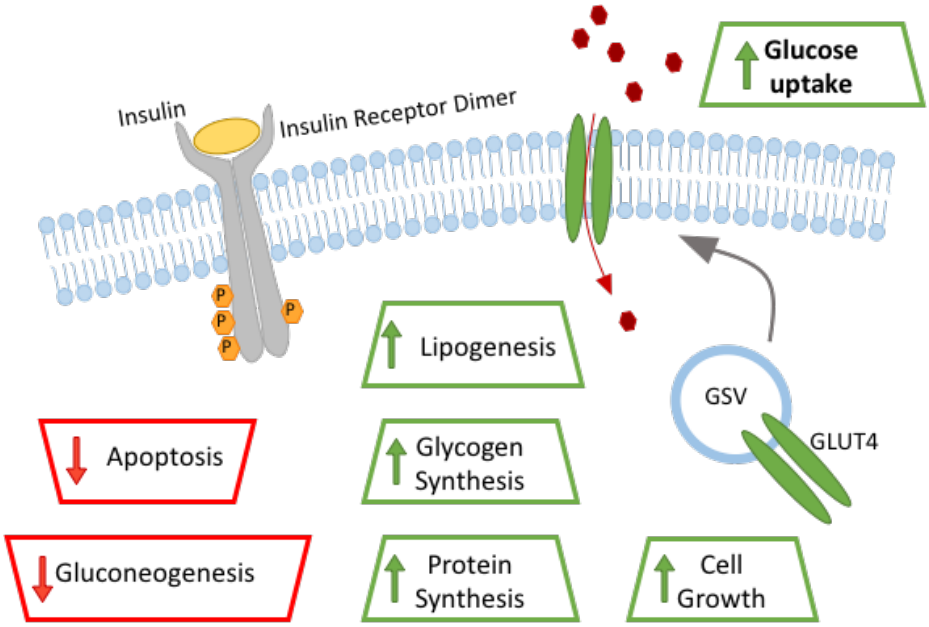

Figure 2: Intracellular effects of insulin stimulation

A schematic showing the various intracellular effects insulin stimulation regulates through insulin receptor binding and activation. The effects can vary between cell types; for example, lipogenesis is a primary effect in adipocyte cells whereas glycogen synthesis is a primary response in hepatic cells.

2.3.1 Insulin receptor substrate (IRS) signalling pathway

There are more than one IR substrate proteins (IRS-1,-2,-3,and-4) which mediate differential signalling cascades in differing cell types (White et al., 1985; Patti *et al.*, 1995; Lavan *et al.*, 1997a, 1997b). IRS-1 and -2 are ubiquitously expressed across all insulin sensitive tissue and are the primary mediators of the insulin signal (White, 2002; Mardilovich *et al.*, 2009). IRS proteins contain no intrinsic enzymatic capabilities, they mediate their function as adaptors to activated IR to organise signalling complexes (Sun *et al.*, 1991). IRS proteins share homology at the N-terminus with two highly conserved regions, the pleckstrin homology (PH) and the phosphotyrosine binding (PTB) domains (Voliovitch Hedva *et al.*, 1995; Sawka-verhelle *et al.*, 1996; Yenush *et al.*, 1996; Backer *et al.*, 1997).

Insulin action in muscle and adipose tissue is a result of IRS-1 action (White, 2002). IRS-1 activation results in the activation phosphatidylinositol 3-kinase (PI3K) and generation of phosphatidylinositol 3,4,5 triphosphate (PI-3,4,5P_3) at the inner leaflet

of the plasma membrane (Okada *et al.*, 1994; Collins *et al.*, 2003). The generation of these PI 3,4,5 P_3 allows for docking of phosphoinositide dependant kinase 1 (PDK1) and Protein kinase B (Akt) through via pleckstin homology (PH) binding domain (Rowland *et al.*, 2011).

2.3.1.1 Adaptor protein with Pleckstrin homology and Src homology domains (APS) signalling pathway

Some studies suggest that IR stimulates two signalling cascades which are both required for GLUT4 translocation: the insulin receptor substrate (IRS) pathway outlined above (2.1.1.1), and the adaptor protein with pleckstrin homology and Src homology domains (APS) signalling branches. Both branches are proposed to be required for GLUT4 translocation, and depicted in Figure 3(Isakoff, 1995; Wiese *et al.*, 1995). The APS signalling cascade is less well characterised in comparison to the IRS pathway. It is suggested that APS activation results in the recruitment of c-CBL associated protein (CAP) which in turn recruits c-CBL (Liu *et al.*, 2002). The final result is the recruitment of the guanine nucleotide exchange factor (GEF) C3G via CRK recruitment by c-CBL (Knudsen *et al.*, 1994; Liu *et al.*, 2003). The GEF activity of C3G promotes the exchange of GDP for GTP within the effector TC10 (Neudauer *et al.*, 1998; Chiang *et al.*, 2001; Chang *et al.*, 2002). Active TC10 is able to bind to Cdc42-interacting protein 4 (CIP4) and exocyst machinery aiding the translocation of GLUT4 to the plasma membrane (Chang *et al.*, 2002).

2.3.1.2 Akt and AS160 activation

Akt is a serine/threonine protein kinase (aka protein kinase B), binding to PI 3,4,5 P_3 via its PH domain results in activation of kinase activity due to conformational changes allowing for the phosphorylation of Thr^{308} by PDK1(Stephens *et al.*, 1998; Song *et al.*, 2005). Akt activity is required for the translocation of GLUT4 to the plasma membrane, specifically Akt2 activation is sufficient to translocate GLUT4 (Ng *et al.*, 2008). A major target of Akt is AS160 (Akt substrate of 160kDa), which contains a GTPase activating protein (GAP) domain. The GAP domain of AS160 promotes GTP hydrolysis, preventing the GTP loading and activation of its effectors. In adipocytes the primary target of this activity is Rab10, a component linked to the translocation of GLUT4 storage vesicles (GSVs) to the plasma membrane. Active AS160 inhibits Rab10 activity, and Akt phosphorylation of AS160 inhibits this activity,

allowing Rab10 GTP loading and effector activation (Sano *et al.*, 2007; Chen and Lippincott-Schwartz, 2013).

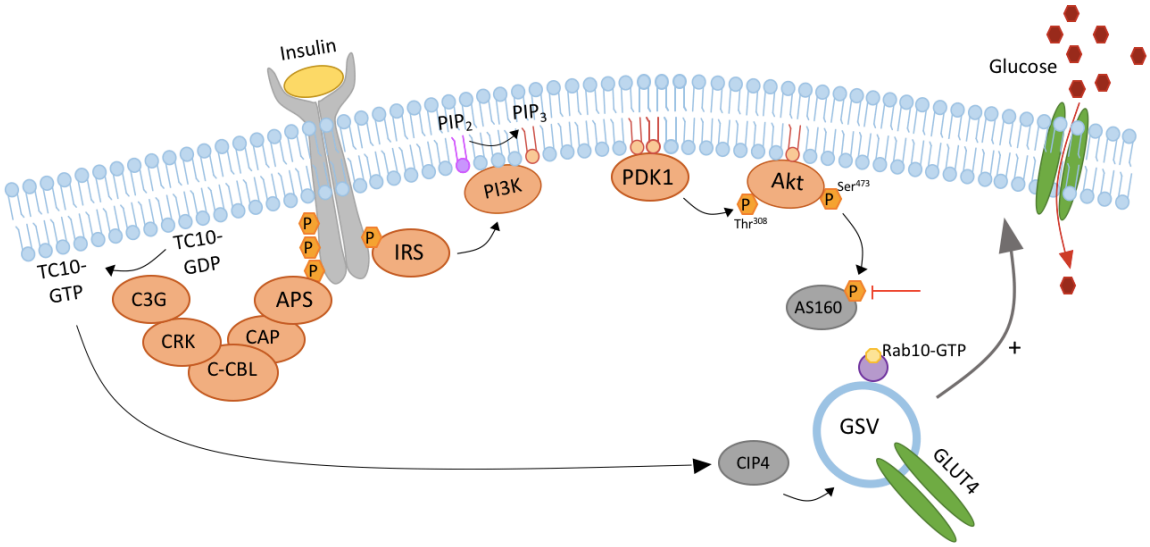

Figure 3: Schematic diagram of insulin signalling cascade for GLUT4 translocation.

Schematic of the two branches of IR signalling required for GLUT4 translocation. The IRS branch results in the formation of PIP_3 patches for PH domain containing PDK1 and AKt to localise to. PH domain localisation results in protein kinase activation, PDK1 phosphorylation of Akt1 results in AS160 inhibition, which allows for Rab10 to remain bound with GTP and therefore active. Rab10 activity is intrinsic to translocate GSV to the PM. The second APS branch of IR signalling is less well characterised, however results in the activation of the effector TC10-GTP, which is able to aid exocyst machinery CIP4 allowing for GLUT4 translocation.

2.4 GLUT4

The human hexose transporters family is composed of 14 expressed proteins. GLUT4 is the only insulin responsive glucose transporter. GLUT4 is an integral membrane protein composed of 12 transmembrane domains. This transporter is expressed in insulin sensitive tissues; striated muscle and adipose tissue. GLUT4 at the PM is dependent on insulin signalling. At the cell surface GLUT4 acts as a facilitative glucose transporter, allowing the excess post-prandial glucose to be absorbed from the blood stream (Huang and Czech, 2007).

2.4.1 GLUT4 Intracellular Trafficking

In the absence of insulin signalling GLUT4 is predominantly stored intracellularly with some GLUT4 present at the PM. GLUT4 is primarily localised to low density membrane (LDM) vesicles known as GLUT4 storage vesicles (GSVs). GSVs have been identified as a specialised pool of insulin sensitive vesicles primed to respond to insulin signalling. To achieve this GLUT4 must be trafficked and sorted within the cell, this is achieved through two distinct but interlinked cycles. The GLUT4 cycle has been well documented. GLUT4 is internalised via clathrin and cholesterol dependant endocytosis (Blot and McGraw, 2006, 2008; Hresko *et al.*, 2016). Once endocytosed GLUT4 has been shown to co-localised with TfR, an example of a PM protein which populates the prototypical endosomal cycle. We understand that GLUT4 from the PM traffics through the prototypical endosomal cycle, as most PM proteins do, and from this cycle GLUT4 is sequestered into a second cycle, shown in Figure 4, which delivers GLUT4 into GSVs. These two cycles have been investigated by various endosomal blocks (Zeigerer et al., 2002; Livingstone et al., 1996; Martin et al., 1996) The formation of GSVs from cycle one is shown to be through the *trans*-Golgi network (TGN), removing GLUT4 from the rapidly recycling pool. GSVs act as a pool of GLUT4 within the cell which react to insulin signalling and are delivered to the plasma membrane.

Much of the understanding of GLUT4 sorting is derived from specific motifs on GLUT4 at the N- and C- terminals. Initial studies showed that the chimera GLUT1 or transferrin receptor protein containing the final C-terminal 30 AA sequence from GLUT4 results in internalisation and retention of these proteins in a similar manner to GLUT4 (Corvera *et al.*, 1994). Similarly chimeras of the first 8 amino acids of

GLUT4 result in sorting to perinuclear compartments which are localised with endogenous GLUT4 (Piper *et al.*, 1993).

2.4.1.1 GLUT4 C-terminal mediated trafficking

In regards to the C terminal, within this sorting motif the double leucine motif L_{489}, L_{490} has been shown to be essential (Verhey and Birnbaum, 1994). This LL sequence is not the only signal however, as mutation does not inhibit internalisation of GLUT4 but does slow the retention of GLUT4 in cells where insulin stimulation has ended (Blot and McGraw, 2006). This is evidence that GLUT4 internalisation and retention is reliant on more than this motif; this may reflect what appears to be a complex endocytic profile of GLUT4. We also know that TELEYLGP (498-505) sequence is important for the sequestering of GLUT4 to GSVs from the endosomal cycle, as mutations within this sequence result in a block and GLUT4 being stuck in the endosomal cycle (Shewan *et al.*, 2000). Subsequent studies showed that the mutation of the E_{499} and E_{501} points to alanine reduces GLUT4 within GSV compartments but does not entirely inhibit the formation of GSVs (Shewan *et al.*, 2000).

2.4.1.2 GLUT4 N-terminal mediated trafficking

N-terminus mediated GLUT4 localisation is determined by the first 8 amino acids, in particular F_5 (Piper *et al.*, 1993; Palacios *et al.*, 2001). After insulin signalling GLUT4 internalisation is dependent on cholesterol, the C-terminal LL $_{489,490}$ motif, and the N-terminus $FQQI_{5\text{-}8}$ motif (Piper *et al.*, 1993; Blot and McGraw, 2006). F_5 to S mutation prevents entry into the perinuclear compartment and targets GLUT4 for degradation (Palacios *et al.*, 2001). F_5 mutation to alanine results in decreased GSV formation, and increases GLUT4 in the endosomal cycle (Blot and McGraw, 2008). Suggesting F_5 is required for the sequestering of GLUT4 after endocytosis.

GLUT4 internalisation is altered in accordance to whether the cell is stimulated or not by insulin. The $FQQI_{5\text{-}8}$ and LL $_{489,490}$ motifs appear to allow for GLUT4 to be trapped intracellularly in GSVs in the absence of insulin signalling. This tells us that the formation of these GSVs are key to the GLUT4 function (Omata *et al.*, 2000; Yeh *et al.*, 2007; Bryant and Gould, 2011; Kioumourtzoglou *et al.*, 2014).

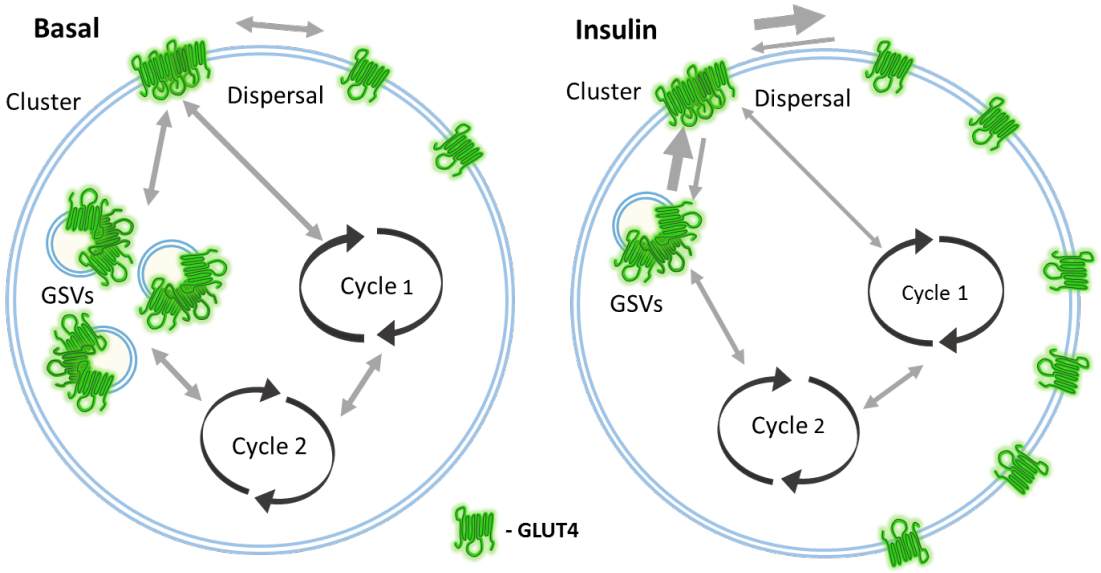

Figure 4: Schematic of intracellular GLUT4 trafficking

GLUT4 is sequestered into storage vesicles (GSVs) that upon insulin stimulation translocate to the plasma membrane (PM). The sequestering of GLUT4 into GSVs requires the sorting of GLUT4 from the pro-typical endosomal cycle (cycle 1) into a specialised GLUT4 sorting cycle (cycle 2). GLUT4 sorts through the *trans*-Golgi network before the formation of GSVs. Upon insulin stimulation GSVs translocate en mass to the PM. It is hypothesised that the fusion of GSVs to the PM delivers GLUT4 as a cluster. These clusters may be re-endocytosed in a "kiss-and-run" like fashion during the absence of insulin signalling. Insulin triggered GSV translocation accounts for an initial burst of GLUT4 delivery at the PM, however to potentiate this effect GLUT4 is dispersed across the plasma membrane. We hypothesise that GLUT4 dispersal at the PM in response to insulin stimulation results in an increased dwell time at the PM, which in turn allows for a sustained glucose uptake period.

2.4.2 Proteins associated with GLUT4 translocation

2.4.2.1 IRAP (Insulin-regulated Aminopeptidase)

IRAP is a zinc-dependent membrane aminopeptidase which is expressed in a variety of cell types (Nikolaou *et al.*, 2014). This protein was initially identified as a component of GSVs, known as vp165, making the association with GLUT4 in an insulin responsive manner the most characterised behaviour of IRAP (Mastick *et al.*, 1994). IRAP is composed of a N-terminus tail, a single transmembrane domain and a large C-terminal domain, which contains aminopeptidase catalytic activity (Keller *et al.*, 1995). IRAP localises to intracellular vesicles in the absence of insulin stimulation and upon insulin stimulation increases at the PM 8-fold, in parallel with GLUT4 translocation (Ross *et al.*, 1997, 1998). The single trans-membrane domain structure and co-localisation with GSVs allows IRAP to be used during investigations of GSV fusion to the PM (Stenkula *et al.*, 2010). Experimental data suggests that IRAP and GLUT4 may have a functional interaction, as the knockout of IRAP or GLUT4 affects the expression stability of the other (Jiang *et al.*, 2001; Keller *et al.*, 2002; Abel *et al.*, 2004). IRAP knockdown results in an increase in GLUT4 present in endosomes, therefore miss-sorted away from GSVs. IRAP KD combined with the GLUT4 FQQI (F^5A) mutation has an additive effect in the miss-sorting from the endosomal compartment to GSV compartment. Together this showed IRAP has an independent role for retention of GLUT4 in the absence of insulin stimulation, specifically the sorting of GLUT4 from endosomes to the GSVs (Jordens *et al.*, 2010). IRAP specific inhibitors such as HFI-419 do not affect blood glucose concentrations in normal or diabetic mouse models, indicating that IRAP enzymatic activity has a minimal role in glucose homeostasis (Albiston *et al.*, 2017).

2.4.2.2 Tankyrase

Tankyrases are a family of poly(ADP-ribose) polymerases which was initially identified from a yeast two-hybrid showing the ANK domain of Tankyrase interacts with the telomeric protein TRF-1 (Smith *et al.*, 1998). Cloning and characterisation revealed a family of TNKS with high identities and near identical domain structures (Kuimov *et al.*, 2001). Tankyrase localisation has been shown to be cell-cycle dependent (Smith and Lange, 1999). It has been shown that the cytosolic domain of IRAP binds to TNKS1/2, and co-localises with a pool of GSVs in 3T3-L1 adipocytes

(Chi and Lodish, 2000). Knockdown of Tankyrase results in impaired glucose uptake, inhibition of GLUT4 and IRAP translocation, and alters intracellular distribution of these proteins (Yeh *et al.*, 2007). TNKS2 forms a complex with the proteins Axin and KIF3A which is critical for translocation of GLUT4 in response to insulin stimulation. TNKS1 has overlapping effect to TNKS2 in this system, pointing to a compensatory effect between homologs (Guo *et al.*, 2012). The exact role for Tankyrase is not fully defined but a role within insulin stimulated GLUT4 translocation, and sorting is forming.

2.4.2.3 SNARE and SM proteins

SNARE (soluble *N*-ethlmaleimide-sensitive factor activating protein receptor) proteins are capable of driving membrane fusion *in vitro* (Weber *et al.*, 1998). This makes SNAREs of interest in stimulated trafficking events such as the insulin dependent GLUT4 trafficking to the PM (Bryant and Gould, 2011). SNARE proteins contain the ~60 amino acid SNARE domain essential for function, and are anchored to the membrane via a transmembrane region or palmitoylation (Hong, 2005). The SNARE hypothesis postulates that a vesicle with specific v-SNARE can only fuse with the appropriate target membrane containing the complementary t-SNAREs, shown in 5. The recognition of complimentary SNARE domains of the approaching vesicle allow for docking of the vesicle by the formation of the *trans*-SNARE complex (Fukuda, 2000; Kioumourtzoglou, *et al.*, 2014). The *trans*-SNARE complex is a helical bundle made up of four complimentary SNARE domains arranged in parallel which has been visualised using x-ray crystallography (Sutton *et al.*, 1998). The formation of the *trans*-SNARE complex initiates zippering of the SNARE proteins and is sufficient to drive membrane fusion. SNARE proteins are commonly regulated through phosphorylation, direct or indirect through the phosphorylation of regulatory proteins such as NSF (*N*-ethylmaleimide-sensitive factor), Munc18, and Sec1 (Matveeva *et al.*, 2001; Snyder *et al.*, 2006; Jewell *et al.*, 2011; Laidlaw *et al.*, 2017). Insulin signalling is mediated through tyrosine phosphorylation, and insulin dependent tyrosine phosphorylation of Munc18c at amino acid positions Y219 and Y521 has been found (Jewell *et al.*, 2011).

The specificity of SNAREs means that separate SNAREs and SM proteins regulate the various stages of GLUT4 trafficking. Key SNAREs involved in GLUT4 trafficking

include; t-SNAREs Sx4 and SNAP-23 at the PM; v-SNARE VAMP2 at the PM; t-SNAREs Sx16 and Sx6 intracellularly; v-SNAREs VAMP3, VAMP4 and VAMP8 intracellularly (Schoch *et al.*, 2001; Perera *et al.*, 2003; Shewan *et al.*, 2003; Proctor *et al.*, 2006; Williams and Pessin, 2008). In relation to GSV approach to the PM GSVs are known to be enriched with the v-SNARE VAMP2, which bind on arrival at the PM to the complimentary t-SNAREs identified as Sx4 and SNAP-23, shown in Figure 5(Sadler, et al., 2015). The SNARE regulatory SM proteins Munc18c and mVps45 are implicated in insulin stimulated GLUT4 vesicle fusion events (Khan et al., 2001; Sadler, Roccisana, et al., 2015).

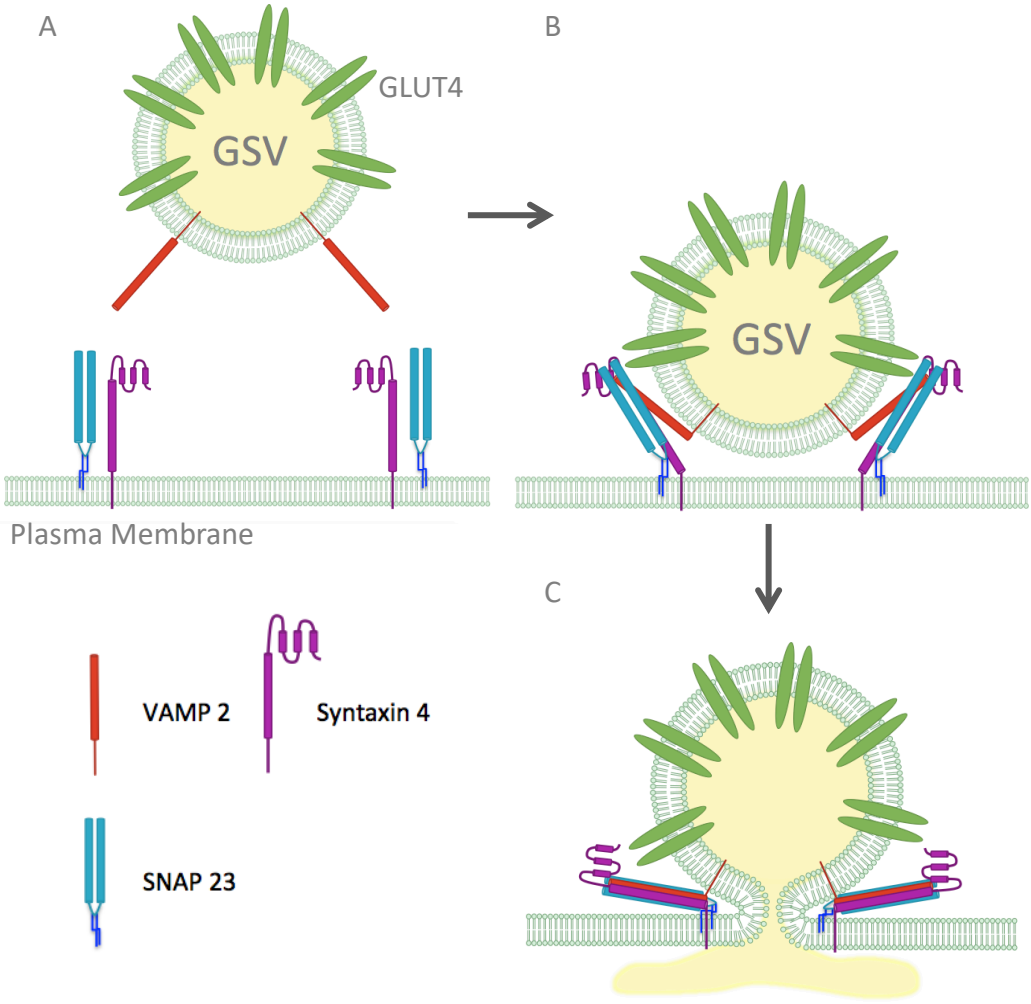

Figure 5: Schematic of SNARE mediated GSV docking to the PM.

The lipid bilayer is thermodynamically stable, which means membrane fusion such as GSVs to the plasma membrane requires accessory proteins to facilitate fusion and overcome the energy requirement for fusion. A. GSV containing V-SNARE VAMP2 approach the target membrane. B. Docking of GSV to plasma membrane through binding of complimentary t-SNAREs; SNAP23 and syntaxin4. C. The formation of the *trans*-SNARE complex leads to zippering, where the tight binding of this complex over comes the energy required for membrane fusion.

2.4.2.4 Cytoskeletal proteins

Cytoskeletal proteins play an important role in the delivery of GSVs to the PM in response to insulin stimulation, as well as the sequestering of GLUT4 in GSVs in the absence of insulin stimulation. Studies which visualise the mobilisation of GSVs to the PM in response to insulin stimulation have shown co-localisation of movement of GSVs along the tubulin positions (Semiz *et al.*, 2003). TIRF microscopy observing mCherry-tubulin and HA-GLUT4-eGFP identified a role for microtubules in the delivery of GSVs to the PM, depicted in Figure 6 A (Dawicki-McKenna *et al.*, 2012). Time-lapse images from the TIRF zone showed that the microtubule density increases in an insulin dependent manner beneath the PM. In addition to increased microtubule density the population of microtubules at the PM within the cell display an increase in curvature upon insulin stimulation. IRAP-pHluorin is used to determine the sites of GSV fusion, pHluorin is a pH sensitive fluorescent tag which is quenched at low pH found in small intracellular vesicles. Upon fusion with the plasma membrane IRAP-pHluorin is exposed to neutral pH which allows for GSV fusion to be visualised and to occur in close proximity to the microtubules populations near the PM, these are correlative and insulin dependent effects (Dawicki-McKenna *et al.*, 2012).

The trafficking of GSVs to the PM in response to insulin stimulation has been attributed to myosin and kinesin proteins, specifically; KIF5B, MYO5A, and MYO1C (Semiz *et al.*, 2003; Boguslavsky *et al.*, 2012; Sun *et al.*, 2014). The microtubule kinesin KIF5B has been identified as highly expressed in adipocytes (Semiz *et al.*, 2003; Cui *et al.*, 2016). KIF5B was shown to be partially co-localised with intracellular GLUT4 and is required for the transport of GLUT4 to the PM (Semiz *et al.*, 2003). Myo1c, a actin based motor protein is associated with GLUT4 translocation in response to insulin stimulation (Toyoda *et al.*, 2011). The tethering of GSVs at the PM in response to insulin stimulation is mediated by Myo1c binding at the sub PM actin population, shown in Figure 6 B (Boguslavsky *et al.*, 2012). In both muscle and fat cells insulin stimulation results in a the rapid formation of cortical actin projections, and the trafficking of GLUT4 is dependent on the formation of these structures (Kanzaki and Pessin, 2001; Brozinick *et al.*, 2004).

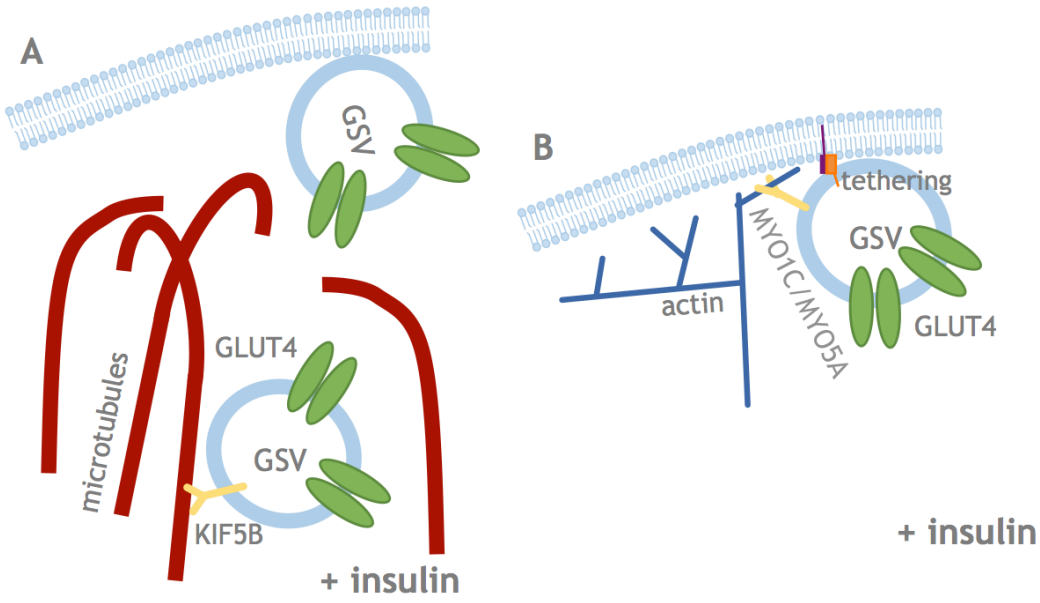

Figure 6: Schematic of Cytoskeletal activity in response to insulin signalling.

A. The activity of microtubule network in response to insulin stimulation alters in two key ways. The density of microtubules at the TIRF zone increases upon insulin stimulation in adipocytes. The curvature of microtubules Microtubule network at the PM increases in curvature. Kinesin KIF5B has been shown to have a role in the insulin dependent translocation of GLUT4 to the Pm and sites of fusion are linked to areas of high microtubule density. B. The actin network beneath the PM is efficiently restructured in response to insulin stimulation forming new projections. The motor proteins Myo1c and Myo5a are involved in actin based GSV transport and tethering to the PM in response to insulin stimulation in adipocytes and striated muscle cells.

2.4.2.5 GTPase proteins

The activation of GTPase family proteins regulate almost every facet of intracellular membrane trafficking, and insulin stimulated GLUT4 translocation is no different (Sano *et al.*, 2003; Mizuno-Yamasaki *et al.*, 2012). GTPase proteins activity is dependent on the state of protein binding to GTP or GDP. In the GTP bound state GTPase proteins bind to specific effector proteins to orchestrate membrane trafficking events (Mizuno-Yamasaki *et al.*, 2012). The activation of Rho family GTPase TC10 has been demonstrated to be required for insulin stimulated glucose uptake, and GLUT4 translocation (Chiang *et al.*, 2001). TC10 activity induces actin

filament formation, which has been observed to be an important part of GSV mobilisation as well as part of the insulin response in adipocytes. Activation of TC10 in response to Insulin stimulation is a PI3K independent pathway. The activation of TC10 requires translocation to lipid rafts of Cbl, CrkII, and C3G, shown in Figure 3 (Chiang et al., 2001).

The Rab GTPase Rab10 is a downstream target of AS160, one of the downstream effectors of the insulin receptor tyrosine kinase activity (Larance *et al.*, 2005; Sano *et al.*, 2007). Rab10 has been identified as the only Rab protein component of GSVs (Brewer *et al.*, 2016). One downstream effector for Rab10 has been identified as SEC16A, a protein required for the organisation of endoplasmic reticulum exit sites, both proteins have been shown to be required for GLUT4 trafficking to GSVs in adipocytes (Bruno *et al.*, 2016). Rab10 has been identified as the major Rab protein involved in GLUT4 translocation to the PM, shown in Figure 3 (Chen and Lippincott-Schwartz, 2013). The Rab protein Rab14 has been identified in GLUT4 positive endosomal compartments. Rab14 has a proposed role for the recycling of GLUT4 which has arrived from the PM to the early endosomes into the Golgi network (Reed *et al.*, 2013). Rab14 is required for this recycling and the presence of dominant negative Rab14Q70L results in GLUT4 stalling within enlarged vesicles. The other Rab proteins involved in the intracellular recycling of GLUt4; Rab4a, Rab4B and Rab8A (Kaddai *et al.*, 2009; Sun *et al.*, 2014).

2.5 GLUT4 MOBILISATION AT THE PLASMA MEMBRANE

As previously stated the ability for GLUT4 to remain sequestered intracellularly until required at the PM is essential to its function in lowering blood glucose. The control of when GLUT4 arrives at the PM is therefore tightly regulated. Insulin is the predominant signal for GLUT4 mobilisation to the PM in adipocytes (Bryant *et al.*, 2002). This study will focus on the insulin-mediated response of GLUT4.The other documented GLUT4 translocation signals are skeletal muscle contraction and, in the brain, neuronal activity (Bradley *et al.*, 2015, Ashrafi *et al.*, 2017). It is important to appreciate these other regulatory pathways, but as insulin is the primary influence when lowering blood glucose concentration, it is the focus of this thesis. New understanding of insulin stimulated GLUT4 regulation is based upon the behaviour of GLUT4 at the plasma membrane.

2.5.1 GLUT4 behaviour at the plasma membrane

Further understanding of GLUT4 regulation and behaviour has been directed at the plasma membrane. Observations using super resolution microscopy techniques have shown that GLUT4 behaviour at the plasma membrane is affected by insulin signalling. GLUT4-containing vesicles continually recycle to and from the membrane in a non-stimulated adipocytes and other GLUT4 containing cell types (Stenkula *et al.*, 2010; Lizunov, Lee, *et al.*, 2013; Lizunov, Stenkula, *et al.*, 2013).

2.5.1.1 GSV fusion behaviour altered by insulin

Evidence suggesting that GLUT4 behaviour once in the plane of the PM was also modulated by insulin came from Stenkula et al., 2010. Results were gathered using total internal reflection (TIRF) microscopy, and the pH sensitive tag pHluorin to the N-terminus of IRAP. IRAP is co-localised with GLUT4 within GSVs and acts with Tankyrase protein to enhance GSV translocation to the PM (Yeh *et al.*, 2007). TIRF microscopy only visualises the first 100nm of sample, ideal for the study of PM protein interactions (Kudalkar *et al.*, 2016). pHluorin is quenched at low pH such as that found in small intracellular vesicles like GSVs, pHluorin flashes when the vesicle fuse with the PM and it is exposed to the neutral extracellular pH (Kavalali and Jorgensen, 2014). Therefore, the flash of IRAP-pHluorin corresponds directly to GSV fusion with the PM. Time lapse images of the TIRF zone of HA-GLUT4-mcherry and IRAP-pH positive adipocytes not stimulated with insulin show GSVs arriving into the

TIRF zone at a constant, slow, constitutive rate. The arrival of GSVs at the PM can be measured in two distinct fashions termed as; fusion with retention and fusion with dispersal, a schematic of these events is depicted in Figure 7.

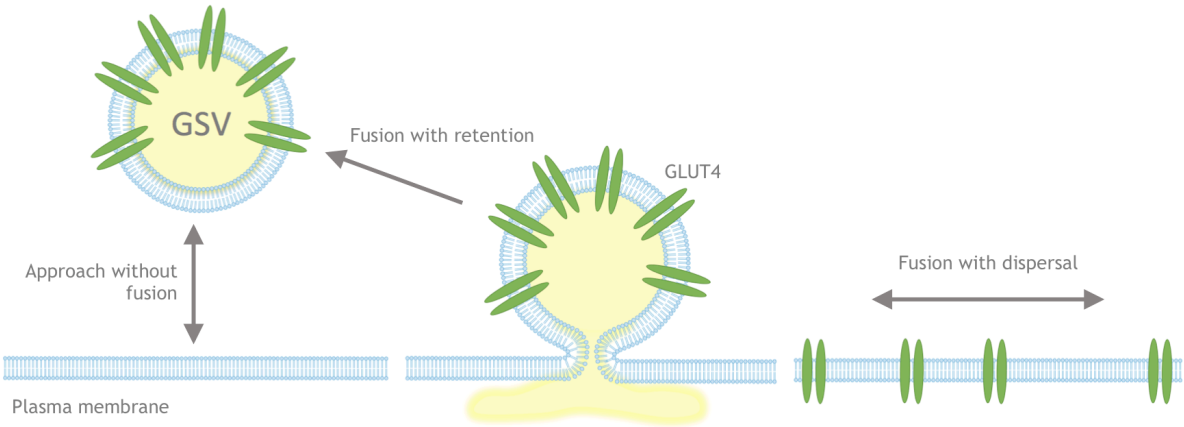

Figure 7: Schematic of GSV fusion events

Arrival of GSVs at the plasma membrane (PM) has been investigated and characterised. GSVs approach and dock without fusion. GSVs fuse with the PM and are re-endocytosed, known as fusion with retention. GSV arrive and fuse at the PM with the dispersal of GLUT4 across the PM.

Fusion with retention is characterised by once the flash of IRAP-pH has occurred signalling fusion the cluster of GLUT4-mcherry remains intact and disappears from the TIRF zone in the Z-direction as a cluster. This fusion with retention is similar to a kiss and run type fusion event. Fusion with retention is the most common event observed in an un-stimulated cell. In response to insulin stimulation fusion with retention occurs at a slightly increased rate in the stimulated adipocyte cell (~2-fold increase) in comparison to the basal cell. This increase is indicative of increased GSV trafficking to the PM in response to insulin signalling. The fusion with dispersal is characterised by IRAP-pH flash and the GLUT4-mcherry cluster signal diffuses at the PM. This diffusion of GLUT4-mcherry shows GLUT4 remaining at the PM and is hypothesised to increase GLUT4 dwell time at the PM. The measured fusion with dispersal events increases 60-fold in response to insulin stimulation; the effect on insulin stimulation on GSV fusion events is depicted in Figure 8. GSVs fusion with dispersal is one of the most up regulated trafficking processes in response to insulin stimulation in adipocytes. Fusion with dispersal occurs at the greatest rate in an insulin-stimulated cell in comparison to fusion with retention, this combined with the fold. Increase indicates that insulin stimulates the dispersal of GLUT4 at the PM (Stenkula *et al.*, 2010). This reported dispersal of GLUT4 at the PM in response to insulin stimulation is further validated using the GSV associated SNARE protein VAMP2. VAMP2-pHluorin is validated to co-localise with GLUT4 and was utilised to investigate GSV arrival at the PM. This study confirmed the occurrence of “kiss-and-run” GSV fusion events are most prevalent in un stimulated adipocytes, and that insulin stimulation resulted in increased dispersal of GLUT4 at the plasma membrane (Xu *et al.*, 2011). This study further highlighted that the dispersal of GLUT4 at the PM is an insulin-stimulated event, providing further credence to this observation.

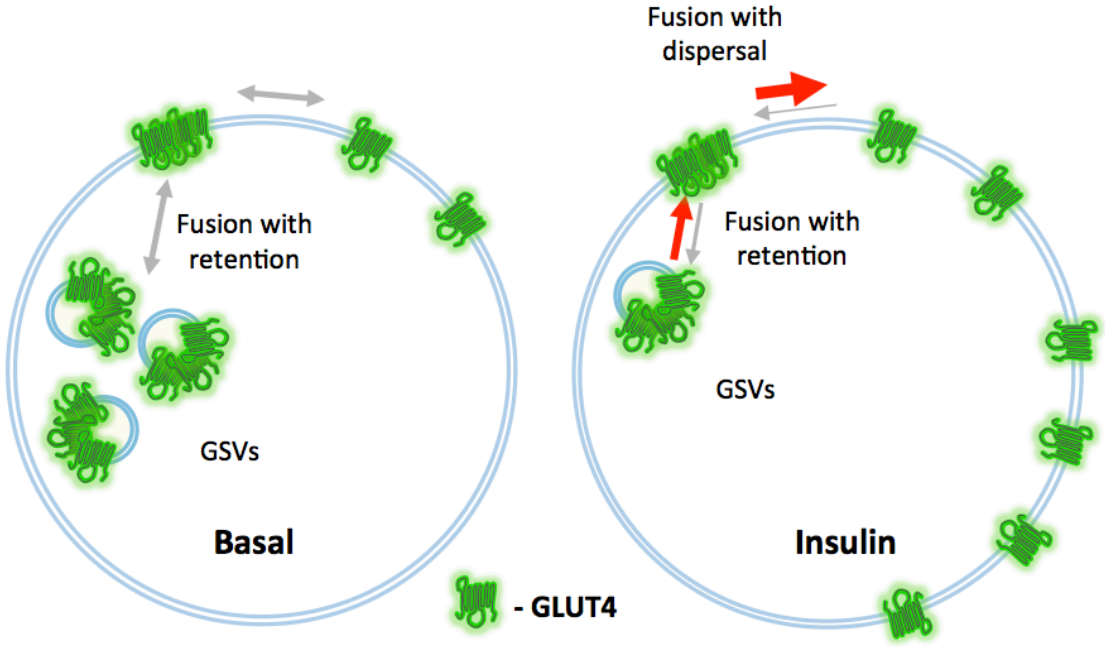

Figure 8: Schematic model of GLUT4 fusion at the plasma membrane

The delivery of GSVs to the PM is an insulin-regulated process. GSVs are sequestered in the cell in the absence of insulin signalling. The fusion of GSVs to the PM has been characterised into two modes, fusion with retention and fusion with dispersal. GSVs undergo a slow and constant recycling to the PM in the absence of insulin stimulation. In the absence of insulin stimulation, the majority of arriving GSVs arriving undergo fusion with retention, similar to a "kiss-and-run" event. Therefore, the majority of fusion events do not lead to GLUT4 retention at the PM in the basal cell. In the insulin stimulated cell there is an increase in GSV delivery at the PM. The GSVs that arrive show fusion of the vesicle with GLUT4 dispersal across the membrane. This is defined as fusion with dispersal, which is increased 60-fold in insulin stimulated cell. The fusion with dispersal step is hypothesised to allow for increased dwell time of GLUT4 at the PM. Red arrows denote increases in events in response to insulin stimulation.

2.5.1.2 Single Molecule tracking of GLUT4 at the PM

Single molecule tracking imaging at the TIRF zone has been harnessed in further studies of GLUT4 at the PM, this allowed for tracking and characterisation of individual GLUT4 molecule behaviour at the PM (Lizunov, Stenkula, *et al.*, 2013). These results gathered when following the trajectory of GLUT4 at the TIRF zone led to the categorization of three distinct forms of GLUT4 motion at the PM; random free diffusion, confined motion and directed motion. Schematic representations of the trajectories of GLUT4 within these definitions is shown below in Figure 9.

Random free diffusion is characterised by an indirect and constant motion of GLUT4

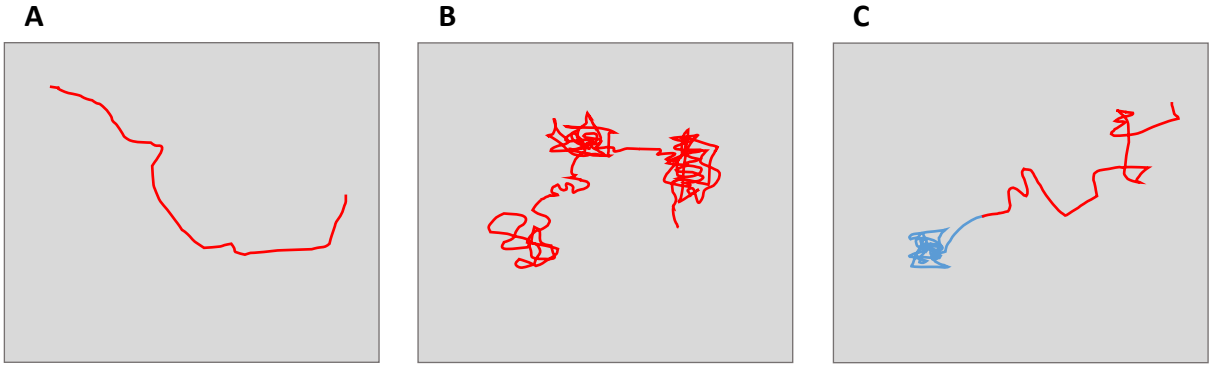

Figure 9: Schematic representation of GLUT4 trajectories at the PM

Schematic of GLUT4 trajectory at the PM of different types of motion. A. Directed motion, defined by a long distance travelled and minimal lateral diffusion B. Free lateral diffusion is characterised by constant motion within a confined area of the PM. C. Confined diffusion is shown by a period of constant motion within a confined area as defined in the picket and fence model.

at the PM. Confined motion is characterised by constant motion within a confined area at the PM, as defined in the picket and fence model, described in detail below 2.5.1.3 (Nakada *et al.*, 2003). Directed motion of GLUT4 is characterised by long distance travel of GLUT4 at the PM with minimal random free diffusion (Lizunov, Stenkula, *et al.*, 2013). The stimulation of 3T3-L1 adipocytes with insulin results in an increase in free diffusion and a decrease in confined GLUT4 motion at the PM. Directed motion is the least prominent form of GLUT4 trajectory at the TIRF zone and is seen at marginally increased levels in the un-stimulated cell compared to the insulin stimulated cell. The directed motion is correlated vesicular transport, which would be GLUT4 pre-fusion to the PM.

To further characterise the clusters of GLUT4 at the PM super resolution microscopy techniques; fluorescence photo-activation localization microscopy (FPALM) and electron microscopy (EM) were used in this study (Lizunov, Stenkula, *et al.*, 2013). The clusters of GLUT4 at the PM where characterised as 110 ± 20nm patches which are not circular, but oblong. Within these clusters the GLUT4 is constantly mobile. The mobility of GLUT4 within the cluster eliminates the hypothesis of simple cluster models such as cross-linking and solid phase domain for GLUT4 at the PM. This points to a separate method of corralling for GLUT4 at the PM in adipocytes. Rates for GLUT4 dissociation from the clusters and the endocytosis of the clusters were measured. KCN was used to deplete ATP and block GLUT4 endocytosis to separate the two events, hypothesising that endocytosis requires ATP but GLUT4 dissociation from clusters is a ATP independent function (Kono *et al.*, 1971). The measurements showed that diffusion from clusters is increased ~3-fold in response to insulin stimulation. Insulin stimulation resulted in endocytosis events decreasing ~2-fold (Lizunov, Stenkula, *et al.*, 2013).

Due to the complex nature of both T1D and T2D future therapeutics which target umbrella steps, such as the dispersal of GLUT4 at the PM, during the insulin response could be of particular interest.

2.5.1.3 Picket and fence plasma membrane model

The understanding of the plasma membrane has moved beyond the random dispersal and diffusion of lipids hypothesised in the lipid mosaic model. Current understanding is based on a more defined structured hypothesis, the picket and fence model (Nakada *et al.*, 2003; Kusumi *et al.*, 2005). It has been demonstrated that proteins and lipids do not freely disperse across the PM as once thought. The composition of the lipid bilayer is understood to affect protein diffusion and movement. Therefore, proteins that are involved with lipid dynamics are of particular interest when investigating the membrane dynamics of a PM protein such as GLUT4 (Di Paolo and De Camilli, 2006; Shisheva, 2008; van den Bogaart *et al.*, 2013; Hresko *et al.*, 2016).

To investigate the mobility of proteins at the PM techniques were required which permitted single particle tracking at a high resolution. Unravelling the detailed mobility of proteins required a high speed camera at the TIRF zone for the observation of cell surface components (Fujiwara *et al.*, 2002; Nakada *et al.*, 2003).

The picket and fence hypothesis was originally developed in studies investigating the transmembrane transferrin receptor (TfR) and the unsaturated phospholipid L-α-dioleoylphosphatidylethanolamine (DOPE) using Cy3 to fluorescently label and track these membrane components (Fujiwara *et al.*, 2002; Nakada *et al.*, 2003). TfR and DOPE both displayed confinement within the membrane, in which free diffusion of both occurred within a 230 ηm^2-confined space. The average residency time of DOPE within a 230 ηm^2 compartment is measured at 13 ms, which is much shorter than the measured compartment confinement time of 65 ms for TfR. This suggests a hindrance to diffusion for the larger TfR (Fujiwara *et al.*, 2002). These studies showed the model of free diffusion required updating and diffusion at the membrane is suppressed within a 230 ηm^2-confined area. This proposed model is described as the anchored membrane-protein picket model (Fujiwara *et al.*, 2002). This model hypothesized that due to the effects of steric hindrance and friction-like effects theorized in various transmembrane proteins. A variety of transmembrane proteins are anchored to the actin-based cytoskeleton. These act as rows of pickets following the underlying cytoskeletal network (Dodd *et al.*, 1995).

The confinement at the membrane is regularly overcome in a rapid hop like diffusion event (Suzuki *et al.*, 2005). Diffusion of a G-protein coupled receptor, μ-opioid receptor (μOR) was observed using colloidal gold probes. This study was able to obtain long term trajectories, without fluorophore bleaching, of individual receptors at the PM known as, single particle tracking (SPT). These results showed short-term confinement within a compartment, followed by slow hop diffusion into a new compartment. The average hop rate measured was once per 45 ms (Suzuki *et al.*, 2005). Further evidence for the picket fence model is collected from a study gathering three-dimensional (3D) images using electron tomography of 0.85 ηm thick sections made 100 ηm below the PM surface. This methodology corresponds with 3D images of the structures under the PM, of the cell type used, normal rat kidney fibroblasts. The actin filaments at the near boundary to the PM correspond to the boundaries of lateral diffusion, PM 230 ηm^2 compartments which were described in previous studies (Morone *et al.*, 2006).

The confinement and hop diffusion rates of proteins at the PM are altered depending on the conditions for the protein. As explained above the behaviour of GLUT4 within

the PM is altered by insulin stimulation, with increased mobility stimulated by insulin signalling. Therefore, the understanding of the mechanism behind this is a new field of interest.

2.5.1.4 Insulin resistance and GSVs at the PM

The effect of insulin resistance on GLUT4 behaviour at the PM has been studied in samples from insulin-resistant human adipose cells (Lizunov, Lee, *et al.*, 2013). Using TIRF microscopy the mobility of GSVs at the cell surface area was calculated. In a healthy individual the mobile GSVs detected at the PM in adipose cells significantly decreases, (3-fold), in response to insulin stimulation. Systematic insulin resistance resulted in no effect on the basal level of GSV mobility but affected the insulin response. Increased insulin resistance resulted in a non-significant minimal decrease in GSV mobility, with mobility being similar to that of basal cells. The mobility of GSVs is correlated to GLUT4 remaining clustered at the PM and not dispersing. Fusion of GSVs upon insulin stimulation increases as demonstrated in previous studies. In samples from high insulin resistant subjects the increase in GSV fusion events is diminished in comparison to healthy samples (Lizunov, Lee, *et al.*, 2013). Fusion of GSVs is integral to the delivery and dispersal of GLUT4. The evidence shows that insulin resistance results in the failure of proper GSV fusion and GLUT4 dispersal at the PM, both steps are essential for proper insulin stimulated glucose uptake.

Increased dispersal of GLUT4 clusters and increased mobility of GLUT4 at the PM in response to insulin stimulation has been demonstrated in these studies using super resolution microscopy techniques (Stenkula *et al.*, 2010; Xu *et al.*, 2011; Lizunov, Stenkula, *et al.*, 2013). The studies carried out show that insulin stimulation increases GLUT4 mobility at the plasma membrane, increases the diffusion of GLUT4 across the plasma membrane and concurrently inhibiting endocytosis of GLUT4. This data collected reveal that the dwell time of GLUT4 is increase in insulin-stimulated adipocytes; increased dwell time of GLUT4 is hypothesised to be critical for sustained glucose uptake resulting in lowered blood glucose concentrations. The results from these observations when taken together show that insulin sensitivity is imperative for proper GSV mobility. GSV mobility is indicated as a positive effect of

insulin signalling which is critical for proper glucose homeostasis. The results from patients with uncontrolled blood glucose homeostasis showed limited mobility. Future studies have potential to demonstrate if the mobility of GLUT4 at the PM improves glucose uptake and is a requirement for proper homeostasis. Understanding the molecular mechanism behind GLUT4 mobility is not yet defined. This study aims to investigate a potential role for EFR3 in GLUT4 dispersal at the PM.

2.5.2 Identification of a potential molecular mechanism behind GLUT4 dispersal

Genetic model organisms, such as *S. cerevisiae,* have long been a tool for identifying proteins of interest when understanding new molecular mechanisms (Botstein and Fink, 2011). It has been shown that GLUT4 trafficking has been demonstrated to be a conserved process from yeast *S. cerevisiae* to mammals (Lamb *et al.*, 2010; Shewan *et al.*, 2013). Studies have showed that mammalian GLUT4 expressed in *S. cerevisiae* traffic through the yeast Golgi in an ubiquitin dependent manner, this same process has been shown in adipocytes (Lamb *et al.*, 2010).

Yeast provides an ideal model organism as the simplest form of eukaryotic cell, with a haploid genetic makeup used in this screen. This along with fast growth makes yeast a valuable tool to gain insight into molecular interactions. To investigate potential interactions for GLUT4 a *S. cerevisiae* strain deficient in hexose transporters (Δhxt) was developed by Wieczorke et al., 2003. This is a temperature sensitive strain, in which hexose transporters are depleted at restrictive growth temperatures, above 30^{o}C. This system was used to characterise the mammalian glucose transporters GLUT (Wieczorke *et al.*, 2003). Mammalian GLUT4 expressed in the Δhxt strain is incapable of maintaining life when fed glucose at restrictive growth temperatures. Visualisation of GLUT4-GFP in this system shows intracellular localisation within structures resembling the endoplasmic reticulum or endosome like organelles similar to GSVs (Wieczorke *et al.*, 2003).

Reasoning that the expressed GLUT4 is unable to rescue the mutant and sustain life when fed glucose at restrictive temperatures due to this localisation within GSV like post Golgi compartments within the cell. Simply put no GLUT4 at the PM results in no glucose uptake and therefore cell death. A genetic screen was preformed using a suppressor model to generate mutations which have selective advantages to the

yeast and allow for survival of the cell. It is theorised any mutations which result in cell survival are involved in the delivery of GLUT4 to the PM. The Δhxt GLUT4 expressing strain of yeast are incubated for prolonged periods on glucose medium after irradiation with UV-light to induce spontaneous genetic mutations. The suppressor colonies able to consume glucose as the sole carbon source were analysed. This screen revealed that the mutation double mutation *fgy1-1 fgy4X* rescues the phenotype allowing for GLUT4 mediated cell growth on glucose medium. The term FGY stands for **f**unctional expression of **G**lut4 in **y**east (Wieczorke *et al.*, 2003). The mutation *fgy1-1* is a recessive mutation of allele FGY1, which corresponds to the protein Efr3 (PHO **E**ighty **F**ive **R**equiring) (Voss, 2005). Efr3 is a membrane localised protein required for the localisation of the PI kinase Stt4 complex to the PM (Baird *et al.*, 2008). The mutation *fgy4X* is a recessive mutation of allele FGY4, which corresponds to the protein Erg4 (Dlugai, 2003). Erg4 is a sterol reductase involved in the final stage of ergosterol biosynthesis (H.Lai *et al.*, 1994). The mutation within Efr3 and Erg4 required for GLUT4 arrival to the PM in yeast is not clear, as a gain or loss of function mutation. This study focuses on the behaviour of GLUT4 at the PM and how insulin mediates dispersal and increased motility of GLUT4 at the PM. Therefore, the investigation is focused on Efr3; a membrane localised protein involved in membrane lipid regulation.

2.6 EFR3

2.6.1 EFR3 biological function

Efr3 in yeast *S. cerevisiae* and the homolog RBO in *Drosophila* have been shown to be essential genes (Faulkner *et al.*, 1998; Baird *et al.*, 2008; Vijayakrishnan *et al.*, 2010). Efr3 and its binding partners are conserved from yeast to mammals, with two EFR3 homologs, A & B, present in mammalian genome (Baird *et al.*, 2008). In *Drosophila* RBO is a transmembrane PIP_2-DAG pathway lipase, with lipase independent functions (F.-D. Huang *et al.*, 2004; Huang, 2006; Vijayakrishnan *et al.*, 2010). Yeast and mammalian EFR3 have no lipase function domains, this has allowed for yeast to be a model organism for the discovery and initial study of Efr3 function (Vijayakrishnan *et al.*, 2010). The mammalian homologs EFR3A and EFR3B have a 64% amino acid sequence identity and 78% positive alignment. This indicates a homologous protein but scope for differences in molecular function. For simplicity EFR3 is used when discussing general mammalian protein features unless homolog is specified assume both are mentioned.

2.6.2 EFR3 interacting proteins

Homology from yeast to mammals has allowed for the study of proteins, which are associated with EFR3 to be carried out in a yeast model system. It has been shown that EFR3 is required for the localisation of Stt4 in yeast to the PM, and that EFR3 is the membrane associated portion of the Stt4 machinery (Baird *et al.*, 2008; Wu *et al.*, 2014). In yeast the lipid kinase Stt4, orthologue of mammalian phosphatidylinositol-4 kinases, has been shown to cluster in distinct PM patches enriched with Stt4 protein (Audhya and Emr, 2002; Baird *et al.*, 2008). A genome wide protein interaction study found that Efr3 in yeast interacts with the protein Ypp1, orthologue of mammalian TTC7 (Tarassov *et al.*, 2008). EFR3 binds to TTC7 (Ypp1) which in turn binds with PI4KIIIα (Stt4). In yeast the two primary components, which have been identified as required for Stt4 (PI4KIIIα) localisation to the PM, are Ypp1 and Efr3, with Efr3 providing membrane localisation and Ypp1 providing linkage between PI4KIIIα and Efr3.

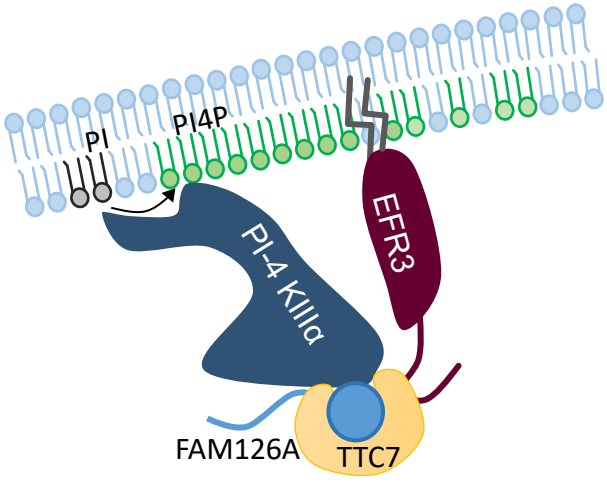

Figure 10: Schematic of EFR3A and PI4KIIIα localisation to the membrane

Schematic shows PI4KIIIα (Stt4 in yeast) localisation to the PM mediated by EFR3. Palmitoylation of the N-terminus of EFR3 allows anchoring to the PM, EFR3 us hypothesised to localise to the PM through a conserved basic patch (yeast K12, R46, K49, and K52). PI4KIIIα is localised to EFR3 through intermediary proteins, this is crucial to membrane localisation of PI4KIIIα. Identified linker proteins include TTC7 (Ypp1 in yeast) and FAM126A. These both act as the intermediary linkers between both EFR3 and PI4KIIIα in mammalian cells, it is not defined if both are required or if they are found in different cell types. PI4KIIIα is a 230kDa PI kinase, which phosphorylates the inositol ring at position 4' of phosphoinositide. PI4KIIIα activity is responsible for generation of distinct PI4P patches at the PM.

Studies using mouse brain extracts have showed that PI4KIIIα (Stt4) immuno-precipitates two interacting proteins, EFR3B and TTC7B. These results correlate with the yeast results as both are the mammalian homologues of yeast EFR3 and Ypp1 respectively (Nakatsu, Jeremy M. Baskin, *et al.*, 2012). This confirmed that EFR3 functions to localise PI4KIIIα/Stt4 to the membrane through intermediary linker proteins and that this is a conserved process from yeast to mammals. TTC7, the second component of this PI4-KIIIα localization machinery, is composed of HEAT-repeat domains. The HEAT-repeat domains are arranged into a dumbbell shape of TTC7. Both the C-terminal component of EFR3 and TTC7 are required for protein-protein interaction (Baird *et al.*, 2008). In mammalian cells TTC7 has been shown to

not be the only linker protein involved as the intermediary interaction of PI4KIIIα to EFR3. The protein FAM126A has also been shown to also play a role in forming the PI4KIIIα complex at the PM with TTC7 (Baskin *et al.*, 2016). A other protein which can localise PI4KIIIα to the PM is TMEM150A, which is able to localise PI4KIIIα independent of TTC7 (Chung *et al.*, 2015). TMEM150A is a transmembrane protein which interacts with both EFR3 and PI4KIIIα, however it does not bypass the role of EFR3 (Chung et al., 2015). Figure 10 depicts the localisation of PI4KIIIα through TTC7 and FAM126A association to EFR3.

2.6.3 EFR3 structural insights

In mammalian cells EFR3 mediates the localisation of PI4KIIIα to the PM. The N-terminal palmitoylation of EFR3 is required for membrane association in mammalian cells (Wu *et al.*, 2014). It is hypothesized that a conserved basic patch, from yeast to mammals, at the N-terminus (yeast K12, R46, K49, and K52) is further able to localize EFR3 to the PM specifically. This patch is shown in Figure 11, denoted by magenta residues and arrows to highlight. The conserved basic patch is the primary source of membrane localisation in yeast which do not have palmitoylation post translational modification (Wu *et al.*, 2014). The conserved basic patch is hypothesised to direct localisation to the PM as a consequence of electrostatic interactions between the negatively charged inner leaflet of the lipid bilayer associated with the PM in the absence of palmitoylation modifications. Architecturally EFR3 has a disordered C-terminal and ordered N-terminus domain. The results from x-ray crystallography are only viable when the disordered C-terminal domain is disregarded; the ordered N terminal structure is shown in Figure 11. Therefore the x-ray crystallography results carried out by (Wu *et al.*, 2014) are of the N8–562 region. The mapping of the N terminal reveals an entirely α-helical secondary structure. The EFR3 N-terminus represents a ~120 Å long rod, composed of VHS, ARM and HEAT repeat domains (Wu *et al.*, 2014). Combined EFR3, TTC7 and other proteins may form a rigid scaffold for PI4KIIIα to catalyse PI4P production at the PM, seen in Figure 10 (Nakatsu, Jeremy M Baskin, et al., 2012; Wu et al., 2014; Chung et al., 2015). The interaction between EFR3 and TTC7 is required for membrane localisation of PI4KIIIα (Baird *et al.*, 2008; Wu *et al.*, 2014). This

interaction between the EFR3 and Ypp1 is localised to the C-terminal (651-782) region of EFR3. Using database searches of EFR3 we know that this C-terminal region has over 20 predicted phosphorylation sites, four of which are highly conserved, S681, S684, T687, and T690 (http://www.phosphogrid.org). Double phospho-mimetic mutations of the S and T sites respectively resulted in a weakened binding between EFR3 and Ypp1 (Wu *et al.*, 2014). Furthermore, full phospho-mimetic

mutations of all four sites results in a 10% reduction in PI4P levels and a significant portion of PI4KIIIα is re-localised to the cytosol.

2.6.3.1 Phosphatidylinositol 4 Kinase IIIa activity

There are two subsets of the PI4-kinase family, type II and type III, which have been characterised based on molecular weight and inhibitor sensitivity (Nakagawa *et al.*,

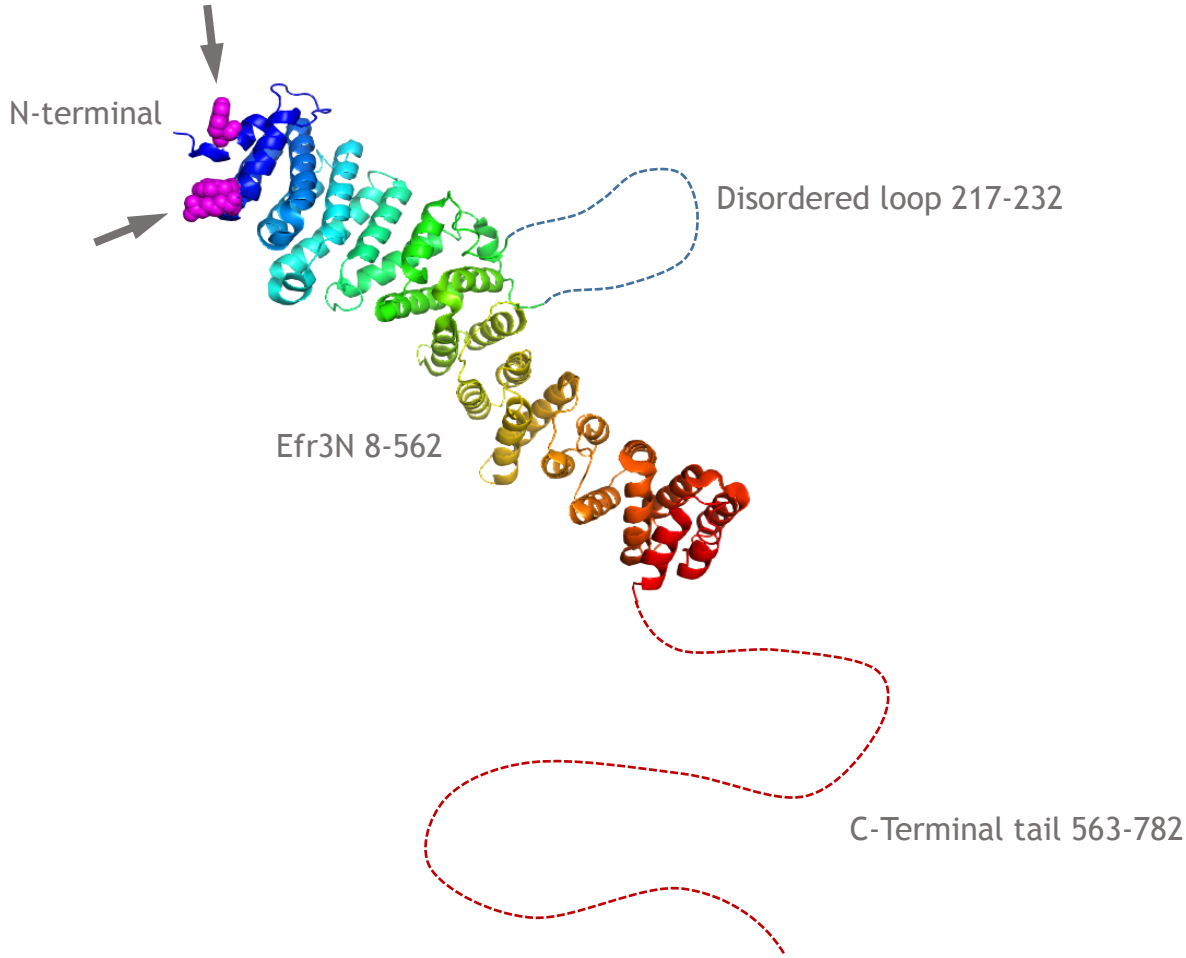

Figure 11: Structure of Efr3

X-ray crystallography solved structure of yeast Efr3 N-terminal from Wu et al., 2015. Helical repeats from N-terminal (8-562) sequence form a structured rod. The disordered loop (217-232) structure was not solved. The C-terminal tail (563-782) is responsible for PI4KIIIα localisation to the PM. Denoted by grey arrows and marked in magenta spheres is the conserved basic patch (K12, R46, K49, and K52) responsible for PM localisation of Efr3.

1996; Barylko *et al.*, 2001; Minogue *et al.*, 2001; Balla *et al.*, 2002). PI4K type III are sensitive to wortmannin, and within the PI4K family there is the large molecular weight (230kDa) and phenylarsine oxide (PAO) sensitive isoform PI4-kinase IIIα (Nakagawa *et al.*, 1996). PI4K type III are conserved from yeast to humans (Barylko *et al.*, 2001). Stt4 is the yeast orthologue for PI4KIIIα and in yeast Stt4 accounts for the production of 40% of the total cellular PI4P in yeast (Strahl and Thorner, 2007). Stt4 localises to the PM, and the loss of Stt4 function results in defective yeast cell walls, defective polarisation during growth, and abnormal cytoskeleton (Audhya and Emr, 2002; Strahl and Thorner, 2007). In yeast loss of Stt4 phenotypes can be rescued with the expression of yeast PI5K Mss4. The double Stt4/Mss4 mutation results in actin cytoskeletal miss-organisation phenotype which is rescued when the PI4P phosphatase Sac1 is inactivated (Foti *et al.*, 2001). Together this information shows that Stt4 activity in yeast is important for cytoskeletal function and that PI4P production is an important precursor for $PI4,5P_2$ in yeast. The bulk of $PI4,5P_2$ at the PM in yeast is dependent on Stt4 activity, and the production of PI4P as a precursor. In mammalian cells PI4P has established further roles than $PI4,5P_2$ precursor, which is discussed below in 2.7.2.1 (Strahl and Thorner, 2007).

2.6.3.2 PI4KIIIα localisation

The initial localisation of PI4KIIIα was reported to be in the endoplasmic reticulum and perinuclear compartments (Wong *et al.*, 1997). However PM localisation had also been suggested due to its importance for PI4P production at the PM specifically (Balla *et al.*, 2002). Later studies using GFP tagged PI4KIIα showed that PI4KIIIα is cytosolically localised with no particular membrane localisation. This study found that PI4KIIIα is dynamically targeted to the PM through the complex formed with EFR3, as explained above in 2.6.2 (Nakatsu, Jeremy M Baskin, *et al.*, 2012). IN PI4KIIIα knock-out MEFs the levels of $PI4,5P_2$ are reduced by 20%, a relatively modest change in comparison to the 75% loss of PI4P in these cells (Nakatsu, Jeremy M Baskin, *et al.*, 2012). Localisation of PI4P in PI4KIIIα KO MEFs showed that the PM pool was ablated, and the Golgi complex was unaffected with PI4P localising to the Golgi still. PI4KIIIα KO MEFs have reduced PM cholesterol and increased total cholesterol. The loss of PI4KIIIα resulted in a loss of plasma membrane identity and miss-localisation of PM associated integral membrane proteins such as M1 muscarinic receptor and myristoylated/palmitoylated Lck membrane anchor were found to be

localised intracellularly (Nakatsu, Jeremy M Baskin, *et al.*, 2012). Taken together this provides a wealth of evidence that PI4KIIIα activity is important for the function of the PM in mammalian cells and established the PM localisation.

2.6.3.3 PI4KIIIα and EFR3; a link to Hepatitis C virus

Approximately 3% of the world's population is chronically infected with Hepatitis C virus HCV, due to limited therapeutic options (Wasley and J., 2000). HCV is a positive stranded RNA virus, and as such in order for HCV to replicate the host cellular membranes must be reorganised to establish suitable sites for replication (Miller and Krijnse-Locker, 2008). The initial HCV protein synthesis occurs at the rough endoplasmic reticulum, and HCV viral replication is achieved with modified cellular membranes which have protease and nuclease resistant properties, to protect viral replication from cellular defences (Yang *et al.*, 2004; Quinkert *et al.*, 2005). As membrane re-assortment is integral to HCV replication the identification of membrane trafficking associated genes involved during HCV infection was studied. A membrane trafficking gene siRNA library was utilised to identify genes involved in HCV replication. The identified genes included; actin proteins (CDC42 & ROCK2), GTPase (RAB7L1), endosomal proteins (EEA1 & RAB5A), and PI-kinases (PIK3C2G & PIK4CA). The gene PIK4CA corresponds to the protein PI4KIIIα, PI4KIIIα has been shown to significantly co-localise with dsRNA and the HCV viral protein NS5A (Berger *et al.*, 2009). The expression and activity of PI4KIIIα is required for HCV replicase formation (Berger *et al.*, 2009, 2011). The effect of HCV infection on total cell PI4P production was measured using mass spectrometry, this showed that infection increases the level of PI4P but not the expression levels of PI4KIIIα in cells in comparison to control cells (Berger *et al.*, 2011). The phosphoprotein NS5A has been described to co-localise using with PI4KIIIα using confocal microscopy (Berger *et al.*, 2009). NS5A is a critical component of HCV host factor interactions during the regulation of viral replication (Bartenschlager *et al.*, 2010). This resulted in the relationship of endogenous PI4KIIIα enzymatic activity and HCV replication (Harak *et al.*, 2014). PI4KIIIα directly interacts with NS5a in co-immunoprecipitation experiments. Mapping the site of interaction serial deletions at the N and C terminals of PI4KIIIα showed that multiple interaction sights are available for PI4KIIIα interaction, as no single deletion resulted in inhibition of PI4KIIIα and NS5A protein interaction. PI4KIIIα activity during HCV viral replication is not dependent on the N-

terminus Δ1-1101 amino acids and function of PI4KIIIα is not compromised by major N-terminus deletions (Harak *et al.*, 2014). Of further interest is the ability of HCV to hijack PI4KIIIα localisation, as well as PI4KIIIα has been identified as a co-factor for viral replication (Borawski et al., 2009; Berger et al., 2011; Reiss et al., 2011; Altan-Bonnet and Balla, 2012). In cells infected with HCV PI4KIIIα is miss-localised away from the PM and instead found in endoplasmic-reticulum-associated HCV replication compartment (Reiss *et al.*, 2011). PI4KIIIα catalytic activity is believed to be an essential host factor during HCV replication.

This is interesting as many epidemiological studies have linked the development of T2D and those suffering from chronic HCV infections (Antonelli, 2014). This investigation revealed an increased correlation between patients suffering from chronic HCV and the development of T2D. Therefore, if EFR3 and its role for PI4KIIIα localisation is important for GLUT4 and glucose uptake this could provide the causative link between the correlation of these two chronic illnesses.

2.7 PHOSPHATIDYLINOSITOL 4 PHOSPHATE

2.7.1 Phosphatidylinositol

The compartmentalisation of eukaryotic cells allows for specialisation zones within the cell to preform functions efficiently. Coordination within these organelles relies on a variety of signalling methods, including the phospholipid identity of the membrane (Tan and Brill, 2014). The phosphatidylinositol (PI) lipid is a member of the glycerphospholipid family containing a *myo*-inositol head group. The PI family is a minor fraction of total lipid composition with far reaching capabilities; from signal transduction to membrane identity and trafficking of vesicles to specific regions (Mueller-Roeber and Pical, 2002; Balla and Balla, 2006; Altan-Bonnet and Balla, 2012). PI is able to exert this regulatory function due to the large variability of phosphorylation of the hydroxyl groups at 3',4' & 5' position of the inositide ring, shown in Figure 12, providing convertible signals to the cell (Tan and Brill, 2014; Bryant *et al.*, 2015). This allows for diverse range of identities, and modification intermediaries which have differing degrees of negative charge as a result. These phosphoinositide's are able to contribute to wide varying physiological mechanisms within the cell including; vesicle trafficking, transmembrane signalling and ion channel regulation (De Camilli *et al.*, 1996; Di Paolo and De Camilli, 2006; Balla *et al.*, 2009; Kim *et al.*, 2013; Billcliff and Lowe, 2014). Localisation to specific membranes within the cell is a key identifier that PI identity plays an important role within membrane trafficking. The distribution of PI at intracellular membranes can be seen in Figure 13. Early evidence showed that the regulation of vesicular trafficking by PI composition involved $PI4,5P_2$ synthesis during exocytic vesicle priming (Eberhard *et al.*, 1990). The breakdown of $PI4,5P_2$ by phosphoinositide specific phospholipase C into the signalling molecules diacylglycerol (DAG) and the soluble inositol 1,4,5 tri-phosphate (IP_3) has long been studied for its ubiquitous role within cell Ca^{2+} signalling (Berridge, 1983; Streb *et al.*, 1983; Thévenod *et al.*, 1986). With this in mind PI4P was long been associated as a precursor for the production of $PI4,5P_2$ with few roles attributed to PI4P, however P14P has since been shown to be involved in a variety of mechanisms (D'Angelo *et al.*, 2008).

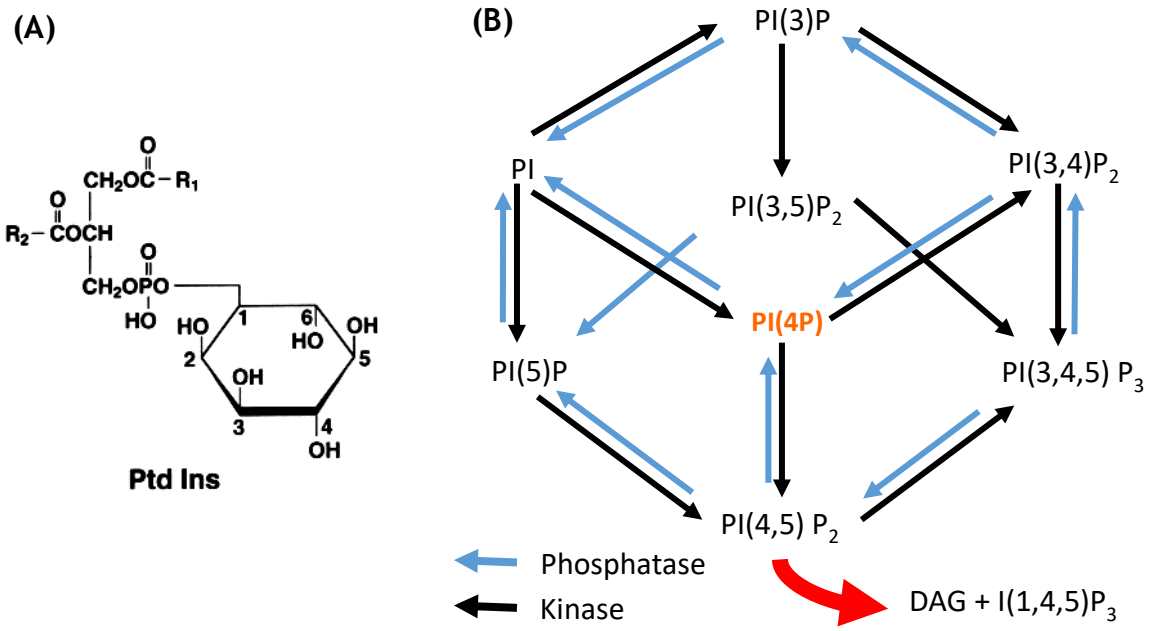

Figure 12 Schematic of Phosphatidylinositol cycle.

(A) The cytosolic phosphatidylinositol (PI) *myo*-inositol head group, phospho- available sights at the ring position 3', 4', and 5'. **(B)** Depiction of the PI phosphorylation cycle, with kinase pathway in black and phosphatase pathways in blue. This represents the complex and variety of regulatory pathways involved in phosphoinositide identity. Kinase and phosphatase regulation allow for the PI family to actively participate in many signalling.

2.7.2 Roles for Phosphatidylinositol groups during insulin signalling

Mentioned above is the insulin signalling pathway, where a key part of the pathway is activation of PI3K and formation of $PI3,4,5P_3$. Roles for other PIs during insulin stimulated GLUT4 dynamics have been identified. HPLC analysis suggests a transient increase in PI3P in response to insulin stimulation and that PI3P generation is believed to occur at the PM, as part of a lipid raft recruitment of PI3K-C2α (Maffucci *et al.*, 2003; Falasca *et al.*, 2007). Over expression of the PI 3-phosphatase myotubularin and depletion of PI3K-C2α result in reduced insulin stimulated glucose uptake independently. This is suggestive that lowering of PI3P levels affects insulin stimulated GLUT4 mediated glucose uptake (Chaussade *et al.*, 2003; Falasca *et al.*, 2007). Using over expression of polyphosphate 5-phosphatse to increase PI3P levels at the PM results in an increase in PM GLUT4, however there is no increase in glucose

uptake as a result (Kong *et al.*, 2006). This suggests a role for PI3P during GLUT4 delivery to or near the PM, and a secondary mechanism is required for the full effect of GLUT4 mediated glucose uptake.

$PI3,5P_2$ is a minor constituent of the PI population (>0.2%) in adipocytes (Sbrissa and Shisheva, 2005). Varying results have been published in relation to $PI3,5P_2$ levels in response to insulin signalling, with reports of increases in intracellular $PI3,5P_2$ and no increase measured in total $PI3,5P_2$ (Sbrissa and Shisheva, 2005; Ikonomov *et al.*, 2007). $PI3,5P_2$ has been linked to the formation of secretory vesicles specifically during the fission and maturation process. In HeLa cells $PI3,5P_2$ production has been identified to be important for trafficking out of the endocytic cycle to the TGN (Rutherford *et al.*, 2006; Sbrissa *et al.*, 2007). In contrast PI5P, which is usually undetectable in most cell types, represents <3% of the PI population in adipocytes and increases 2.5 fold in response to insulin stimulation (Sbrissa *et al.*, 2002, 2004). PI5P production correlates with the F-actin stress fibre break down during insulin signalling, and this break down is controlled by PI5P production (Sbrissa *et al.*, 2004). This increase in PI5P is thought to be linked to the kinase PIKfyve. In response to insulin signalling PIKfyve translocate to intracellular compartments from the cytosol, which plausibly accounts for the increase in PI5P (Shisheva *et al.*, 2001). It is important to note that PIKfyve is important for $PI3,5P_2$ production and is up regulated during the differentiation of 3T3-L1 fibroblasts to adipocytes (Sbrissa *et al.*, 2002; Ikonomov *et al.*, 2007). Delivery of PI5P to adipocytes through cytoplasmic microinjections results in increased PM GLUT4 in an insulin independent manner. Introduction of exogenous $PI3,5P_2$ does not increase PM GLUT4. When PI5P is sequestered, therefore enabling binding, the insulin stimulated translocation of GLUT4 to the PM is inhibited (Sbrissa *et al.*, 2004). In myotubes delivery of exogenous PI5P results in increased Akt phosphorylation and GLUT4 translocation to the PM is triggered in a PI3K dependent fashion, suggesting PI5P production in response to insulin signalling may promote PI3K signalling (Grainger *et al.*, 2011). This points to a role in exocytosis for these PIs in the exocytosis phase of GLUT4 stimulation by insulin.

In contrast to the above PIs $PI4,5P_2$ is an abundant fraction in mammalian cells, including muscle and adipocytes. $PI4,5P_2$ is established to have roles within

endocytosis and regulated secretion (Di Paolo and De Camilli, 2006). Specifically $PI4,5P_2$ is found at the PM, enriched in certain regions which co-localise with endocytic machinery, such as clathrin heavy chains (S. Huang *et al.*, 2004). Inhibition of $PI4,5P_2$ arrests clathrin mediated endocytosis in 3T3-L1 adipocytes, independent of F-actin inhibition (Kanzaki *et al.*, 2004; S. Huang *et al.*, 2004). Inhibition of $PI4,5P_2$ binding through sequestering with PLCδ1-PH expression inhibits TfR endocytosis post insulin stimulation (S. Huang *et al.*, 2004). PI5K over expression increases the production of $PI4,5P_2$, in adipocytes this results in the inhibition of both TfR and GLUT4 endocytosis (Kanzaki *et al.*, 2004). This result is counter intuitive to previous findings. $PI4,5P_2$ action during endocytosis is believed to be through clathrin mediated endocytosis. The over production of $PI4,5P_2$ may have an effect on the established requirement for $PI4,5P_2$ hydrolysis early on during clathrin mediated endocytosis. This over production may result in hindering the formation of invagination (Czech, 2003; Di Paolo and De Camilli, 2006).

2.7.2.1 Phosphatidylinositol 4 Phosphate

PI4P is an abundant member of the PI family. Early characterisation of GLUT4 containing vesicles isolated from both muscle and adipose tissue rat simples included abundant insulin-independent PI4P synthesising activity, however no PI4K has been definitively linked to this activity (Del Vecchio and Pilch, 1991; Kristiansen *et al.*, 1998). The injection of exogenous PI4P into adipocytes does not increase GLUT4 delivery to the PM as others PI populations are capable of, as discussed above (Sbrissa *et al.*, 2004).

With this in mind PI4P was long been associated as a precursor for the production of $PI4,5P_2$ with few roles attributed to PI4P at the PM. However, PI4P has since been shown to be involved in a variety of mechanisms intracellularly and to have a distinct presence at the PM other than precursor lipid (D'Angelo *et al.*, 2008; Hammond *et al.*, 2012; Billcliff and Lowe, 2014). PI4P is generated from PI by members of the PI 4-kinase family, or as a result of INPPE5 phosphatase activity on $PI4,5P_2$ (Behar-Bannelier and Murray, 1980; Collins and Wells, 1982; Hammond *et al.*, 2012). Many of the PI4P associated protein effectors are lipid transfer proteins and vesicle coat proteins (Levine and Munro, 1998; Wang *et al.*, 2003). PI4P has been demonstrated to have involvement in cargo sorting and bud formation, in particular within the

trans-Golgi network (TGN), this function of PI4P is conserved within yeast to mammalian cells (Heldwein *et al.*, 2004; Wang *et al.*, 2007; Ren *et al.*, 2013). As further supported by the fact that many TGN sorting proteins have PI4P binding motifs, an example of which being the EpsinR protein (Hirst *et al.*, 2003). EpsinR binds PI4P via its ENTH domain allowing for the assembly of adaptor protein 1 and soluble *n*-ethylmaleimide sensitive factor adaptor protein receptor into clathrin coated vesicles (Hirst *et al.*, 2004).

PI4P is abundant in the Golgi apparatus and a significant pool is present on the inner leaflet of the PM, shown in Figure 13(Nakatsu, Jeremy M Baskin, et al., 2012; Hammond et al., 2014). Due to the known high level of PI4K activity in GSVs it is conceivable that GSVs are enriched with PI4P. This further goes in hand with the fact that GLUT4 is trafficked through the PI4P enriched TGN during the formation of GSVs (Shewan *et al.*, 2003; Bryant and Gould, 2011; Rowland *et al.*, 2011). The intracellular trafficking from TGN to the PM has been demonstrated to require PI4K activity and PI4P for successful direction to the PM in yeast (Thomas and Fromme, 2016). The improved and evolving understanding of the lipid bilayer reveal that dynamics of the membrane can be tightly regulated and associated with the lipid identity (Kusumi *et al.*, 2005). It is therefore plausible that the delivery of GLUT4 clusters to the PM may be regulated by the lipid identity of either the GSVs or the PM at the regions of GSV fusion.

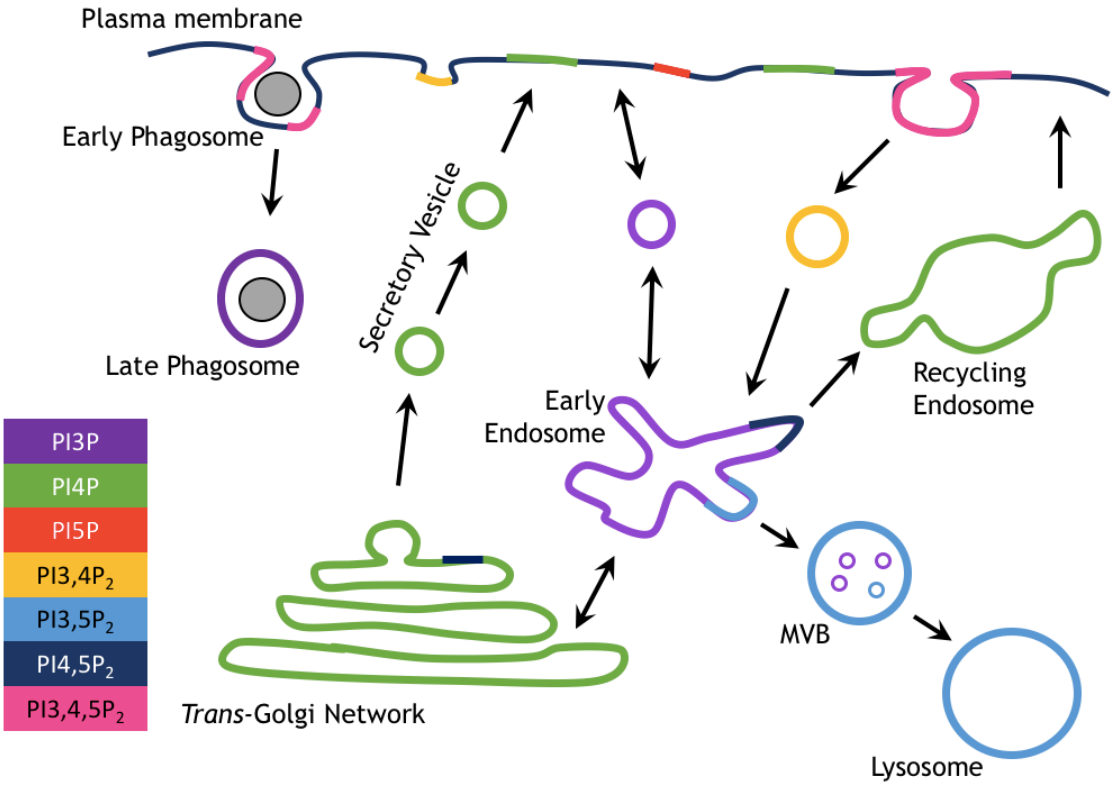

Figure 13: Schematic of phosphoinositide (PI) membrane identity.

Phosphoinositide groups enriched at various intracellular membranes. PI4P is shown in blue and can be seen predominantly associated with recycling endosomes, the *trans*-Golgi network and distinct pools have been shown to exist at the PM. The importance of PI4P pools at the plasma membrane a thought to play a critical role in the trafficking process to and from the PM. The flow of various PI populations can also be seen in this image taken from (Billcliff and Lowe, 2014).

2.8 AIMS AND HYPOTHESIS

This investigation aims to address the evolving understanding of the mechanism behind the insulin response of GLUT4 within adipocytes, with focus on the dynamics of GLUT4 at the PM. EFR3 has been identified as potential mechanism of control for GLUT4 arrival to the PM. EFR3 is of noteworthy interest due to the established role of EFR3 as a membrane localisation protein for the lipid kinase PI4KIIIα. PI4P is enriched in GSVs, and isolated GSVs have increased PI4P synthesising activity. EFR3 and PI4P are membrane components with the potential to regulate GLUT4 at the PM. The molecular method behind the dispersal of GLUT4 at the PM is as of yet not understood. We believe that EFR3 and associated machinery proteins are involved during the insulin dependent dispersal of GLUT4 at the PM, a schematic of our working hypothesis is shown in Figure 14. The ability of EFR3 to regulate this system is hypothesised to be a result of the pools of PI4P produced by PI4KIIIα. A yeast genetic screen identified a mutant allele of Efr3 was required for PM GLUT4 in yeast, the literature doesn't indicate a loss or gain of function mutation. As EFR3 has been demonstrated to regulate PI4P levels through the interaction with PI4KIIIα. PI4KIIIα is responsible for the formation of PI4P populations at the PM. The formation of PI4P PM pools are theorised to be capable of maintaining the cluster of GLUT4 once fused at the PM. We hypothesis that the presence of PI4P at the PM is a corralling regulator for GLUT4 arrival at the PM, this would indicate that the *fgy1-1* mutant allele of Efr3 is a loss of function as loss of corralling effect of PI4P would allow for GLUT4 increased mobility and dispersal. Insulin stimulation results in GLUT4 dispersal across the PM, and therefore our hypothesis is that insulin stimulation inhibits PI4P production at the PM. The aim of this thesis is to investigate a role of the protein EFR3 and the regulation of PI4P levels at the PM during insulin dependent GLUT4 dispersal. We aim to test this hypothesis through a variety of microscopy and biochemical techniques.

This project aims to characterise EFR3 in adipose model cell line 3T3-L1 adipocytes. This aim will aid the understanding of EFR3 in an insulin sensitive system. Characterisation of PI4P in an insulin sensitive model system is carried out as a product of the EFR3 regulated enzyme PI4KIIIα. This thesis aims to understand the effect insulin has on PI4P, and if PI4P has a regulatory role during the dispersal of

GLUT4 at the PM. Finally this thesis aims to demonstrate a regulatory role for EFR3 machinery during insulin stimulated GLUT4 dispersal at the PM in 3T3-L1 adipocytes.

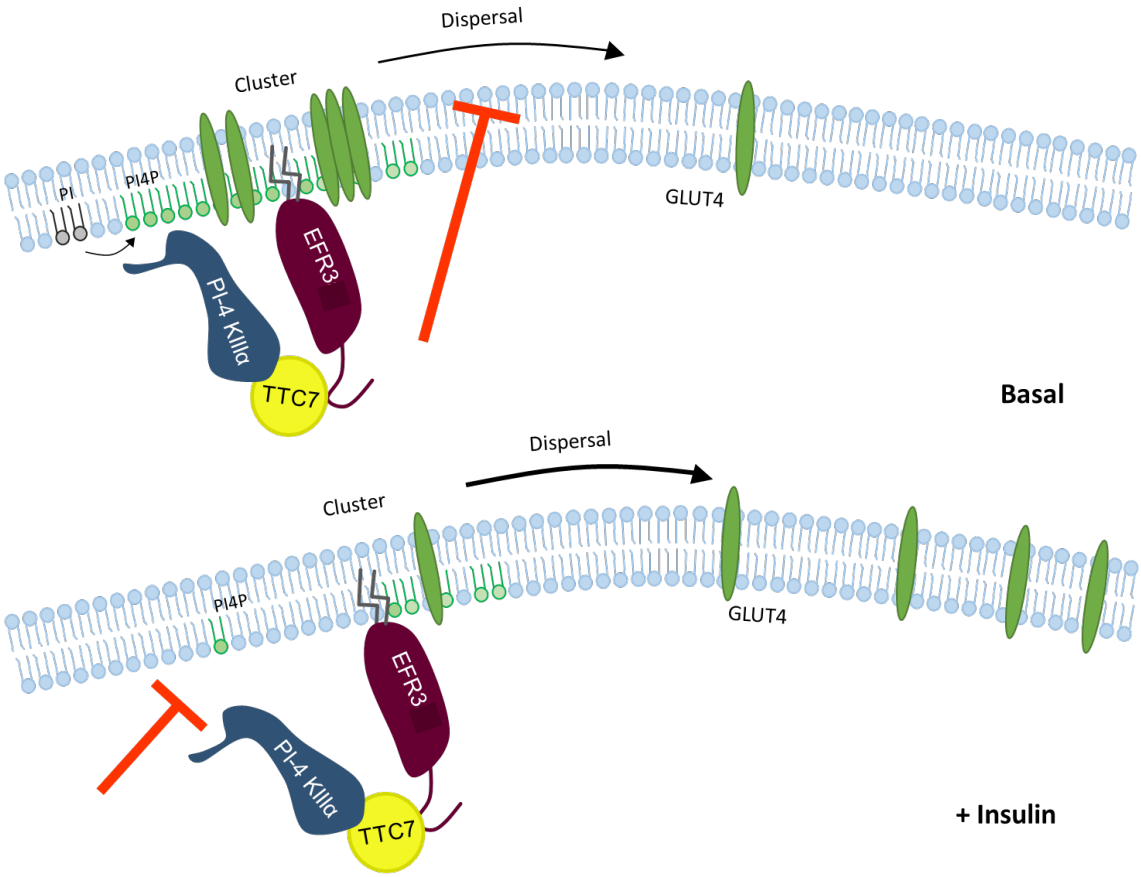

Figure 14: Schematic of proposed molecular mechanism for EFR3 and PI4P during GLUT4 response to insulin at the plasma membrane.

This is a representation of the hypothesis of this investigation. A proposed role for EFR3 and PI4P during the insulin response of GLUT4 at the plasma membrane (PM) is to act in the basal cell when GLUT4 is confined within dynamic clusters at the PM. It is hypothesised that the population of PI4P generated at the PM inner leaflet by PI4KIIIα is responsible for aiding the confinement of GLUT4 clusters upon delivery to the PM via GSVs. Upon insulin stimulation the maintenance of PI4P at the PM is disturbed. Disruption of the PI4P patches results in the dispersal of GLUT4 at the PM. This hypothesis is proposed based on the assumption that the *fgy1-1* mutant allele of Efr3 is a loss of function mutation.

3 MATERIALS AND METHODS

3.1 GENERAL REAGENTS AND ENZYMES

Applied Biosystems
Power SYBR® green PCR master mix (#4367659)
dNTP Mix (#4367381)
10 x RTP buffer (#4368813)
25 mM $MgCl_2$ (#4368813)
RNAase Inhibitor 20 U/µL (#4368813)
Multiscribe 50 U/µL (#4368813)
Random Hexamers 50 µM (TO3166)

BD Biosciences, Oxford UK
Syringes
24 Gauge needles
26 ⅝ Gauge needles

BioRad Labatories Ltd, Hemel Hemstead, Hampshire, UK
Precision Plus Protein™ All Blue Standards (#161-0373)
Gene Pulser®/MicroPulser™ Electroporation Cuvettes, 0.2 cm gap (#1652086)

Clontech, France
TakaRa, Lenti-X™ GoStix™ (#631243)

Fisher Scientific UK Ltd., Loughborough, Leicestershire, UK
2-[4-(2-hydroxyethyl)-1-piperazine] ethanesuphonic acid (HEPES)
3mm filter paper
Ethanol
Glycine
ImmunoMount
L-Glucose
Pierce™ Micro BCA™ Protein Assay Kit
Tris(hydroxymethyl)aminoethane Base (Tris Base)

Formedium Ltd., Hunstanton, Norfolk, UK
Bacterial agar
Yeast extract powder

GE Healthcare BioSciences Ltd, Chalfont, Buckinghamshire, UK
Protein A Sepharose Fast-Flow

Melford Laboratories Ltd., Chelsworth, Ipswich, UK
Dithiothreitol (DTT)

New England Bioscience (UK) Ltd., Hitchin, Hertfordshire, UK
All endonucleases used in this study
1 kb DNA ladder

100 bp DNA ladder
6x DNA loading buffer Chapter 2 56
Shrimp Alkaline Phosphatase (rSAP)
CutSmart® Buffer (10X)

Life Technologies, Paisley, UK
Dulbecco's Modified Eagle Medium (DMEM),
Foetal Bovine Serum (FBS)
Gateway® LR Clonase® II enzyme mix
Lipofectamine® 2000 transfection reagent
Newborn Calf Serum (NCS)
One Shot Chemically Competent TOP10 E. coli
One Shot® Stbl3™ Chemically Competent E. coli
Opti-MEM®
Penicillin-Streptomycin (10,000 U/mL)
SYBR ® Safe DNA Gel Stain
Trypsin-EDTA (0.05%), phenol red

Pall Life Sciences, Portsmouth, UK
Nitrocellulose transfer membrane, 0.2 µM pore size

Promega, Southampton, UK
Wizard® Plus SV Minipreps DNA Purification System

Qiagen Ltd., Crawley, West Sussex, UK
QIAfilter™ Plasmid Maxi Kit
QIAquick Gel Extraction Kit
miRNAeasy Mini Kit

Roche Diagnostic Ltd., Burgess Hill, UK
Agarose MP
Complete™ Protease Inhibitor Cocktail Tablets
Complete™ EDTA-free Protease Inhibitor Cocktail Tablets

Severn Biotech Ltd., Kidderminster, Worcestershire, UK
30 % Acrylamide [Acrylamide: Bis-acrylamide ratio 37.5:1]

Sigma-Aldrich Ltd., Gillingham, Dorset, UK
Ammonium acetate
Ammonium persulphate (APS)
Ampicillin
ß-mercaptoethanol
Bovine serum albumin (BSA)
Brilliant Blue-R
Bromophenol blue
Dimethyl suphoxide (DMSO)
Dexamethasone
Ethylenediaminetetracetic acid (EDTA)
Gelatine from cold water fish skin

Goat serum
L-Glutathione reduced
Glycerol
G418 disulphate salt Chapter 2 57
3-isobutylmethylxanthine (IBMX)
Isopropanol
Kanamycin
Methanol
N'-Tetramethylethylenediamine (TEMED)
Paraformaldehyde
Ponceau S
Porcine insulin
Potassium hydroxide (KOH)
Reduced glutathione
Sodium fluoride (NaF)
Sodium hydrogen carbonate (NaHCO3)
Sodium dihydrogen phosphate (NaH2PO4)
Sodium orthovanadate (Na4VO3)
Sodium dodecyl sulphate (SDS)
Thrombin (Bovine)
Triton-X100
Troglitazone
Tween -20

Spectrum Europe BV., Breda, The Netherlands
Float-a-lyzer, 5 mL 5 kDa MWCO
Float-a-lyzer, 5 mL 20 kDa MWCO

System Biosciences (SBI)
Lentiviral expression plasmid pCDH-CMV-MCS-EF1-puro
Lentivirus packaging kit pPACKH1™

TaKaRa
10-minute Lentiviral Titer Test – Lenti-X™ GoStix™

VWR International Ltd., Lutterworth, Leicestershire, UK
Glacial Acetic Acid
Glass cover slips (3mm diameter)
Disodium hydrogen orthophosphate (Na_2HPO_4)
Potassium Acetate
Potassium Chloride (KCl)
Potassium dihydrogen orthophosphate (KH_2PO_4)
Sodium Chloride (NaCl)
Sodium Hydroxide (NaOH)

3.2 SOLUTIONS

2x LaemmLi Sample Buffer (LSB)	100mM Tris, HCl pH 6.8, 4% (w/v) SDS, 20% (v/v) glycerol, 0.2% (w/v) bromophenol blue, 10% (v/v) β-mercaptoethanol
2YT	1.6% (w/v) tryptone, 1.0% (w/v) yeast extract, 0.5% (w/v) NaCl (20% Agar)
Coomassie	0.05% (w/v) Coomassie brilliant blue R-250, 50% (v/v) methanol, 10% (v/v) acetic acid
Coomassie Destain	15% (v/v) methanol, 15% (v/v) acetic acid
ECL solution 1	100mM Tris-HCl, pH 8.5, 2.25mM luminol in 2% (v/v) DMSO, 0.4 mM ρ-coumaric acid in 1% (v/v) DMSO
ECL solution 2	100mM Tris-HCl, pH 8.5, 0.018% (v/v) H2O2
HEPES/EDTA/Sucrose (HES) buffer	250 mM Sucrose, 20 mM HEPES pH 7.4, 1 mM EDTA
immunoprecipitation (IP) buffer	50 mM HEPES pH 7.5, 5 mM EDTA, 10 mM sodium pyrophosphate, 10 mM NaF, 150 mM NaCl, 2 mM β-Glycerophosphate, 1 mM DTT
Immunofluorescence (IF) buffer	1X PBS, 0.5% (w/v) fish gelatin, 0.1% (v/v) donkey serum
PBS	140mM NaCl 3mM KCl, 1.5mM KH_2HPO_4, 8mM Na_2HPO_4
PBST	140mM NaCl 3mM KCl, 1.5mM KH_2HPO_4, 8mM Na_2HPO_4, 0.1% (v/v) Tween-20
Ponceau S	0.2% (w/v) Ponceau S, 1% (v/v) acetic acid
RIPA Buffer	50mM Tris, HCl pH8, 150mM NaCl, 2mM $MgCl_2$, 1% Triton, 0.5% sodium deoxycholate (w/v), 0.1% (w/v) SDS, 1mM DTT, 50 units/mL Benzonase
SDS-PAGE running buffer	25mM Tris, 190mM glycine, 0.1% (w/v) SDS
SDS-PAGE transfer buffer	25 mM Tris-HCl, 192 mM glycine, 20% (v/v) methanol
SDS-PAGE transfer buffer (semi-dry)	50 mM Tris base, 40 mM glycine, 0.1% (w/v) SDS, 10% (v/v) methanol
SOC	2% tryptone, 0.5% yeast extract, 10 mM NaCl, 2.5 mM KCl, 10 mM MgCl2, 10 mM $MgSO_4$, and 20 mM glucose
TAE buffer	40mM Tris, 1mM EDTA 20 mM Acetic Acid

TBST	20 mM Tris-HCl, pH 7.5, 137 mM NaCl, 0.1% (v/v) Tween-20
TE buffer	1 M Tris pH 8.0, 100 mM EDTA
TST	50mM Tris HCl pH7.6, 150mM NaCl, 0.05% (v/v) Tween-20
Yeast lysate binding buffer	40mM HEPES pH7.4 KOH, 150mM KCl, 1mM DTT, 1 mM EDTA 0.5% Triton X 100

3.2.1 Primary Antibodies

Antigen	Working Dilution	Description	Source
GLUT4	IB: 1:1000	Rabbit, polyclonal	Synaptic Systems (235 003)
HA	IF: 1:3000	Mouse, monoclonal	Covance Research Products (MMS 101P)
HA	FACS: 1:100	Rat monoclonal	Roche applied sciences (11 867 423 001)
GAPDH	IB : 1:10000	Mouse, monoclonal	Applied Biosystems (AM4300)
EFR3A	IB : 1:250	Rabbit, polyclonal	Sigma-Aldrich (HPA023092)
PI4KIIIα	IB : 1:250	Rabbit, polyclonal	Abcam (ab111565)
PDI	IB : 1:5000	Rabbit, polyclonal	Cell Signalling (2446S)
TfR	IB : 1:1000	Mouse, monoclonal	Life Technologies (13 6800)
Sx4	IB : 1:1000	Rabbit, polyclonal	Synaptic Systems (110 042)
B-tubulin	IF : 1:500	Rabbit Polyclonal	Cell Signalling (2146)

3.2.2 Secondary Antibodies

Antigen	Working Dilution	Description	Source
Donkey anti Rabbit 680	IB : 1:10000	Donkey, infrared dye-labelled secondary antibodies against rabbit IgG	LI-COR Biosciences (925 68023)
Goat anti Mouse 680	IF : 1:10000	Goat, infrared dye-labelled secondary antibodies against mouse IgG	LI-COR Biosciences (925 68070)
Goat anti Mouse 800	IF : 1:10000	Goat, infrared dye-labelled secondary antibodies against mouse IgG	LI-COR Biosciences (926 32210)
Anti-Rat AlexaFluor® 647	FACS : 1:300	Goat, infrared dye-labelled against rat IgG	LI-COR Biosciences (A-21247)

3.2.3 Plasmids

Plasmid	Description	Source
GFP-P4M-SidM	CMV promoter, Neomycin/Kanamycin Resistance, expressing	Addgene (51469)
mCherry-P4M-SidM	CMV promoter, Neomycin/Kanamycin Resistance	Addgene (51471)
PH-PLCδ1-GFP	CMV promoter, Neomycin/Kanamycin Resistance	Addgene (51407)
EFR3A-mcherry	CMV promoter, Neomycin/Kanamycin Resistance, expressing EFR3A tagged with mCherry at the C-terminal	Construct provided by Pietro De Camilli
EFR3B-mcherry	CMV promoter, Neomycin/Kanamycin Resistance, expressing EFR3B tagged with mCherry at the C-terminal	Construct provided by Pietro De Camilli
EFR3A(C6-9S)-tdtomato	CMV promoter, Neomycin/Kanamycin Resistance, expressing EFR3A tagged with tdtomato at the C-terminal with mutation of palmitoylation sites C6-9 to S6-9 (C6-9S).	Construct provided by Pietro De Camilli

LYN11-FRB-CFP	CMV promoter, Neomycin/Kanamycin Resistance, expressing the PM anchor LYN11 linked with FKBP rapamycin binding (FRB) protein tagged with CFP	Addgene (38003)
mRFP-FKBP-Pseudojanin	CMV promoter, Neomycin/Kanamycin Resistance,	Addgene (37999)
mRFP-FKBP-PJ-Sac	CMV promoter, Neomycin/Kanamycin Resistance,	Addgene (38000)
mRFP-FKBP-PJ-INPPE5	CMV promoter, Neomycin/Kanamycin Resistance,	Addgene (38001)
mRFP-FKBP-PJ-Dead	CMV promoter, Neomycin/Kanamycin Resistance,	Addgene (38002)

3.3 MOLECULAR METHODS

3.3.1 Transformation of plasmid into bacterial cells

Competent XL1-blue bacterial cells were thawed on ice. 1 µL of plasmid DNA was added to 20 µL of bacteria cells, this was incubated on ice for 1 hour. Heat shock was used to insert the plasmid DNA into the bacteria cells, 42°C for 45 seconds. Cells returned to ice for 5 minutes before 300µL pre-warmed SOC media was added to the cells. Cells were incubated for 1 hour at 37°C on a shaking platform. Onto pre-warmed 2YT bacto-agar plates containing the corresponding selection antibiotic (in most cases it was 50 µg/mL Kanamycin or 100 µg/mL ampicillin) 50µL of the bacteria was streaked and incubated at 37°C overnight.

3.3.2 Plasmid DNA purification

50 mL 2YT culture containing the correlating selection antibiotic was inoculated using a single colony from the transformation. This was grown for 8 hours at 37°C in a shaking incubator and then transferred into 800 mL of 2YT culture overnight. Plasmid DNA was isolated using the Qiagen QIAfilter™ Plasmid Maxi Kit. Plasmid DNA concentration was measured using ThermoFischer Scientific NanoDrop 1000. The plasmid DNA was digested with restriction endonucleases were required and analysed using agarose gel electrophoresis.

3.3.3 Agarose Gel Electrophoresis

1% agarose (w/v) gels were made up in TAE buffer (40mM Tris, 1mM EDTA). The DNA stain used was SYBR safe DNA gel stain (1 in 10,000 dilutions in TAE). Gels were run at 70V in TAE buffer. Samples prepared as stated below in 3.3.4 and was mixed with 6x DNA loading buffer. The gel was run using 5µL of New England BioLabs Quick-Load 1Kb DNA ladder. When required DNA fragments were extracted from agarose gels using the QIAquick extraction kit (Qiagen) according to the manufacturer's instructions.

3.3.4 DNA Plasmid Digestion using Endonucleases

DNA plasmid was incubated with the corresponding endonuclease in the buffer most suitable according to the manufacturers' recommendations between 2 and 6 hours at 37°C in a final volume of 20µL. 1 unit of enzyme was used per µg of DNA, and 1µg

of DNA was digested per digestion. When plasmid DNA required digestion at two or more sites using two or more different restriction endonucleases the buffer chosen for digestion was compatible with the least stable restriction enzyme.

3.3.5 DNA Plasmid Ligation

DNA plasmid containing the desired vector was digested using endonucleases as described above (3.3.4) using the corresponding restriction sites in the target plasmid multi cloning site. The vector was extracted using agarose gel electrophoresis as described above (3.3.3). The 5' position linearized target plasmid was dephosphorylated to inhibit self-ligation of the target plasmid using Shrimp Alkaline Phosphatase (rSAP). 1 µg of plasmid DNA was dephosphorylated using 2 µL CutSmart® Buffer (10X) and 0.5 µL rSAP made up to 20 µL with nuclease-free water. This was incubated at 37°C for 30 minutes, and then 5 minutes at 65°C to stop the reaction. For the ligation 1 µL T4 DNA ligase was used with 2 µL T4 DNA ligase buffer (10X), 50 ηg vector DNA, 37 ηg insert DNA, which was made up to 20 µL using nuclease-free water. This was gently mixed then incubated for 1 hour at room temperature and heat inactivated at 65°C for 10 minutes. The mixture was transformed into XL-1 blue cells as described above (3.3.1).

3.4 Cell Culture Methods

3.4.1 Growth and maintenance of 3T3-L1 Adipocytes

3T3-L1 murine adipocytes were originally purchased from ATCC (USA), cells expressing HA-GLUT4-GFP had previously been generated in the lab. To culture cells DMEM (Dulbecco's Modified Eagle's Medium) supplemented with 10% (v/v) Newborn Calf Serum (NCS) was used. Cells were incubated in a 10% CO_2 humid atmosphere incubator at 37°C. Cells were fed every second day until cells were ready for adipocyte differentiation or for passage.

3.4.2 3T3-L1 adipocyte passage

Cells were passaged at 70% confluence, cells were not used past passage 13. The media was aspirated, and the cells were washed with 5mL pre-warmed sterile D-PBS and 1 mL 0.05% trypsin was added. Cells were incubated for 2-5 minutes at 37°C till cells had detached from the flask. DMEM NCS was added to stop the trypsin reaction

and the cell suspension was split, no more than 1 in 12 from the original flask. To each T75 flask 15 mL of DMEM NCS cell suspension was added, 10 mL to each 10cm plate, 1 mL to each well of a 12 well plate, 500 µL to each well of a 24 well plate, and 100 µL to each well of a 96 well plate.

3.4.2.1 Seeding cells onto glass coverslips

Coverslips were sterilised by dipping into 100% ethanol and placed onto the edge of the well to dry in the cell culture hood ventilation for 15 minutes. The coverslips were knocked into the wells and left under UV light for a minimum of 45 minutes. Before use wells were washed with D-PBS to remove residual ethanol. If coating with collagen wells were filled with 1 mL 0.1% (v/v) rat tail collagen type IV and incubated for 10 minutes. The collagen was removed, and the wells allowed to dry. Wells were washed with D-PBS 3 times to lower the acidity. Cells added as described in the passage methods.

3.4.2.2 Fixing cells on glass coverslips

Cells serum starved for 2 hours pre-fixing and were washed 3 times using PBS. Coverslips were fixed using 4% paraformaldehyde solution for 90 minutes at room temperature. Coverslips were quenched using 25mM glycine for 5 minutes and washed using PBS.

3.4.3 3T3-L1 adipocyte differentiation

Cells were differentiated 2 days post confluence and followed an 8-day protocol. Day 0 differentiation media was made up using DMEM supplemented with 10% (v/v) Foetal Calf Serum (FCS), 1 µM insulin, 1 ηM troglitazone, 0.5 mM 3-isobutyl-1-methylxanthine (IBMX), and 0.25 µM dexamethasone. 3 days post the start of differentiation media was changed for Day 3 differentiation media. Day 3 differentiation media was DMEM supplemented with 10% (v/v) FCS, 1 µM insulin, and 1 ηM troglitazone. 6 days post the start of the differentiation the media was changed for day 6, DMEM supplemented with 10% (v/v) FCS. Cells were fully differentiated and ready for use by day 8 of the process. Cells to be used by day 12 of differentiation and media to be changed every second day after day 6 with DMEM supplemented with 10% (v/v) FCS.

3.4.4 3T3-L1 fibroblast cryo-preservation

Cells were preserved in liquid nitrogen. Cells were prepared when at 70% confluence using the passage method, after cells have detached 5 mL of DMEM supplemented with 10% (v/v) NCS was added and cells were pelleted using centrifugation at 500 x g for 5 minutes. The cell pellet was re-suspended in 1 mL, per flask, freeze down media, FCS supplemented with 10% (v/v) dimethyl sulfoxide (DMSO). Cells were transferred into 1.8 mL cryo-vials. Cells were stored overnight in Nalgene "Mr. Frosty" containing isopropanol at -80^{o}C. Cells were transferred to liquid nitrogen for long term storage.

3.4.4.1 Resurrection of cells

Cells were removed from liquid nitrogen and thawed at 37^{o}C before adding to 15mL of pre-warmed growth media in a T75 flask. 12 hours later growth media was replaced to remove DMSO.

3.4.5 Growth of HeLa cells

The human cervical carcinoma HeLa cells were purchased from ATCC (USA), cells expressing HA-GLUT4-GFP were previously generated by the group. Cells were cultured in DMEM, 10% (v/v) FCS, 1% (v/v) Glutamine. The media was changed every second day until cells were ready for passage or use. Cells were incubated at 5% CO_2 at 37^{o}C in a humid atmosphere incubator.

3.4.6 HeLa cell passage

At 70% confluence cells were passaged, the media was aspirated, and the cells were washed in pre-warmed D-PBS. 1 mL 0.05% (w/v) trypsin was added and cells were incubated at 37^{o}C for 2-5 minutes till cells had detached from the flask. DMEM growth media was added to stop the trypsin reaction and cells were split no more than 1 in 6. Volumes were as described in section 3.4.2. Cells added to coverslips which were prepared as described in 3.4.2.1.

3.5 PREPARATION OF MICROSCOPY SAMPLES

3.5.1 Transfection of Hela cells

Hela cells were cultured on glass cover slips, prepared as described in section 3.4.2.1 till 70% confluence was reached when they were transfected with Lipofectamine 2000 (LF2K). A ratio of 0.75 µg DNA to 1.5 µL LF2K per well in a 12 well plate was used and incubated for 5 hours in Opti-MEM®. 48 hours post transfection cover slips where fixed using paraformaldehyde as stated in 3.4.2.2.

3.5.2 Immunofluorescence staining of HA epitope tag for confocal microscopy imaging

Cells prepared according to type onto coverslip glass (HeLa) or µ-slide IBIDI 8 well (3T3-L1 adipocytes). Cells fixed using paraformaldehyde as described in 3.4.2.2 and was blocked for 30 minutes at room temperature using immunofluorescence (IF) buffer (1X PBS, 0.5% (w/v) fish gelatin, 0.1% (v/v) donkey serum). Cells were not permeabilised for this technique to distinguish between extracellular and intracellular HA. Primary mouse anti HA antibody was applied to the cells for 1 hour at room temperature at a 1 in 3000 concentrations in IF buffer. Cells were carefully washed using IF buffer 3 times and was placed on the platform shaker at low setting for 5 minutes between washes. Secondary donkey anti-mouse AlexaFluor® 647ηm antibody was applied to the cells for 45 minutes at room temperature at a 1 in 5000 concentrations in IF buffer. Cells were carefully washed 3 times using IF buffer. Coverslips were mounted onto slides using ImmunoMount and IBIDI wells were filled with 1 x PBS and stored at 4ºC. Confocal images were gathered on a

3.5.3 Preparation of HA-GLUT4-GFP HeLa cells for FACS analysis

HeLa cells (~150000 cells/well) were seeded into a 6 well plate 48 hours pre-analysis. When required cells were transfected as per the LF2K transfection described in 3.5.1 24 hours prior to analysis. Prior to analysis cells were serum starved for two hours, half of the samples were stimulated with 1 µM insulin for 20 minutes at 37°C. The plates were then placed on ice and all subsequent steps were performed on ice and use ice cold solutions.

In the well cells were washed three times with PBS, cells were fixed with 1% (w/v) electron microscopy grade, methanol free PFA for 20 minutes. Cells were washed two times in PBS and blocked with 2 % BSA (w/v) in PBS for 45 minutes on ice. Surface GLUT4 was stained for using the HA-epitope tag. Primary anti-HA antibody was incubated with cells for 45 minutes and used at 1 in 200 concentrations in PBS supplemented with 2 % (w/v) BSA. Cells were washed three times in PBS. Secondary antibody conjugated with AlexaFluor® 647 (ThermoFischer) was incubated for 45 minutes at a 1 in 300 concentrations in 2 % (w/v) BSA in PBS. Cells were washed 3 times in 2 % (w/v) BSA in PBS.

The cells were gently dissociated from the tissue culture dish using a cell lifter. Dissociated cells were collected and centrifuged at 600 g for 8 minutes at 4°C. The resulting pellet of cells was suspended in 350 µL of 2 % (w/v) BSA in PBS. Samples were analysed on a BD LSRFortessa X20. Data was collected and analysed using Summit Software v4.3.

3.6 Production of Cell Lysates

3.6.1 Production of Protein Lysates

Cells were serum starved using serum free DMEM for 2 hours at 37ºC. Cells were washed 3 times in PBS and scraped in RIPA buffer (50 mM Tris pH 8, 150mM BaCl, 2mM $MgCL_2$,1% Triton (v/v), 0.5% sodium deoxycholate (w/v), 0.1% (w/v) SDS, 1mM DTT, 50 units/mL Benzonase) containing EDTA free protease inhibitor (Roche), 200µL per 10 cm plate. Samples were homogenised using a 26-gauge needle 8 times. Samples were rested on ice for 10 minutes and insoluble material was pelleted from the homogenate using 12470 x g centrifugation at 4ºC. Lysates were stored at -80ºC till required.

3.6.2 mRNA extraction

Cells were serum starved using serum free DMEM for 2 hours at 37ºC. Cells were scraped in Qiagen buffer RLT to produce a lysate. mRNA was extracted using Qiagen miRNAeasy mini kit as per the instructions. mRNA concentration was measured using ThermoFischer Scientific NanoDrop 1000.

3.7 CELL LYSATE TECHNIQUES

3.7.1 Differential Centrifugation

Twelve 10cm plates of fully differentiated 3T3-L1 adipocytes between day 8 and 10 were serum starved using serum free DMEM for 2 hours, 6 of the plates were stimulated with 1 μM porcine insulin for 30 minutes. Plates were washed using sterile HES buffer, scraped and homogenised using a dounce homogeniser. The lysate was centrifuged at 10,000 x g at 4ºC for 20 minutes, resulting in a pellet of the plasma membrane, mitochondria and nuclei. This pellet was re-suspended in HES buffer and carefully layered onto high sucrose (1.12M sucrose in HES) cushion and centrifuged in a swing out rota at 41,000 x g at 4oC for 60 minutes. The pellet, mitochondria & nucleus fraction, was re-suspended in 100 μL 1 x Laemelli sample buffer (LSB) and the interphase was collected, as the plasma membrane, re-suspended in 4 mL HES buffer and centrifuged at 140, 000 x g at 4oC for 60 minutes. The pellet was re-suspended in 100 μL 1 x LSB. Simultaneously the supernatant from the original lysate spin, which contains the low-density membrane (LDM); high density membrane (HDM); and soluble protein fraction, was centrifuged at 12, 500 x g at 4oC for 20 minutes to pellet the HDM, which was re-suspended in 100 μL 1 x LSB. The supernatant from this was centrifuged at 140, 000 x g at 4oC for 60 minutes and the pellet, containing the LDM, was re-suspended in 100 μL 1 x LSB. TCA precipitation was used to recover the soluble protein fraction from the supernatant, this was re-suspended in 100 μL 1 x LSB.

3.7.2 Western Blotting

SDA-polyacrylamide gel electrophoresis was used to resolve the protein samples. Protein samples were boiled prior to loading at 95ºC for 5 minutes or 65ºC for 10 minutes when probing for GLUT4. BioRad Precision Plus Protein Standards All Blue Markers was used as molecular weight ladder. Following transfer to nitrocellulose, the membranes were stained using Ponceau solution prior to immuno-labelling. Nitrocellulose was blocked for 30 minutes using 3% BSA in PBS-T solution. Blot was incubated O/N at 4ºC or 1 hour at room temperature with primary antibody in 3% BSA PBS-T solution. Primary antibody was washed for 10 minutes in PBS-T 3 times. Blot was incubated with Alexa Flour® conjugated secondary antibody for 1 hour at

room temperature. Unspecific binding was washed using PBS-T for 10 minutes 3 times. The western blot was visualised using LICOR.

3.7.3 Immunoprecipitation of 3T3-L1 adipocytes

3T3-L1 adipocytes were used on day 10 of the differentiation protocol. 10 cm dishes of 3T3-L1 adipocytes were serum starved for 2 hours. For the last 20 min, 1 µM insulin was added to the medium of half the dishes. Cells washed in ice-cold PBS 3 times and then cells were scraped in IP buffer supplemented with 1% or 0.5% Triton-X. Samples were lysed using a 26G needle and transferred into a clean tube to be incubated on ice for 30 minutes. Lysates were centrifuged at 500 x g for 20 minutes at 4˚C. The supernatant was transferred to a clean tube. To determine the whole lysate protein concentrations of the sample a Bradford assay was performed. Total protein of 1 mg per sample was used per group. To each sample of protein antibody/serum was added; EFR3A (2 µg), PI4KIIIα (5µg) or random rabbit IgG (5µg). Samples were rotated for 2 hours at 4˚C, and then centrifuged at 500 x g for 1 minute at 4˚C. The pellet was washed 3 times in IP buffer supplemented with 1% or 0,5% Triton-X and then washed 1x with IP buffer supplemented with 10 times reduced Triton-X, 0,1% or 0,05% respectively. Samples were centrifuged at 500 x g for 1 minute at 4˚C. This pellet was mixed with directly with 2x LSB and boiled at 95˚C for 5 minutes. Samples were stored at -20˚C until subjected to immunoblotting.

3.8 SEMI-QUANTITATIVE REVERSE TRANSCRIPTASE PCR (RTPCR)

3.8.1 cDNA preparation

cDNA was prepared from mRNA using Applied Biosystems reagents for RT-PCR. mRNA concentration required was 200 ηg/µL to be prepared in a 96 well PCR plate on ice, each reaction was 20 µL. To the reaction 2 µL 10X buffer, 4.4 µL 25 mM $MgCl_2$, 4 µL 10 mM dNTPs, 1 µL 50 µM random hexamers, 0.4 µL 20 U/µL RNAase inhibitors, 0.5 µL 50 U/µL multiscribe, 1 µg mRNA sample, and 5.7 µL nuclease free water. PCR plate was sealed, and PCR run under cycle conditions; 25ºC for 10 minutes, 48ºC for 30 minutes, 95ºC for 5 minutes, and 4ºC to end the reaction.

3.8.2 Quantitative PCR using SYBR® green

Synthesised cDNA prepared as shown above (3.7.1) was used. A master mix containing; 6.25 µL Applied Biosystems Power SYBR® green PCR master mix, 0.05 µL 100 µM forward primer, 0.05 µL 100 µM reverse primer, and 3.25 µL RNAase free water; was prepared per well of PCR reaction. To the master mix 2.5 µL of RT cDNA was added to the well. Plates were loaded onto Taqman and thermal cycling parameters were set to; 48ºC for 30 minutes, 95ºC for 10 minutes, 40 cycles of denature 95ºC for 15 seconds, and anneal/extend 60ºC for 1 minute.

3.9 ANTI-PEPTIDE RABBIT SERUM PURIFICATION

3.9.1 Column purification

ThermoFischer® scientific protein purification column was used. The EFR3A peptide was added to the column according the protocol of the manufacturer to bind covalently with the matrix in the column. This was stored ON at 4˚C using the degassed buffer from the Kit. The next day, the column was washed with 10 mL 1x PBS, and the degassed buffer flows out of the column. Meanwhile 0.2 mL of 10X PBS was added to 1.8 mL of the thawed rabbit serum. The serum was added to the column and incubated for 15 minutes at room temperature. The serum was collected after incubation and added to the column for a second 15-minute incubation. The matrix was washed thoroughly with 2 mL of 1x PBS 5 times. To release the bound proteins from the column matrix, 4.5 mL glycine (2M; pH 2.0) was added to the column and 8 aliquots of 0.5 mL of the flow-out containing the EFR3A anti-peptide antibodies were collected. To determine protein concentration the OD-values were measured using the spectrometer.

3.9.2 Sepharose-A bead purification

100 µL Sepharose-protein A beads were added to 1 mL of serum and 100 µL 10x PBS. Serum with beads was rotated for 2 hours at 4˚C after which the beads were spun down for about 15 seconds in the microfuge. Supernatant was removed, and the remaining beads were washed 3x with 1x PBS. 1 mL of 2M glycine was added to the beads and incubated for 10 minutes at RT. The samples were spun briefly, and the supernatant was collected, this was repeated twice. The OD-values of the 3 fractions were measured using the spectrometer.

3.9.3 Purified Antibody Concentration

Using spectrometer absorption spectra of 280λ, the density of antibodies in the aliquots was calculated. The aliquots with the highest values were pooled together. This pooled sample was purified using a Slide-A-Lyzer™ 3.5K MWCO dialysis cassette (ThermoFischer), which was done O/N at 4°C. After dialysis, the purified EFR3A-antibody was collected, aliquoted in 50 µL aliquots and stored at -80°C.

3.10 TRANSFECTION OF 3T3-L1 ADIPOCYTES

3.10.1 Electroporation of 3T3-L1 adipocytes with plasmid DNA

Cells used at day 4 of differentiation, cells were washed 3 times in 10 mL D-PBS (no Ca and no Mg). To detach the pre-adipocytes 3mL of equal 0.05% trypsin: 2mg/ml collagenase was added and incubated for 5 minutes at 37ºC. Once detached add 10mL complete media to the plate and transfer to a 50mL conical centrifuge tube. Cells were pelleted using 500 x g for 2 minutes and re-suspended in 30mL D-PBS, this was repeated twice more. Cells were re-suspended in 0.5mL D-PBS per 10 cm plate used. 0.4mL of re-suspended cells was added to a 0.2cm BIO-RAD Gene Pulser® electroporation cuvette and 75µg plasmid DNA. Using the BIO-RAD GENE PULSER® II set at 0.18kV and 975µF and pulse. Add 1mL complete media to the cuvette and stand for 1 minute before removing the fat from lysed cells before adding the cells to 6mL pre-warmed complete media and rest for 10 minutes. Only remove the top 6mL of media and add 300µL per well of collagen coated glass bottom ibidi® µ-Slide 8 well. Use cells for visualisation 72 hours post electroporation.

3.10.2 Electroporation of 3T3-L1 adipocytes with siRNA

Cells used at day 6 of differentiation, cells were washed 3 times in 10 mL D-PBS (no Ca and no Mg). To detach the pre-adipocytes 3mL of equal 0.05% trypsin: 2mg/ml collagenase was added and incubated for 5 minutes at 37ºC. Once detached add 10mL complete media to the plate and transfer to a 50mL conical centrifuge tube. Cells were pelleted using 500 x g for 2 minutes and re-suspended in 30mL D-PBS, this was repeated twice more. Cells were re-suspended in 0.5mL D-PBS per 10 cm plate used. 0.65mL of re-suspended cells was added to a 0.2cm BIO-RAD Gene Pulser® electroporation cuvette and 3ηmol Silencer® select pre-designed siRNA. Using the BIO-RAD GENE PULSER® II set at 0.25kV and 950µF and pulse. Add 1mL complete

media to the cuvette and stand for 1 minute before removing the fat from lysed cells before adding the cells from 3 electroporation's to 12mL pre-warmed complete media and rest for 10 minutes. Only remove the top 12mL of media and add 500µL per well of 24 well falcon plate. Use cells for glucose uptake assay 72 hours post electroporation.

3.11 GENERATION OF A STABLE CELL LINE IN 3T3-L1 ADIPOCYTES

Fibroblast 3T3-L1 adipocytes were transfected when at 70% confluence using LF2K as described above in 3.4.7 with plasmids containing the neomycin resistance gene. 24 hours post transfection split cells 1:10 into growth medium before selection medium (containing 0.75mg/ml G418) was applied daily. When single colonies appear after applying selection media the cells were split to 1 cell/100µl and added to a 96 well plate in selection media. Wells which were positive for single colonies were expanded and expression of protein was confirmed by visualisation.

4 CHARACTERISATION OF EFR3 IN 3T3-L1 ADIPOCYTES

4.1 INTRODUCTION

Much of our understanding of EFR3 comes from studies of the yeast orthologues and from studies of adherent fibroblast cell types (Wu *et al.*, 2014; Bojjireddy *et al.*, 2015). EFR3 has been shown to be membrane associated, not transmembrane, in both yeast and mammalian cells. In both yeast and mammals EFR3 was shown to be localised to the plasma membrane (Baird *et al.*, 2008; Wu *et al.*, 2014). The N-terminus was required for membrane association in yeast and mammals. In yeast the presence of a conserved basic patch at the N-terminus (K12A, R46D, K49A, K52A, H67E, and R69A) has been determined to be essential for membrane association and PM localisation (Wu *et al.*, 2014). In mammalian cells EFR3 localisation was dependent on N-terminus palmitoylation (C6/C7/C8/C9 for EFR3A and C5/C7/C8 for EFR3B), and residues 1-37 are sufficient to direct GFP to the PM (Bojjireddy *et al.*, 2015).

In mammalian cell lines two homologs of EFR3 have been identified, EFR3A and EFR3B which have 64% sequence identity (Bojjireddy *et al.*, 2015). Previous studies have shown that EFR3 a and b are ubiquitously expressed in mouse tissue, with notably high expression of EFR3A in the testis and EFR3B in the brain (Bojjireddy *et al.*, 2015). In skeletal muscle and heart samples expression of EFR3A and EFR3B are similar. The expression levels in skeletal muscle show that EFR3A was slightly less expressed than EFR3B and vice versa in the heart sample. Skeletal and cardiac muscle are examples of insulin responsive tissue containing GLUT4. This information confirms a presence of EFR3A and EFR3B in insulin responsive tissues. There was no data for the expression levels of EFR3A and EFR3B in adipose tissue.

The effect insulin signalling has on GLUT4 trafficking can be experimentally demonstrated using subcellular fractionation. This technique allows for the trafficking of proteins from vesicles to the PM in response to insulin to be observed of the endogenous protein in adipocyte cell lines. The trafficking of proteins with GLUT4 in response to insulin signalling may indicate a regulatory role within vesicle trafficking. Plasma membrane localisation indicates a role within cell surface dynamics. The location of endogenous EFR3 and PI4KIIIα will be analysed using this technique.

HeLa cells are used in this study as a model system, as a cell line expressing HA-GLUT4-GFP will be used to measure the effect of EFR3 on GLUT4 at the PM. The HA epitope tag is extracellularly exposed when GLUT4 is fused at the PM, allowing assay of the levels of GLUT4 on the surface in the presence and absence of insulin (Lizunov *et al.*, 2012; Sadler *et al.*, 2013; Kioumourtzoglou *et al.*, 2015). The GFP tag was cytosolic and therefore acts as a measure of total GLUT4 in the cell. HeLa cells do no express endogenous GLUT4 but do exhibit insulin-stimulated GLUT4 delivery to the plasma membrane, and thus are a useful cell line for mechanistic studies of this process ((Kioumourtzoglou *et al.*, 2015)). Therefore, characterisation of EFR3 in HeLa cells was carried out concurrent with studies in 3T3-L1 adipocytes.

4.2 AIMS

This chapter aims to characterise EFR3 in 3T3-L1 adipocytes and the model cell line HeLa expressing HA-GLUT4-GFP. Semi-quantitative reverse transcriptase PCR will be employed to measure EFR3 homolog distribution in cells used in this investigation. Subcellular fractionation and fluorescently labelled EFR3 cell imaging will be used to determine membrane localisation. This chapter aims to characterise the protein levels of EFR3 and PI4KIIIα in samples from mice models of insulin resistance.

4.3 EFR3 HOMOLOG DISTRIBUTION

Semi quantitative reverse transcriptase polymerase chain reaction (rtPCR) was used to determine the relative levels of EFR3 mRNA homologs A and B in cell lines in HeLa cells, 3T3-L1 fibroblasts and adipocytes, shown in Figure 15. The primer sequences used correspond to an intron region of EFR3A, EFR3B and GAPDH. Primers where validated using PCR of DNA, all primers resulted in appropriate PCR product. GAPDH was used as a housekeeper gene to facilitate the relative quantification of EFR3A and EFR3B mRNA expression levels. The cycle threshold (Ct) values and the relative quantification to GAPDH values indicate that EFR3B was virtually undetectable in all cell types investigated. In 3T3-L1 adipocytes EFR3A was found at 0.7 relative to the Ct level of GAPDH. In 3T3-L1 fibroblasts EFR3A was found at 1.7 relative to the level of GAPDH.

These results, shown in graph form in Figure 15, indicate that EFR3A was a relatively abundant transcript product. The high transcript levels infer an abundant protein in the cell. This information informed our focus on EFR3A in future investigations of the role of EFR3A during GLUT4 dispersal at the PM in 3T3-L1 adipocytes.

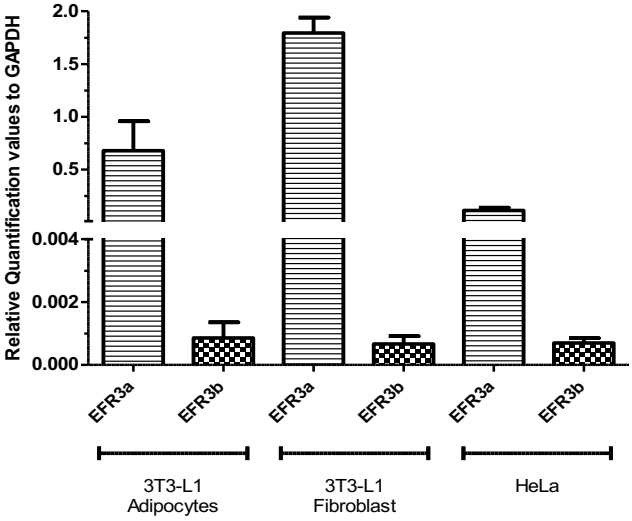

Figure 15: Semi-quantitative reverse transcriptase PCR relative quantification to GAPDH results

HeLa and 3T3-L1 fibroblast (pre-differentiation) and adipocyte (day 8 post differentiation) mRNA was extracted and gene expression in each cell type assessed using EFR3 homolog A and B probes with GAPDH utilised for normalisation. n=3. Primer sequences are shown in the supplemental data.

4.4 SUBCELLULAR FRACTIONATION

Differential centrifugation of 3T3-L1 adipocyte lysates was used to track the membrane localisation of EFR3A and PI4KIIIα. The results are shown in relation to GLUT4 and in response to insulin stimulation. Cell lysates were separated into plasma membrane (PM), high density membrane (HDM), low density membrane (LDM), and the soluble protein fraction using differential centrifugation as described (Claude, 1946; Hepp *et al.*, 2005). The fractions were immunoblotted for GLUT4, PI4KIIIα, EFR3A and various endosomal membrane markers and a typical set of data was presented in Figure 16. The results confirm that GLUT4 was enriched in the LDM fraction in the absence of insulin stimulation. Twenty-minute insulin stimulation results in GLUT4 being enriched at the PM fraction and the levels at the LDM are diminished in comparison to non-stimulated samples. This was indicative of the translocation of LDM vesicles to the PM in response to stimulation. EFR3A and PI4KIIIα WERE predominantly localised to the PM in the absence of insulin stimulation, Figure 16. With regards to PI4KIIIα and EFR3A the results from subcellular localisation show

that insulin stimulation does not result in substantial differences in localisation of either proteins; EFR3A or PI4KIIIα. Both proteins remain enriched at the PM in both insulin and non-insulin stimulated cells. The subcellular fraction markers used were; syntaxin 4 (Sx4) as a PM marker; protein disulphide-isomerase (PDI) as a HDM marker; Transferrin receptor as a LDM marker; and GAPDH as a soluble fraction marker. All markers showed equal distribution between insulin and non-insulin stimulated samples allowing for confidence that PI4KIIIα and EFR3A localisation does not change in response to insulin stimulation.

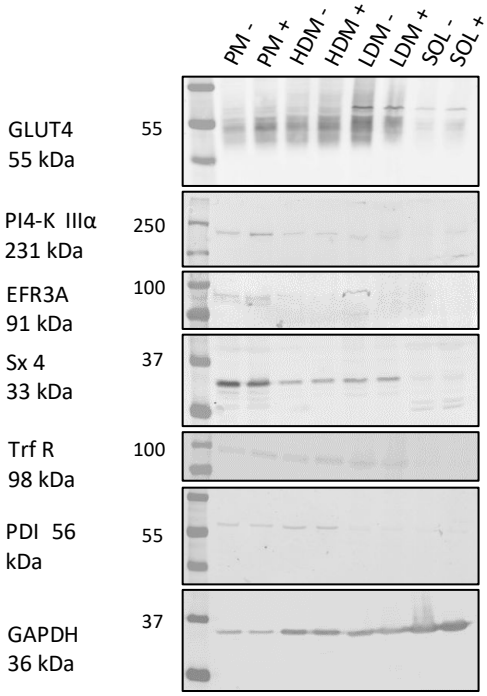

Figure 16: Representative immunoblot of subcellular localisation of EFR3A and PI4KIIIα in 3T3-L1 adipocytes.

Immunoblot of subcellular fractionation of 3T3-L1 adipocyte lysate. Fraction controls, which remain unaltered in the presence of insulin stimulation, include; Syntaxin (Sx) that was enriched in the PM fraction, transferrin receptor (Trf R) is enriched in the LDM, protein disulphide-isomerase (PDI) was enriched in the HDM fraction, and glyceraldehyde-3-phosphate dehydrogenase (GAPDH) is enriched in the soluble fraction. Western blot lanes denoted with – or + for insulin stimulation. Fractions; plasma membrane (PM), high density membrane (HDM), low density membrane (LDM), soluble (SOL). Insulin stimulation was carried out for 20 minutes with 0.1 μM insulin.

4.5 CONFOCAL MICROSCOPY VISUALISATION OF EFR3

4.5.1 HeLa cell visualisation

Fluorescently labelled EFR3 (A and B) tagged with mCherry at the C terminal was expressed in HeLa cells using plasmid DNA transfection. EFR3(A/B)-mCherry was under CMV promoter control, resulting in the over expression of the protein in transfected cells. The confocal images of EFR3A-mCherry and EFR3B-mCherry are shown in Figure 17. The images of EFR3 (A and B), shown in the indicated panel of Figure 17, exhibit PM localisation which does not vary between homolog A and B. Some cells exhibit an intracellular localisation of EFR3 (A and B), denoted with blue arrows, near the nucleus of the cell. Results from adipocyte whole cell lysates shown in Figure 17 show no corresponding high-density membrane localisation in the immunoblots. This intracellular localisation was therefore believed to be a product of over expression of EFR3 using plasmid transfection under CMV promoter control. The intracellular localisation was discounted and was attributed as artefact of over expression. At the PM EFR3A and EFR3B show similar localisation, denoted with white arrows in Figure 17 and 18. This localisation pattern at the PM was expected to be a result of PM furrowing in HeLa's and not a patch localisation feature of EFR3 at the PM.

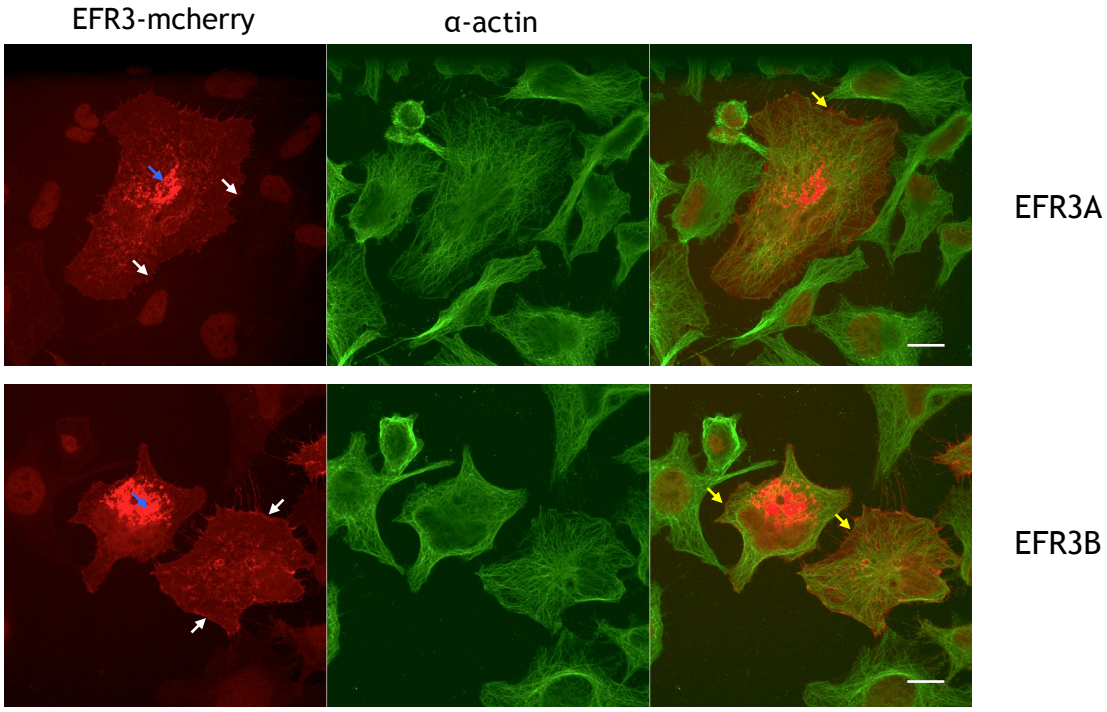

Figure 17: Confocal images of HeLa cells expressing EFR3.

HeLa cells transfected with EFR3A and EFR3B plasmids respectively imaged using confocal microscopy. Intracellular concentration (blue arrows). EFR3 localise in puncta at the PM (white arrows), α-actin fluorescent immune-staining, and antibody concentration in methods Scale bar 20 μm. Images have been brightened for printing purposes.

4.5.2 Visualisation of the effect of insulin stimulation on EFR3A at the plasma membrane

The results of subcellular fractionation above in Figure 16 showed that in 3T3-L1 whole lysates that there was no insulin-dependent change in subcellular distribution of EFR3 or PI4KII. Previous images in Figure 17 showed EFR3A was localised to the PM in HeLa cells. Transfection confirms a membrane-associated proteins with characteristic morphology. Insulin stimulation of HeLa cells which express mammalian GLUT4 results in translocation of GLUT4 to the PM (Sadler et al., 2013). We therefore examined whether insulin stimulation altered the distribution of EFR3A-mCherry at the plasma membrane, depicted in Figure 18. The data indicated that insulin stimulation did not result in any visual morphological changes of EFR3A at the PM, shown in Figure 18. This indicated that any affect EFR3A has on GLUT4 during insulin stimulation was not a result of a translocation event and supports the

hypothesis that EFR3A acts at the PM. This indicates that any effect insulin stimulation has on EFR3A is at the protein level, potentially via the binding or activity of PI4KIIIα.

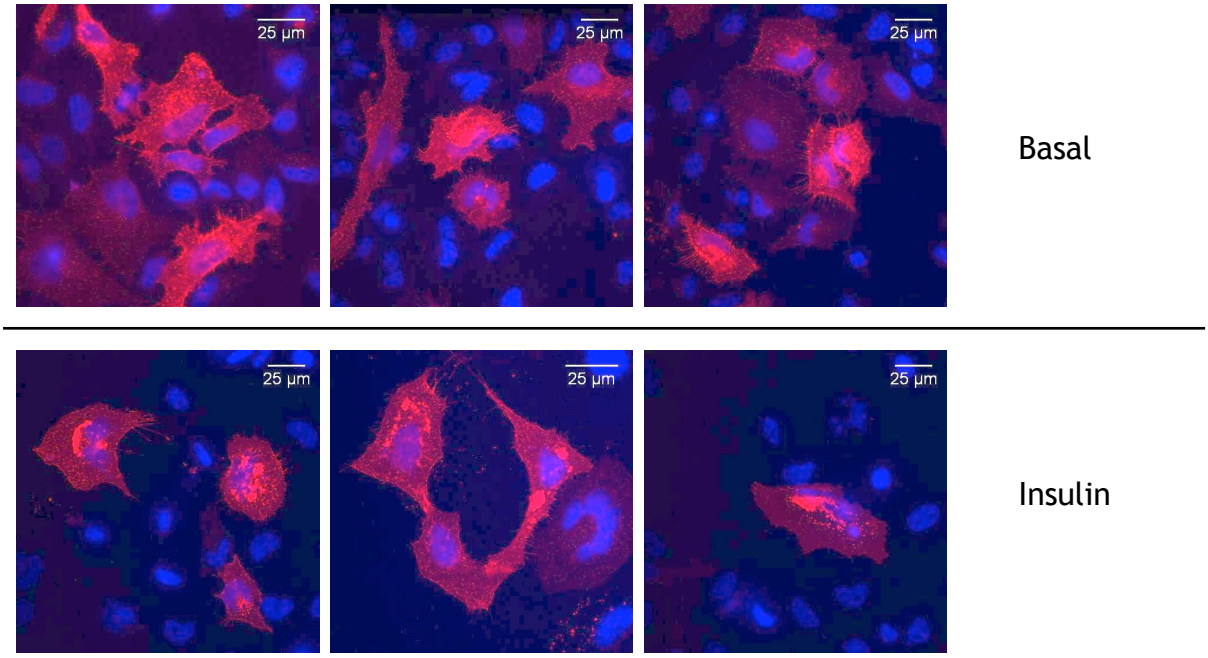

Figure 18: Confocal images of EFR3A-mcherry in HeLa cells with insulin stimulation.

EFR3A-mcherry transfection using plasmid DNA under CMV promoter control in HeLa cells. No significant morphological change to the PM organisation of EFR3A was noted in response to insulin signalling. Therefore, insulin stimulation does not alter global localisation of EFR3A at the PM. Scale bar 25µm. Cells are stimulated with 0.1 µM insulin after 1 hour 30 minutes serum free media starvation, 3 technical repeats with n=10 per condition. Brightness of images has been increased for printing purpose.

4.5.3 3T3-L1 adipocyte EFR3A-mCherry

The introduction of fluorescently labelled proteins to adipocyte cells was restricted as a consequence of the difficulty in transfecting terminally differentiated cells in addition to the high lipid content of the adipocyte cell. To overcome this, electroporation was utilised to introduce plasmid DNA and drive the overexpression of EFR3A in 3T3-L1 adipocytes (Okada et al., 2003). 48 hours post transfection 3T3-L1 adipocytes show a distinctive PM distribution of EFR3A-mcherry, indicated by white arrows in Figure 19. Localization of EFR3A was also visible in an intracellular compartment, indicated by yellow arrows in Figure 19. The size and position of this intracellular compartment was suggestive of endoplasmic reticulum localization. Previous studies have shown that EFR3A localizes to the PM exclusively in both yeast and mammalian cells (Nakatsu, 2012) (Baird, 2008), the intracellular localization shown in Figure 17, 18, & 19 was hypothesised to be a result of the over expression of CMV promoter controlled EFR3A-mCherry. There was no significant difference of EFR3A localization at the PM upon insulin stimulation. The above results using sub cellular localisation have shown that EFR3A was predominantly localized to the PM, as seen in Figure 16. This information compliments the localization of EFR3A shown in the microscopy images below in Figure 19.

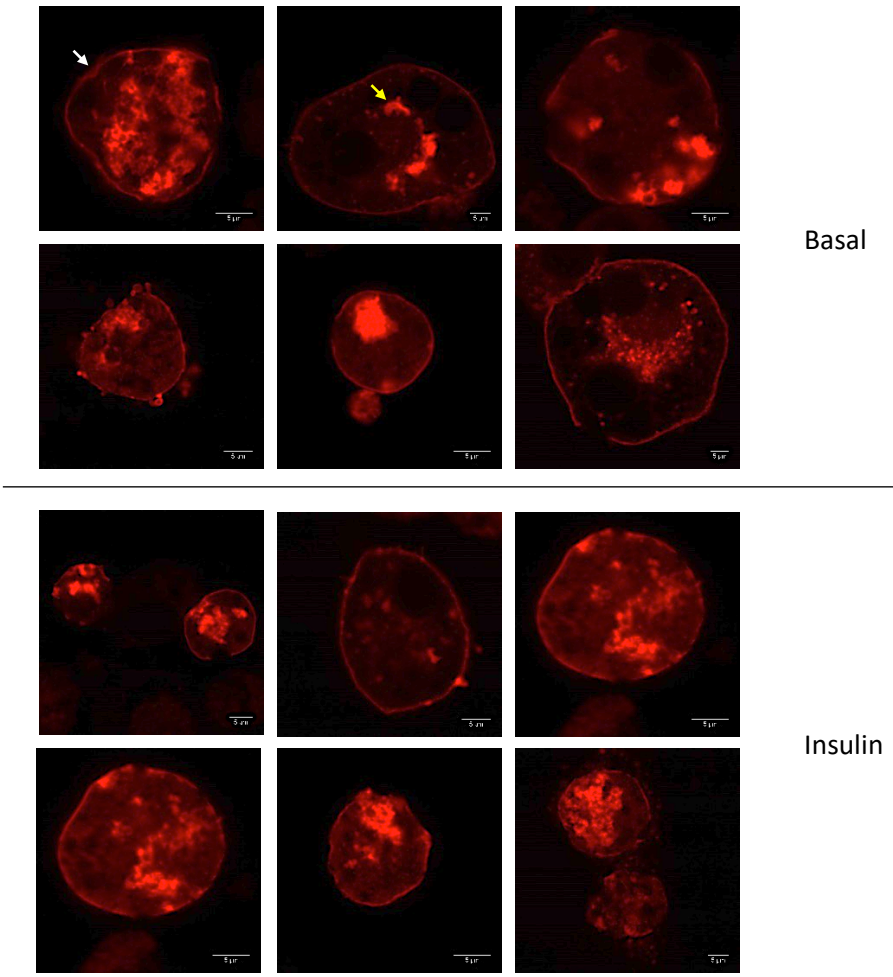

Figure 19: Visualisation of EFR3A in 3T3-L1 adipocytes.

Representative confocal images of 3T3-L1 cell over-expressing EFR3A-mcherrry fusion protein, treated with or without 0.1μM insulin for 20 minutes. Images show PM ring around the cell, indicated with white arrows. An intracellular population was also denoted using yellow arrows. Three technical repeats and n=10 cells examined per condition. Scale bar 5μm. Brightness of images has been increased for printing purposes.

4.6 GENERATION OF AN ANTI-EFR3A ANTIBODY

To further investigate and characterise the role of EFR3A in insulin stimulated GLUT4 dispersal the development of a potent antibody to use when investigating the endogenous protein levels was required. Imaging results obtained using CMV promoter expression of EFR3A have shown variance in comparison to results obtained using subcellular fractionation, Figure 16Figure 19. This variability is believed to be a product of the over expression. Visualisation of endogenous EFR3A through immunofluorescence labelling of EFR3A was a way to negate the effect of protein over production through the CMV promoter. Immunoprecipitation of endogenous EFR3A in 3T3-L1 adipocytes would also be a powerful technique to investigate proteins which co-immunoprecipitate with EFR3A. Of special interest would be if any changes in immunoprecipitation result as a response to insulin stimulation. The current commercially available anti-EFR3A antibodies did not have a high enough affinity for either of the desired techniques. Therefore, we sought to generate anti-EFR3A antibodies raised against EFR3A specific peptide sequences. Two separate sequences were tested, both were C-terminus sequences predicted to be exposed for antibody binding on the protein. For each sequence two rabbits were inoculated with peptide sequences, the T96 batch were raised against the sequence (C)-SVPVYEMKFPDLCVY, and the CRB batch were raised against the sequence (C)-VPQVTDEDRLSRRKSIV. Peptide sequence position within EFR3A shown in Figure 20 below, both sequences are within the disordered C-terminal shown in Figure 11 and 20.

MPTRVCCCCSALRPRYKRLVDNIFPEDPKDGLVKADMEKLTFYAVSAPEKLDRIGAYLAERLSRDVV
RHRSGYVLIAMEALDQLLMACHSQSIKPFVESFLHMVAKLLESGEPKLQVLGTNSFVKFANIEEDT
PSYHRRYDFFVSRFSAMCHSCHSDPEIRTEIRIAGIRGIQGVVRKTVNDELRATIWEPQHMDKIVP
SLLFNMQKIEEVDSRLGPPSSPSAADKEENPAVLAESCFRELLGRATFGNMNNAVRPVFAHLDHH
KLWDPNEFAVHCFKIIMYSIQAQYSHHVIQEILGHLDARRKDSPRVRAGIIQVLLEAVAIAAKGSIGP
TVLEVFNTLLKHLRLSVELEANDSQKGSVGSVTVSSKDNDEKIVQNAVIQTIGFFGSNLPDYQRSEI
MMFIMGKVPVFGTSTHTLDISQLGDLGTRRIQIMLLRSLLMVTSGYKAKTIVTALPGSFLDPLLSPS
LMEDYELRQLVLEVMHNLMDRHDNRAKLRGIRIIPDVADLKIKREKICRQDTSFMKKNGQQLYRH
IYLGCKEEDNVQKNYELLYTSLALITIELANEEVVIDLIRLAIALQDSAIINEDNLSMFHRCGIMALVA
AYLNFVSQMIAVPAFCQHVSKVIETRTMEAPYFLPEHIFRDKCMLPKSLEKHDKNLYFLTNKIAES
LGGSGYSVERLTVPYVPQVTDEDRLSRRKSIVDTVSIQVDILSNSVPSDDVVSNTEEITFEALKKAI
DTNGMEEQEKEKRRLVIEKFQKAPFEEIAAQCESKANLLHDRLAQILELTIRPPPSPSGTLTVTSG
HTQYQSVPVYEMKFPDLCVY

Figure 20: EFR3A amino acid sequence

Amino acid sequence of mouse EFR3A, in bold is the disordered C-terminal region aligned from yeast sequence. The two peptide sequences used as antigens are highlighted and underlined in blue and red. The red highlighted sequence refers to the T96 peptide. The blue highlighted sequence refers to the CRB peptide.

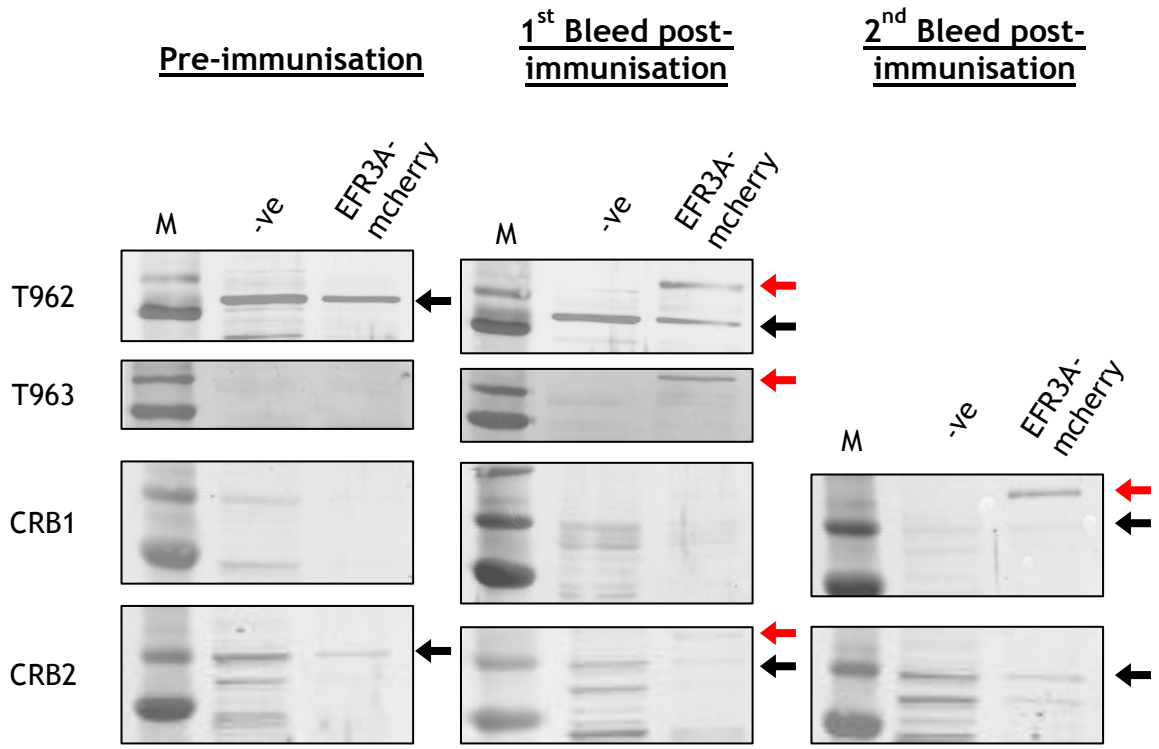

Figure 21: Immunoblots of anti-peptide EFR3A rabbit serums.

Immunoblot with rabbit serum, pre and post EFR3A peptide immunisation, used for EFR3A detection of HeLa cell lysates. MW of EFR3A was 93kDa, as a positive control HeLa cells transfected with EFR3A-mcherry (MW of 120kDa) are also tested. Red arrows denote bands at the predicted MW for EFR3A-mcherry. Black arrows denote bands at the predicted MW for EFR3A. Gels loaded with 40µL 100µg/mL Bradford assay normalised lysate samples, serum diluted 1:200 in 3% BSA

4.6.1 Anti-peptide serum testing

To investigate the initial serum affinity to the target endogenous protein and identify candidates for further purification the whole serum was tested using immunoblots. Whole HeLa cell lysate were screened and compared with HeLa cells transfected with EFR3A-mCherry are used as a positive control. Endogenous EFR3A has a molecular weight (MW) of 93 kDa and EFR3A-mcherry has a higher MW of 120kDa. The results are shown in Figure 21. Pre and post immunisation serum was used as primary antibodies to account for any non-specific binding. The red arrows denote bands at the correct MW for EFR3A-mcherry. The animals with serum showing

positive bands at the MW of EFR3A-mcherry are T962, T963, CRB1 (2nd bleed) and CRB2 (1st bleed only). Animals with strong positive bands for endogenous EFR3A are T962 and CRB2, however both animals have bands at a similar position when the pre-immunised serum is tested with the same lysates. CRB1 has a weak positive band at the molecular weight for endogenous EFR3A. The results from both of the T96 animal serums raised against the same peptide (SVPVYEMKFPDLCVY) are not promising from these initial immunoblots. The strong signal detected under the 100kDa marker seen in the pre-immunised serum of T962 indicates non-specific binding of a protein of similar MW to EFR3A, therefore making the serum unsuitable for further purification. This is despite T962 serum displaying a specific positive band at 120 kDa correlating to EFR3A-mCherry, which is only seen in the EFR3A-mCherry transfected HeLa samples of the post-immunisation serum. The non-specific binding of a protein near endogenous EFR3A resulted in the discontinuation of use for this serum. T963 has a positive band at the MW for EFR3A-mCherry in the post immunisation serum; this band is not present pre-immunisation serum blots. There is a weak visible band at the MW for endogenous EFR3A in T963 making this candidate suitable for IgG purification and concentration. The serum from CRB1 2nd bleed has a strong visible band at MW for EFR3A-mcherry and a weaker band at the endogenous EFR3A. These bands are not visible in the pre-immunisation serum and the 1st bleed. This indicates that immunity is built up against the specific peptide and it is reactive to endogenous EFR3A were present, making it a suitable candidate for IgG purification and concentration. CRB2 has a weak band at the MW for EFR3A-mcherry and endogenous EFR3A at the 1st bleed. However, the band for EFR3A-mcherry disappears in the 2nd bleed sample. This makes CRB2 a weaker candidate for further IgG purification as the majority of serum is from the second bleed. The sum result from this indicates that the whole serum is not very promising and IgG purification to improve the specificity of the CRB2 serum is crucial. Serum from rabbits T963, CRB1, and CRB2 were taken forward for further purification and investigation.

4.6.2 Serum purification

To improve the antibody reactivity the serum was IgG purified using two approaches, column and sepharose A bead purification. Column purification involved binding to the peptide used during serum production, which should concentrate peptide specific binding proteins. IgG purification was used to concentrate whole IgG population of the serum using protein A beads. Post purification, protein concentrations where measured using a spectrometer, this is to ensure protein is present in the eluted sample post purification. The post column purification concentration of T693 serum yielded low levels which resulted in the discontinuation of this sample. Shown in Figure 22 was a SDS-gel electrophoresis Coomassie staining containing the serum samples post purification. IgG antibody heavy chain MW was predicted at 50 kDa and light chain MW was predicted at 23 kDa. Only samples that have undergone IgG peptide column purification have strong bands at the heavy and light chain MW, denoted with * in Figure 22. This indicates that peptide bound column purification results in IgG protein purification. As CRB2 preliminary tests showed it to be the most promising we tested this against commercially available EFR3A antibody, immunoblot results shown in Figure 23. Protein samples used were 3T3-L1 adipocyte whole cell lysate, a 1:2 diluted 3T3-L1 adipocyte sample, HeLa cell lysate and HeLa cells transfected with EFR3A-mcherry. In the immunoblot probed with the commercial antibody a band at the expected MW for endogenous EFR3A was seen in all lanes, denoted by the black * in Figure 23A. In the commercial blot a distinct band at the expected MW for EFR3A-mCherry was only seen in the HeLa EFR3A-mCherry sample, shown in Figure 23A with red *. Immunoblots using column purified CRB2 as primary antibody, shown in Figure 23B, indicate that no distinct band was present for the MW for endogenous EFR3A in any lane. However, a faint band for endogenous EFR3A was noted in the lane containing HeLa cells transfected with EFR3A-mcherry. A faint band was visible at the correct MW for EFR3A-mCherry, denoted by a red * in Figure 23B, only in the EFR3A-mCherry transfected sample. Commercial antibody was determined to have the best western blot read out for endogenous EFR3A and was used in further experiments.

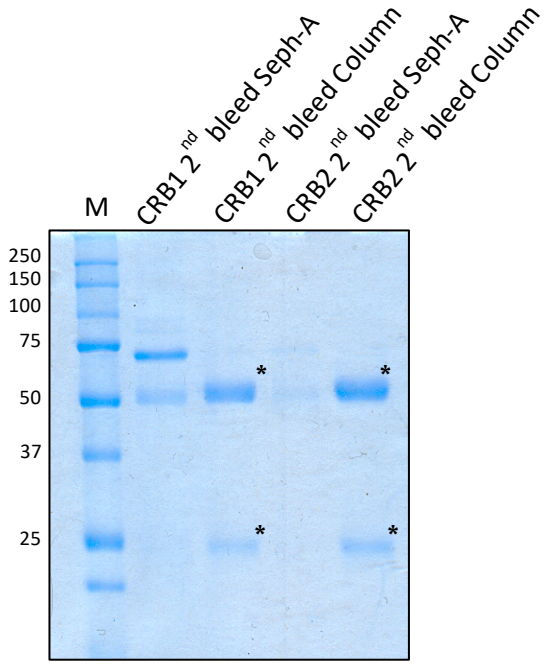

Figure 22: Coomassie staining of purified anti-peptide serums

Coomassie stain of the purified samples from the CRB peptide serum. The two forms of purification used are peptide bound column purification (denoted with Column), and sepharose-A bead (denoted with Seph-A) purification. The Heavy chain band was visible at 50kDa and light chain band was visible at 23kDa, marked with *, in the peptide column purifications. Equal volume of elution's prepared from each purification, 5µL of elute loaded per lane.

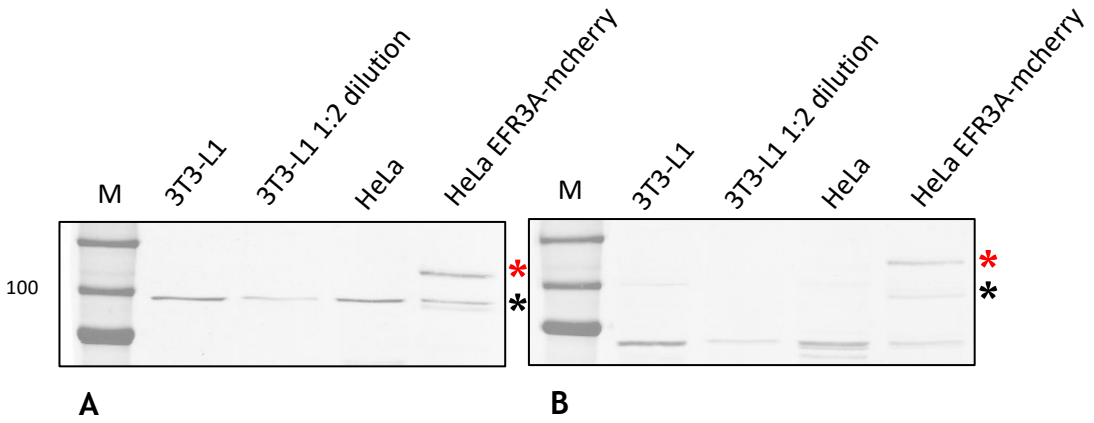

Figure 23: Immunoblot using commercial EFR3A antibody and purified EFR3A anti-peptide serum

Comparative immunoblots of the commercial EFR3A antibody and purified EFR3A peptide antibody. A. Immunoblot using commercial EFR3A antibody. B. Immunoblot using CRB1 2nd bleed peptide column purified serum. Samples used for comparison are in order from left to right; 3T3-L1 adipocyte, 1:2 diluted 3T3-L1 adipocyte, HeLa lysate and HeLa transfected with EFR3A-mcherry. Black * denotes the position for endogenous EFR3A. The red * denotes the position for EFR3A-mcherry. Samples normalized using Bradford assay and 40µL 20µg/lysate per lane, 1:2 dilution denotes sample dilution to 10µg/mL according to normalization. A. Commercial antibody used at 1:250 as stated in materials and methods 3.2.1 in 3% BSA B. CRB1 peptide column purified serum used at 1:200 in 3% BSA.

4.7 IMMUNOPRECIPITATION OF EFR3A

To investigate the effect insulin has on the molecular complex that EFR3A and PI4KIIIα form in 3T3-L1 adipocytes immunoprecipitation was performed. This was carried out using commercial antibodies for both EFR3A and PI4KIIIα antibodies. Samples from the immunoprecipitation were immunoblotted, as shown in Figure 24. Two stringencies of elution conditions were tested, 1% and 0.5% Triton-X100 IP buffer. These stringencies are tested as low detergent may result in unspecific binding, whereas high detergent may result in sample wash. The results suggest a successful immunoprecipitation using the PI4KIIIα antibody, as a clear strong band was visible at the expected MW for PI4KIIIα in both 0.5% and 1% Triton-X100 IP buffer. In the EFR3A immunoblot of the PI4KIIIα immunoprecipitation a band at the expected MW for EFR3A was visible, bands are depicted using red arrows in Figure 24. This suggests a positive co-immunoprecipitation, validating that EFR3A and PI4KIIIα interact in 3T3-L1 adipocytes.

The results for the EFR3A immunoprecipitation indicate that the commercial antibody cannot immunoprecipitate, since the anti-EFR3A blot does not have defined bands at the MW for EFR3A. There are however non-specific bands visible at the expected MW for PI4KIIIα in the EFR3A immunoprecipitation sample. This indicates an unsuccessful immunoprecipitation, and that the commercially available antibody was not appropriate for this technique.

All samples are incubated with random rabbit IgG and show negligible visible bands. This result support the bands present in the PI4KIIIα immunoprecipitation are specific. Additionally, it was expected that no GAPDH will co-immunoprecipitate with either of the samples. The blots show that GAPDH was not found in the immunoprecipitate and was only found in the whole cell lysates and flow through, this was shown in the Supplemental Figure 1.

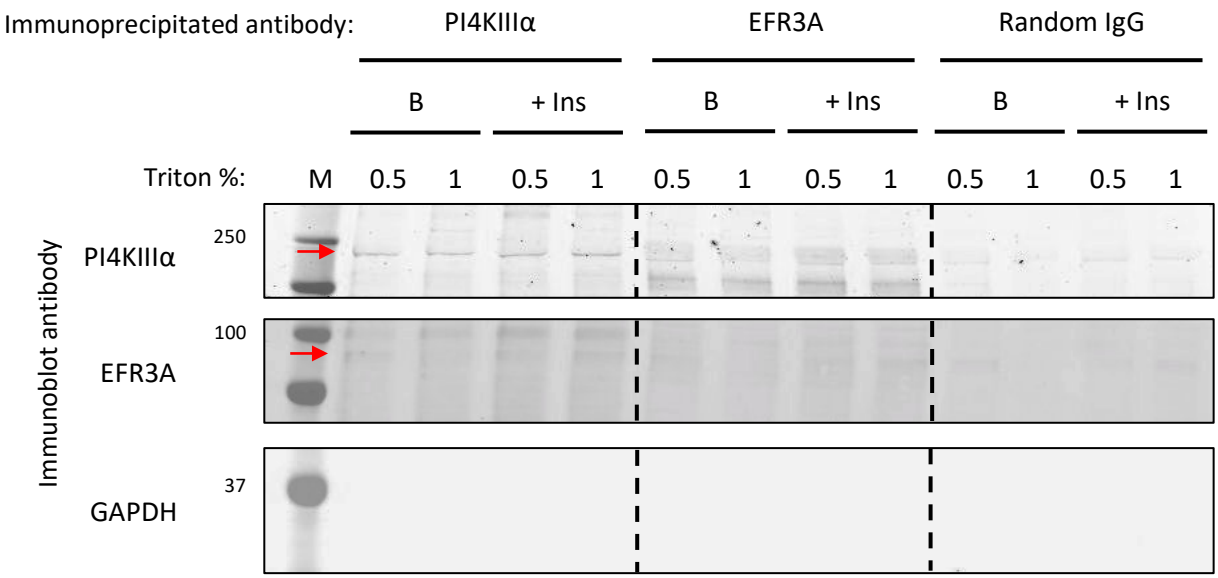

Figure 24: Immunoprecipitation of EFR3A and PI4KIIIα

Immunoblots from samples immunoprecipitated with EFR3A, PI4KIIIα, and random IgG. Whole 3T3-L1 lysate was immunoprecipitated and blotted for PI4KIIIα, EFR3A, and GAPDH. 1% and 0.5% Triton-X concentrations where used in the IP buffer. Red arrows indicate bands at the expected MW for the corresponding antibody. 3T3-L1 adipocytes were insulin stimulated for 20 minutes with 0.1 μM insulin. Samples normalised using Bradford's assay before immunoprecipitatation. Commercial anti-EFR3a antibody used at 1:250 in 3% BSA and commercial anti-PI4KIIIα antibody used at 1:250

4.8 Characterisation of EFR3A and PI4KIIIα protein levels in striated muscle samples from CHOW v HFD Mice.

4.8.1 Heart Sample Analysis

Mice heart samples from normal (CHOW) and high fat diet (HFD) fed animals were obtained and the whole organ was lysed as described. Work carried out by Dr Anna White pre-cull showed the mice glucose tolerance tests confirmed that mice on HFD have impaired glucose tolerance compared to their Chow-fed littermates, shown in Figure 25, which is in line with previous findings (Andrikopoulos *et al.*, 2008). Impaired glucose tolerance is a common diagnostic indicator of insulin resistance and a hallmark on the road to the development of type II diabetes. Previous studies have shown that GLUT4 protein levels in these animals remain unchanged (Gurley *et al.*, 2016) however there is no data on either EFR3A or PI4KIIIα protein levels. We therefore measured protein levels using immunoblotting. The results showed that both PI4KIIIα and EFR3A are elevated in HFD mouse cardiac muscle samples, figure 26. From the mean values of normalised EFR3A immunoblot band intensity values show a 2.20-fold increase in HFD mice compared to CHOW fed mice. The mean values of normalised PI4KIIIα immunoblot band intensity values show a 2.09-fold increase in HFD mice compared to CHOW fed mice. However, the cohort obtained is too small to reliably statistically analyse and future work will aim to test this result from a larger cohort of mice.

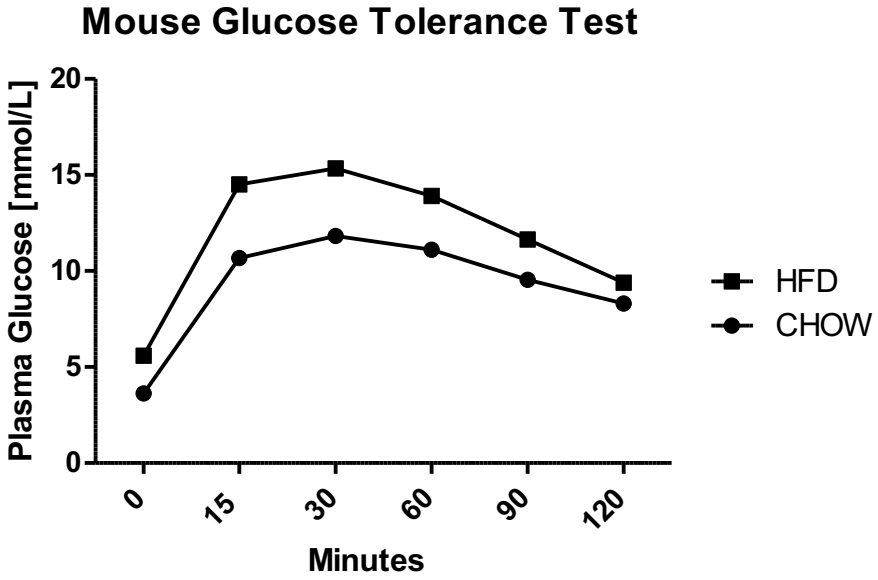

Figure 25: Glucose tolerance test

Glucose tolerance test preformed on mice at 10-week stage by Dr Anna White. Mice injected with 2mg glucose/g body weight and samples measured across time points. The CHOW fed mice plasma glucose is lower in comparison to HFD mice pre-injection with glucose. HFD mice have increased plasma membrane glucose post injection which remains elevated for longer in comparison to CHOW fed population. These results are indicative of lowered glucose tolerance. Per condition n=6 mice, samples from which are used in the immunoblots below.

4.8.2 Quadriceps Sample Analysis

Samples from CHOW and HFD mice quadriceps where obtained and the protein levels of EFR3A and PI4KIIIα where probed using western blotting. As with the heart samples the HFD mice samples showed elevated levels of both proteins in comparison to the CHOW fed mice, shown in Figure 27. As with the heart samples, not enough samples where obtained to preform statistical analysis of the cohort probed. The measured mean values of normalised EFR3A immunoblot band intensity reveal a 1.47-fold increase in HFD mice compared to CHOW fed mice. The measured mean values of normalised PI4KIIIα immunoblot band intensity reveal a 2.72-fold increase in HFD mice compared to CHOW fed mice.

Heart and quadriceps are both examples of striated muscle which are GLUT4 positive and insulin sensitive (Kobayashi *et al.*, 1996). Both exhibit a visible increase in EFR3A and PI4KIIIα protein levels when immunoblotted when mice are fed a HFD. The samples where obtained from different cohorts of mice, in both samples the HFD mice had impaired glucose tolerance results. The heart and quadriceps cohorts analysed both are of low numbers, which inhibits statistical analysis. However, the two separate cohorts exhibit the same trend of increased EFR3A and PI4KIIIα protein levels therefore giving bigger leaning to the fact that the elevation was due to the HFD of these mice, giving correlation between HFD and the increase in protein levels.

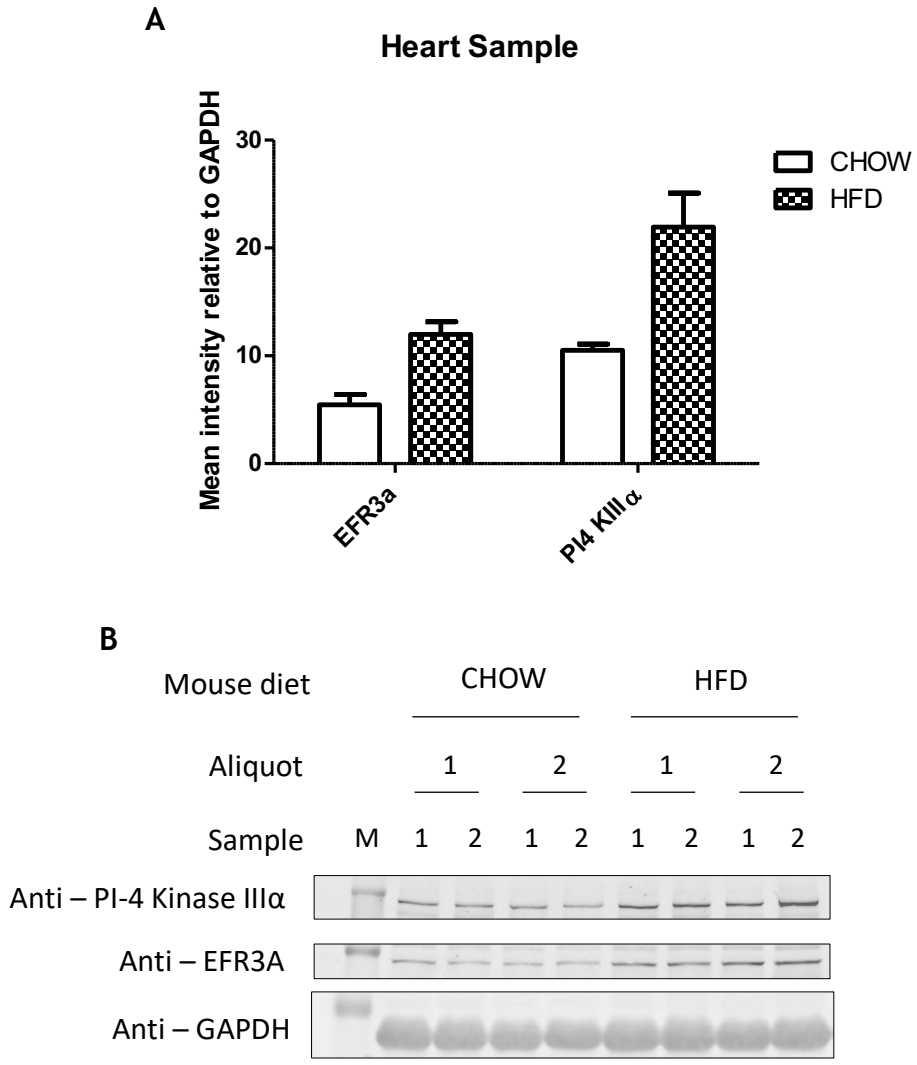

Figure 26: HFD mouse comparison of EFR3A and PI4KIIIα in cardiac tissue.

Mouse samples obtained from CHOW fed or high fat diet (HFD) fed (10 weeks diet) mice of same age. B. Immunoblot of whole heart lysates against PI4KIIIα, EFR3A and GAPDH. A. Mean intensity of bands was measured using imageJ and normalised to GAPDH bands from corresponding samples. Sample number too low to statistically analyse, to fully characterise this effect new samples of a greater cohort would need to be obtained. From the mean values of normalised EFR3A increase 2.20-fold in HFD mice compared to CHOW fed mice. From the mean values of normalised PI4KIIIα increase 2.09-fold in HFD mice compared to CHOW fed mice. Total protein level in samples normalised using BCA assay. 40µL 36 µg/ml normalised sample run on 12% gel, same gel is probed for all proteins. Antibodies used with concentrations described in materials and methods 3.2.1.

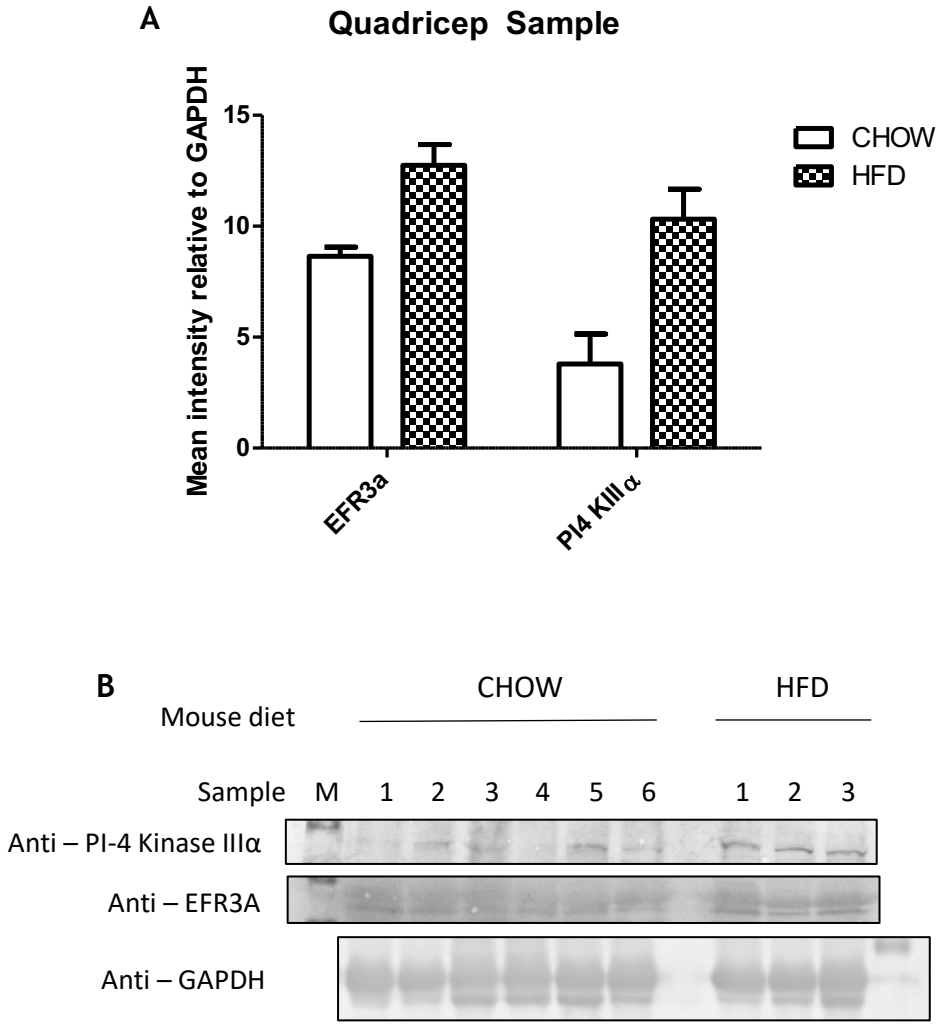

Figure 27: HFD mouse comparison of EFR3A and PI4KIIIα in quadricep samples.

Mouse samples obtained from CHOW fed or high fat diet (HFD) fed (10 weeks diet) mice of same age. B. Immunoblot of whole quadriceps lysates against PI4KIIIα, EFR3A, and GAPDH. A. Mean intensity of bands was measured using imageJ and normalised to GAPDH bands from corresponding samples. Sample number too low to statistically analyse, to fully characterise this effect new samples of a greater cohort would need to be obtained. From the mean values of normalised EFR3A increase 1.47-fold in HFD mice compared to CHOW fed mice. From the mean values of normalised PI4KIIIα increase 2.72-fold in HFD mice compared to CHOW fed mice. Total protein level in samples normalised using BCA assay. 40µL 36µg/mL normalised sample run on 12% gel, same gel is probed for all proteins. Antibodies used with concentrations described in materials and methods 3.2.1.

4.9 DISCUSSION

4.9.1 Homolog distribution

Current insight into EFR3A has previously been gathered using the yeast orthologue (Baird *et al.*, 2008; Wu *et al.*, 2014). In mammalian cells the two EFR3 homologs (EFR3A and EFR3B) share 64% amino acid sequence identity and 78% positive sequence alignment, previous work has shown that homolog distribution greatly varies across some tissues (Bojjireddy *et al.*, 2015). To assess the homolog distribution of EFR3 a and b in cell lines used; 3T3-L1 adipocytes and HeLa cells, qPCR provides an accurate, tried and tested methodology (Bojjireddy *et al.*, 2015). In 3T3-L1 and HeLa cell lines EFR3A was the predominantly expressed homolog and EFR3B was virtually undetectable. The qPCR results guided the focus for this study on EFR3A, and the role for EFR3A plays in an insulin responsive system.

4.9.2 EFR3A localisation

To examine the endogenous localisation of EFR3A in 3T3-L1 adipocytes subcellular fractionation of the whole lysate membranes was employed. This technique has previously been used to characterise the translocation of endogenous GLUT4 in adipocytes in response to insulin stimulation (Marette *et al.*, 1992). The results show that EFR3A was predominantly found at the PM. Populations of EFR3A was not seen in intracellular compartments, and re-distribution in response to insulin signalling was not observed. EFR3A serves to localise PI4KIIIα to the membrane and the endogenous localisation of PI4KIIIα was shown to be at the PM, in accompaniment with the localisation of EFR3A. No intracellular compartment localisation or cytosolic localisation was found for PI4KIIIα. These results demonstrate that EFR3A and PI4KIIIα remain bound to the PM during insulin signalling and re-localisation from an inner compartment was not responsible for any effect EFR3A may have on PM GLUT4. This data informs that any effect insulin signalling may have on EFR3A was at the PM, and may involve domain localisations at the PM.

To visualise the localisation of EFR3A in the model HeLa system and 3T3-L1 adipocytes confocal microscopy was used. To assess the localisation of EFR3 proteins C-terminal mCherry tagged proteins were expressed using plasmid transfection. This technique allowed for visualisation of EFR3A and EFR3B in the relevant cell lines.

Results showed that EFR3A and EFR3B are both localised at the PM in a uniform manner in both HeLa and 3T3-L1 adipocytes. Noted from the confocal images are intracellular localisations, which are not observed in the results from the subcellular fractionation of endogenous protein in 3T3-L1 adipocytes. This visualised intracellular localisation was believed to be a facet of the plasmid transfection, in which the protein transcription was under CMV promoter control. CMV promoter was used in mammalian cells for high level production of recombinant proteins (Wang *et al.*, 2017). To circumvent issues with the over expression of proteins the development of a CRISPR EFR3A C-terminal fluorescently tagged cell line should be undertaken for future investigations. This would allow for the visualisation of endogenous EFR3A in adipocytes to negate for the effects of over expression on localisation in the cell (Ratz *et al.*, 2015). Transient transfection of EFR3A-mCherry was achieved using electroporation and LF2K. These techniques result in a potential number of plasmids may be present in per cell, which cannot be controlled for. To further investigate EFR3A localisation and co-localisation at the PM future investigations would improve results using super-resolution microscopy. The limiting resolution of confocal microscopy, 240 ηm, does not allow for the finer details of PM localisation to be observed (Huang *et al.*, 2010). TIRF microscopy in conjunction with fPALM would provide a greater insight into the effect of insulin on EFR3A at the PM specifically (Hess *et al.*, 2006). The visualisation of circular objects of unknown size, such as domains at the PM, was greatly improved using fPALM in opposed to dSTORM. This was due to the antibody labelling required for dSTORM results in an affected size of the visualisation (Tam and Merino, 2015).

4.9.3 Immunoprecipitation and Generation of EFR3A antibody

To investigate the interaction between EFR3A and PI4KIIIα at the PM this investigation aimed to immunoprecipitation EFR3A and PI4KIIIα to investigate this interaction between the proteins in response to insulin stimulation in 3T3-L1 adipocytes. The commercial antibodies available for EFR3A and PI4KIIIα are used. EFR3A antibody does not immunoprecipitation. PI4KIIIα antibody appears to yield a successful immunoprecipitation and the generation of a EFR3A specific anti-peptide antibody was conducted.

This was not achieved in this study and future studies will require an affinity purified high specificity antibody to carry out immunoprecipitation investigations, this was beyond the scope of this work.

4.9.4 Characterisation of EFR3A and PI4KIIIα in mouse tissue

Samples from mouse cohorts which for ten weeks before culling have been divided into normal diet (CHOW) or high fat diet (HFD). Mice fed with HFD have impaired glucose tolerance in comparison to the CHOW fed mice, shown in Figure 25 (Wang and Liao, 2012). Impaired glucose tolerance is a hallmark of insulin resistance and type II diabetes (Costa *et al.*, 2002). Samples from the heart and quadriceps were obtained from different mice. Striated muscle found in the heart and quadriceps are insulin responsive with (Mueckler, 2001). The obtained sample cohort was supplied from Dr Anna White to investigate any changes. The numbers are too low to draw any significant conclusions from, however the presence of a similar trend in both the quadriceps and cardiac sample was promising. The result may hint at a compensatory effect by up regulating EFR3A when insulin resistance was developed. In genetic models where proteins have been knocked down compensations are a widespread occurrence (El-Brolosy and Stainier, 2017). It was conceivable that multi-faceted diseases such as type II diabetes have a degree of phenotypic compensation as the disease develops. Further investigation of non-insulin responsive tissue would be an important control to ensure this elevation was specific to GLUT4 containing tissue and not a universal response to HFD. Either result would be of interest. Proteins which are upregulated during the development of obesity, such as adipokines, are of interest in the study of the growing obesity epidemic (Ouchi *et al.*, 2011).

These results indicate that EFR3A and PI4KIIIα are potentially positive regulators of glucose uptake if increased protein expression is a result of compensation during the development of insulin resistance and continued increased blood glucose levels. This indicated the original hypothesis based on the assumption that *fgy1-1* being a loss of function mutation may be incorrect and in fact this may be a gain of function mutation in yeast allowing for mammalian GLUT4 to be dispersed at the PM in yeast. The next chapters aim to generate a better understanding of how EFR3A and PI4P

may affect GLUT4 at the PM, and if this effect is a positive or negative one for GLUT4 dispersal.

4.10 CONCLUSION

The findings in this chapter show that EFR3A is the dominant homolog in 3T3-L1 adipocytes. This allows future avenues of study to focus on the EFR3A homolog. The findings confirm EFR3A was primarily PM localised in 3T3-L1 adipocytes and HeLa cells. The combination of visualisation and subcellular fractionation allows for the effects of over expression for visualisation to be negated for. Future studies looking into the behaviour and co-localisation of EFR3A with other proteins in response to insulin stimulation will require the generation of an antibody capable of immunoprecipitation. Preliminary work with tissue samples show an increase in EFR3A and PI4KIIIα in mice fed HFD. This will require a larger cohort to further investigate fully however results in this chapter are intriguing.

5 CHARACTERISATION OF PLASMA MEMBRANE PI4P IN AN INSULIN SENSITIVE SYSTEM

5.1 INTRODUCTION

The study of phospholipids in adipocytes in response to insulin signalling has predominantly been focused on PI3,4,5P_3 (Kanzaki *et al.*, 2004; Funaki *et al.*, 2006; Grainger *et al.*, 2011; Ijuin and Takenawa, 2012). In response to insulin stimulation PI3,4,5P_3 is generated in adipocytes by the phosphorylation of PI4,5P_2 by phosphatidylinositol 3-kinase (PI3K). PI3K is activated through SH2 domains of the regulatory p85 subunit binding in response to insulin receptor auto phosphorylation (Levy-toledano *et al.*, 1995; Shepherd *et al.*, 1998). PI3,4,5P_3 acts as an allosteric regulator of phosphoinositide-dependent kinase (PDK) which in turn is able to phosphorylate to activate Akt and PKC isoforms (PKC$_z$ and PKC$_1$) (Alessi *et al.*, 1997; Le Good *et al.*, 1998). The activation of PI3K and generation of PI3,4,5P_3 through catalytic manipulation or external introduction was not capable of mimicking insulin signalling (Isakoff, 1995; Wiese *et al.*, 1995). Thus, showing that insulin signalling requires a variety of concurrent signals to induce GLUT4 translocation and glucose uptake.

PI4P has long been established as a component of the *trans*-Golgi network (Wang *et al.*, 2007). PI4P has recently been shown to have a distinct role at the PM, separate from being the building blocks for PI4,5P_2 production (Hammond *et al.*, 2012; Dickson *et al.*, 2014). The visualisation of phosphoinositide's such as PI4P and PI4,5P_2 in the cell has been achieved using fluorescently labelled protein domains which specifically bind to the PI of interest. This technique was of particular use when characterising PIP and PIP$_2$ as these protein domains only bind to the specific PI with the corresponding phosphorylated inositol ring positions. Therefore, PI4P can be differentiated from PI5P or PI3P and likewise for PI4,5P_2 over other PIP$_2$ groups (Idevall-Hagren and De Camilli, 2015).

Previous studies into phosphoinositide levels in cells have used inhibitors of PI kinases such as LY294002 and phenylarsine oxide (PAO). These techniques are limited in that there are off target effects and the membrane which was depleted cannot be controlled using inhibitors in this manner. A technique which allows the direct manipulation of PI4P and/or PI4,5P_2 levels at the PM has been developed and investigated using mammalian COS-7 cells (Hammond *et al.*, 2012). This technique used the rapamycin-inducible dimerization of FRB (fragment of mTOR that binds

rapamycin) and FKBP (FK506 binding protein 12) (Heo *et al.*, 2006; Varnai *et al.*, 2006). The rapamycin-inducible dimerization components FRB and FKBP was bound to a membrane specific anchor and phosphatase respectively. To selectively manipulate PI4P and PI4,5P_2 a chimera protein containing the 5' phosphatase INPP5E (inositol polyphosphate-5-phosphatase E) and the 4' phosphatase sac1 phosphatase named pseudojanin was produced by Hammond et al. (Guo *et al.*, 1999; Varnai *et al.*, 2006; Hammond *et al.*, 2012). To direct this system to the PM specifically a LYN11 anchor was fused with the FRB component, a schematic is shown in Figure 28. This system can be used to selectively remove different populations of PI by using double and individual active versions of the chimera phosphatase to disrupt specifically PI4P or PI4,5P_2 into PI4P or into PI. Upon the addition of rapamycin the pseudojanin was localised to the PM within 2 minutes and levels of the PI are decreased (Hammond *et al.*, 2012). A double dead pseudojanin can be used as a control for the effect of rapamycin on cellular processes.

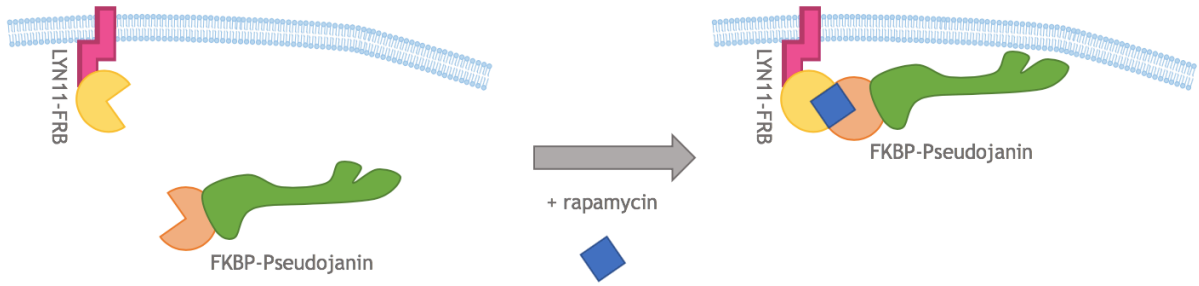

Figure 28: Schematic of rapamycin induced phosphatase system

The proteins FKBP and FRB (FKBP rapamycin binding) bind in the presence of rapamycin. This allows for inducible co-localisation of these two proteins. Linking of the FKBP component to the pseudojanin phosphatase enzyme allows for dephosphorylation of the 4' and 5' position phosphate of phosphoinositide. The pseudojanin is composed of two phosphates and is capable of double position dephosphorylation or single position dephosphorylation. The FRB component is linked to a membrane anchor, in this case LYN11, which specifically targets the FRB to the plasma membrane. The introduction of rapamycin results in localisation of the pseudojanin phosphatase to the plasma membrane, providing precise temporal control for the reduction of specific phosphoinositide populations at the plasma membrane inner leaflet.

To observe the effect depletion of these specific PI groups at the PM specifically have on glucose uptake would provide informative insight as to if PI4P modulates GLUT4 dispersal or in fact aids the clustering of GLUT4 at the PM in the absence of insulin stimulation. This experiment required high transfection of the above mentioned FRB and FKBP components to allow for any measured differences to be related to the depletion of the PI identities and not a result of rapamycin addition to the cells. High transfection is challenging when working with terminally differentiated cells such as 3T3-L1 adipocytes, further more traditional transfection using lipid reagents is inhibited when working with high adiposity of adipocyte cell lines.

5.2 AIM

This chapter aims to characterise localisation of PI4P in 3T3-L1 adipocytes. This aim will allow for the characterisation of phosphoinositide behaviour at the PM in response to insulin signalling in HeLa and 3T3-L1 adipocyte cell types. This chapter aims to directly manipulate PI levels at the PM of adipocytes to monitor the effects of P14P depletion and proliferation on PM GLUT4 and glucose uptake.

5.3 VISUALISATION OF PI4P AND PI4,5P$_2$ IN HELA

The protein SidM is secreted by the *Legionella pneumophila* and binds to PI4P specifically through the P4M domain (Brombacher *et al.*, 2009; Hammond *et al.*, 2014). HeLa cells were transfected with PI4P binding GFP-SidM-P4M probe. Images show PI4P localisation to the PM as an even distribution in HeLa cells, which was consistent with previous studies, depicted in Figure 29 denoted by white arrows. A concentration of intracellular GFP-SidM-P4M was consistent with previous findings of Golgi concentrations of PI4P, denoted with red arrows in Figure 29 (Hammond *et al.*, 2014).

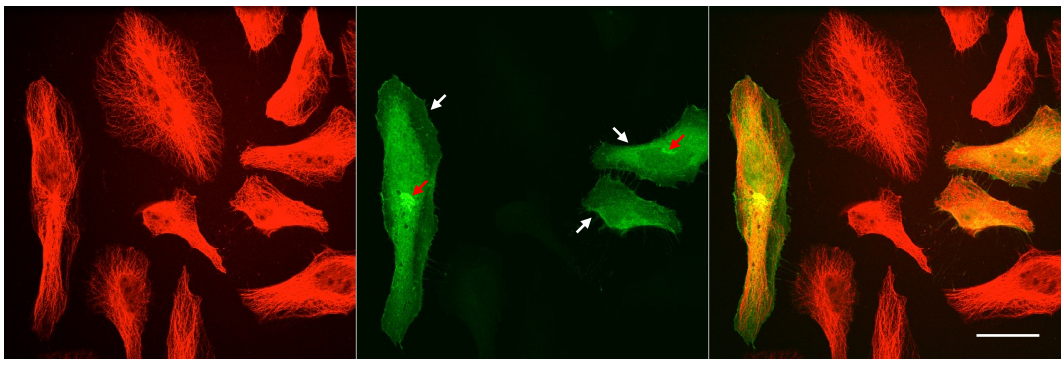

Figure 29: Confocal images of SidM-P4M-GFP expressing HeLa cells.

Representative confocal images of the PI4P binding probe GFP-SidM-P4M expressed in HeLa cells. The left red panel is fluorescent immuno-labelled ß-tubulin, the middle green panel is GFP-SidM-P4M, and the right panel is the merged image. White arrows denote the PM localised PI4P, and the red arrow denotes the intracellular Golgi PI4P localisation. Scale bar represents 25 µm.

The probe PH-PLCδ1-GFP was derived from the pleckstrin homology (PH) domains of phospholipase C (PLC)δ. PH-PLCδ1-GFP binds specifically to PI4,5P2 via the PH domain (Várnai and Balla, 1998). Images shown in Figure 30 show confocal microscopy views of HeLa cells fluorescently immuno-labelled expressing PH-PLCδ1-GFP. PI4,5P2 localisation in HeLa cells was membrane localise to the PM, as shown in previous studies (S. Huang et al., 2004). The patches of PI4,5P2 at the PM, denoted by the white arrows in Figure 30, have been associated with clusters of PI4,5P2 required for focal adhesions (Cai et al., 2008). These patches are now mostly associated with the formations of furrows of the PM giving the appearance of clustering (Ji et al., 2015). The majority of PI4,5P2 localisation was seen at the PM

but intracellular perinuclear localisation was also noted in the HeLa cells as previous studies have shown, signified by the purple arrow in the merged panel in Figure 30 (Tan et al., 2015).

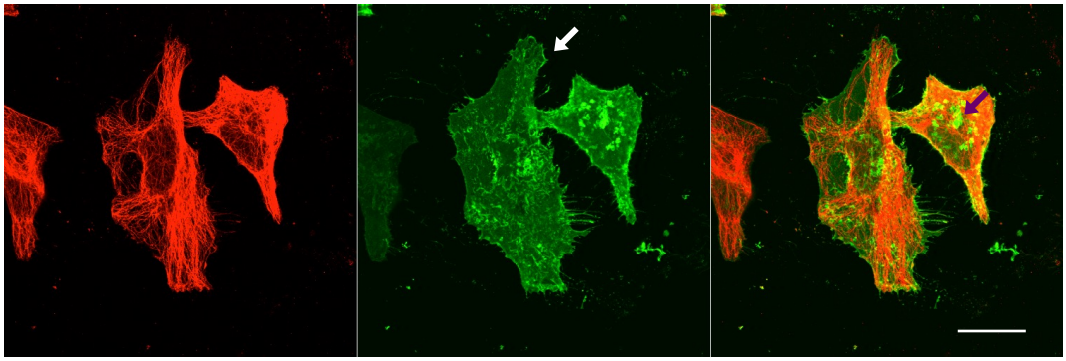

Figure 30: Confocal images of PH-PLCδ1-GFP expressing HeLa cells.
Representative confocal images of the $PI4,5P_2$ binding probe PH-PLCδ1-GFP expressed in HeLa cells. The left red panel is fluorescent immuno-labelled ß-tubulin, the middle green panel is PH-PLCδ1-GFP, and the right panel is the merged image. White arrows denote the patches of PM localised $PI4,5P_2$, and the purple arrow denotes the intracellular perinuclear localisation. Scale bar represents 25 µm.

5.4 Visualisation of PI4P and $PI4,5P_2$ in 3T3-L1 Adipocytes

Confocal microscopy images of the PI4P probe SidM-P4M-GFP show distinct patch localisation in 3T3-L1 adipocytes, shown in Figure 31. Plasmid DNA was introduced to day 4 post-differentiation 3T3-L1 cells via electroporation. This results in smaller adipocytes due to the transfection process. Arrows denote the patch visualisation of GFP-SidM-P4M in adipocytes, which is distinct from when visualising GFP-SidM-P4M in HeLa cells. In HeLa cells PI4P localisation was noticeably PM with concentrations associated with folds in the PM. The patch visualisation in 3T3-L1 was seen at the PM and as fainter intracellular localisations, denoted with white and red arrows respectively.

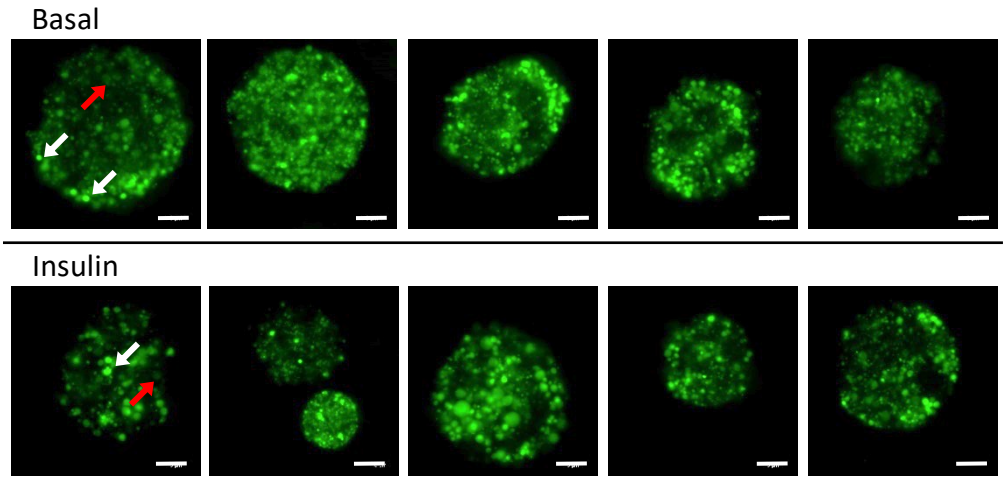

Figure 31: Confocal images of SidM-P4M-GFP expressing 3T3-L1 adipocytes.

Representative confocal images of the PI4P binding probe GFP-SidM-P4M expressed in 3T3-L1 adipocyte cells. White arrows denote the brighter PI4P patches believed to be PM, and the red arrow denotes the fainter potentially intracellular PI4P patch localisation. Cells serum starved for 2 hours and stimulated with 0.1 μM insulin for 20 minutes pre PFA fixing. Scale bar represents 5 μm.

Confocal microscopy images of the PI4,5P_2 probe PH-PLCδ1-GFP show predominant PM localisation in 3T3-L1 adipocytes, shown in Figure 32. White arrows denote PM localised PI4,5P2, there was no difference in PI4,5P2 localisation in cells stimulated with insulin. However, significant intracellular localisation was noted in the majority of 3T3-L1 adipocytes in comparison to HeLa cells, denoted with red arrows in Figure 32.

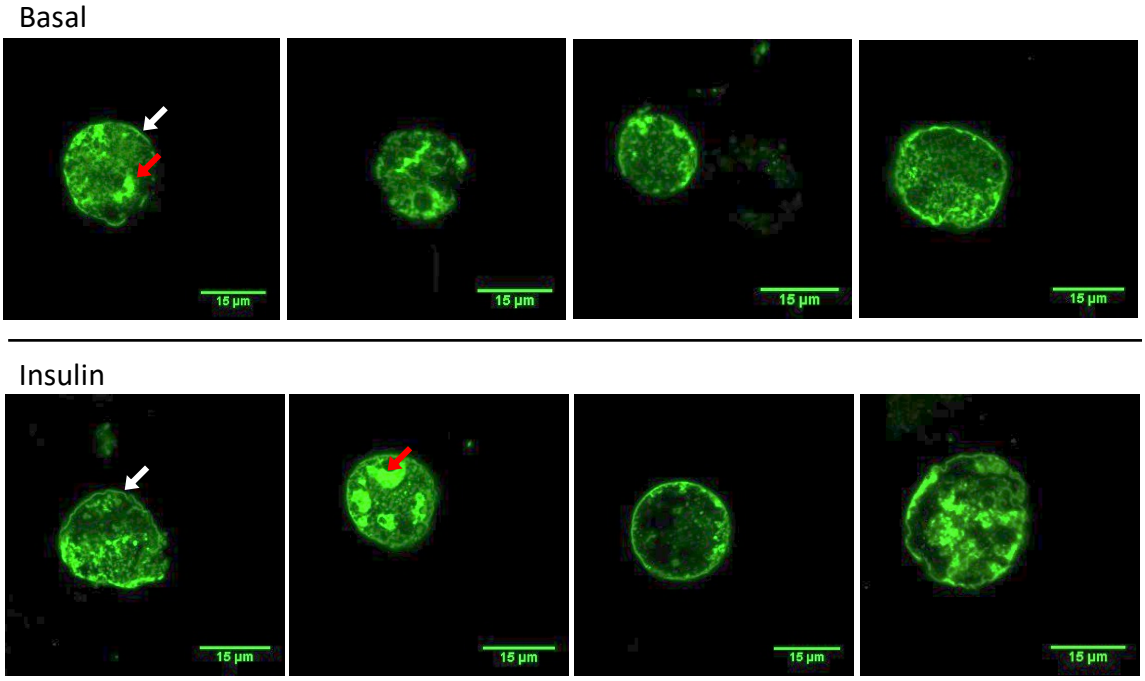

Figure 32: Confocal images of PLCδ1-GFP expressing 3T3-L1 adipocytes.

Representative confocal images of the PI4,5P_2 binding probe PH-PLCδ1-GFP expressed in 3T3-L1 adipocyte cells. The top panel shows non-insulin stimulated cells. The bottom panel shows insulin stimulated cells. White arrows denote the PM localised PI4,5P_2, and the red arrow denotes the intracellular localisation. Cells were serum starved for 2 hours and stimulated with 0.1 µM insulin for 20 minutes pre PFA fixing. Scale bar represents 15 µm.

5.5 THE EFFECT OF INSULIN STIMULATION ON VISUALIZED POOLS OF PI4P

Confocal images of 3T3-L1 adipocytes expressing the PI4P binding probe SidM-P4M-mcherry show distinct patches of PI4P in 3T3-L1 adipocytes, shown in Figure 31. This was unlike the PI4,5P2 binding probe PLCδ1-GFP, shown in Figure 32, which showed a more uniform PM localisation with no visible changes in distribution in response to insulin stimulation. Using ImageJ, the intensity threshold was adjusted to allow for the number of foci at the PM to be measured per cell. Threshold intensity was automatically set using Fiji clustering threshold to remove biases from the sample evaluated (Sezgin and Sankur, 2004). The results shown in Figure 33 are that insulin stimulation results in a significant decrease in the number of patches per cell of PI4P. The decrease in the number of foci per cell was 3-fold in the population measured.

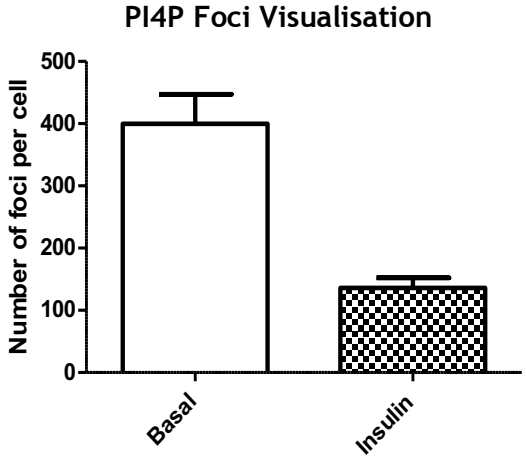

Figure 33: Measurement of the visualisation of PI4P patches in 3T3-L1 adipocytes.

Graph showing the number of patches per cell, cells that are insulin stimulated have a marked decreased in the number of PI4P patches. Over 30 cells where measured per condition. Cells were transfected using electroporation as described in 3.10.1, serum starved for 2 hours and insulin stimulated for 20 minutes using 0.1 μM insulin.

5.6 GENERATION OF PSEUDOJANIN PHOSPHATASE SYSTEM

5.6.1 Expression of Pseudojanin in HeLa cells

The plasmids containing the PI manipulation system, shown in Figure 28, was composed of the FRB-LYN11 PM anchor component and the FKBP-pseudojanin phosphatase component. The pseudojanin phosphatase was a chimera protein containing the 4' phosphatase Sac1 and the 5' phosphatase INPPE5. The FKBP and FRB proteins bind in the presence of rapamycin allowing the phosphatase to be directed to appropriate membrane. There are four phosphatase chimeras versions; the double active pseudojanin (PJ), the two single active Sac1 or INPPE5, and the double dead PJ-dead developed by Hammond (Hammond *et al.*, 2014). Confocal images confirm that the FRB-LYN11 component was plasma membrane localised, shown in Figure 34 A. Images confirm that all four of the FKBP-phosphatases are cytosolic localised in the absence of the FRB-LYN11 plasmid and rapamycin, shown in Figure 34B-E.

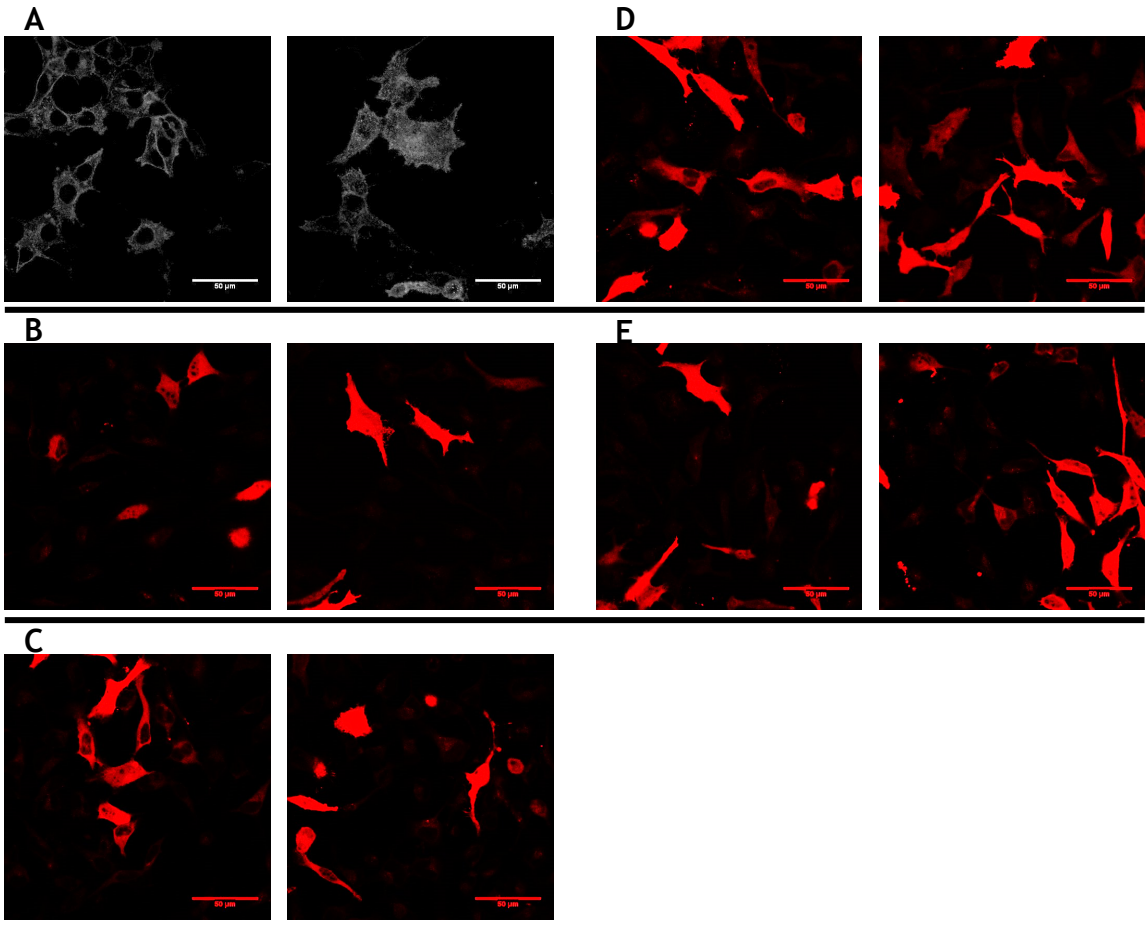

Figure 34 :Confocal images of pseudojanin system components in HeLa cells
Confocal images of HeLa cells transfected with plasmid DNA expressing the A. LYN11-FRB-CFP; B. FKBP-PJ-mCherry, C. FKBP-PJSac1-mcherry, D. FKBP-PJINPPE5-mcherry, E. FKBP-PJdead-mCherry. The LYN11-FRB-CFP anchor shows distinctive plasma membrane localisation, as per the LYNN11 protein. The Pseudojanin (B-E) all show typical cytosolic localisation in the absence of co-transfection with the LYN11-FRB-CFP and rapamycin treatment. Scale bar represents 50 µm.

5.6.2 Generation of a stable FRB-LYN11 anchor 3T3-L1 cell line

Due to the high lipid content of 3T3-L1 adipocytes transfection with plasmid DNA was inhibited. The disruption of PI at the plasma membrane requires introduction of two plasmids. This makes the visualisation of GLUT4 behaviour at the PM in a few cells which are transfected not feasible. To assess the effect of PI depletion on glucose uptake in adipocytes a high transfection rate must be achieved. Therefore, a stable cell line containing FRB-LYN11 was developed. This will allow for a high rate of FRB-LYN11 positive cells and improve double expression with the FKBP-PJ component to perform the uptake assay.

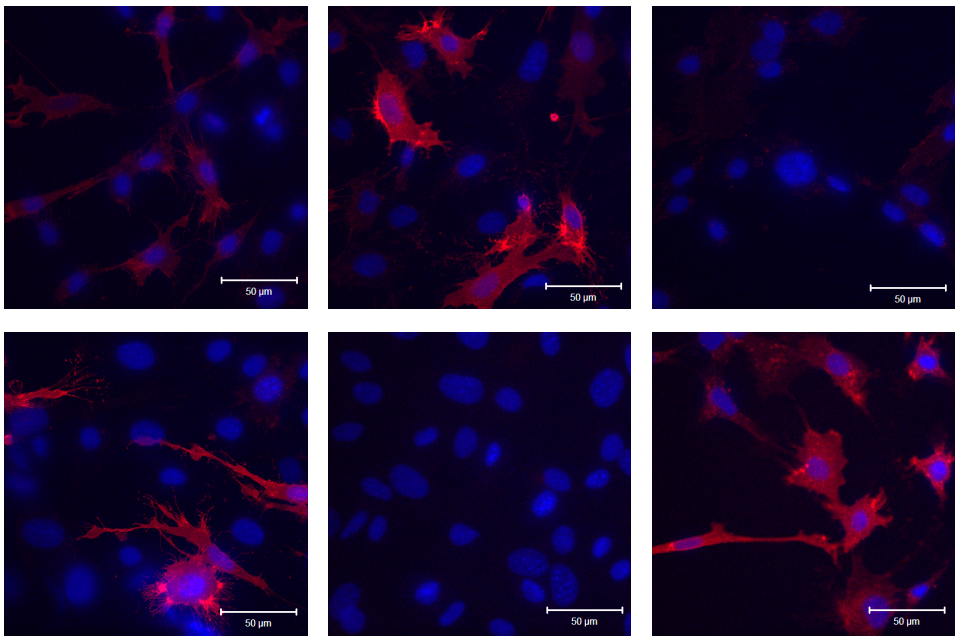

Figure 35: Confocal images of FRB-LYN11-mcherry stable expression 3T3-L1 cell line generated through limiting dilution

Representative confocal images of limiting dilution generated 3T3-L1 fibroblasts stably expressing FRB-LYN11-mcherry as a polyclonal cell line. Random views from single colonies show that less than 30% of cells display a successful stable transfection of FRB-LYN11-mcherry. None of the colonies had a stable transfection rate of above 30%. Scale bar represents 50 µm.

A stable cell line of the FRB-LYN11-mcherry and FRB-LYN11-CFP was generated using G418 media, as the plasmid contains neomycin resistance. To obtain colonies from single cells the transfected 3T3-L1 fibroblasts are submitted to limiting dilution to

generate cell colonies from a single G418 resistant cells. Confocal images from a single colony show LYN11-FRB-mcherry positive and negative cells, shown in Figure 35. 10 colonies in total were tested and none of the colonies have more than 40% positive cells. This result shows that this technique for generating a stable cell line was inappropriate.

To improve the percentage of stable transfected 3T3-L1 fibroblasts FACS sorting was used to sort for mCherry positive cells from cells which are G418 resistant. Images show that FACS sorting did not improve the percentage of LYN11-FRB-mcherry cells, shown in Figure 36. This result concluded the use of stable cell line for this investigation.

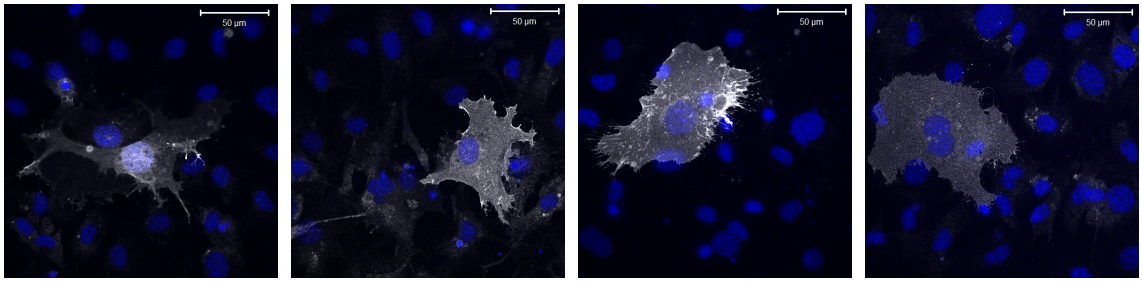

Figure 36: Confocal images of 3T3-L1 fibroblast cell which stably express FRB-LYN11-mcherry and have been FACS sorted.

Representative confocal images of FACS sorted 3T3-L1 fibroblasts stable polyclonal line expressing FRB-LYN11-mcherry. As is shown in the confocal images FRB-LYN11-mcherry positive expressing cells make up less than 10% of cells viewed. Scale bar represents 50 µm.

5.6.3 Lentivirus production

The lentiviral expression construct was co transfected with the packing plasmids into producing cells, HEK293FT. The packaging plasmids used are the pPACKH1™ constructs from system biosciences. Virus production was tested using Lenti-X™ GoStix™, the titre test was positive for all components and viral supernatant was tested on HeLa cells for efficacy. Images from infected 3T3-L1 fibroblast cells show no expression of plasmid inserts, shown in Figure 38. To test that the lentiviral expression constructs express the plasmid inserts HEK293FT cells are transfected and visualised. Results from lentiviral expression construct transfection are shown in Figure 37. The plasmids successfully express mCherry which was cytosolically localised, as previous expected for the PJ phosphatases (Hammond *et al.*, 2014). The expression of the vectors containing active PJ phosphatases results in a significant proportion of cells positive for the PJ phosphatase becoming multinucleated, Figure 37A-C. Multinucleation was an indication that cells are not able to divide properly when expressing the PJ phosphatases. This indicates issues with cytokinesis and viral budding as both of these processes require membrane scission. The phosphatases are active when expressed and it was possible that this was causing an imbalance in the PI population at the membrane affecting scission (Berger *et al.*, 2011; Altan-Bonnet and Balla, 2012).

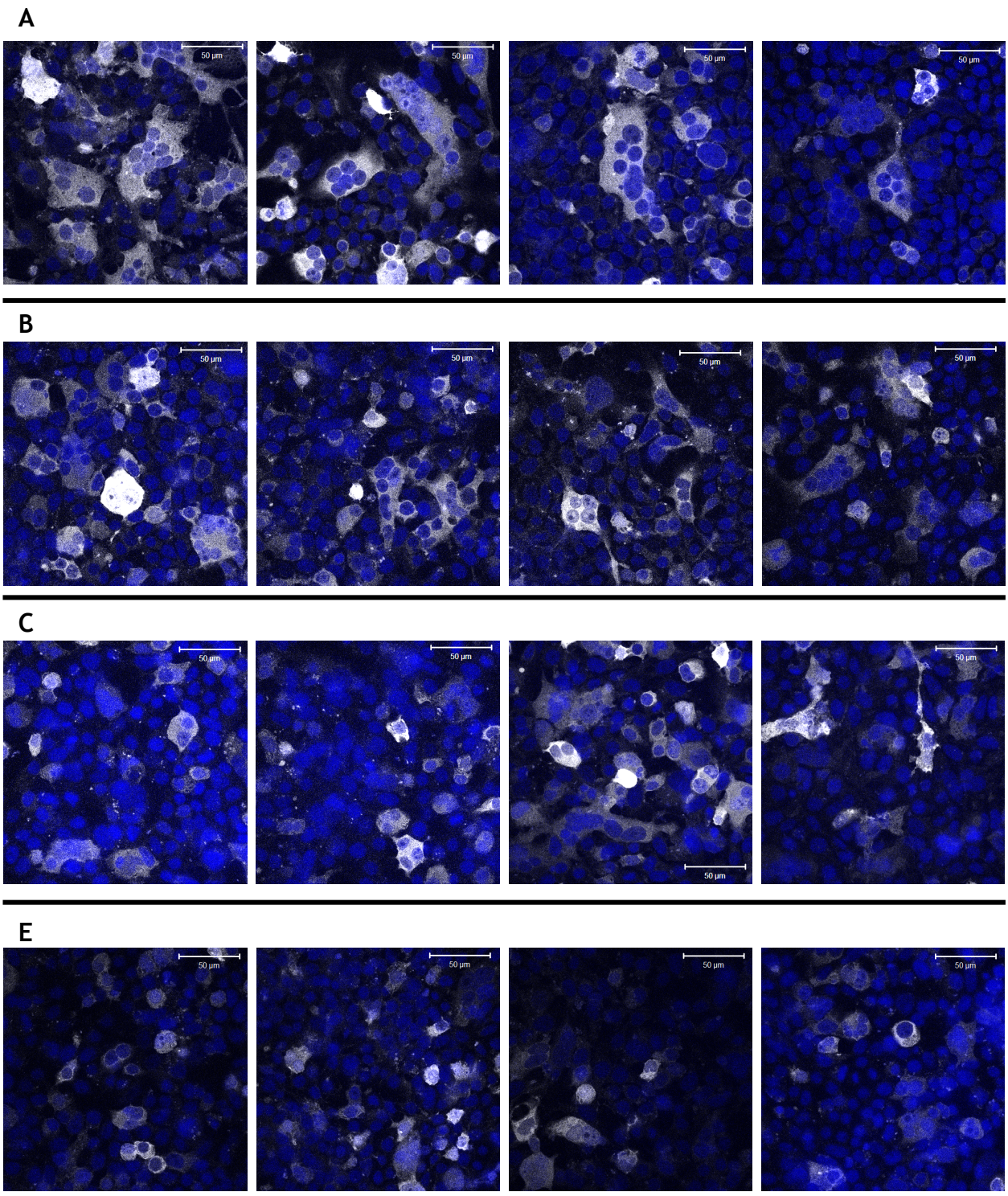

Figure 37: Confocal images of lentiviral plasmid pCDH-FKBP-Pseudojanin-mcherry expressed in HEK293FT

Representative confocal images of HEK293FT cells transfected with plasmid expressing mcherry tagged A. pCDH-FKBP-PJ B. pCDH-FKBP-PJ (Sac1) C. pCDH-FKBP-PJ (INPPE5) E. pCDH-FKBP-PJdead constructs. Multinucleated cells make up a large proportion of transfected cells for A. 51% B. 40% C. 35% E. 12%. Scale bar represents 50 µm.

A

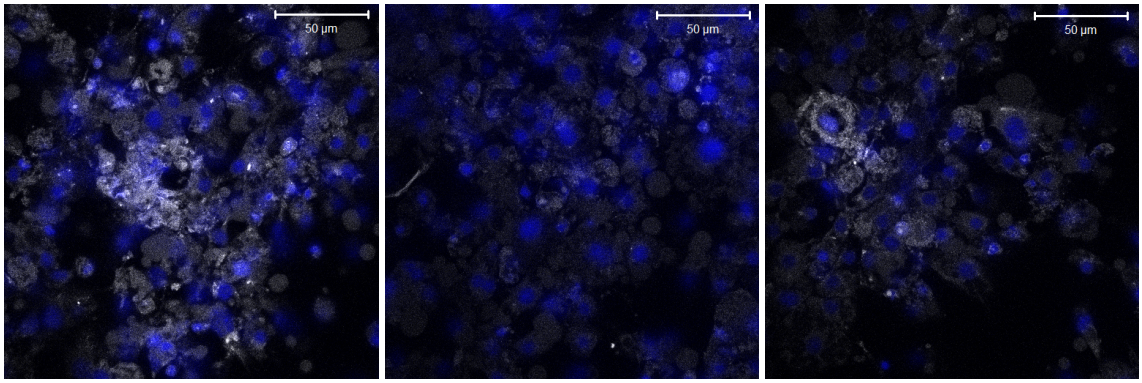

B

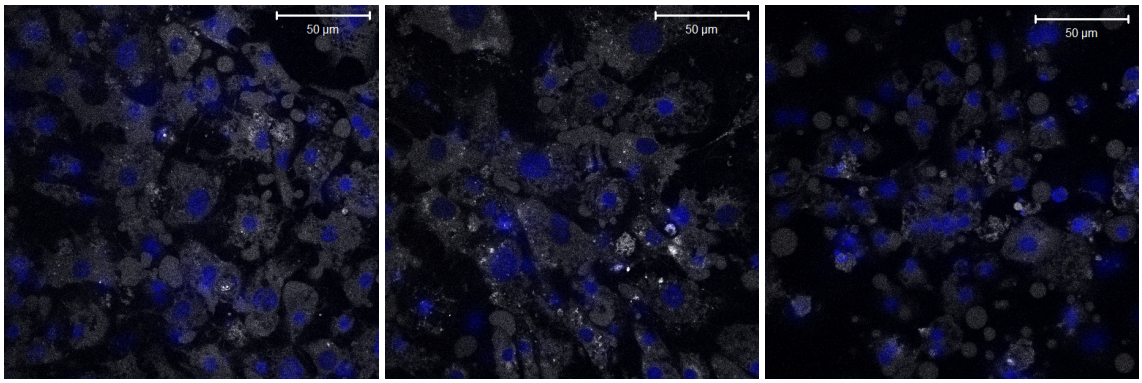

Figure 38 : Confocal images of 3T3-L1 fibroblast infected with pCDH-pseudojanin

A. 3T3-L1 adipocyte cells infected with pCDH-Pseudovirus lentivirus on day 6-post differentiation using recommended TU/million cells. B. 3T3-L1 adipocyte cells that were not infected with lentivirus.

Images taken using the same laser intensity settings to account for 3T3-L1 adipocyte auto fluorescence. Scale bar represents 50 µm.

5.7 DISCUSSION

5.7.1 Visualisation of phosphoinositide's

Visualisation of PI4P and PI4,5P_2 in HeLa cells demonstrates PM localisation. PI4P visualisation shows both intracellular perinuclear compartment localisation, and uniform lawn at the PM. PI4P in HeLa cells have minimal patches at the PM represented in these images. The images from PI4,5P_2 probe show PM localisation with numerous concentrated distinct patches noted at the PM. In 3T3-L1 adipocytes PI4,5P_2 localisation was shown to be at the PM, with patches as seen in HeLa cells. Further intracellular localisation was observed in some cells, this was not consistent across all images and was therefore potentially a result of plasmid DNA delivery.

When studying various PI populations at the PM the use of PH domains was ubiquitous within in the field (Hammond *et al.*, 2012). A new technique to visualise nanoscale landscape PI groups at the PM based on the specific PH probes have been developed using super-resolution fPALM microscopy combined with TIRF (Ji *et al.*, 2015). However, it was important to consider the possibility that not all PH domains have access to all the PIs at the PM due to the presence of endogenous proteins which bind to and sequester specific PIs for function (D'Angelo *et al.*, 2008). The binding of other effector proteins to the PIs would result in inhibition of fluorescent probe binding due to space hindrance. The use of PI probes has previously been employed in studies to inhibit binding, of effector proteins to the specific PI (Wang *et al.*, 2005). It was therefore important to appreciate that the use of these probes in a system may inhibit the molecular mechanisms being investigated.

5.7.2 Future work investigating PI4P foci at the PM in adipocytes.

To improve results when investigating PIs in cells other techniques could be employed for future investigations. Techniques commonly used to identify and quantify PIs in the cell include thin layer chromatography (TLC), and ion-exchange HPLC separation in cells labelled with [^{32}P]inorganic phosphate or [^{3}H]inositol (Milne *et al.*, 2005; Rusten and Stenmark, 2006; Kim *et al.*, 2010). However, the major drawback of these techniques was that the phosphorylation position on the inositol ring cannot be distinguished. Therefore, the difference between PI4P and PI5P cannot be evaluated. This technique was still viable as overall PIP or PIP_2 levels can be analysed, with the knowledge that both PI4P and $PI4,5P_2$ are the predominant PI populations in higher eukaryotes. Therefore, any significant changes in PIP levels are predominantly attributed to be changes in PI4P levels in the cell (Idevall-Hagrena and De Camilli, 2015). However, to distinguish between the distinct populations of PIP, and PIP_2 other techniques are required.

The development of fluorescent probes fused with PI binding domains which are capable of selectively binding to specific PI identities has been integral to the microscopic study of PI (Balla *et al.*, 2005). A large number of PI binding protein domains have been identified for example; the PX domain from Tubby protein and the PH domain from PLCδ1 both selectively bind $PI4,5P_2$ (Várnai and Balla, 1998; Santagata *et al.*, 2001). In particular when studying PIs at the PM TIRF microscopy has been a powerful method for elucidating events at the PM (Knight and Falke, 2009).

Previous studies have shown that the over expression of phosphoinositide binding domain probes has an inhibitory effect on the interaction of other PI binding proteins in the cell. The over expression of both Akt and Btk PH domains which recognise and bind $PI3,4,5P_3$ resulted in the inhibition of $PI3,4,5P_3$ stimulated Akt/PKB activation (Varnai *et al.*, 2005). The over expression of PH binding of other proteins, such as ARO and GRP1, had no such inhibitory effects (Varnai *et al.*, 2005). The activation of the G-protein coupled receptors type 1 muscarinic receptor and bradykinin 2 receptor, results in the phosphorylation of $PI4,5P_2$ and production of $PI3,4,5P_3$. Cells expressing the $PI4,5P_2$ binding probe PLCδ-GFP show that in response to receptor stimulation the probe PLCδ-GFP was displaced from the PM to the cytosol (Wang *et*

al., 2005). Indicating that the probe was displaced upon receptor stimulation and allows for cellular processes to continue uninhibited. These findings show that the binding of the PI binding probes can be used as a tool to visualise specific PI populations without inhibiting cellular processes. However, it was important to be aware that inhibition may occur as a result of over expression of probes containing these binding domains if binding partners and effectors of the specific PI exhibit competitive binding. Results in this chapter show that the PI4P binding probe SidM-P4M-GFP localisation was altered in response to insulin stimulation.

5.7.3 Developing the Pseudojanin system for future studies

Achieving the direct manipulation of PI populations would have been an impressive experiment to observe the effect depletion of specific PI groups ($PI4,5P_2$, PI4P, PI5P) on glucose uptake. This would have revealed if the presence of PI4P at the PM was important for insulin mediated glucose uptake. Therefore, if the function of EFR3 is based on the generation of PI4P at the PM. This experiment required a high expression percentage of two vectors to observe effects on glucose uptake, this was not achieved using the strategy of generating a stable cell 3T3-L1 cell line with the FRB-LYN11 anchor component and a lentiviral vector containing the FKBP-pseudojanin component for infection of terminally differentiated 3T3-L1 adipocytes. Future work may involve changing the CMV promoter of these components as it may not be compatible with 3T3-L1 adipocytes for stable cell line generation. An inducible promoter would be a more appropriate system for introducing the phosphatases due to the formation of multinucleated cells noted in HEK293FT cells when generating lentivirus. Viral budding and cytokinesis are two linked process which both require similar scission machinery for example ESCRT proteins (endosomal sorting complex required for transport) (Wollert *et al.*, 2009).

5.8 CONCLUSION

The findings in this chapter reveal that the phospholipid PI4P is present in a distinct manner in 3T3-L1 adipocytes. PI4P forms foci in 3T3-L1 adipocytes and the number of foci was reduced upon insulin stimulation indicating an insulin dependent effect. Crucial experimentation would involve direct manipulation of PI4P at the PM to elucidate if the effect on PI4P patches at the PM was a causative or correlative

result. Work to achieve this showed the experimental strategy employed was not possible using adipocytes for glucose uptake. As this global approach is beyond current tools future work may be possible observing single cells using 4 colour imaging. This would give a qualitative overview of how PI4P affects the PM GLUT4 of adipocytes opposed to the more quantitative result the experimental strategy followed in this thesis would have yielded. Therefore results herein cannot definitively state if it is the levels of PI4P which affect GLUT4 at the PM in response to insulin stimulation or an unknown function of EFR3. It is however most likely any effect produced by EFR3 is a result of PI4P levels at the PM based on the literature available (Baird *et al.*, 2008; Nakatsu, Jeremy M. Baskin, *et al.*, 2012; Bojjireddy *et al.*, 2015).

6 ROLE OF EFR3A DURING INSULIN STIMULATED GLUT4 DISPERSAL

6.1 INTRODUCTION

Understanding of GLUT4 response to insulin has long focused on the delivery of GLUT4 storage vesicles (GSVs) to the PM (Huang and Czech, 2007). The mechanisms underpinning GLUT4 delivery to the PM in response to insulin stimulation rely on several distinct processes; endocytosis, sorting, sequestering, release, tethering, fusion and dispersal (Shewan *et al.*, 2000; Blot and McGraw, 2006; Stenkula *et al.*, 2010; Bryant and Gould, 2011; Lizunov, Stenkula, *et al.*, 2013; Brewer *et al.*, 2014). Much of the molecular mechanisms behind the majority of these steps have been identified and characterised. GLUT4 dispersal at the PM in response to insulin signalling has recently been identified and characterised, but the molecular mechanism behind this remain uncharacterised (Stenkula *et al.*, 2010; Lizunov *et al.*, 2012; Lizunov, Stenkula, *et al.*, 2013).

To identify a molecular mechanism behind this the results from a previous genetic study in yeast was used (Wieczorke *et al.*, 2003). Yeast have no endogenous GLUT4 transporters, when GLUT4 was expressed it was intracellular sequestered, as in mammalian cells. Yeast strain with all hexose transporters deleted (Δhxt) which are expressing mammalian GLUT4 are however unable to sustain life when fed glucose. This study found that a double mutation *fgy1-1* and fgy4X was required for GLUT4 mediated glucose uptake in yeast. The *fgy1-1* mutation was a mutant allele of gene FGY1, which encodes the protein EFR3 in yeast. GLUT4 transport has been shown to be conserved from yeast to mammals, with yeast capable of sequestering GLUT4 internally in GSV type bodies (Shewan *et al.*, 2013). EFR3A in 3T3-L1 adipocytes and HeLa's has been characterised to localise to the PM in chapter 4. Results from mice samples in chapter 4 indicate that EFR3A and PI4KIIIα protein levels are elevated in insulin sensitive tissue of mice which have impaired glucose tolerance. This is indicative of a compensatory effect as a disease is developed, and therefore indicates our initial hypothesis that *fgy1-1* was a loss of function mutation of Efr3 appears incorrect. This chapter aims to test the hypothesis for how EFR3A may affect GLUT4 at the PM in response to insulin stimulation.

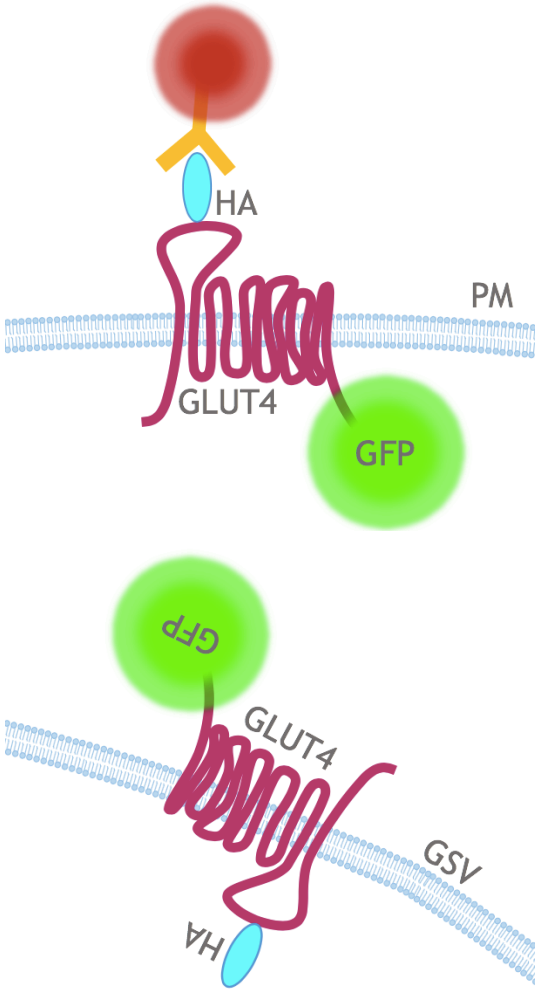

Figure 39: Schematic of HA-GLUT4-GFP plasma membrane staining

HA-GLUT4-GFP expressing cells can be used to measure the plasma membrane GLUT4 levels relative to total GLUT4 levels of the cell. The HA epitope tag expressed on the extracellular loop of GLUT4 is stained using antibody labelling in non-permeabilised cells. Therefore, only HA which is extracellularly exposed (ie GLUT4 fused to the PM) is stained. The GFP signal is seen for both intracellularly localized GLUT4 and PM fused GLUT4 and acts as an internal control for total GLUT4. This technique has been employed by others in both HeLa and 3T3-L1 adipocytes.

HeLa cells provide a model system which can be used to demonstrate an effect on PM GLUT in the cell expressing HA-GLUT4-GFP. 3T3-L1 adipocytes expressing HA-GLUT4-GFP also provide a more physiologically relevant model to investigate PM GLUT4, the schematic of how HA-GLUT4-GFP can be used to quantify plasma

membrane GLUT4 levels is shown above in Figure 39 (Martin *et al.*, 2006; Sadler, Bryant, *et al.*, 2015). The HA-epitope tag is exposed at the extracellular surface when GLUT4 was fused at the PM. This allows for the HA tag to be fluorescently immuno-labelled at the PM in non-permeabilised cells. Therefore in HA-GLUT4-GFP expressing cells HA staining intensity correlates to PM GLUT4 levels and GFP fluorescence intensity correlates to total GLUT4 content of the cell, and therefore can be used to normalise measurements (Kioumourtzoglou *et al.*, 2015). HeLa cells are regularly used in this model despite not expressing endogenous IR and GLUT4, when expressing HA-GLUt4-GFP translocation from intracellular stores to the PM was still triggered by insulin stimulation, the insulin stimulated increase is less than that seen in 3T3-L1 adipocytes and therefore it is possible to miss effects on PM GLUT4 using this model (Haga *et al.*, 2011). The introduction of plasmid DNA to 3T3-L1 adipocytes by traditional methods was inhibited due to the high lipid content of the cell, meaning the introduction of plasmid DNA to adipocytes was not a simple process (Okada *et al.*, 2003). HeLa cells however are readily transfected using standard protocols, the HA-GLUT4-GFP expressing HeLa cells therefore provide a transfectable model system to gather preliminary results in. This can be used to investigate if EFR3A has a positive or negative effect on PM GLUT4 and how insulin stimulation is involved.

The end result of translocation of GLUT4 to the PM is to increase glucose uptake of the cell. This provides a measurable output for how EFR3A and PI4KIIIα may affect GLUT4 via the uptake of glucose within these cells. PI4KIIIα activity can be inhibited using phenylarsine oxide, providing a method for inhibiting the production of PI4P at the PM inner leaflet.

6.2 AIMS

The aim of this chapter was to characterise the role of EFR3A in insulin stimulated GLUT4 behaviour at the PM. Chapter 4 has shown that EFR3A was localised to the PM in adipocytes, as the molecular mechanism behind insulin stimulated GLUT4 behaviour

6.3 The Effect of EFR3 overexpression in GLUT4 expressing HeLa Model System

6.3.1 Confocal visualisation of the effect of EFR3 on GLUT4 at the plasma membrane

Images of HeLa cell line expressing HA-GLUT4-GFP transfected with high copy EFR3A-mcherry or EFR3B-mcherry plasmid are shown in Figure 40 &Figure **41** respectively. As previously characterised in 4.5.1 EFR3A and EFR3B exhibit PM localization in HeLa cells, seen in the white panel of Figure 40 & Figure **41**. HA-staining in cells positive for EFR3A and EFR3B, depicted with white arrows, was increased in comparison to non-transfected cells. HA-staining was increased in insulin stimulated and non-insulin stimulated samples, indicating that there still was an insulin effect, but it was diminished.

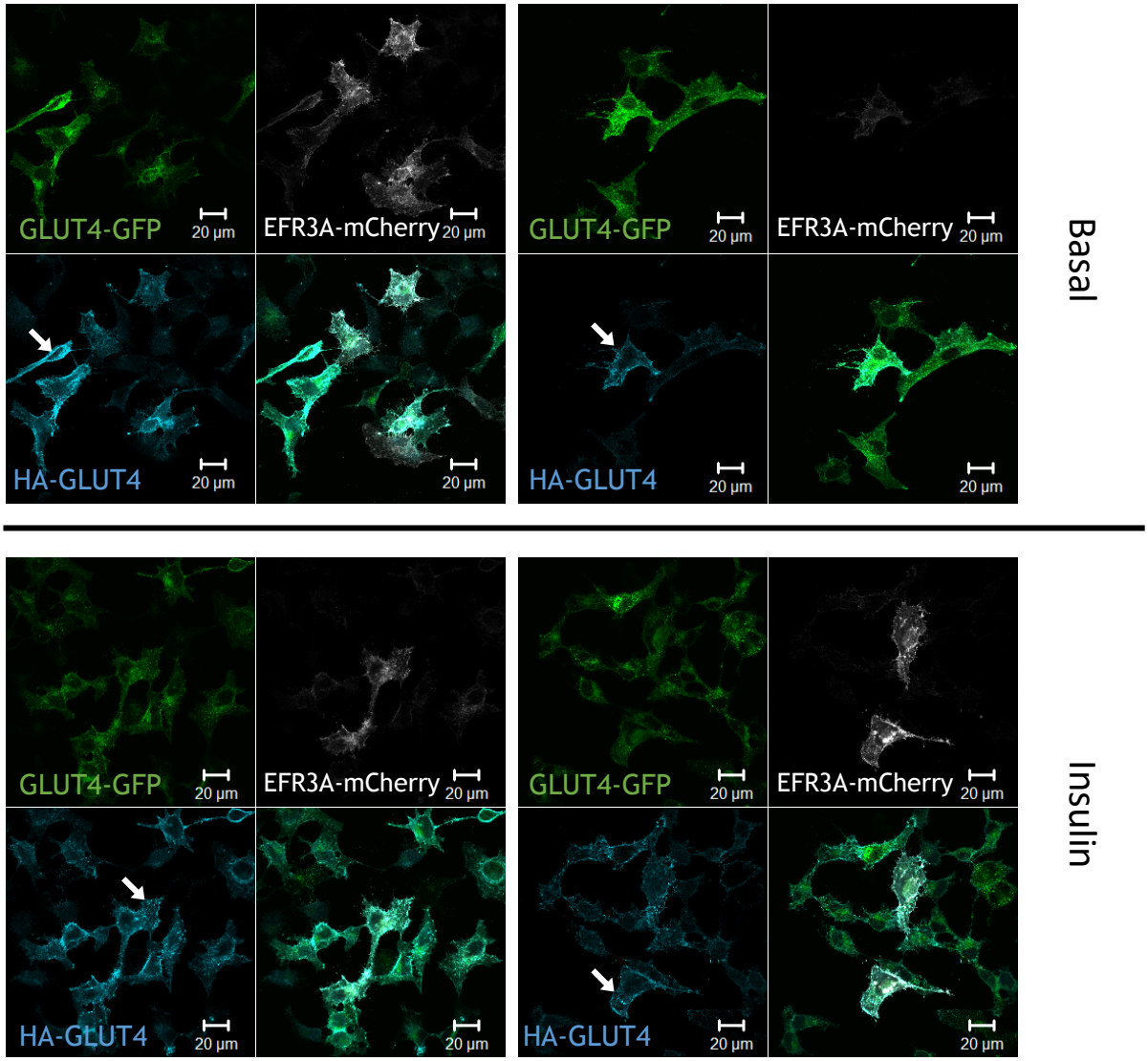

Figure 40: Confocal microscopy images of EFR3A-mcherry expressing HA-GLUT4-GFP HeLa cells

Representative confocal microscopy images of HA-GLUT4-GFP expressing HeLa cells over-expressing with EFR3A-mcherry. EFR3A-mcherry positive expressing cells (white panel), HA-GLUT4 staining (blue panel) and GLUT4-GFP (green panel). HA staining in non-permeabilised cells represents plasma membrane GLUT4. Cells over-expressing EFR3A indicated with white arrows in the blue panel. HeLa cells are serum starved for 3 hours and insulin stimulated for 20 minutes with 0.1 uM insulin.

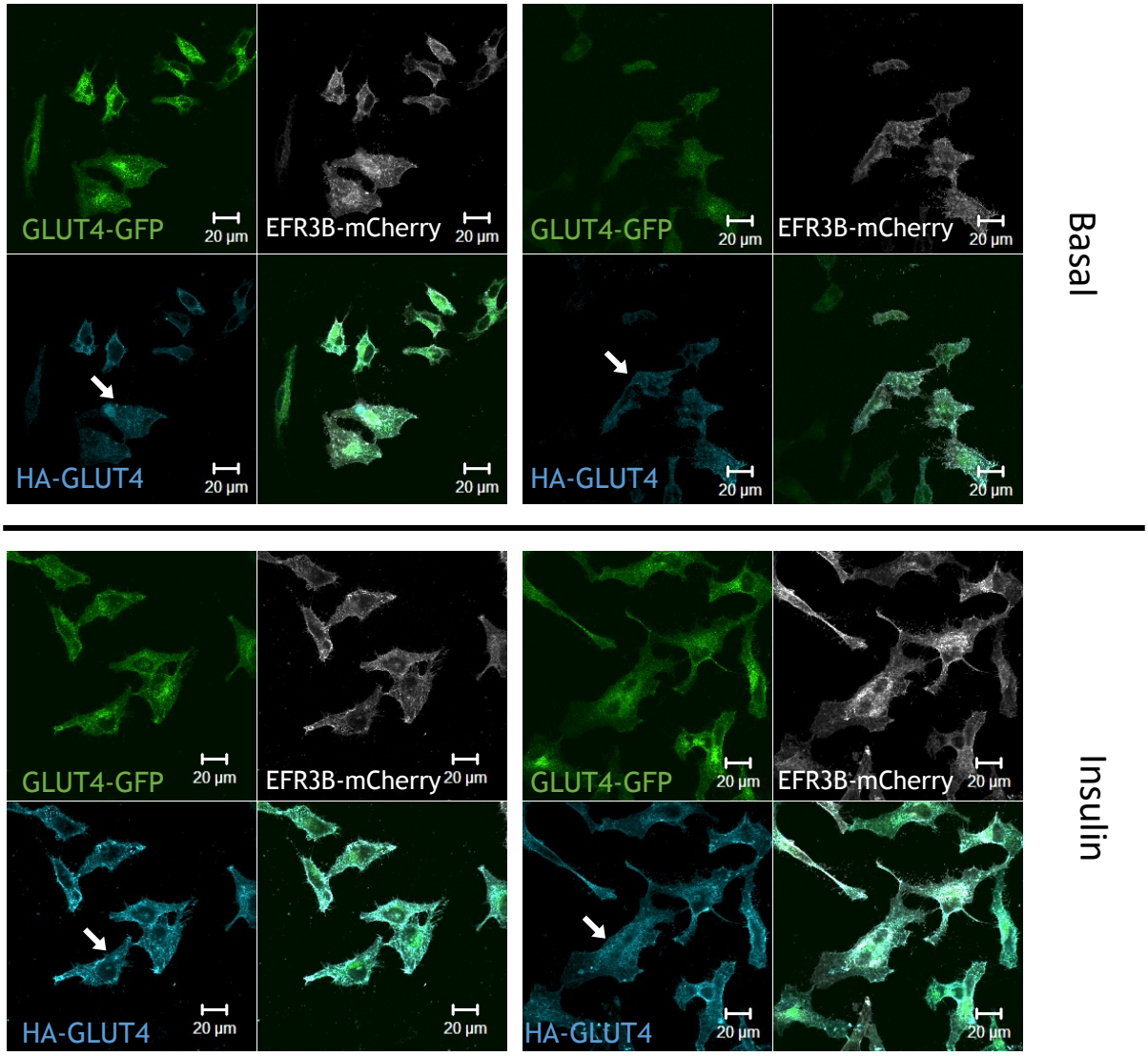

Figure 41: Confocal microscopy images of EFR3B-mcherry expressing HA-GLUT4-GFP HeLa cells

Representative confocal microscopy images of HA-GLUT4-GFP expressing HeLa cells over-expressing with EFR3B-mcherry. EFR3B-mcherry positive expressing cells (white panel), HA-GLUT4 staining (blue panel) and GLUT4-GFP (green panel). HA staining in non-permeabilised cells represents plasma membrane GLUT4. Cells over-expressing EFR3B, indicated with white arrows in the blue panel. HeLa cells are serum starved for 3 hours and are insulin stimulated for 20 minutes with 0.1 uM insulin.

6.3.2 Effect of EFR3 overexpression on plasma membrane GLUT4 in HeLa cells

The HA epitope tag on GLUT4 allows for the relative PM exposed GLUT4 in comparison to the total GLUT4 to be measured using fluorescence microscopy images and ImageJ to measure mean intensity, results are shown in Figure 42. Results show that insulin stimulation of HeLa cells results in a 2.09-fold increase in PM GLUT4. HeLa cells over expressing EFR3A have a 1.50-fold increase in PM GLUT4 and cells expressing EFR3B have a 2.07-fold increase in PM GLUT4 in response to insulin stimulation. HeLa cells stimulated with insulin compared with HeLa cells which are not stimulated with insulin but are over expressing EFR3A or EFR3B have similar measured PM GLUT4 levels, 1.2 ($P>0.1$) and 0.98 (NS) fold difference respectively. The difference in PM GLUT4 levels in insulin stimulated HeLa cells which over express EFR3A and EFR3B was not significant 1.03-fold. The difference between homologs was non-significant apart from the increase in PM GLUT4 in response to insulin stimulation was greater in cells expressing EFR3B. As previous data indicates that EFR3A was the dominantly expressed homolog in HeLa and 3T3-L1 adipocytes future investigation will focus on EFR3A. Results show that cells which are overexpressing EFR3A or the homolog EFR3B have an increase in PM GLUT4 in comparison to the non-transfected HeLa cells.

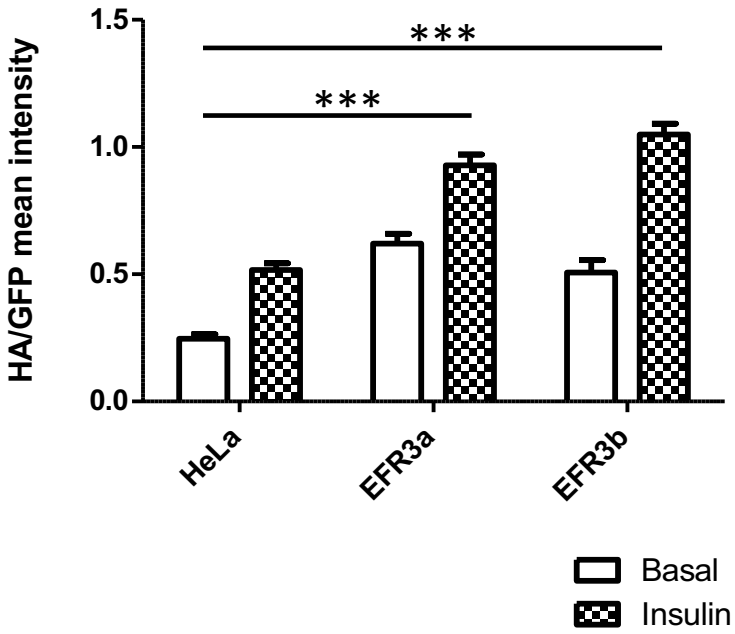

Figure 42 : The effect of over expression of EFR3A and EFR3B on plasma membrane GLUT4 in HeLa cells

HeLa cells stably express HA-GLUT4-GFP were transiently transfected with EFR3A-mcherry and EFR3B-mcherry. The HA epitope tag was stained at the plasma membrane (PM) in non-permeabilised cells. A. Individual cell HA staining fluorescence intensity measurements using imageJ were quantified and normalised to GFP fluorescent intensity, correlating to total cell GLUT4. HeLa cells have a measured 2.09 fold increase in PM GLUT4 in response to 20-minute 0.1 uM insulin stimulation. Cells expressing EFR3A and EFR3B have a measured increase in PM GLUT4 in non-stimulated cells and an insulin stimulated increase in PM GLUT4 is still measured. Error bars represent SEM. Over expression of EFR3 results in increased surface GLUT4 in both insulin stimulated (+) and basal (-) conditions Number of cells measured; EFR3A (+) n=48, EFR3A (-) n=37, EFR3B (+) n= 70, EFR3B (-) n=29, HeLa (+) n=67, HeLa (-) n= 70. *** P value < 0.0001, ** P value < 0.001 from two way ANOVA analysis.

6.3.3 Effect of dominant negative EFR3A mutant EFR3A(C6-9S) on plasma membrane GLUT4 in HeLa cells

6.3.3.1 Visualisation of EFR3A(C6-9S)-tdtomato in HA-GLUT4-GFP HeLa cells

The HeLa cell line stably expressing HA-GLUT4-GFP was transfected with high copy EFR3A (C6-9S) – tdtomato containing plasmid (Nakatsu et al., 2012). Mutation of the palmitoylation sites C6 – 9 to serine inhibits post translational modification. EFR3A was no longer membrane associated and was miss-localised from the PM to the cytosol as shown in the white panels in Figure 43. EFR3A(C6-9S) was still able to bind to the PI4KIIIα intermediator binding protein TTC7, as the binding domain at the C terminal has not been mutated (Nakatsu, et al., 2012; Wu et al., 2014). Therefore EFR3A(C6-9S) overexpression will miss-localise PI4KIIIα acting as a dominant negative mutant. Images of HA-GLUT4-GFP expressing HeLa cells transfected with EFR3A(C6-9S) show decrease in HA staining in the insulin stimulated cells in comparison to non-transfected cells, indicated with white arrows in the HA staining panel of Figure 43.

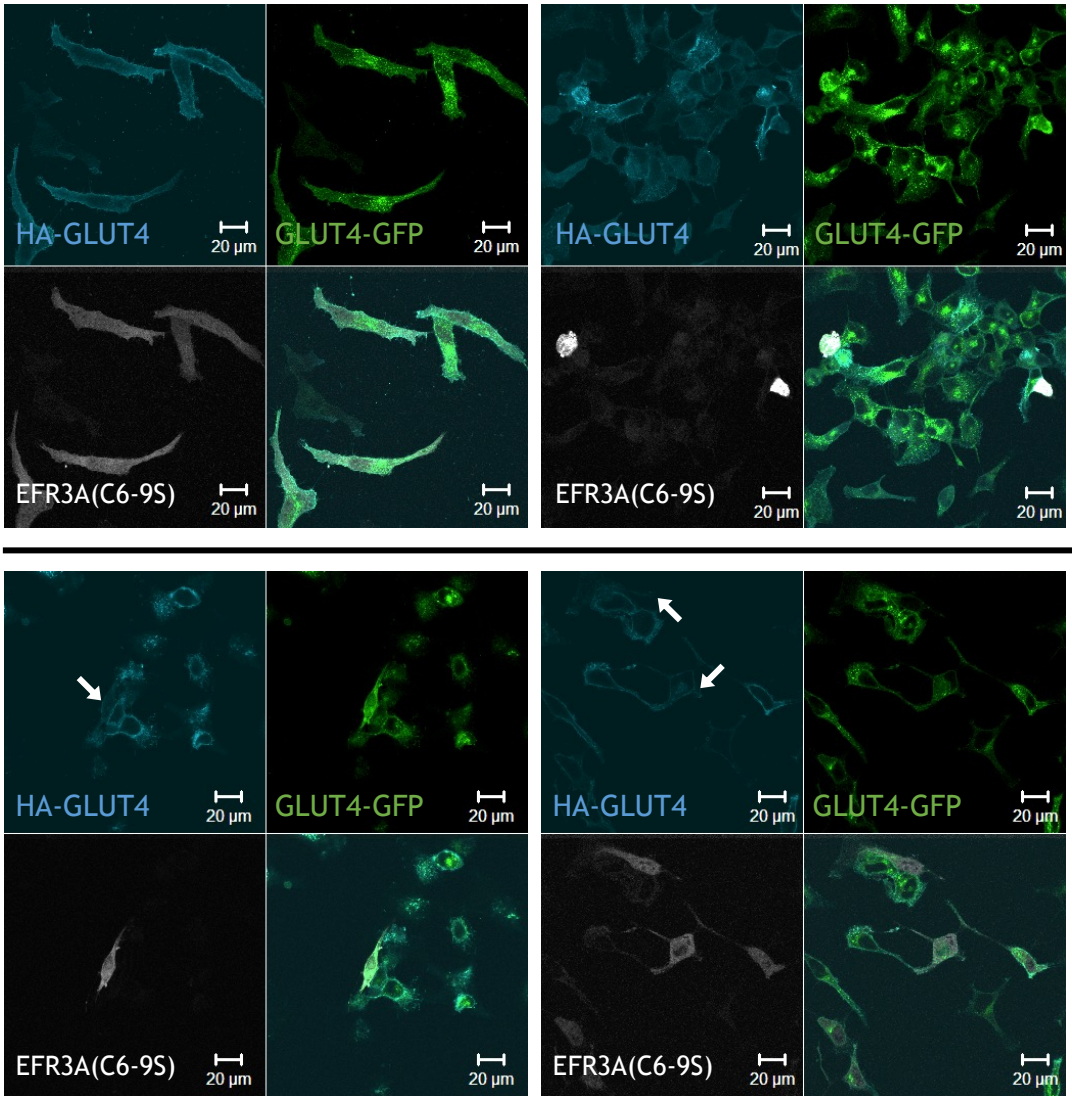

Figure 43: The effect of over expression of EFR3A dominant negative mutant on plasma membrane GLUT4 in HeLa cells

Representative confocal microscopy images of HA-GLUT4-GFP expressing HeLa cells transfected with EFR3A (C6-9S)-tdtomato. EFR3A (C6-9S)-tdtomato positive expressing cells (white panel), HA-GLUT4 staining (blue panel) and GLUT4-GFP (green panel). HA staining in non-permeabilised cells represents plasma membrane GLUT4. HA-staining was diminished in insulin-stimulated cells transfected with EFR3A (C6-9S)-tdtomato, indicated with white arrows. HeLa cells are serum starved for 3 hours and insulin stimulated for 20 minutes with 0.1 uM insulin.

6.3.3.2 Effect of EFR3(C6-9S) overexpression on plasma membrane GLUT4 in HeLa cells

The HA epitope tag on GLUT4 allows for the relative PM exposed GLUT4 compared to total GLUT using the GFP intensity. This can be used to measure PM GLUT4 in a cell expressing HA-GLUT4-GFP and was quantified per cell using ImageJ, the data from images shown in Figure 43 was shown in Figure 44. Results show that insulin stimulation of HeLa cells results in a 1.73-fold increase ($P>0.01$) in PM GLUT4. HeLa cells over expressing EFR3A(C6-9S) have a 0.6901-fold difference (NS) in PM GLUT4 in response to insulin stimulation. There was a 0.77 (NS) fold difference between PM GLUT4 levels in non-insulin stimulated HeLa cells and HeLa cells expressing EFR3A(C6-9S). The difference between PM GLUT4 of HeLa and EFR3A(C6-9S) expressing HeLa insulin stimulated cells was ~3 fold decrease ($P>0.01$). The results show that EFR3A(C6-9S) expression has minimal effect on PM GLUT4 in HeLa cells which are not insulin stimulated. Cells over expressing EFR3A(C6-(S) have eliminated the insulin effect, with no increase in PM GLUT4 in response to insulin stimulation. Over expression of EFR3A(C6-9S) results in a significant decrease in PM GLUT4 in insulin stimulated cells in comparison to non-transfected cells.

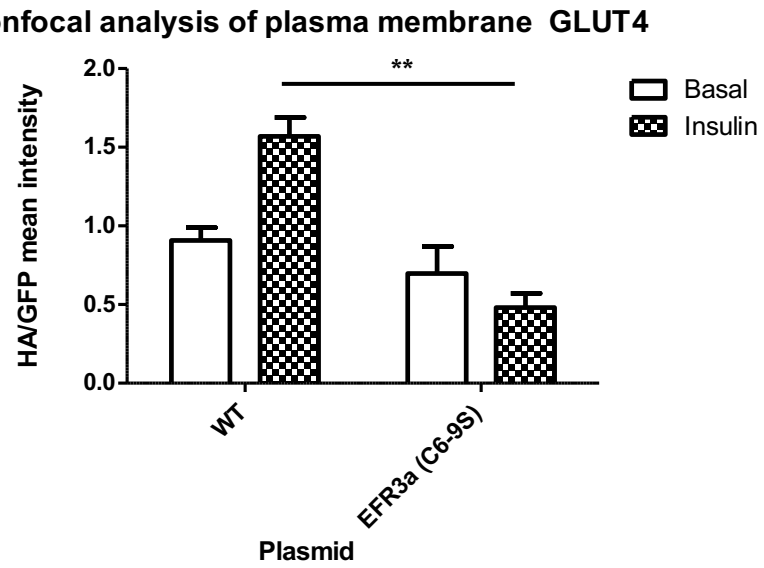

Figure 44: The effect of over expression of EFR3A dominant negative mutant on plasma membrane GLUT4 in HeLa cells

Graph showing the levels of PM GLUT4 in HeLa cells expressing different plasmids in response to insulin stimulation. Images show a representative confocal image of each condition; blue represents HA staining, green represents GFP, and white represents transfected tdtomato labelled protein. Error bars represent SEM. Number of cells measured; EFR3A (C6-9S) (+) n=23, EFR3A (C6-9S) (-) n=34 HeLa (+) n=30, HeLa (-) n= 32. *** P value < 0.001 from two-way ANOVA analysis. Cells are serum starved for 3 hours and insulin stimulated for 20 minutes with 0.1 uM insulin.

6.4 Fluorescence-Activated Cell Sorting Analysis of Plasma Membrane GLUT4 in HeLa Model System

Previous results using confocal microscopy has shown in the HA-GLUT4-GFP expressing HeLa cells that EFR3A over expression affects plasma membrane GLUT4. To confirm these results in a manner which has removed bias from the sample collection and increased cells analysed FACS was used. This technique allows for hundreds and thousands of cells to be analysed in comparison to the tens of cells analysed using microscopy. FACS analysis results, displayed below in Figure 45, show that over expression of EFR3A in this system leads to an increase in plasma membrane GLUT4. FACs analysis of HeLa cells show 1.38 ($P<0.001$) fold increase in PM GLUT4 in response to insulin stimulation. HeLa cells over expressing EFR3A have a measured 1.34 ($P<0.001$) fold increase in PM GLUT4 in response to insulin stimulation. In non-insulin stimulated cells over expressing EFR3A the GLUT4 levels at the PM was 1.23 ($P<0.001$) fold increased in comparison to the non-transfected insulin stimulated HeLa cells. Cells over expressing EFR3A have a 1.69 ($P<0.001$) increase in PM GLUT4 in comparison to un-transfected cells in the absence of insulin stimulation. Over expression of EFR3A results in a larger increase in PM GLUT4 than insulin stimulation in FACS analyses HeLa cells. This result shows EFR3A over expression results in increased PM GLUT4, and an insulin response was still measured. The dominant negative mutant EFR3A (C6-9S) was mutated at the palmitoylation site and therefore no longer localises to the plasma membrane. Microscopy images, shown in Figure 43, confirm this was now a cytosolic localised protein. EFR3A (C6-9sS) was still capable of binding PI4KIIIα machinery, therefore localising this to the cytosol. HeLa expressing this dominant negative EFR3A (C6-9S) show an impaired insulin response, with a non-significant 1.18-fold increase in plasma membrane GLUT4 in response to insulin. Plasma membrane GLUT4 was also significantly lowered in these cells expressing the dominant negative in comparison to non-transfected cells. Insulin stimulated cells expressing EFR3A(C6-9S) have a 1.69 ($P<0.001$) fold decrease in PM GLUT4 in comparison to non-transfected insulin stimulated HeLa cells. The trend observed using confocal microscopy was maintained; over expression of EFR3A increases PM GLUT4 maintaining an insulin effect and over expression of EFR3A (C6-9S) results in decreased PM GLUT4 and inhibition of the insulin effect.

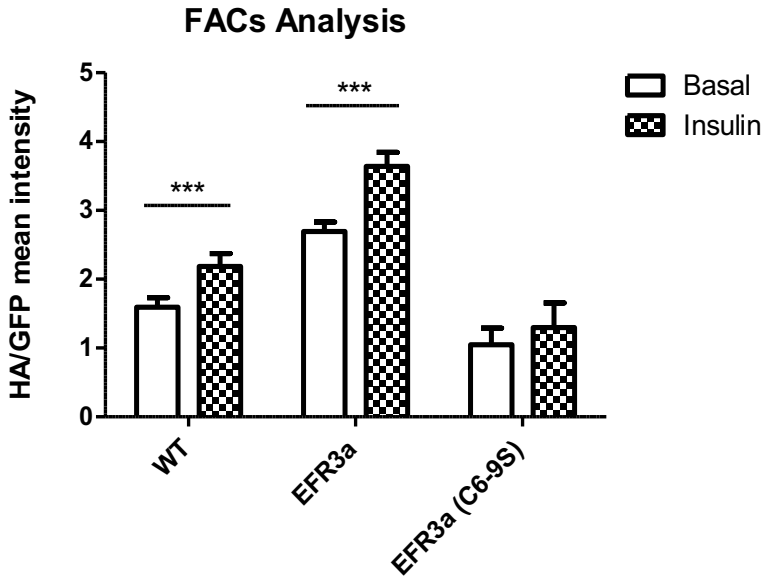

Figure 45 : FACS analysis of the effect of EFR3A and EFR3A (C6-9S) on plasma membrane GLUT4 in HeLa cells

HeLa cells stably expressing mammalian GLUT4 with the epitope tag HA and the fluorescent tag GFP. Cells where transfected using purefection with EFR3A-mcherry or EFR3A(C6-9S)-tdtomato. The HA epitope tag is stained in non-permeabilised cells and the fluorescence is measured of both the HA tag, plasma membrane GLUT4, and GFP, total GLUT4. Difference between plasmids is P>0.001 from two-way ANOVA analysis n numbers as follows; WT basal 13025, WT insulin 12906, EFR3A basal 3071, EFR3A insulin 3691, EFR3A (C6-9S) basal 605, EFR3A (C6-9S) insulin 715. Cells are serum starved for 3 hours and insulin stimulated for 20 minutes with 0.1 uM insulin.

6.5 THE EFFECT OF EFR3A OVER EXPRESSION IN 3T3-L1 ADIPOCYTES.

3T3-L1 adipocytes are a well characterised model for insulin sensitivity as adipocytes are one of the predominant targets of insulin signalling in the body. As with the HeLa model system 3T3-L1 adipocytes stably express HA-GLUT4-GFP. The HA epitope tag allows for the staining and measuring of PM GLUT4 in non-permeabilised cells, shown the blue panel in Figure 46. The internal GFP intensity, shown in the green panel, visualises total GLUT4 in the cell. As shown in Figure 46 below HA staining at the PM was elevated in insulin stimulated adipocytes with a ring formation around the majority of cells, denoted with white arrows. In the unstimulated adipocytes GLUT4-GFP shows a predominantly intracellular localisation, denoted with red arrows. In the insulin stimulated cells GLUT4-GFP fluorescence was localised to the PM in a ring co-localised with the HA staining, denoted by yellow arrows. The effect of insulin was increased in comparison to the model system HeLa cells. Due to the high adiposity of this cell line the delivery of plasmid DNA was inhibited and difficult to overcome with most plasmid DNA transfection techniques. Electroporation offers a robust technique for the transient delivery of plasma DNA to adipocyte cells.

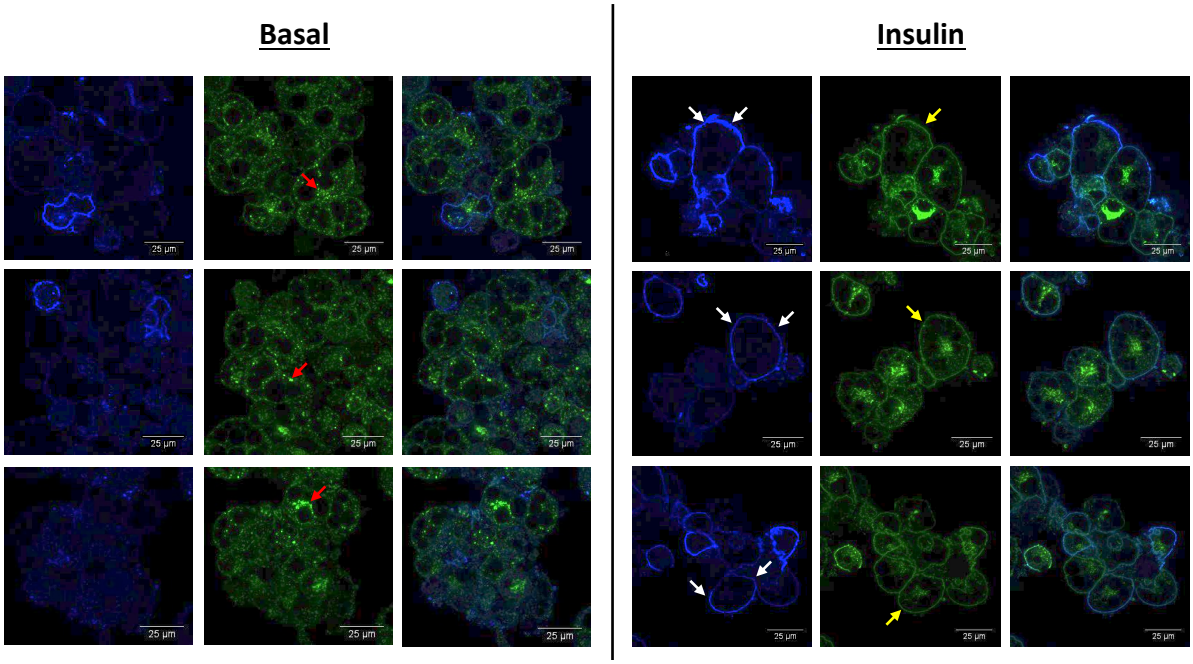

Figure 46: Confocal images of HA-GLUT4-GFP expressing 3T3-L1 adipocytes.

Representative confocal images of 3T3-L1 adipocytes expressing HA-GLUT4-GFP. The left panel represents non-stimulated basal cells and the right panel represents insulin-stimulated cells (20 minutes with 0.1 uM insulin). Blue images are HA epitope tag GLUT4 staining and green images are GLUT4-GFP.

6.5.1 Visualisation of EFR3A in HA-GLUT4-GFP 3T3-L1 Adipocytes

Confocal microscopy of EFR3A-mcherry in HA-GLUT4-GFP expressing adipocytes, shown in Figure 47. Cells expressing EFR3A-mcherry (red panel) have elevated HA staining in the absence of insulin stimulation, denoted by the red arrow in the blue panel of Figure 47A. GLUT4-GFP can be seen at the PM in a ring in the absence of insulin stimulation in cells over expressing EFR3A-mcherry, shown in Figure 47A depicted with the yellow arrow. The HA-staining co-localises with EFR3A in a ring around the cell or across the PM of these cells, depicted in the merged panel with white arrows. In the insulin stimulated cells it can be seen the HA-staining of EFR3A-mcherry positive cells, depicted with red arrows Figure 47B, was in comparison to the un-transfected cells.

Figure 47: Confocal visualisation of EFR3A-mcherry in HA-GLUT4-GFP expressing3T3-L1 adipocytes.

Representative confocal images of 3T3-L1 adipocytes expressing HA-GLUT4-GFP transfected with the EFR3A-mcherry plasmid. Top panel of non-stimulated basal cells. Bottom panel of insulin stimulated cells (20 minutes with 0.1 uM insulin). Blue panel depicts HA epitope staining of GLUT4, green panel depicts GLUT4-GFP, and red panel depicts EFR3A-mcherry positive cells. Red arrows denote EFR3A-mcherry positive cells in the blue panel. Yellow arrows denote GLUT4GFP ring around EFR3A-mcherry positive cells in basal cells. White arrows denote EFR3A-mcherry overlay with GLUT4 in the merge panel. Scale bar denotes 25 μm

Figure 47: Confocal visualisation of EFR3A-mcherry in HA-GLUT4-GFP expressing3T3-L1 adipocytes

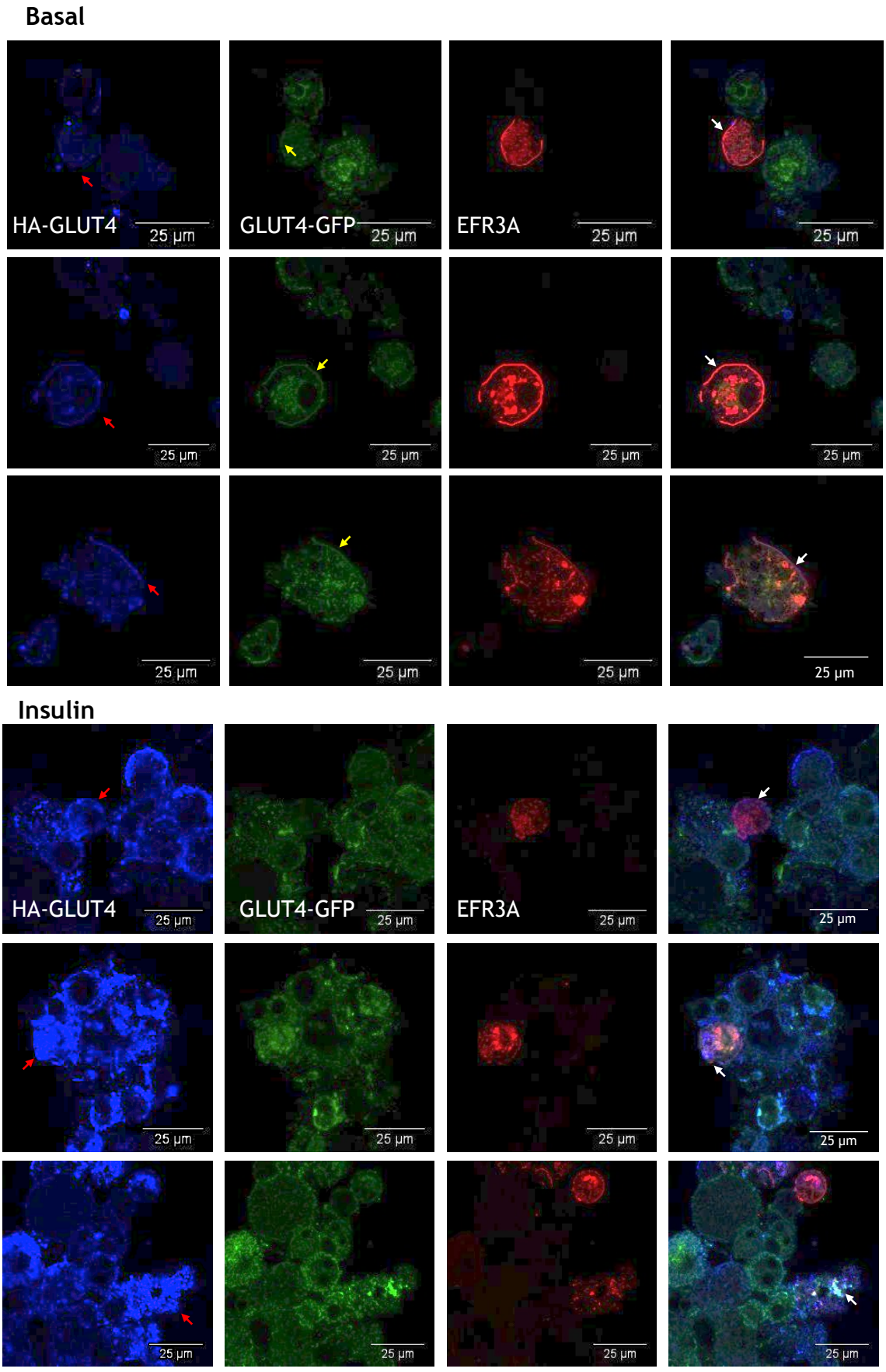

Figure 48: Confocal visualisation of EFR3A (C6-9S)-tdtomato in HA-GLUT4-GFP expressing 3T3-L1 adipocytes

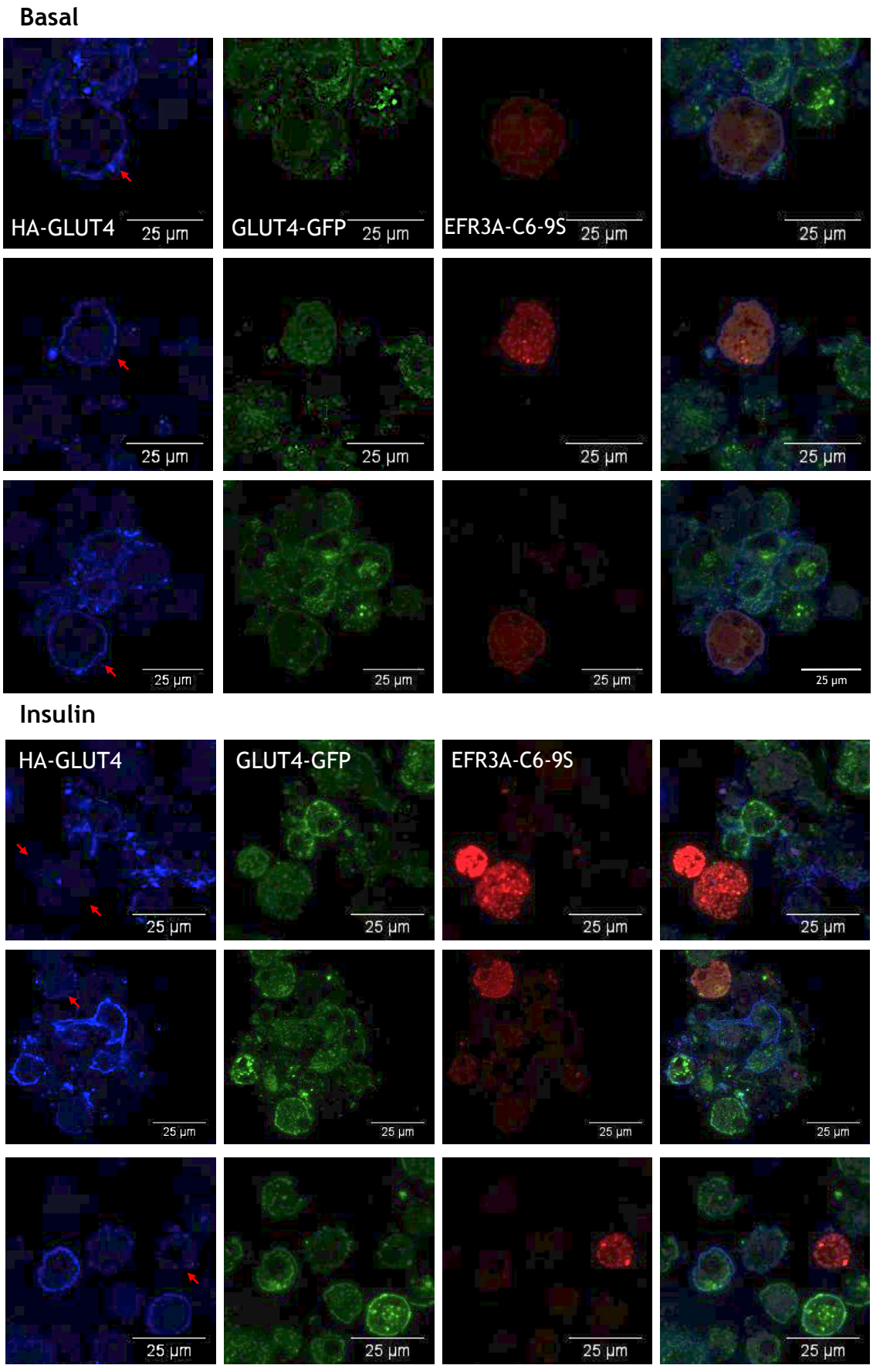

Figure 48: Confocal visualisation of EFR3A (C6-9S)-tdtomato in HA-GLUT4-GFP expressing 3T3-L1 adipocytes.

Representative confocal images of 3T3-L1 adipocytes expressing HA-GLUT4-GFP transfected with the EFR3A (C6-9S)-tdtomato plasmid. Top panel of non-stimulated basal cells. Bottom panel of Insulin stimulated cells (20 minutes with 0.1 uM insulin). Blue panel depicts HA epitope staining of GLUT4, green panel depicts GLUT4-GFP, and red panel depicts EFR3A-mcherry positive cells. Red arrows denote EFR3A (C6-9S)-tdtomato positive cells in the blue panel. Scale bar denotes 25 μm

6.5.2 Visualisation of EFR3A(C6-9S) in HA-GLUT4-GFP Adipocytes

Confocal microscopy of EFR3A dominant negative mutant EFR3A(C6-9S)-tdtomato in HA-GLUT4-GFP expressing adipocytes, shown in Figure 48. EFR3A(C6-9S) was cytoplasmically localised due to the mutation of the palmitoylation sites, shown in red panel in Figure 48. In the absence of insulin cells positive for EFR3A(C6-9S) have increased HA in comparison to non-transfected cells, denoted with a red arrow in the blue panel of Figure 48A. Insulin stimulated cells positive for EFR3A(C6-9S) the HA staining was decreased in comparison to un-transfected cells.

6.5.3 Plasma membrane level of GLUT4 in EFR3A and EFR3A(C6-9S) transfected adipocytes

The HA epitope tag of GLUT4 was stained in non-permeabilised cells to measure the level of PM GLUT4 per individual cell in adipocytes through the HA-staining fluorescence intensity. Individual cells which over express proteins of interest, EFR3A and EFR3A(C6-9S) are analysed and non-transfected cells are used for the positive control. As previously reported in HeLa cells over expression of EFR3A in 3T3-L1 adipocytes results in an increase in measured plasma membrane GLUT4, shown in Figure 49. Non-stimulated adipocyte cells over expressing EFR3A have a 2.60-fold increase in PM GLUT4 in comparison to the WT non-stimulated cells. The difference between insulin stimulated WT and non-stimulated EFR3A over-expressing cells was not significant, at 1.05-fold increase in PM GLUT4. Therefore,

cells over expressing EFR3A have comparable PM GLUT4 levels to insulin stimulated non-transfected adipocytes. This result shows that over expression of EFR3A alone can mimic insulin stimulated GLUT4 translocation to the plasma membrane in adipocytes. Cells over expressing EFR3A have a measured insulin response of 1.25 fold increase in PM GLUT4 in comparison to non-transfected cells, which have a measured 2.47 fold increase in PM GLUT4. Therefore, over expression of EFR3A does not over-ride the insulin response as a measured increase in PM GLUT4 was still seen but the effect was not additive. Over expression of the dominant negative EFR3A(C6-9S) results in a 1.66-fold increase in PM GLUT4 in non-stimulated WT cells. The insulin response of EFR3A(C6-9S) expressing cells was a non-significant 0.76 fold increase in PM GLUT4. The difference between insulin stimulated cells expressing EFR3A(C6-9S) and WT cells was a 0.51 fold increase. Therefore, insulin stimulated PM GLUT4 increase has been inhibited by the expression of EFR3A(C6-9S) in adipocytes. This trend has previously been shown in HeLa cells using both confocal microscopy and FACS analysis.

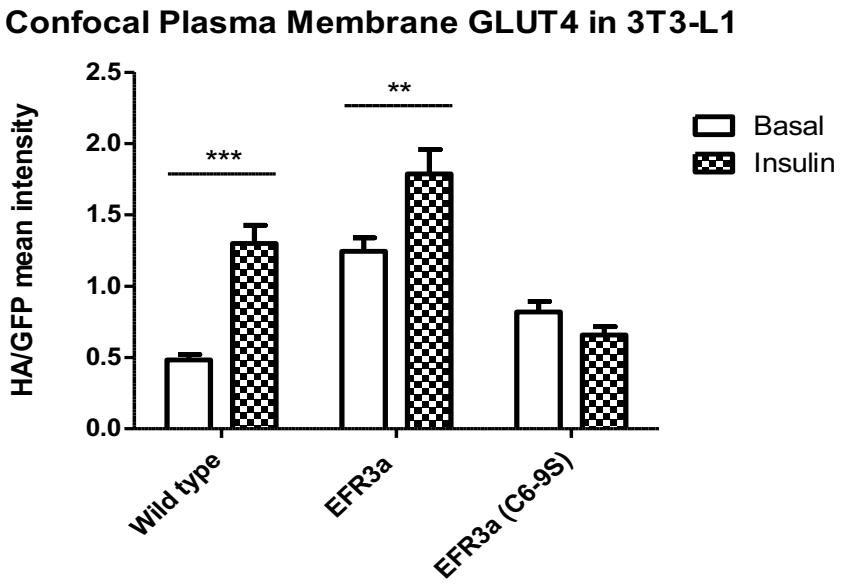

Figure 49 Confocal analysis of plasma membrane GLUT4 in 3T3-L1 adipocytes.

3T3-L1 adipocytes stably expressing mammalian GLUT4 with the epitope tag HA and the fluorescent tag GFP. Cells where transfected using electroporation with EFR3A-mcherry or EFR3A (C6-9S)-tdtomato plasmids. Confocal images where used from figures 47 and 48, cells which where mCherry or tdtomato positive used to measure HA and GFP fluorescence intensity. Difference between plasmids is P>0.001 from two-way ANOVA analysis n numbers as follows; WT basal 33, WT insulin 38, EFR3A basal 31, EFR3A insulin 38, EFR3A (C6-9S) basal 21, EFR3A (C6-9S) insulin 23. Cells are serum starved for 3 hours and insulin stimulated for 20 minutes with 0.1 uM insulin.

6.6 THE EFFECT ON GLUCOSE UPTAKE USING PHENYLARSINE OXIDE INHIBITION OF PI4KIIIA ACTIVITY

Inhibition of PI4K family has been tested using a variety of inhibitors. PI4K type was initially divided based on inhibitors. Phenylarsine oxide (PAO) was determined to be specific to PI4KIIIα at below 2.5 μM concentrations. Using ^{3}H labelled 2-deoxy glucose to measure glucose uptake in 3T3-L1 adipocytes treated with known doses of PAO 4 hours pre-uptake assay, the results from the assay are shown in Figure 50. Un-treated 3T3-L1 adipocytes have measured mean glucose uptake of 10.04 ρmol/min/million cells in the basal sample and 108.61 ρmol/min/million cells in the insulin stimulated sample. This represents a 10.81-fold increase in glucose uptake, typical for 3T3-L1 adipocytes. Cells treated with 0.5 μM PAO have a measured mean glucose uptake of 21.93 μM ρmol/min/million cells in the basal sample and 73.98 μM ρmol/min/million cells in the insulin stimulated sample. This represents a diminished total glucose uptake in response to insulin stimulation. 0.5 μM PAO treatment results in a marked decrease in the fold increase in glucose uptake in response to insulin stimulation, down to 3.4-fold increase in glucose uptake in comparison to 10.8-fold increase in non-treated cells. Cells treated with 1 μM PAO have a measured mean glucose uptake of 55.20 ρmol/min/million cells in the basal sample and 60.89 ρmol/min/million cells in the insulin stimulated sample. This represents a further diminished glucose uptake in response to insulin stimulation. The treatment with 1 μM PAO results in an inhibition of the insulin response with a measured 1.10-fold increase in response to insulin. Basal glucose uptake was markedly increased 5.50-fold in cells treated with 1 μM PAO in comparison to non-treated cells. In cells treated with 1 μM PAO the combined decrease in glucose uptake in response to insulin stimulation compared to non-treated cells and increase in basal glucose uptake compared to non-treated cells results in an inhibition of an insulin effect in these samples. Cells treated with 2.5 μM PAO have a measured mean glucose uptake of 30.48 ρmol/min/million cells in the basal sample and 20.25 ρmol/min/million cells in the insulin stimulated sample. This represents full inhibition of insulin stimulated glucose uptake.

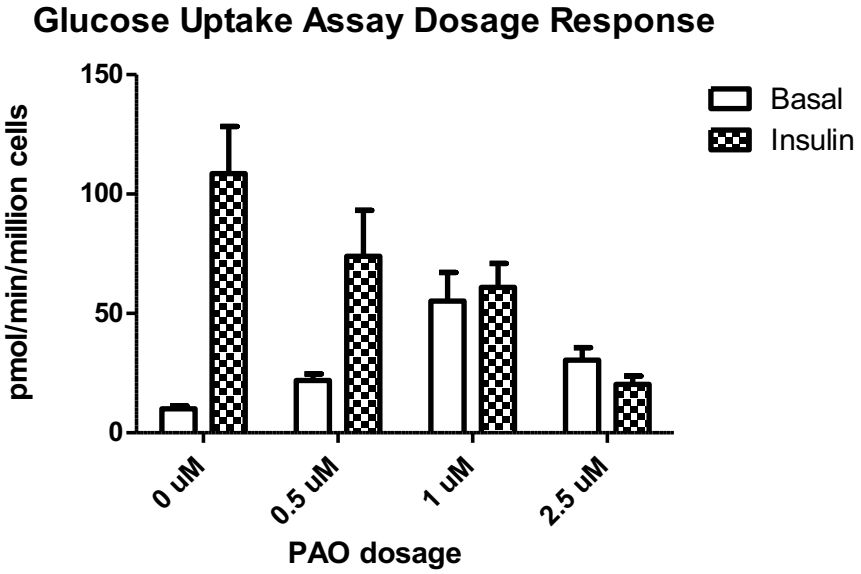

Figure 50: Effect of phenylarsine oxide dosage on glucose uptake in 3T3-L1 adipocytes.

Glucose uptake was measured using ^{3}H labelled 2-deoxy glucose. Cells are incubated with phenylarsine oxide 4 hours prior to uptake assay. Cells are insulin stimulated for 30 minutes with 0.1μM insulin and a 10-minute uptake of the 25 ηmol 2-Deoxyglucose. Data was from 3 technical and 3 biological repeats, graph represents mean ρmol/min/million cells and error bars SEM. Un-treated 3T3-L1 adipocytes have measured mean glucose uptake of 10.04 ρmol/min/million cells in the basal sample and 108.61 ρmol/min/million cells. Cells treated with 0.5 μM PAO have a measured mean glucose uptake of 21.93 μM ρmol/min/million cells in the basal sample and 73.98 μM ρmol/min/million cells in the insulin stimulated sample. Cells treated with 1 μM PAO have a measured mean glucose uptake of 55.20 ρmol/min/million cells in the basal sample and 60.89 ρmol/min/million cells in the insulin stimulated sample 2.5 μM PAO have a measured mean glucose uptake of 30.48 ρmol/min/million cells in the basal sample and 20.25 ρmol/min/million cells in the insulin stimulated sample.

6.7 Characterisation of Glucose uptake in 3T3-L1 adipocytes treated with EFR3A and PI4KIIIα siRNA

We have developed a robust delivery system for siRNA in adipocytes using electroporation. Electroporation of 3T3-L1 adipocytes with EFR3A siRNA results in a 50% KD of EFR3A detected using western blotting, shown in Figure 51. PI4KIIIα siRNA results in 42% KD of PI4KIIIα detected using western blotting, shown in Figure 51. Electroporation has a minimal effect on the insulin stimulated glucose uptake in adipocytes, results shown in Figure 51. The measured glucose uptake of scramble (SC) siRNA treated cells was 9.28 ρmol/min/well in basal cells and 78.04 ρmol/min/well in insulin stimulated cells. The mean measured fold increase in electroporated cells treated with SC siRNA was 8.4-fold in comparison to non-electroporated cells which exhibit a 10-fold increase in glucose uptake. Cells treated with EFR3A siRNA have a mean measured glucose uptake of 4.97 ρmol/min/well in basal cells and 18.38 ρmol/min/well in insulin stimulated cells. Insulin stimulated glucose uptake was inhibited in the adipocytes treated with EFR3A siRNA, results show a 3.4-fold increase in glucose uptake in response to insulin stimulation. Cells treated with PI4KIIIα siRNA have a mean measured glucose uptake of 8.46 ρmol/min/well in basal cells and 26.86 ρmol/min/well in insulin stimulated cells. Insulin stimulated glucose uptake was similarly inhibited in the adipocytes treated with PI4KIIIα siRNA, as with the EFR3A siRNA treated samples, with a measured 3.2-fold increase in glucose uptake in response to insulin stimulation.

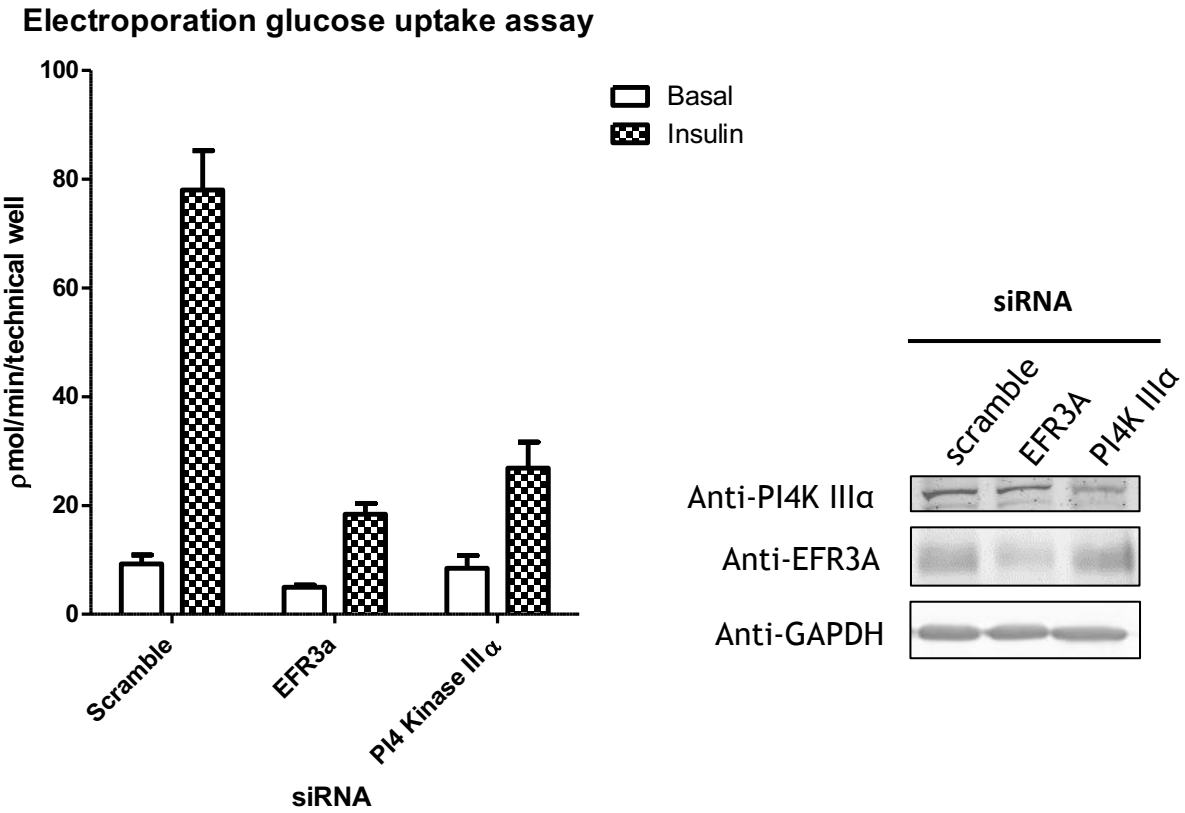

Figure 51 Glucose in 3T3-L1 adipocytes treated with EFR3A siRNA.

Glucose uptake was measured using ^{3}H labelled 2-deoxy glucose. Cells are stimulated for 30 minutes with 0.1μM insulin and a 10-minute uptake of the 25 ηmol 2-Deoxyglucose. Due to this assay requiring electroporation numbers of cells between experiments was variable meaning the fold difference within each biological repeat was represented. The mean measured uptake of the scramble (SC) siRNA samples was 9.28 ρmol/min/well in the basal samples and 78.21 ρmol/min/well in the insulin stimulated cells. The mean measured uptake of the EFR3A siRNA samples was 4.97 ρmol/min/well in the basal samples and 18.38 ρmol/min/well in the insulin stimulated cells. The mean measured uptake of the PI4KIIIα samples was 8.46 ρmol/min/well in the basal samples and 26.86 ρmol/min/well in the insulin stimulated cells. The siRNA knockdown was measured using western blotting and imageJ to measure the band mean intensity a 50% KD was measured for EFR3A and 42% KD was measured for PI4KIIIα. Error bars represent SEM. SC siRNA data from 5 biological replicates, with 5 technical replicates. EFR3A siRNA data from 4 biological repeats, with 5 technical replicates. PI4KIIIα siRNA data from 3 biological repeats, with 5 technical replicates.

6.8 DISCUSSION

6.8.1 The effect on GLUT4 at the PM

6.8.1.1 HeLa Cells

The findings from this chapter have shown a role for EFR3 for GLUT4 at the PM. In confocal microscopy experiments images are taken using the same laser intensity for each experiment. HeLa cells have no endogenous insulin receptor, however stimulation with insulin was possible through tyrosine kinase epidermal growth factor receptor present in HeLa cells. HeLa cells do not express endogenous GLUT4, the HeLa cells use stably express HA-GLUT4-GFP. The output measured was an increase in PM GLUT4 in response to insulin stimulation, this protocol has been established as a model system for GLUT4 (Kioumourtzoglou *et al.*, 2015). This due to the difficulty gaining high numbers for statistical analysis which was introduced when working with 3T3-L1 adipocytes which are not easily manipulated using standard molecular protocols.

The overexpression of EFR3A and the homolog EFR3B in HA-GLUT4-GFP expressing HeLa cells result in an increase in PM GLUT4 in unstimulated cells similar to levels seen in control insulin stimulated cells. The over expression of EFR3A and EFR3B was achieved using transient plasmid transfection, a technique which does not allow for normalisation of expression in transfected cells. To investigate if the level of over expression of EFR3A-mcherry or EFR3B-mcherry had an effect on PM GLUT4 levels the mean intensity of mCherry fluorescence per cell was gathered and plotted against the HA/GFP mean intensity. Increased mCherry fluorescence was correlated with increased EFR3A or EFR3B expression. No correlation between intensity of mCherry fluorescence and HA/GFP was discernible from the sample data, shown in Supplemental Figure 2. Therefore, this data suggests that EFR3A and EFR3B overexpression must reach a threshold for effect with a low number of plasmid transfections. The results show that overexpression of EFR3A and EFR3B results in the maintenance of an insulin response, with increased PM GLUT4 in cells stimulated with insulin. The fold increase in PM GLUT4 was maintained in HeLa cells over expressing EFR3B, with cells over expressing EFR3A exhibiting a lowered fold increase in PM GLUT4, 1.5-fold increase in comparison to 2-fold increase. However,

this fold increase was still significant and indicates that EFR3A and EFR3B overexpression does not inhibit the insulin response and a pool of GSVs are still present and able to respond to insulin in cells over expressing EFR3. Images of HeLa cells over expressing EFR3A which are not insulin stimulated have visible internal pools of GSVs, these are diminished upon insulin stimulation. Together these results indicate that EFR3A and EFR3B overexpression works to capture GLUT4 at the PM.

The effect of the dominant negative EFR3A mutant on PM GLUT4 was analysed in HeLa cells using confocal microscopy. The EFR3A mutant has the N terminal palmitoylation sites mutated (C6-9S), resulting in cytosolic localisation of EFR3A. This mutation does not inhibit EFR3A binding of TTC7 and PI4KIIIα, thus resulting in localisation of the majority of PI4KIIIα to the cytosol and not the PM due to overexpression (Nakatsu, *et al.*, 2012). Images confirm cytosolic localisation of EFR3A(C6-9S) as reported. Results obtained using confocal microscopy in HA-GLUT4-GFP HeLa cells showed that expression of EFR3A(C6-9S) inhibits insulin stimulated increase in PM GLUT4. Levels of PM GLUT4 in cells expressing EFR3A(C6-9S) are significantly reduced in comparison to non-transfected non-stimulated HeLa cells.

To remove implicit bias from the analysis of PM GLUT4 in the HeLa model system FACS analysis was performed. HA-GLUT4-GFP expressing HeLa cells transfected with EFR3A, and the dominant negative mutant EFR3A(C6-9S) were analysed using this technique. Results using FACS followed the same trend observed from the confocal data. The over expression of EFR3A resulted in increased PM GLUT4 in unstimulated cells similar to PM GLUT4 levels seen in insulin stimulated HeLa cells. Cells over expressing EFR3A still exhibit an insulin stimulated increase in PM GLUT4. HeLa cells overexpressing the dominant negative EFR3A(C6-9S) mutant exhibit inhibited insulin response, with a non-significant response to insulin stimulation. EFR3A(C6-9S) expression in HeLa cells results in decreased level of PM GLUT4 in comparison to non-transfected HeLa cells. The fold increase in PM GLUT4 in non-transfected HeLa cells measured using FACS was lower than that from confocal data. However, the result has increased statistical significance due to the number of cells assessed increasing 100 fold when FACS was used in comparison to confocal microscopy. Thus, confirming that FACS analysis was a valuable tool when investigating PM GLUT4 in this model system.

Future investigation into the effect of EFR3A on PM GLUT4 could examine the dwell time of individual GLUT4 molecules at the PM in cells with altered EFR3A expression. The dawn of CRISPR has improved the capability of super-resolution techniques. Introduction of mutations to endogenous EFR3A, such as the C6-9S mutation, may have effects on GLUT4 dwell time at the PM. To elucidate the role for EFR3A in the sequence of GLUT4 arrival and behaviour at the PM the effect EFR3A has on GSV fusion events at the PM. The recent development of a functional GLUT4 tagged with pHluorin would allow for the direction visualisation and co-localisation of GSV fusion events to EFR3A in cells expressing EFR3A-mcherry (Ashrafi *et al.*, 2017).

6.8.1.2 3T3-L1 Adipocytes

The effects of EFR3A and EFR3A(C6-9S) over expression observed in model HA-GLUT4-GFP expressing HeLa cells was maintained when tested in HA-GLUT4-HA expressing 3T3-L1 adipocytes. The analysis of PM GLUT4 in 3T3-L1 adipocytes was only performed by confocal analysis. DNA plasmids are introduced into 3T3-L1 adipocytes using electroporation, as standard methods of DNA transfection are inefficient in 3T3-L1 adipocytes (Okada *et al.*, 2003). Electroporation results in reduced cell size, however results in vastly improved transfection rates if still low in comparison to other cell types (Okada *et al.*, 2003). FACS analysis of 3T3-L1 adipocytes was not possible due to the size and adiposity of this cell type. The lipid content of 3T3-L1 means once ruptured adipocytes cause a cascade of autolysis of cells in the sample. This effect makes FACS an inappropriate technique as the cells are scraped before analysis.

The parallel results of PM GLUT4 in HeLa and 3T3-L1 adipocytes show that HA-GLUT4-GFP expressing HeLa's are an appropriate model for testing the role of EFR3A during insulin stimulated GLUT4 dispersal. This provides a solid representation of results to base future studies of EFR3A and GLUT4 on. These results indicate that EFR3A alone may have a role for GLUT4 PM behaviour as overexpression of EFR3A alone affects PM GLUT4. To confirm that over expression of EFR3A alone has an affect future studies could investigate PI4KIIIα expression in cells over expressing EFR3A. However, as this was a transient expression of 48 hours pre sample analysis it was expected that minimal effects are a result of transcriptional changes of PI4KIIIα.

6.8.2 PAO inhibition of PI4KIIIα

PAO is a trivalent arsenical which is capable of forming stable ring complexes with vicinal dithiols. PAO has been demonstrated to have a variety of effects when applied to 3T3-L1 adipocytes (Frost and Lane, 1985; Gould *et al.*, 1988; Liao *et al.*, 1991). PAO is a known phosphotyrosine phosphatase inhibitor, which has been demonstrated to have a variety of effects in many cell types (Fletchert *et al.*, 1993). Previous studies analysing the effect of PAO on glucose uptake showed a 3 fold increase in glucose uptake in adipocytes when used at 10 μM concentration in 3T3-L1 adipocytes (Gould *et al.*, 1988). Studies using higher concentrations of PAO (10 – 40 μM) show PAO blocks insulin stimulated glucose uptakes with minimal effect on the basal glucose uptake and auto-phosphorylation of IR (Fletchert *et al.*, 1993).

Inhibition of PI4KIIIα using PAO uses lower concentration than previous studies of the effects of PAO on glucose uptake, as PAO was an inhibitor of type III PI4Ks with a greater specificity for PI4KIIIα (IC_{50} 1 – 5 μM) (Dumaresq-Doiron *et al.*, 2010). We assume inhibition of PI4KIIIα activity by PAO is the mechanism of action measured here, but due to the nature of PAO we cannot be certain of this but have minimised other targets with these concentrations. The results show a simultaneous decrease in insulin stimulated glucose uptake and an increase in glucose uptake of unstimulated 3T3-L1 adipocytes. This results in an inhibition of insulin stimulate increase of glucose uptake in 3T3-L1 adipocytes. This effect was comparable to the effect of the overexpression of the dominant negative EFR3A(C6-9S) mutant, which results in the inhibition of increased PM GLUT4 in response to insulin stimulation.

6.8.3 siRNA knockdown of PI4KIIIα and EFR3A

To achieve a knock down of PI4KIIIα and EFR3A electroporation was employed to deliver siRNA. As previously described electroporation affects size of remaining adipocytes and increases distribution of fibroblasts in the sample, as these are a hardier cell type which are less likely to succumb to the effects of electroporation. Using immunoblots from cell lysates the knockdown was measured at 42% and 50% for PI4KIIIα and EFR3A respectively. To obtain a more accurate knockdown level in samples future experiments may evaluate mRNA levels of PI4KIIIα and EFR3A concurrent with immunoblot evaluation. Previous titration results of siRNA treated adipocytes show an importance of timing of sample use. Due to the time constraints

of the glucose uptake assay and mRNA sample preparation could not be concurrently run.

Results from the glucose uptake of both PI4KIIIα and EFR3A siRNA treated adipocytes showed a 3-fold decrease in insulin stimulated glucose uptake individually in comparison to scrambled siRNA-treated cells. Due to the known interaction between PI4KIIIα and EFR3A, the similarity in effect and knockdown levels the results are likely a result of the same pathway during insulin stimulated glucose uptake. Further investigation into the effect of double knockdown could elucidate this for certain. However, as using electroporation does not guarantee siRNA delivery to the same cell, meaning this technique was not optimal to investigate an additive effect. These glucose uptake results coupled with the results from PM GLUT4 experiments indicate that a role for EFR3A and PI4KIIIα exists during insulin mediated PM GLUT4 behaviour.

6.8.3.1 Issues surrounding electroporation

As mentioned electroporation results in reduced cell size of remaining 3T3-L1 adipocytes. The population of 3T3-L1 fibroblasts was increased in electroporated samples as these cell types are more robust than adipocytes to electroporation. Previous studies have determined that electroporation does not affect GLUT4 trafficking (Martin *et al.*, 2006). To determine suitability of 3T3-L1 adipocytes post electroporation initial experiments characterised the effect of electroporation on insulin stimulated glucose uptake, results shown in supplemental data. The results show a 9-fold increase in glucose uptake in response to insulin stimulation. This represents no significant difference in the fold increase in glucose uptake between electroporated cells and electroporated cells treated with SC siRNA. A minimum of a 7-fold increase in glucose uptake was arbitrarily set for future experiments of electroporated cells treated with SC siRNA. To confirm results obtained using electroporated siRNA treated 3T3-L1 adipocytes an EFR3A knockout cell line generated using CRISPR could be used. Knockout of EFR3A would require testing of 3T3-L1 adipocyte differentiation, as EFR3A may be a requirement for differentiation and function of adipocytes. EFR3 was an embryonic lethal knock out gene, however, tissue specific or inducible knockout mice are potentially suitable to study the effect

on glucose uptake *in vivo* (Vijayakrishnan *et al.*, 2010; Mirantes *et al.*, 2013; Ablain and Zon, 2016).

6.8.3.2 Future investigations of GLUT4 at the PM

Kinase deficient PI4KIIIα mutant, K1792L, has been generated based on the ATP binding site and validated in other studies (Harak *et al.*, 2014). CRISPR single nucleotide editing can be utilized in future investigations to confirm results observed using PAO inhibition of PI4KIIIα (Ran *et al.*, 2013). Using single nucleotide editing of endogenous PI4KIIIα protein to the kinase deficient mutant (K1792L) would create a cell line where GLUT4 behaviour at the PM can be investigated. Due to the promiscuous nature of PAO as an inhibitory molecule an experiment carried out using PAO requires validating using a separate methodology to block PI4KIIIα activity. The use of PAO cannot be discounted from future investigation as it provides a transient method of inhibition, which may be a requirement. Super resolution microscopy such as dSTORM has the ability to provide insight into the dispersal of GLUT4 clusters at the PM. Of particular interest would be the effect of siRNA depletion of EFR3A and PI4KIIIα on GLUT4 dispersal.

6.9 CONCLUSIONS

The results indicate that EFR3A alone has a potential role in GLUT4 behaviour at the PM. This was due to the noted effect of EFR3A overexpression alone on PM GLUT4 in HeLa and 3T3-L1 adipocyte cells. It would be of interest to investigate this result further as there may be other roles for EFR3A. The siRNA knockdown of EFR3A represents a significant inhibitory effect on glucose uptake. This effect was concurrent with results defined in HA-GLUT4-GFP expressing cells of EFR3A(C6-9S) mutant, both demonstrate an inhibitory effect on insulin stimulated GLUT4 effects. Inhibition of PI4KIIIα has similar effects to EFR3 this indicates that Inhibition of PI4KIIIα activity through protein depletion using siRNA or using PAO inhibition have similar inhibitory outcomes on insulin stimulated glucose uptake. This result supports the use of PAO at <2.5 μM concentrations within this system to inhibit PI4KIIIα activity. Taken together a role for EFR3A and PI4KIIIα was envisaged in increasing PM GLUT4 and further testing whether mobility of GLUT4 is directly influenced by these factors.

7 SUMMARY OF RESULTS

This project aimed to observe the mechanism behind the dispersal of GLUT4 at the plasma membrane, and as part of this we investigated the role of EFR3, a protein identified to play a role in GLUT4 dispersal in budding yeast. The evidence that GLUT4 behaviour at the PM is regulated by insulin stimulation has been mounting in advance of this work being undertaken. This thesis aimed to determine a molecular mechanism behind insulin stimulated GLUT4 PM behaviour, in particular how EFR3 affects GLUT4 at the PM, and if this is part of the insulin signal to increase GLUT4 dispersal and mobility at the PM in insulin stimulated cells.

Results identify EFR3A as the predominantly expressed homolog in 3T3-L1 adipocytes. Localisation of EFR3A was determined to be PM, and not to undergo translocation in response to insulin stimulation. This indicated that EFR3 and PI4P are involved with GLUT4 control at the PM and not the formation or delivery of GSVs in response to insulin stimulation.

EFR3 was investigated due to the discovery for the requirement of the mutant allele of Efr3, *fgy1-1*, in yeast for mammalian GLUT4 translocation to the PM. The initial hypothesis for the mechanism of control was the generation of PI4P by the PI4KIIIα localised to the membrane by EFR3 served to corral GLUT4 delivered to the PM. In response to insulin stimulation PI4P production is perturbed, a schematic of this is shown in Figure 20. This mechanism of action assumed that the *fgy1-1* mutation was a loss of function mutation as this information is not available.

The results show that increased EFR3A at the PM results in increased GLUT4 at the PM, even in the absence of insulin stimulation. This indicates that EFR3A is positively involved in glucose uptake. These results show that the original hypothesis of PI4P production at the PM inhibits GLUT4 dispersal at the PM was incorrect. The increase in PM GLUT4 in the absence of insulin stimulation may be a result of GLUT4 dispersal resulting in increased retention at the PM, stalling endocytosis of GLUT4. The increase measured may also be a result of increased GSV fusion with retention in the unstimulated cell. The activity of EFR3A on this system is a result of its PM localisation, this was tested using the cytosolic mutant EFR3A(C6-9S). Expression of which resulted in no increase in GLUT4 at the PM in response to insulin stimulation.

The results from samples of striated muscle from HFD mice, a model of insulin-resistance, show increased protein expression of both EFR3A and PI4KIIIα. This is an indication of physiological compensation in response to the HFD and impaired glucose tolerance to improve glucose uptake within the animal. The results showing that EFR3A at the PM is required for increased PM GLUT4 indicate that its role is within localisation of the PI4KIIIα which allows for the production of PI4P. EFR3A(C6-9S) is still capable of binding with this kinase machinery and therefore over-expression will serve to divert PI4KIIIα from its membrane localisation (Nakatsu, *et al.*, 2012). This ties in with the result that inhibition of PI4KIIIα activity with PAO inhibits glucose uptake indicating reduced GLUT4 at the PM. As PAO is not a specific inhibitor inhibition of PI4KIIIα activity these results taken together with the siRNA depletion resulting in similar insulin-stimulated glucose uptake inhibition.

These results indicate that EFR3A and PI4KIIIα are significant at the PM for the insulin-stimulated dispersal of GLUT4, depicted in Figure 52 and that dispersal of GLUT4 is integral to a sustained increase in glucose uptake. Based on the results within this thesis a conceivable mode of action is the production of PI4P at the PM increases lipid mobility by increasing the negative charge of the PM, this allows for the increased mobility of GLUT4 at the PM in insulin stimulated cell and therefore dispersal from the original cluster at fusion.

There is a solid basis to indicate a role which warrants further investigation using techniques described in the chapters. In particular dissecting if EFR3A is involved by its localisation of PI4KIIIα and the production of PI4P. The results indicate a positive role, however to definitively state that increased PI4P production at the PM is responsible for increased GLUT4 mobility and dispersal in response to insulin requires further investigation.

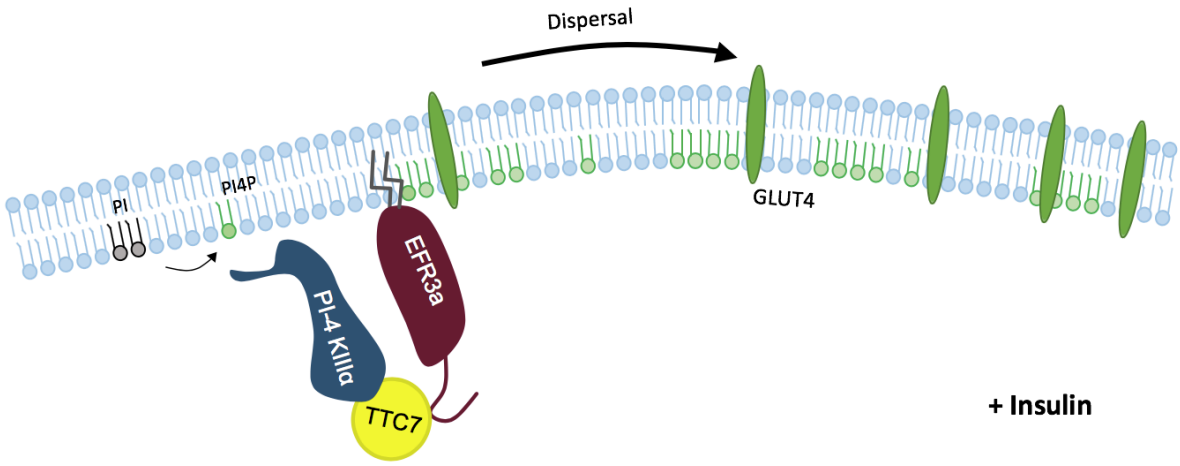

Figure 52: Schematic of EFR3A and PI4P involvement during GLUT4 dispersal

Based on the findings within this thesis the dispersal of GLUT4 at the PM is stimulated by EFR3A machinery. Increased EFR3A in cells result in increased PM GLUT4 in cells. Inhibition of PI4KIIIα using PAO results in decreased glucose uptake, indicating production of PI4P has a role during insulin stimulated glucose uptake. siRNA depletion of both EFR3A and PI4KIIIα results in decreased insulin stimulated glucose uptake. This model postulates that EFR3A and PI4P production is important for the dispersal of GLUT4 across the plasma membrane.

8 SUPPLEMENTAL

8.1 PRIMER

Primer-BLAST from NCBI was used to design primers for qPCR (Ye *et al.*, 2012)

8.1.1 EFR3A

8.1.1.1 Mouse

Left - ggtgacagatgaagatcgcc

Right - ccacatcatcagaaggcaca

8.1.1.2 Human

Left - caaagcttcgagggatcaga

Right - cagctgttgcccattctttt

8.1.2 EFR3B

8.1.2.1 Mouse

Left - aagcccgttcttatccacct

Right - gctgcggctgaattgagta

8.1.2.2 Human

Left - tcaagcctgttctcatccatc

Right - tgcggctgaattgagtacat

8.1.3 GAPDH

8.1.3.1 Mouse

Left - gttgtctcctgcgacttca

Right - ggtggtccagggtttctta

8.1.3.2 Human

Left - gtctcctctgacttcaacagcg

Right - accaccctgttgctgtagccaa

8.2 IMMUNOPRECIPITATION FLOW THROUGH BLOT

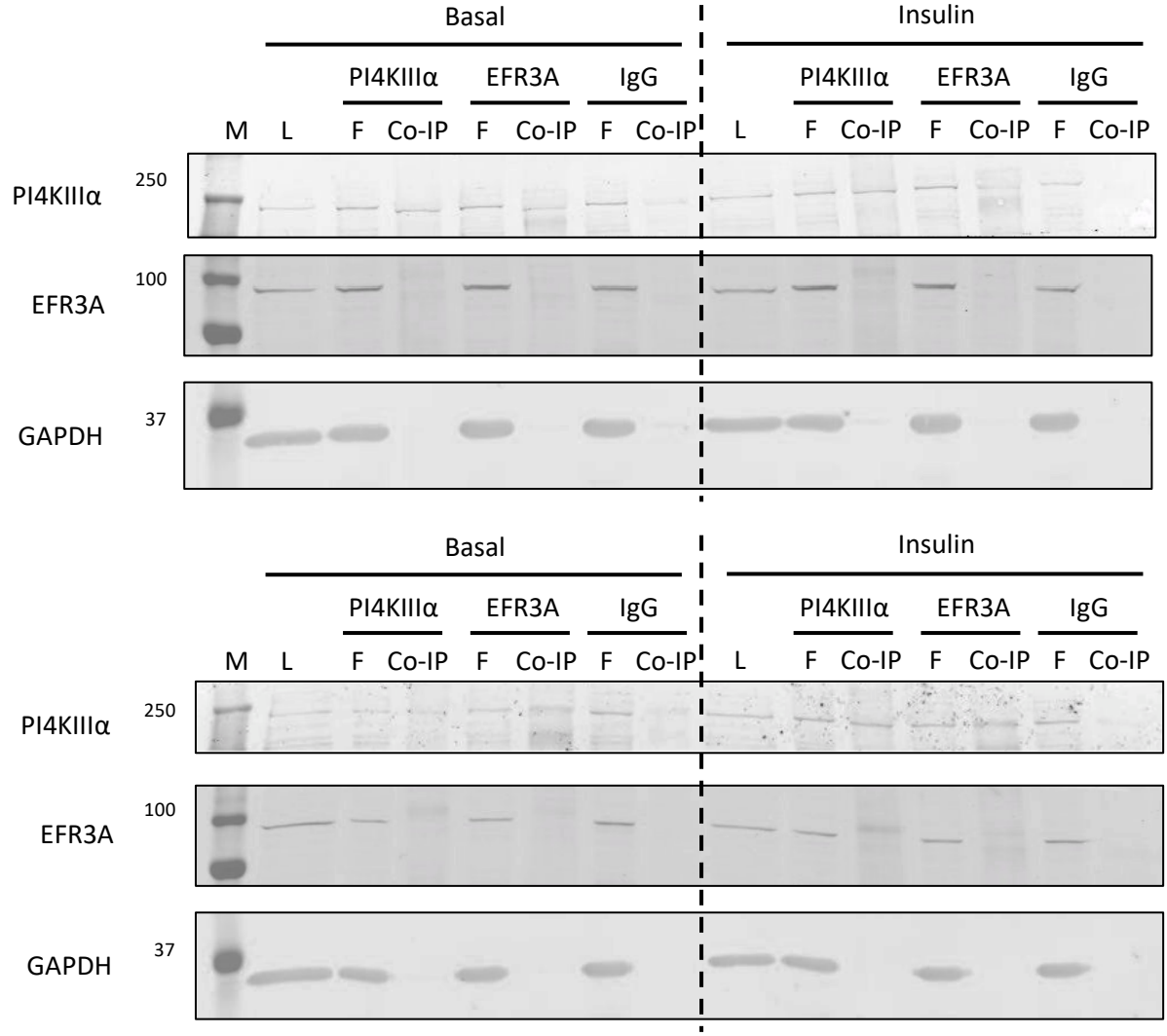

Supplemental Figure 1: Immunoprecipitation immunoblot

Immunoblot from immunoprecipitation experiments. The antibodies used during immunoprecipitation are shown in the top lane, commercial EFR3A, PI4KIIIα, and random IgG as a control. Total cell lysate (L) as a control, the flow through (F), and immunoprecipitant eluted sample (Co-IP) is loaded for each precipitation. Elution stringency of 0.5% and 1% Triton-X 100 is shown in the top and bottom panel respectively.

8.3 EFR3A-mCherry intensity against Plasma membrane GLUT4 intensity.

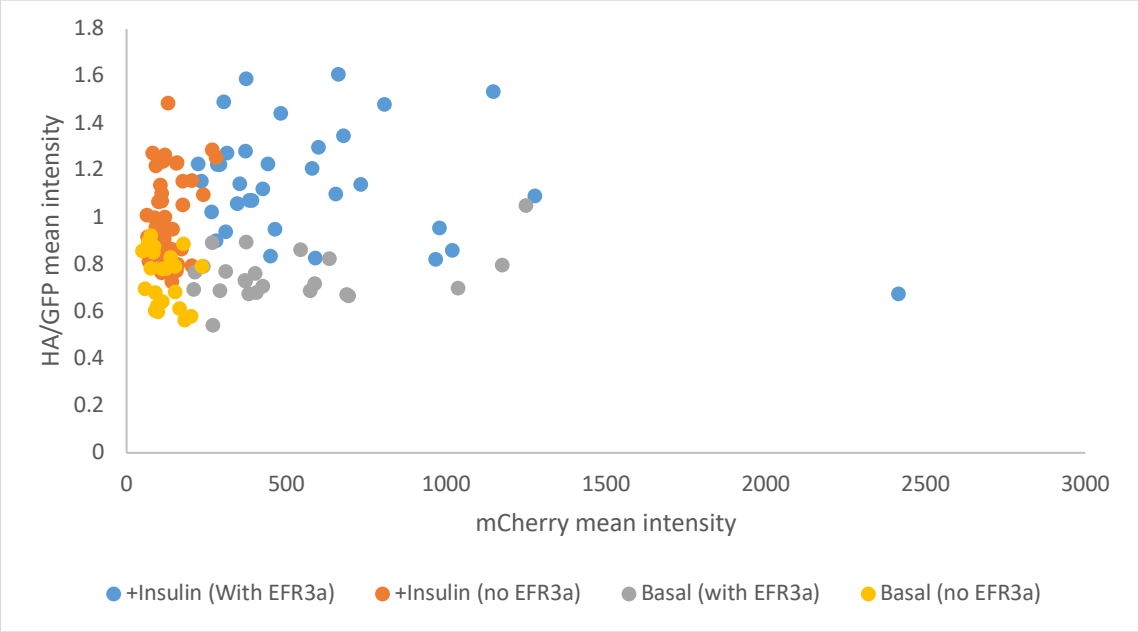

Supplemental Figure 2: HA/GFP mean intensity vs mCherry mean intensity

Effect of EFR3A-mCherry intensity on HA/GFP mean intensity. EFR3A-mCherry intensity correlates to expression levels of plasmid product. HA/GFP mean intensity correlates to level of PM GLUT4 in the cell. Increased HA/GFP mean intensity is shown in response to insulin stimulation. EFR3A-mCherry mean intensity shows no correlation to increased HA/GFP mean intensity. HeLa cells are serum starved for 3 hours prior to 20 min stimulation with 1μM insulin. n>30.

9 BIBLIOGRAPHY

Abel, E. D. *et al.* (2004) 'Regulation of Insulin-Responsive Aminopeptidase Expression and Targeting in the Insulin-Responsive Vesicle Compartment of Glucose Transporter Isoform 4-Deficient Cardiomyocytes', *Molecular Endocrinology*, 18(10), pp. 2491–2501. doi: 10.1210/me.2004-0175.

Abel, J. J. (1926) 'Crystaline insulin', *Proceedings of the National Academy of Sciences of the United States of America*, 12(2), pp. 132–6.

Ablain, J. and Zon, L. I. (2016) 'Tissue-specific gene targeting using CRISPR/Cas9', *Methods Cell Biol*, 135, pp. 189–202. doi: 10.1158/1940-6207.CAPR-14-0359.Nrf2-dependent.

Albiston, A. L. *et al.* (2017) 'Insulin-regulated aminopeptidase inhibitors do not alter glucose handling in normal and diabetic rat', *Molecular Endocrinology*.

Alessi, D. R. *et al.* (1997) 'Characterization of a 3-phosphoinositide-dependent protein kinase which phosphorylates and activates protein kinase Bα', *Current Biology*, 7(4), pp. 261–269. doi: 10.1016/S0960-9822(06)00122-9.

Altan-Bonnet, N. and Balla, T. (2012) 'Phosphatidylinositol 4-kinases: Hostages harnessed to build panviral replication platforms', *Trends in Biochemical Sciences*. Elsevier Ltd, 37(7), pp. 293–302. doi: 10.1016/j.tibs.2012.03.004.

American Diabetes Association (2010) 'Diagnosis and classification of diabetes mellitus', *Diabetes Care*, 33(SUPPL. 1). doi: 10.2337/dc10-S062.

Andrikopoulos, S. *et al.* (2008) 'Evaluating the glucose tolerance test in mice', *Marine Drugs*, 14(12), pp. 1323–1332. doi: 10.1152/ajpendo.90617.2008.

Antonelli, A. (2014) 'Hepatitis C virus infection and type 1 and type 2 diabetes mellitus', *World Journal of Diabetes*, 5(5), p. 586. doi: 10.4239/wjd.v5.i5.586.

Ashrafi, G. *et al.* (2017) 'GLUT4 Mobilization Supports Energetic Demands of Active Synapses', *Neuron*. Elsevier Inc., pp. 1–10. doi: 10.1016/j.neuron.2016.12.020.

Audhya, A. and Emr, S. D. (2002) 'Stt4 Pl 4-kinase localizes to the plasma membrane and functions in the Pkc1-mediated MAP kinase cascade', *Developmental Cell*, 2(5), pp. 593–605. doi: 10.1016/S1534-5807(02)00168-5.

Backer, J. M., Wjasow, C. and Zhang, Y. (1997) 'In Vitro Binding and Phosphorylation of Insulin Receptor Substrate 1 by the Insulin Receptor', *European Journal of Biochemistry*. Blackwell Science Ltd, 245(1), pp. 91–96. doi: 10.1111/j.1432-1033.1997.t01-1-00091.x.

Baird, D. *et al.* (2008) 'Assembly of the PtdIns 4-kinase Stt4 complex at the plasma membrane requires Ypp1 and Efr3', *Journal of Cell Biology*, 183(6), pp. 1061–1074. doi: 10.1083/jcb.200804003.

Balla, A. *et al.* (2002) 'Characterization of type II phosphatidylinositol 4-kinase isoforms reveals association of the enzymes with endosomal vesicular compartments', *Journal of Biological Chemistry*, 277(22), pp. 20041–20050. doi: 10.1074/jbc.M111807200.

Balla, A. *et al.* (2005) 'A Plasma Membrane Pool of Phosphatidylinositol 4- Phosphate Is Generated by Phosphatidylinositol 4-Kinase Type-III Alpha: Studies with the PH Domains of the Oxysterol Binding Protein and FAPP1', *Molecular biology of the cell*, 16, pp. 1282–1295. doi: 10.1091/mbc.E04.

Balla, A. and Balla, T. (2006) 'Phosphatidylinositol 4-kinases: old enzymes with emerging functions', *Trends in Cell Biology*. Elsevier, 16(7), pp. 351–361. doi: 10.1016/j.tcb.2006.05.003.

Balla, T., Szentpetery, Z. and Kim, Y. J. (2009) 'Phosphoinositide Signaling: New Tools and Insights', *Physiology*, 24(4), pp. 231–244. doi: 10.1152/physiol.00014.2009.

Bartenschlager, R., Cosset, F.-L. and Lohmann, V. (2010) 'Hepatitis C virus replication cycle', *Journal of Hepatology*. Elsevier, 53(3), pp. 583–585. doi: 10.1016/j.jhep.2010.04.015.

Barylko, B. *et al*. (2001) 'A Novel Family of Phosphatidylinositol 4-Kinases Conserved from Yeast to Humans', *Journal of Biological Chemistry*, 276(11), pp. 7705–7708. doi: 10.1074/jbc.C000861200.

Baskin, J. M. *et al*. (2016) 'The leukodystrophy protein FAM126A (hyccin) regulates PtdIns(4)P synthesis at the plasma membrane.', *Nature cell biology*, 18(1), pp. 132–8. doi: 10.1038/ncb3271.

Behar-Bannelier, M. and Murray, R. K. (1980) 'An Electrophoretic Study of Endogenous Phosphorylation in vitro of the Polypeptides of Microsomal Membrane Fractions of Mouse Liver', *Biochem. J.*, 187, pp. 147–156.

Bennett, D. L. *et al*. (1992) 'Identification of the type 2 proinsulin processing endopeptidase as PC2, a member of the eukaryote subtilisin family', *Journal of Biological Chemistry*, 267(21), pp. 15229–15236.

Berger, K. L. *et al*. (2009) 'Roles for endocytic trafficking and phosphatidylinositol 4-kinase III alpha in hepatitis C virus replication.', *Proceedings of the National Academy of Sciences of the United States of America*, 106(18), pp. 7577–7582. doi: 10.1073/pnas.0902693106.

Berger, K. L. *et al*. (2011) 'Hepatitis C Virus Stimulates the Phosphatidylinositol 4-Kinase III Alpha-Dependent Phosphatidylinositol 4-Phosphate Production That Is Essential for Its Replication', *Journal of Virology*, 85(17), pp. 8870–8883. doi: 10.1128/JVI.00059-11.

Berridge, M. J. (1983) 'Rapid accumulation of inositol trisphosphate reveals that agonists hydrolyse polyphosphoinositides instead of phosphatidylinositol.', *The Biochemical journal*, 212(3), pp. 849–58. doi: 10.1042/bj2120849.

Billcliff, P. G. and Lowe, M. (2014) 'Inositol lipid phosphatases in membrane trafficking and human disease', *Biochemical Journal*, 461(2).

Blot, V. and McGraw, T. E. (2006) 'GLUT4 is internalized by a cholesterol-dependent nystatin-sensitive mechanism inhibited by insulin.', *The EMBO journal*, 25(24), pp. 5648–5658. doi: 10.1038/sj.emboj.7601462.

Blot, V. and McGraw, T. E. (2008) 'Molecular Mechanisms Controlling GLUT4 Intracellular Retention', *Molecular and Cellular Neuroscience*, 19, pp. 3477–3487. doi: 10.1091/mbc.E08.

van den Bogaart, G., Lang, T. and Jahn, R. (2013) *Microdomains of SNARE proteins in the plasma membrane*. 1st edn, *Current Topics in Membranes*. 1st edn. Elsevier Inc. doi: 10.1016/B978-0-12-417027-8.00006-4.

Boguslavsky, S. *et al*. (2012) 'Myo1c binding to submembrane actin mediates insulin-induced tethering of GLUT4 vesicles', 23. doi: 10.1091/mbc.E12-04-0263.

Bojjireddy, N. *et al*. (2015) 'EFR3s are palmitoylated plasma membrane proteins that control responsiveness to G-protein-coupled receptors', *J Cell Sci*, 128(1), pp. 118–128. doi: 10.1242/jcs.157495.

Borawski, J. *et al.* (2009) 'Class III Phosphatidylinositol 4-Kinase Alpha and Beta Are Novel Host Factor Regulators of Hepatitis C Virus Replication', *Journal of Virology*, 83(19), pp. 10058–10074. doi: 10.1128/JVI.02418-08.

Botstein, D. and Fink, G. R. (2011) 'Yeast: An experimental organism for 21st century biology', *Genetics*, 189(3), pp. 695–704. doi: 10.1534/genetics.111.130765.

Bradley, H. *et al.* (2015) 'Visualization and quantitation of GLUT4 translocation in human skeletal muscle following glucose ingestion and exercise.', *Physiological reports*, 3(5), p. e12375. doi: 10.14814/phy2.12375.

Brelje, T. C., Scharp, D. W. and Sorenson, R. L. (1989) 'Three-dimensional imaging of intact isolated islets of Langerhans with confocal microscopy', *Diabetes*, 38(6), pp. 808–814. doi: 10.2337/diab.38.6.808.

Brewer, P. D. *et al.* (2014) 'Insulin-regulated Glut4 translocation: Membrane protein trafficking with six distinctive steps', *Journal of Biological Chemistry*, 289(25), pp. 17280–17298. doi: 10.1074/jbc.M114.555714.

Brewer, P. D. *et al.* (2016) 'Glut4 is sorted from a Rab10 GTPase-independent constitutive recycling pathway into a highly insulinresponsive Rab10 GTPase-dependent sequestration pathway after adipocyte differentiation', *Journal of Biological Chemistry*, 291(2), pp. 773–789. doi: 10.1074/jbc.M115.694919.

Brissova, M. (2005) 'Assessment of Human Pancreatic Islet Architecture and Composition by Laser Scanning Confocal Microscopy', *Journal of Histochemistry and Cytochemistry*, 53(9), pp. 1087–1097. doi: 10.1369/jhc.5C6684.2005.

Brombacher, E. *et al.* (2009) 'Rab1 guanine nucleotide exchange factor SidM is a major phosphatidylinositol 4-phosphate-binding effector protein of Legionella pneumophila', *Journal of Biological Chemistry*, 284(8), pp. 4846–4856. doi: 10.1074/jbc.M807505200.

Brozinick, J. T. *et al.* (2004) 'Disruption of Cortical Actin in Skeletal Muscle Demonstrates an Essential Role of the Cytoskeleton in Glucose Transporter 4 Translocation in Insulin-sensitive Tissues *', 279(39), pp. 40699–40706. doi: 10.1074/jbc.M402697200.

Bruno, J. *et al.* (2016) 'SEC16A is a RAB10 effector required for insulinstimulated GLUT4 trafficking in adipocytes', *Journal of Cell Biology*, 214(1), pp. 61–76. doi: 10.1083/jcb.201509052.

Bryant, K. L., Baird, B. and Holowka, D. (2015) 'A novel fluorescence-based biosynthetic trafficking method provides pharmacologic evidence that PI4-kinase IIIα is important for protein trafficking from the endoplasmic reticulum to the plasma membrane.', *BMC cell biology*, 16(1), p. 5. doi: 10.1186/s12860-015-0049-5.

Bryant, N. J. and Gould, G. W. (2011) 'SNARE Proteins Underpin Insulin-Regulated GLUT4 Traffic', *Traffic*, 12(6), pp. 657–664. doi: 10.1111/j.1600-0854.2011.01163.x.

Bryant, N. J., Govers, R. and James, D. E. (2002) 'Regulated transport of the glucose transporter GLUT4', *Nature Reviews Molecular Cell Biology*, 3(4), pp. 267–277. doi: 10.1038/nrm782.

Cai, X. *et al.* (2008) 'Spatial and Temporal Regulation of Focal Adhesion Kinase Activity in Living Cells', *Molecular and Cellular Biology*, 28(1), pp. 201–214. doi: 10.1128/MCB.01324-07.

De Camilli, P. *et al.* (1996) 'Phosphoinositides as Regulators in Membrane Traffic', *Science*, 271(5255), p. 1533 LP-1539. Available at: http://science.sciencemag.org/content/271/5255/1533.abstract.

Chang, L., Adams, R. D. and Saltiel, A. R. (2002) 'The TC10-interacting protein CIP4/2 is required for insulin-stimulated Glut4 translocation in 3T3L1 adipocytes.', *Proceedings of the National Academy of Sciences of the United States of America*, 99(20), pp. 12835–40. doi: 10.1073/pnas.202495599.

Chaussade, C. *et al.* (2003) 'Expression of Myotubularin by an Adenoviral Vector Demonstrates Its Function as a Phosphatidylinositol 3-Phosphate [PtdIns(3) *P*] Phosphatase in Muscle Cell Lines: Involvement of PtdIns(3) *P* in Insulin-Stimulated Glucose Transport', *Molecular Endocrinology*, 17(12), pp. 2448–2460. doi: 10.1210/me.2003-0261.

Chen, Y. and Lippincott-Schwartz, J. (2013) 'Rab10 delivers GLUT4 storage vesicles to the plasma membrane', *Communicative and Integrative Biology*, 6(3), pp. 3–5. doi: 10.4161/cib.23779.

Chi, N. W. and Lodish, H. F. (2000) 'Tankyrase is a Golgi-associated mitogen-activated protein kinase substrate that interacts with IRAP in GLUT4 vesicles', *Journal of Biological Chemistry*, 275(49), pp. 38437–38444. doi: 10.1074/jbc.M007635200.

Chiang, S. H. *et al.* (2001) 'Insulin-stimulated GLUT4 translocation requires the CAP-dependent activation of TC10.', *Nature*, 410(6831), pp. 944–948. doi: 10.1038/35073608.

Chung, J. *et al.* (2015) 'Plasticity of PI4KIIIα interactions at the plasma membrane.', *EMBO reports*, 16(3), pp. 312–320. doi: 10.15252/embr.201439151.

Claude, A. (1946) 'FRACTIONATION OF MAMMALIAN LIVER CELLS BY DIFFERENTIAL CENTRIFUGATION', *The Journal of Experimental Medicine*, 84(1), p. 61 LP-89. Available at: http://jem.rupress.org/content/84/1/61.abstract.

Collins, B. J. *et al.* (2003) 'In vivo role of the PIF-binding docking site of PDK1 defined by knock-in mutation', *EMBO Journal*, 22(16), pp. 4202–4211. doi: 10.1093/emboj/cdg407.

Collins, C. A. and Wells, W. (1982) 'Phosphatidylinositol Kinase', *The Journal of Biological Chemistry*, 258(4), pp. 2130–2135.

Corvera, S. *et al.* (1994) 'A double leucine within the GLUT4 glucose transporter COOH-terminal domain functions as an endocytosis signal', *Journal of Cell Biology*, 126(4), pp. 979–989. doi: 10.1083/jcb.126.4.979.

Costa, À., Conget, I. and Gomis, R. (2002) 'Impaired Glucose Tolerance', *Treatments in Endocrinology*, 1(4), pp. 205–210. doi: 10.2165/00024677-200201040-00001.

Cui, J. *et al.* (2016) 'Conventional kinesin KIF5B mediates adiponectin secretion in 3T3-L1 adipocytes', *Biochemical and Biophysical Research Communications*. Elsevier Ltd, 476(4), pp. 620–626. doi: 10.1016/j.bbrc.2016.06.008.

Cushmans, S. W. and Wardzalafj, L. J. (1980) 'Potential Mechanism of Insulin Action on Glucose Transport in the Isolated Rat Adipose Cell', *The Journal of Biological Chemistry*, 255(10), pp. 4758–4762.

Czech, M. P. (2003) 'Dynamics of phosphoinositides in membrane retrieval and insertion', *Annu Rev Physiol*, 65, pp. 791–815. doi: 10.1146/annurev.physiol.65.092101.142522.

D'Angelo, G. *et al.* (2008) 'The multiple roles of PtdIns(4)P -- not just the precursor of PtdIns(4,5)P2', *J Cell Sci*, 121(Pt 12), pp. 1955–1963. doi: 10.1242/jcs.023630.

Dawicki-McKenna, J. M., Goldman, Y. E. and Ostap, E. M. (2012) 'Sites of glucose transporter-4 vesicle fusion with the plasma membrane correlate spatially with microtubules', *PLoS ONE*, 7(8). doi: 10.1371/journal.pone.0043662.

Deng, D. *et al.* (2014) 'Crystal structure of the human glucose transporter GLUT1', *Nature*.

Nature Publishing Group, a division of Macmillan Publishers Limited. All Rights Reserved., 510(7503), pp. 121–125. Available at: http://dx.doi.org/10.1038/nature13306.

Diabetes, D. O. F. and American Diabetes Association (2010) 'Diagnosis and classification of diabetes mellitus', *Diabetes Care*, 33(SUPPL. 1). doi: 10.2337/dc11-S062.

Diabetes UK (2016) *Prevalence of diabetes*, *Facts and stats*. doi: 10.1007/s11245-009-9073-4.

Dickson, E. J., Jensen, J. B. and Hille, B. (2014) 'Golgi and plasma membrane pools of PI(4)P contribute to plasma membrane PI(4,5)P2 and maintenance of KCNQ2/3 ion channel current.', *Proceedings of the National Academy of Sciences of the United States of America*, 111(22), pp. E2281-90. doi: 10.1073/pnas.1407133111.

Dimitriadis, G. *et al*. (2011) 'Insulin effects in muscle and adipose tissue', *Diabetes Research and Clinial Practise*, 93, p. 7. Available at: http://ac.els-cdn.com/S0168822711700146/1-s2.0-S0168822711700146-main.pdf?_tid=70c6974a-fff4-11e6-9707-00000aab0f01&acdnat=1488533781_de7093e359942da750a7f4f9d11b7a97.

Dlugai, S. (2003) *Untersuchungen zur funktionellen Expression des humanen Glukosetransporters GLUT4 in der Hefe Saccharomyces cerevisiae und der Nachweis möglicher Interaktionspartner*. Universität Düsseldorf.

Dodd, T. L. *et al*. (1995) 'Numerical simulations of the effect of hydrodynamic interactions on diffusivities of integral membrane proteins', *J. Fluid Mech*, 293, pp. 147–180.

Dodson, G. and Steiner, D. (1998) 'The role of assembly in insulin's biosynthesis', *Current Opinion in Structural Biology*, 8(2), pp. 189–194. doi: 10.1016/S0959-440X(98)80037-7.

Dumaresq-Doiron, K. *et al*. (2010) 'The phosphatidylinositol 4-kinase PI4KIII is required for the recruitment of GBF1 to Golgi membranes', *Journal of Cell Science*, 123(13), pp. 2273–2280. doi: 10.1242/jcs.055798.

Eberhard, D. A. *et al*. (1990) 'Evidence that the inositol phospholipids are necessary for exocytosis. Loss of inositol phospholipids and inhibition of secretion in permeabilized cells caused by a bacterial phospholipase C and removal of ATP', *The Biochemical journal*, 268(1), pp. 15–25. doi: 10.1042/bj2680015.

El-Brolosy, M. A. and Stainier, D. Y. R. (2017) 'Genetic compensation: A phenomenon in search of mechanisms', *PLoS Genetics*, 13(7), pp. 1–17. doi: 10.1371/journal.pgen.1006780.

Falasca, M. *et al*. (2007) 'The role of phosphoinositide 3-kinase C2α in insulin signaling', *Journal of Biological Chemistry*, 282(38), pp. 28226–28236. doi: 10.1074/jbc.M704357200.

Faulkner, D. L., Dockendorff, T. C. and Jongens, T. A. (1998) 'Clonal analysis of cmp44E, which encodes a conserved putative transmembrane protein, indicates a requirement for cell viability in Drosophila', *Developmental Genetics*, 23(4), pp. 264–274. doi: 10.1002/(SICI)1520-6408(1998)23:4<264::AID-DVG2>3.0.CO;2-6.

Fletchert, M. C., Samelson, L. E. and June, C. H. (1993) 'Complex effects of phenylarsine oxide in T cells: Induction of tyrosine phosphorylation and calcium mobilization independent of CD45 expression', *Journal of Biological Chemistry*, 268(31), pp. 23697–23703.

Foti, M., Audhya, A. and Emr, S. D. (2001) 'Sac1 lipid phosphatase and Stt4 phosphatidylinositol 4-kinase regulate a pool of phosphatidylinositol 4-phosphate that functions in the control of the actin cytoskeleton and vacuole morphology.', *Molecular biology of the cell*, 12(8), pp. 2396–411. doi: 10.1091/mbc.12.8.2396.

Frost, S. C. and Lane, M. D. (1985) 'Evidence for the involvement of vicinal sulfhydryl groups in insulin-activated hexose transport by 3T3-L1 adipocytes', *Journal of Biological*

Chemistry, 260(5), pp. 2646–2652.

Fujiwara, T. *et al*. (2002) 'Phospholipids undergo hop diffusion in compartmentalized cell mem- brane.', *Journal of Cell Biology*, 157, p. 1071–1081.

Fukuda, R. (2000) 'Functional architecture of an intracellular membrane t-SNARE', *Nature*. Nature Publishing Group, 407, pp. 198–202. Available at: http://dx.doi.org/10.1038/35025084.

Fukumoto, H. *et al*. (1989) 'Cloning and characterization of the major insulin-responsive glucose transporter expressed in human skeletal muscle and other insulin-responsive tissues', *The Journal of biological chemistry*, 264(14), pp. 7776–9.

Funaki, M., DiFransico, L. and Janmey, P. A. (2006) 'PI 4,5-P2 stimulates glucose transport activity of GLUT4 in the plasma membrane of 3T3-L1 adipocytes', *Biochimica et Biophysica Acta*, 1763, pp. 889–899.

Gammeltoft, S. and Van Obberghen, E. (1986) 'Protein kinase activity of the insulin receptor.', *The Biochemical journal*, 235(1), pp. 1–11. Available at: http://www.ncbi.nlm.nih.gov/pubmed/3017297%5Cnhttp://www.pubmedcentral.nih.gov/articlerender.fcgi?artid=PMC1146640.

Genuth, S. *et al*. (2003) 'Follow-up Report on the Diagnosis of Diabetes Mellitus', *Diabetes Care*, 26(11), pp. 3160–3167. doi: 10.2337/diacare.26.11.3160.

Gibbs, E. M., Lienhard, G. E. and Gould, G. W. (1988) 'Insulin-Induced Translocation of Glucose Transporters to the Plasma Membrane Precedes Full Stimulation of Hexose Transport', *Biochemistry*, 27(18), pp. 6681–6685. doi: 10.1021/bi00418a006.

Le Good, J. A. *et al*. (1998) 'Protein Kinase C Isotypes Controlled by Phosphoinositide 3-Kinase Through the Protein Kinase PDK1', *Science*, 281(5385), p. 2042 LP-2045. Available at: http://science.sciencemag.org/content/281/5385/2042.abstract.

Gould, G. W. *et al*. (1988) 'Phenylarsine oxide stimulates hexose transport in 3T3-L1 adipocytes by a mechanism other than an increase in surface transporters', *Biochemistry and Biophysics*, 268(1), pp. 264–275.

Gould, G. W. and Holman, G. D. (1993) 'The glucose transporter family: structure, function and tissue-specific expression.', *Biochemical Journal*, 295(Pt 2), pp. 329–341.

Grainger, D. L. *et al*. (2011) 'Involvement of phosphatidylinositol 5-phosphate in insulin-stimulated glucose uptake in the L6 myotube model of skeletal muscle', *Pflügers Archiv - European Journal of Physiology*, 462(5), p. 723. doi: 10.1007/s00424-011-1008-4.

Guo, H. *et al*. (2012) 'The Axin / TNKS complex interacts with KIF3A and is required for insulin-stimulated GLUT4 translocation', 22(8), pp. 1246–1257. doi: 10.1038/cr.2012.52.

Guo, S. *et al*. (1999) 'SAC1-like domains of yeast SAC1, INP52, and INP53 and of human synaptojanin encode polyphosphoinositide phosphatases', *Journal of Biological Chemistry*, 274(19), pp. 12990–12995. doi: 10.1074/jbc.274.19.12990.

Gurley, J. M., Griesel, B. A. and Olson, A. L. (2016) 'Increased skeletal muscle GLUT4 expression in obese mice after voluntary wheel running exercise is posttranscriptional', *Diabetes*, 65(10), pp. 2911–2919. doi: 10.2337/db16-0305.

H.Lai, M. *et al*. (1994) 'The identification of a gene family in the Saccharomyces cerevisiae ergosterol biosynthesis pathway', *Gene*. Elsevier, 140(1), pp. 41–49. doi: 10.1016/0378-1119(94)90728-5.

Haga, Y., Ishii, K. and Suzuki, T. (2011) 'N-glycosylation is critical for the stability and

intracellular trafficking of glucose transporter GLUT4', *Journal of Biological Chemistry*, 286(36), pp. 31320–31327. doi: 10.1074/jbc.M111.253955.

Hammond, G. R. V. V, Machner, M. P. and Balla, T. (2014) 'A novel probe for phosphatidylinositol 4-phosphate reveals multiple pools beyond the Golgi', *Journal of Cell Biology*, 205(1), pp. 113–126. doi: 10.1083/jcb.201312072.

Hammond, G. R. V *et al.* (2012) 'PI4P and PI(4,5)P2 Are Essential But Independent Lipid Determinants of Membrane Identity', *Science*, 337(August), pp. 727–730. doi: 10.1126/science.1222483.

Harak, C. *et al.* (2014) 'Mapping of Functional Domains of the Lipid Kinase Phosphatidylinositol 4-Kinase Type III Alpha Involved in Enzymatic Activity and Hepatitis C Virus Replication.', *Journal of virology*, 88(17), pp. 9909–26. doi: 10.1128/JVI.01063-14.

Hediger, M. A. *et al.* (1987) 'Expression cloning and cDNA sequencing of the Na+/glucose co-transporter', *Nature*, 330(6146), pp. 379–381. doi: 10.1038/330379a0.

Heldwein, E. E. *et al.* (2004) 'Crystal structure of the clathrin adaptor protein 1 core.', *Proceedings of the National Academy of Sciences of the United States of America*, 101(39), pp. 14108–13. doi: 10.1073/pnas.0406102101.

Heo, W. Do *et al.* (2006) 'PI(3,4,5)P3 and PI(4,5)P2 Lipids Target Proteins with Polybasic Clusters to the Plasma Membrane', *Science*, 314(5804), pp. 1458–1461. doi: 10.1126/science.1134389.

Hepp, R. *et al.* (2005) 'Phosphorylation of SNAP-23 regulates exocytosis from mast cells', *Journal of Biological Chemistry*, 280(8), pp. 6610–6620. doi: 10.1074/jbc.M412126200.

Herman, M. a and Kahn, B. B. (2006) 'Glucose Transport and sennsing in the maintenance of glucose homeostasis and metabolic harmony', *The Journal of Clinical Investigation*, 116(7), pp. 1767–1775. doi: 10.1172/JCI29027.The.

Hess, S. T., Girirajan, T. P. K. and Mason, M. D. (2006) 'Ultra-High Resolution Imaging by Fluorescence Photoactivation Localization Microscopy', *Biophysical Journal*, 91(11), pp. 4258–4272. doi: 10.1529/biophysj.106.091116.

Hex, N. *et al.* (2012) 'Estimating the current and future costs of Type1 and Type2 diabetes in the UK, including direct health costs and indirect societal and productivity costs', *Diabetic Medicine*, 29(7), pp. 855–862. doi: 10.1111/j.1464-5491.2012.03698.x.

Hirst, J. *et al.* (2003) 'EpsinR: an ENTH Domain-containing Protein that Interacts with AP-1', *Molecular Biology of the Cell*, 14(February), pp. 625–641. doi: 10.1091/mbc.E02.

Hirst, J. *et al.* (2004) 'EpsinR Is an Adaptor for the SNARE Protein Vti1b', *Molecular biology of the cell*, 15(1), p. 55935602. doi: 10.1091/mbc.E04.

Hong, W. (2005) 'SNAREs and traffic', *Biochimica et Biophysica Acta (BBA) - Molecular Cell Research*, 1744(2), pp. 120–144. doi: 10.1016/j.bbamcr.2005.03.014.

Howel, S. . *et al.* (1978) 'Role of zinc and calcium in the formation and storage of insulin in the pancreatic beta-cell.', *Cell Tissue Research*, 188(1), pp. 107–118.

Hresko, R. C. *et al.* (2016) 'Mammalian glucose transporter activity is dependent upon anionic and conical phospholipids', *Journal of Biological Chemistry*, 291(33), pp. 17271–17282. doi: 10.1074/jbc.M116.730168.

Huang, B., Bates, M. and Zhuang, X. (2010) 'Super resolution fluorescence microscopy', *Annual Review of Biochemistry*, 78, pp. 993–1016. doi: 10.1146/annurev.biochem.77.061906.092014.Super.

Huang, F.-D. *et al.* (2004) 'Rolling blackout, a newly identified PIP2-DAG pathway lipase required for Drosophila phototransduction.', *Nature neuroscience*, 7(10), pp. 1070–8. doi: 10.1038/nn1313.

Huang, F.-D. (2006) 'Rolling Blackout Is Required for Synaptic Vesicle Exocytosis', *Journal of Neuroscience*, 26(9), pp. 2369–2379. doi: 10.1523/JNEUROSCI.3770-05.2006.

Huang, S. *et al.* (2004) 'Phosphatidylinositol-4,5-bisphosphate-rich plasma membrane patches organize active zones of endocytosis and ruffling in cultured adipocytes.', *Molecular and cellular biology*, 24(20), pp. 9102–23. doi: 10.1128/MCB.24.20.9102-9123.2004.

Huang, S. and Czech, M. P. (2007) 'The GLUT4 Glucose Transporter', *Cell Metabolism*, 5(4), pp. 237–252. doi: 10.1016/j.cmet.2007.03.006.

Huang, X. F. and Arvan, P. (1995) 'Intracellular transport of proinsulin in pancreatic beta-cells. Structural maturation probed by disulfide accessibility.', *The Journal of biological chemistry*, pp. 20417–20423. doi: 10.1074/jbc.270.35.20417.

Idevall-Hagren, O. and De Camilli, P. (2015) 'Detection and manipulation of phosphoinositides', *Biochimica et Biophysica Acta - Molecular and Cell Biology of Lipids*. Elsevier B.V., 1851(6), pp. 736–745. doi: 10.1016/j.bbalip.2014.12.008.

Idevall-Hagrena, O. and De Camilli, P. (2015) 'Detection and manipulation of phosphoinositides', *Biochim*, 1851(6), pp. 736–745. doi: 10.1016/S2215-0366(16)30284-X.Epidemiology.

Ijuin, T. and Takenawa, T. (2012) 'Regulation of insulin signaling and glucose transporter 4 (GLUT4) exocytosis by phosphatidylinositol 3,4,5-trisphosphate (PIP 3) phosphatase, skeletal muscle, and kidney enriched inositol polyphosphate phosphatase (SKIP)', *Journal of Biological Chemistry*, 287(10), pp. 6991–6999. doi: 10.1074/jbc.M111.335539.

Ikonomov, O. C. *et al.* (2007) 'ArPIKfyve-PIKfyve interaction and role in insulin-regulated GLUT4 translocation and glucose transport in 3T3-L1 adipocytes', *Exp. Cell. Res.*, 313(11), pp. 2404–2416. doi: 10.1038/nrm2621.

Isakoff, S. J. (1995) 'The inability of PI 3-kinase activation to stimulate GLUT4 translocation indicates additional signaling pathways are required for insulin-stimulated glucose uptake.', *Proc. Natl Acad. Sci. USA*, 92, pp. 10247–10251.

James, D. ., Strube, M. and Mueckler, M. (1989) 'Molecular cloning and characterization of an insulin-regulatable glucose transporter.', *Nature*, 338(6210), pp. 83–87.

Jewell, J. L. *et al.* (2011) 'Munc18c phosphorylation by the insulin receptor links cell signaling directly to SNARE exocytosis', *The Journal of Cell Biology*, 193(1).

Ji, C. *et al.* (2015) 'Nanoscale landscape of phosphoinositides revealed by specific pleckstrin homology (PH) domains using single-molecule superresolution imaging in the plasma membrane', *Journal of Biological Chemistry*, 290(45), pp. 26978–26993. doi: 10.1074/jbc.M115.663013.

Jiang, H. *et al.* (2001) 'GLUT4 Ablation in Mice Results in Redistribution of IRAP to the Plasma Membrane', *Biochemical and Biophysical Research Communications*, 525, pp. 519–525. doi: 10.1006/bbrc.2001.4994.

Jordens, I. *et al.* (2010) 'Insulin-regulated Aminopeptidase Is a Key Regulator of GLUT4 Trafficking by Controlling the Sorting of GLUT4 from Endosomes to Specialized Insulin-regulated Vesicles', *Molecular Biology of the Cell*, 21, pp. 2034–2044. doi: 10.1091/mbc.E10.

Kaddai, V. *et al.* (2009) 'Rab4b is a small GTPase involved in the control of the glucose

transporter GLUT4 localization in adipocyte', *PLoS ONE*, 4(4). doi: 10.1371/journal.pone.0005257.

Kahn, S. E., Cooper, M. E. and Del Prato, S. (2014) 'Pathophysiology and treatment of type 2 diabetes: Perspectives on the past, present, and future', *The Lancet*. Elsevier Ltd, 383(9922), pp. 1068–1083. doi: 10.1016/S0140-6736(13)62154-6.

Kahn, S. E., Hull, R. L. and Utzschneider, K. M. (2006) 'Mechanisms linking obesity to insulin resistance and type 2 diabetes', *Nature*, 444(7121), pp. 840–846. doi: 10.1038/nature05482.

Kanzaki, M. *et al.* (2004) 'Phosphatidylinositol 4,5-bisphosphate regulates adipocyte actin dynamics and GLUT4 vesicle recycling', *Journal of Biological Chemistry*, 279(29), pp. 30622–30633. doi: 10.1074/jbc.M401443200.

Kanzaki, M. and Pessin, J. E. (2001) 'Insulin-stimulated GLUT4 Translocation in Adipocytes Is Dependent upon Cortical Actin Remodeling * □', 276(45), pp. 42436–42444. doi: 10.1074/jbc.M108297200.

Kasuga, M., Karlsson, F. A. and Kahn, C. R. (1982) 'Insulin Stimulates the Phosphorylation of the 95,000-Dalton Subunit of Its Own Receptor', *Science*, 215(4529), pp. 185–186.

Kavalali, E. T. and Jorgensen, E. M. (2014) 'Visualizing presynaptic function', *Nat Neurosci*. Nature Publishing Group, a division of Macmillan Publishers Limited. All Rights Reserved., 17(1), pp. 10–16. Available at: http://dx.doi.org/10.1038/nn.3578.

Keller, S. R. *et al.* (1995) 'Cloning and Characterization of a Novel Insulin-regulated Membrane Aminopeptidase from Glut4 Vesicles *', 270(40), pp. 23612–23618.

Keller, S. R., Davis, A. C. and Clairmont, K. B. (2002) 'Mice Deficient in the Insulin-regulated Membrane Aminopeptidase Show Substantial Decreases in Glucose Transporter GLUT4 Levels but Maintain Normal Glucose Homeostasis *', *The Journal of Biological Chemistry*, 277(20), pp. 17677–17686. doi: 10.1074/jbc.M202037200.

Khan, A. H. *et al.* (2001) 'Munc18c Regulates Insulin-stimulated GLUT4 Translocation to the Transverse Tubules in Skeletal Muscle', *Journal of Biological Chemistry*, 276(6), pp. 4063–4069. doi: 10.1074/jbc.M007419200.

Kim, Y. *et al.* (2010) 'Mass spectrometry based cellular phosphoinositides profiling and phospholipid analysis: A brief review', *Experimental and Molecular Medicine*, 42(1), p. 1. doi: 10.3858/emm.2010.42.1.001.

Kim, Y. J., Hernandez, M. L. G. and Balla, T. (2013) 'Inositol lipid regulation of lipid transfer in specialized membrane domains', *Trends in Cell Biology*. Elsevier Ltd, 23(6), pp. 270–278. doi: 10.1016/j.tcb.2013.01.009.

Kioumourtzoglou, D., Sadler, J. B. A., *et al.* (2014) 'Studies of the regulated assembly of SNARE complexes in adipocytes', *Biochemical Society Transactions*, 42(5), p. 1396 LP-1400. Available at: http://www.biochemsoctrans.org/content/42/5/1396.abstract.

Kioumourtzoglou, D., Sadler, J. B. A., *et al.* (2014) 'Studies of the regulated assembly of SNARE complexes in adipocytes GLUT4 trafficking uses SNARE proteins', *Biochemical Society Transactions*, 42(5). doi: 10.1042/BST20140114.

Kioumourtzoglou, D. *et al.* (2015) 'Alternative routes to the cell surface underpin insulin-regulated membrane trafficking of GLUT4', *Journal of Cell Science*. The Company of Biologists, 128(14), pp. 2423–2429. doi: 10.1242/jcs.166561.

Knight, J. D. and Falke, J. J. (2009) 'Single-molecule fluorescence studies of a PH domain: New insights into the membrane docking reaction', *Biophysical Journal*. Biophysical Society, 96(2), pp. 566–582. doi: 10.1016/j.bpj.2008.10.020.

Knudsen, B. S., Feller, S. M. and Hanafusa, H. (1994) 'Four proline-rich sequences of the guanine-nucleotide exchange factor C3G bind with unique specificity to the first Src homology 3 domain of crk.', *J. Biol. Chem.*, 269, pp. 32781–32787.

Kobayashi, M. *et al.* (1996) 'Expression and localization of insulin-regulatable glucose transporter (GLUT4) in rat brain', *Neuroscience Letters*, 213(2), pp. 103–106. doi: 10.1016/0304-3940(96)12845-7.

Kong, A. M. *et al.* (2006) 'Phosphatidylinositol 3-phosphate [PtdIns3P] is generated at the plasma membrane by an inositol polyphosphate 5-phosphatase: endogenous PtdIns3P can promote GLUT4 translocation to the plasma membrane', *Molecular and cellular biology*, 26(16), pp. 6065–6081. doi: 10.1128/MCB.00203-06.

Kono, T. *et al.* (1971) 'Action of Insulin in Fat Cells', *The Journal of Biological Chemistry*, 7(April), pp. 2226–2233.

Kristiansen, S., Ramlal, T. and Klip, A. (1998) 'Phosphatidylinositol 4-kinase, but not phosphatidylinositol 3-kinase, is present in GLUT4-containing vesicles isolated from rat skeletal muscle', *Biochemical Journal*, 335, pp. 351–356. Available at: http://www.ncbi.nlm.nih.gov/pubmed/12518000.

Kudalkar, E. M., Davis, T. N. and Asbury, C. L. (2016) 'Single-Molecule Total Internal Reflection Fluorescence Microscopy', *Cold spring harbor protocol*, 5. doi: 10.1016/S2215-0366(16)30284-X.Epidemiology.

Kuimov, A. N. *et al.* (2001) 'Cloning and characterization of TNKL, a member of tankyrase gene family', *Genes And Immunity*. Macmillan Publishers Limited, 2, p. 52. Available at: http://dx.doi.org/10.1038/sj.gene.6363722.

Kusumi, A. *et al.* (2005) 'Paradigm Shift of the Plasma Membrane Concept from the Two-Dimensional Continuum Fluid to the Partitioned Fluid: High-Speed Single-Molecule Tracking of Membrane Molecules', *Annual Review of Biophysics and Biomolecular Structure*, 34(1), pp. 351–378. doi: 10.1146/annurev.biophys.34.040204.144637.

Laidlaw, K. M. E. *et al.* (2017) 'SNARE phosphorylation : a control mechanism for insulin-stimulated glucose transport and other regulated exocytic events', pp. 1–7.

Lamb, C. A. *et al.* (2010) 'Insulin-regulated trafficking of GLUT4 requires ubiquitination', *Traffic*, 11(11), pp. 1445–1454. doi: 10.1111/j.1600-0854.2010.01113.x.

Larance, M. *et al.* (2005) 'Characterization of the role of the Rab GTPase-activating protein AS160 in insulin-regulated GLUT4 trafficking', *Journal of Biological Chemistry*, 280(45), pp. 37803–37813. doi: 10.1074/jbc.M503897200.

Lavan, B. E. *et al.* (1997a) 'A novel 160 kDa phosphotyrosine protein in insulin-treated embryonic kidney cells is a new member of the insulin receptor substrate family', *J.Biol.Chem.*, 272(34), pp. 21403–21407. doi: 10.1074/jbc.272.34.21403.

Lavan, B. E. *et al.* (1997b) 'The 60-kDa Phosphotyrosine Protein in Insulin-treated Adipocytes Is a New Member of the Insulin Receptor Substrate Family*', *J.Biol.Chem.*, 272(17), pp. 11439–11443. doi: 10.1074/jbc.272.34.21403.

Leney, S. E. and Tavaré, J. M. (2009) 'The molecular basis of insulin-stimulated glucose uptake: Signalling, trafficking and potential drug targets', *Journal of Endocrinology*, 203(1), pp. 1–18. doi: 10.1677/JOE-09-0037.

Levine, R. and Goldstein, M. . (1958) 'On the mechanism of action of insulin.', *Hormoner*, 11(2), pp. 2–22.

Levine, T. P. and Munro, S. (1998) 'The pleckstrin homology domain of oxysterol-binding

protein recognises a determinant specific to Golgi membranes', *Current Biology*, 8(13), pp. 729–739. doi: 10.1016/S0960-9822(98)70296-9.

Levy-toledano, R. *et al.* (1995) 'Insulin-induced Activation of Phosphatidylinositol (PI) 3-Kinase', 270(50), pp. 30018–30022.

Liao, K., Hoffman, R. D. and Lane, M. D. (1991) 'Phosphotyrosyl turnover in insulin signaling', *Journal of Biological Chemistry*, 266(10), pp. 6544–6553.

Liu, J. *et al.* (2002) 'APS Facilitates c-Cbl Tyrosine Phosphorylation and GLUT4 Translocation in Response to Insulin in 3T3-L1 Adipocytes APS Facilitates c-Cbl Tyrosine Phosphorylation and GLUT4 Translocation in Response to Insulin in 3T3-L1 Adipocytes', *Society*, 22(11), pp. 3599–3609. doi: 10.1128/MCB.22.11.3599.

Liu, J. *et al.* (2003) 'The roles of Cbl-b and c-Cbl in insulin-stimulated glucose transport', *Journal of Biological Chemistry*, 278(38), pp. 36754–36762. doi: 10.1074/jbc.M300664200.

Livingstone, S. J. *et al.* (2015) 'Estimated life expectancy in a scottish cohort with type 1 diabetes, 2008-2010', *JAMA - Journal of the American Medical Association*, 313(1), pp. 37–44. doi: 10.1001/jama.2014.16425.

Lizunov, V. A. *et al.* (2012) 'Insulin stimulates fusion, but not tethering, of GLUT4 vesicles in skeletal muscle of HA-GLUT4-GFP transgenic mice', *American Journal of Physiology - Endocrinology and Metabolism*. Bethesda, MD, MD: American Physiological Society, 302(8), pp. E950–E960. doi: 10.1152/ajpendo.00466.2011.

Lizunov, V. A., Lee, J. P., *et al.* (2013) 'Impaired tethering and fusion of GLUT4 vesicles in insulin-resistant human adipose cells', *Diabetes*, 62(9), pp. 3114–3119. doi: 10.2337/db12-1741.

Lizunov, V. A., Stenkula, K., *et al.* (2013) 'Insulin Regulates Glut4 Confinement in Plasma Membrane Clusters in Adipose Cells', *PLoS ONE*, 8(3). doi: 10.1371/journal.pone.0057559.

Maffucci, T. *et al.* (2003) 'Insulin induces phosphatidylinositol-3-phosphate formation through TC10 activation', *EMBO Journal*, 22(16), pp. 4178–4189. doi: 10.1093/emboj/cdg402.

Mardilovich, K., Pankratz, S. L. and Shaw, L. M. (2009) 'Expression and function of the insulin receptor substrate proteins in cancer', *Cell Communication and Signaling*, 7(1), p. 14. doi: 10.1186/1478-811X-7-14.

Marette, A. *et al.* (1992) 'Insulin Induces the Translocation of GLUT4 From a Unique Intracellular Organelle to Transverse Tubules in Rat Skeletal Muscle', *Diabetes*, 41(12), p. 1562 LP-1569. Available at: http://diabetes.diabetesjournals.org/content/41/12/1562.abstract.

Martin, O. J., Lee, A. and McGraw, T. E. (2006) 'GLUT4 distribution between the plasma membrane and the intracellular compartments is maintained by an insulin-modulated bipartite dynamic mechanism', *Journal of Biological Chemistry*, 281(1), pp. 484–490. doi: 10.1074/jbc.M505944200.

Mastick, C. C. *et al.* (1994) 'Characterization of a Major Protein in GLUT4 Vesicles', *The Journal of Biological Chemistry*, 269(8), pp. 6089–6092.

Matveeva, E. A. *et al.* (2001) 'Phosphorylation of the N-Ethylmaleimide-sensitive Factor Is Associated with Depolarization-dependent Neurotransmitter Release from Synaptosomes', *Journal of Biological Chemistry*, 276(15), pp. 12174–12181. doi: 10.1074/jbc.M007394200.

Mayer, J. P., Zhang, F. and DiMarchi, R. D. (2007) 'Insulin Structure and Function', *Peptide Science*, 88, pp. 687–713. doi: 10.1002/bip.

Miller, S. and Krijnse-Locker, J. . (2008) ‘Modification of intracellular membrane structures for virus replication.’, *Nature Reviews Microbiology*, 6, pp. 363–374.

Milne, S. B. *et al.* (2005) ‘A targeted mass spectrometric analysis of phosphatidylinositol phosphate species’, *Journal of Lipid Research*, 46(8), pp. 1796–1802. doi: 10.1194/jlr.D500010-JLR200.

Minogue, S. *et al.* (2001) ‘Cloning of a Human Type II Phosphatidylinositol 4-Kinase Reveals a Novel Lipid Kinase Family’, *Journal of Biological Chemistry*, 276(20), pp. 16635–16640. doi: 10.1074/jbc.M100982200.

Mirantes, C. *et al.* (2013) ‘An inducible knockout mouse to model the cell-autonomous role of PTEN in initiating endometrial, prostate and thyroid neoplasias’, *Disease Models & Mechanisms*. The Company of Biologists Limited, 6(3), pp. 710–720. doi: 10.1242/dmm.011445.

Mizuno-Yamasaki, E., Rivera-Molina, F. and Novick, P. (2012) ‘GTPase Networks in Membrane Traffic’, *Annual Review of Biochemistry*, 81, pp. 637–659. doi: 10.1016/j.neuron.2009.10.017.A.

Mohan, S. *et al.* (2010) ‘Molecular dynamics simulation studies of GLUT4: Substrate-free and substrate-induced dynamics and ATP-mediated glucose transport inhibition’, *PLoS ONE*, 5(12). doi: 10.1371/journal.pone.0014217.

Mohan, S. S. *et al.* (2009) ‘Homology Modeling of GLUT4, an Insulin Regulated Facilitated Glucose Transporter and Docking Studies with ATP and its Inhibitors’, *Journal of biomolecular structure and dynamics*, 26(4), pp. 455–464.

Morone, N. *et al.* (2006) ‘Three-dimensional reconstruction of the membrane skeleton at the plasma membrane interface by electron tomography’, *Journal of Cell Biology*, 174(6), pp. 851–862. doi: 10.1083/jcb.200606007.

Mueckler, M. (1994) ‘Facilitative glucose transporters’, *European Journal of Biochemistry*. Blackwell Publishing Ltd, 219(3), pp. 713–725. doi: 10.1111/j.1432-1033.1994.tb18550.x.

Mueckler, M. (2001) ‘Insulin resistance and the disruption of glut4 trafficking in skeletal muscle’, *Journal of Clinical Investigation*, 107(10), pp. 1211–1213. doi: 10.1172/JCI13020.

Mueller-Roeber, B. and Pical, C. (2002) ‘Inositol phospholipid metabolism in Arabidopsis. Characterized and putative isoforms of inositol phospholipid kinase and phosphoinositide-specific phospholipase C.’, *Plant physiology*, 130(1), pp. 22–46. doi: 10.1104/pp.004770.

Nakada, C. *et al.* (2003) ‘Accumulation of anchored proteins forms membrane diffusion barriers during neuronal polarization’, *Nature Cell Biology*, 5(7), pp. 626–632. doi: 10.1038/ncb1009.

Nakagawa, T., Goto, K. and Kondo, H. (1996) ‘Cloning , Expression , and Localization of 230-kDa Phosphatidylinositol 4-Kinase *’, 271(20), pp. 12088–12094.

Nakatsu, F., Baskin, J. M., *et al.* (2012) ‘Ptdins4P synthesis by PI4KIIIα at the plasma membrane and its impact on plasma membrane identity’, *Journal of Cell Biology*, 199(6), pp. 1003–1016. doi: 10.1083/jcb.201206051.

Nakatsu, F., Baskin, J. M., *et al.* (2012) ‘Ptdlns4P synthesis by PI4KIIIa at the plasma membrane and its impact on plasma membrane identity’, 199(6), pp. 1003–1016. doi: 10.1083/jcb.201206095.

Neudauer, C. L. *et al.* (1998) ‘Distinct cellular effects and interactions of the rho-family GTPase TC10.’, *Curr. Biol.*, 8, pp. 1151–1160.

Ng, Y. *et al*. (2008) 'Rapid Activation of Akt2 Is Sufficient to Stimulate GLUT4 Translocation in 3T3-L1 Adipocytes', *Cell Metabolism*, 7(4), pp. 348–356. doi: 10.1016/j.cmet.2008.02.008.

Nikolaou, A. *et al*. (2014) 'Presence and regulation of insulin-regulated aminopeptidase in mouse macrophages', *Journal of the Renin-Angiotensin-Aldosterone System*, 15(4), pp. 466–479. doi: 10.1177/1470320313507621.

Okada, S., Mori, M. and Pessin, J. E. (2003) 'Introduction of DNA into 3T3-L1 Adipocytes by Electroporation', in Özcan, S. (ed.) *Diabetes Mellitus: Methods and Protocols*. Totowa, NJ: Humana Press, pp. 93–96. doi: 10.1385/1-59259-377-1:093.

Okada, T. *et al*. (1994) 'Essential role of PI 3-kinase in insulin-induced glucose transport and antilipolysis in rat adipocytes. Studies with a selective inhibitor wortmannin.', *J. Biol. Chem.*, 269, pp. 3568–3573.

Omata, W. *et al*. (2000) 'Actin filaments play a critical role in insulin-induced exocytotic recruitment but not in endocytosis of GLUT4 in isoloated rat adipocytes.', *Biochem. J.*, 346, pp. 321–328.

Ouchi, N. *et al*. (2011) 'Adipokines in inflammation and metabolic disease', *Nat.Rev.Immunol.*, 11(2), pp. 85–97. doi: 10.1038/nri2921.Adipokines.

Palacios, S. *et al*. (2001) 'Recycling of the insulin-sensitive glucose transporter GLUT4: Access of surface internalized GLUT4 molecules to the perinuclear storage compartment is mediated by the Phe5-Gln6-Gln7-Ile8 motif', *Journal of Biological Chemistry*, 276(5), pp. 3371–3383. doi: 10.1074/jbc.M006739200.

Di Paolo, G. and De Camilli, P. (2006) 'Phosphoinositides in cell regulation and membrane dynamics.', *Nature*, 443(7112), pp. 651–657.

Park, G. . and Johnson, L. . (1955) 'Effect of insulin on transport of glucose and galactose into cells of rat muscle and brain', *American Journal of Physiology*, 182, pp. 17–23.

Patti, M. E. *et al*. (1995) '4PS/IRS-2 is the alternative substrate of the insulin receptor in IRS-1 deficient mice', *J.Biol.Chem.*, 270(42), pp. 24670–24673.

Perera, H. K. I. *et al*. (2003) 'Syntaxin 6 Regulates Glut4 Trafficking in 3T3-L1 Adipocytes', 14(July), pp. 2946–2958. doi: 10.1091/mbc.E02.

Perley, M. and Kipnis, D. M. (1966) 'Plasma Insulin Responses to Glucose and Tolbutamide of Normal Weight and Obese Diabetic and Nondiabetic Subjects', *Diabetes*, 15(12), p. 867 LP-874. Available at: http://diabetes.diabetesjournals.org/content/15/12/867.abstract.

Piper, R. C. *et al*. (1993) 'GLUT-4 NH2 terminus contains a phenylalanine-based targeting motif that regulates intracellular sequestration', *Journal of Cell Biology*, 121(6), pp. 1221–1232.

Proctor, K. M. *et al*. (2006) 'Syntaxin 16 controls the intracellular sequestration of GLUT4 in 3T3-L1 adipocytes', 347, pp. 433–438. doi: 10.1016/j.bbrc.2006.06.135.

Quesada, I. *et al*. (2008) 'Physiology of the pancreatic α-cell and glucagon secretion: Role in glucose homeostasis and diabetes', *Journal of Endocrinology*, 199(1), pp. 5–19. doi: 10.1677/JOE-08-0290.

Quinkert, D., Bartenschlager, R. and Lohmann, V. (2005) 'Quantitative Analysis of the Hepatitis C Virus Replication Complex', *Journal of Virology*. American Society for Microbiology, 79(21), pp. 13594–13605. doi: 10.1128/JVI.79.21.13594-13605.2005.

Ran, F. A. *et al*. (2013) 'Genome engineering using the CRISPR-Cas9 system.', *Nat Protoc*,

8(11), pp. 2281–2308. doi: 10.1038/nprot.2013.143.

Ratz, M. *et al.* (2015) 'CRISPR/Cas9-mediated endogenous protein tagging for RESOLFT super-resolution microscopy of living human cells', *Scientific Reports*, 5, pp. 1–6. doi: 10.1038/srep09592.

Reed, S. E. *et al.* (2013) 'A role for Rab14 in the endocytic trafficking of GLUT4 in 3T3-L1 adipocytes', *Journal of Cell Science*, 126(9), pp. 1931–1941. doi: 10.1242/jcs.104307.

Reiss, S. *et al.* (2011) 'Recruitment and activation of a lipid kinase by hepatitis C virus NS5A is essential for integrity of the membranous replication compartment', *Cell Host and Microbe*, 9(1), pp. 32–45. doi: 10.1016/j.chom.2010.12.002.

Ren, X. *et al.* (2013) 'Structural basis for recruitment and activation of the AP-1 clathrin adaptor complex by Arf1', *Cell*, 152(4), pp. 755–767. doi: 10.1016/j.cell.2012.12.042.

Röder, P. V. *et al.* (2014) 'The role of SGLT1 and GLUT2 in intestinal glucose transport and sensing', *PLoS ONE*, 9(2), pp. 20–22. doi: 10.1371/journal.pone.0089977.

Ross, S. A. *et al.* (1997) 'Trafficking Kinetics of the Insulin-Regulated Membrane Aminopeptidase in 3T3-L1 Adipocytes', *Biochemical and Biophysical Research Communications*, 251(239), pp. 247–251.

Ross, S. A., Keller, S. R. and Lienhard, G. E. (1998) 'Increased intracellular sequestration of the insulin-regulated aminopeptidase upon differentiation of 3T3-L1 cells', *Biochem. J*, 1008, pp. 1003–1008.

Rowland, A. F., Fazakerley, D. J. and James, D. E. (2011) 'Mapping Insulin/GLUT4 Circuitry', *Traffic*, 12(6), pp. 672–681. doi: 10.1111/j.1600-0854.2011.01178.x.

Rusten, T. E. and Stenmark, H. (2006) 'Analyzing phosphoinositides and their interacting proteins', *Nature Methods*, 3(4), pp. 251–258. doi: 10.1038/nmeth867.

Rutherford, A. C. *et al.* (2006) 'The mammalian phosphatidylinositol 3-phosphate 5-kinase (PIKfyve) regulates endosome-to-TGN retrograde transport', *Journal of Cell Science*, 119(19), pp. 3944–3957. doi: 10.1242/jcs.03153.

Sadler, J. B. A. *et al.* (2013) 'Posttranslational modifications of GLUT4 affect its subcellular localization and translocation', *International Journal of Molecular Sciences*, 14(5), pp. 9963–9978. doi: 10.3390/ijms14059963.

Sadler, J. B. A., Roccisana, J., *et al.* (2015) 'mVps45 knockdown selectively modulates VAMP expression in 3T3-L1 adipocytes', (June), pp. 2–5.

Sadler, J. B. A., Bryant, N. J. and Gould, G. W. (2015) 'Characterization of VAMP isoforms in 3T3-L1 adipocytes: implications for GLUT4 trafficking.', *Molecular biology of the cell*. American Society for Cell Biology, 26(3), pp. 530–6. doi: 10.1091/mbc.E14-09-1368.

Sano, H. *et al.* (2003) 'Insulin-stimulated phosphorylation of the rab GTPase-activating protein TBC1D1 regulates GLUT4 translocation', *Journal of Biological Chemistry*, 278(17), pp. 14599–14602. doi: 10.1074/jbc.M109.035568.

Sano, H. *et al.* (2007) 'Rab10, a Target of the AS160 Rab GAP, Is Required for Insulin-Stimulated Translocation of GLUT4 to the Adipocyte Plasma Membrane', *Cell Metabolism*, 5(4), pp. 293–303. doi: 10.1016/j.cmet.2007.03.001.

Santagata, S. *et al.* (2001) 'G-protein signaling through tubby proteins', *Science*, 292(5524), pp. 2041–2050. doi: 10.1126/science.1061233.

Sawka-verhelle, D. *et al.* (1996) 'Insulin Receptor Substrate-2 Binds to the Insulin',

Biochemistry, pp. 5980–5983.

Sbrissa, D. *et al*. (2002) 'Phosphatidylinositol 5-phosphate biosynthesis is linked to PIKfyve and is involved in osmotic response pathway in mammalian cells', *Journal of Biological Chemistry*, 277(49), pp. 47276–47284. doi: 10.1074/jbc.M207576200.

Sbrissa, D. *et al*. (2004) 'Role for a novel signaling intermediate, phosphatidylinositol 5-phosphate, in insulin-regulated F-actin stress fiber breakdown and GLUT4 translocation', *Endocrinology*, 145(11), pp. 4853–4865. doi: 10.1210/en.2004-0489.

Sbrissa, D. *et al*. (2007) 'Core protein machinery for mammalian phosphatidylinositol 3,5-bisphosphate synthesis and turnover that regulates the progression of endosomal transport: Novel Sac phosphatase joins the ArPIKfyve-PIKfyve complex', *Journal of Biological Chemistry*, 282(33), pp. 23878–23891. doi: 10.1074/jbc.M611678200.

Sbrissa, D. and Shisheva, A. (2005) 'Acquisition of unprecedented phosphatidylinositol 3,5-bisphosphate rise in hyperosmotically stressed 3T3-L1 adipocytes, mediated by ArPIKfyve-PIKfyve pathway', *Journal of Biological Chemistry*, 280(9), pp. 7883–7889. doi: 10.1074/jbc.M412729200.

Schoch, S. *et al*. (2001) 'SNARE function analyzed in synaptobrevin/VAMP knockout mice', *Science*. Nature Publishing Group, 294(5544), pp. 1117–1122. Available at: http://dx.doi.org/10.1126/science.1064335.

Semiz, S. *et al*. (2003) 'Conventional kinesin KIF5B mediates insulin- stimulated GLUT4 movements on microtubules', 22(10), pp. 2387–2399.

Seshasai, S. R. K. *et al*. (2014) 'Diabetes Mellitus, Fasting Glucose, and risk of Cause-Specific Death', *New England Journal of Medicine*, 364(9), pp. 829–841. doi: 10.1056/NEJMoa1008862.Diabetes.

Sezgin, M. and Sankur, B. (2004) 'Survey over image thresholding techniques and quantitative performance evaluation Mehmet', *Journal of Electronic Imaging*, 13(1), p. 220. doi: 10.1117/1.1631316.

Shepherd, P. R., Withers, D. J. and Siddle, K. (1998) 'Phosphoinositide 3-kinase : the key switch mechanism in insulin signalling', *Biochem. J*, 333, pp. 471–490. doi: 10.1042/BJ3330471.

Shewan, A. M. *et al*. (2000) 'The cytosolic C-terminus of the glucose transporter GLUT4 contains an acidic cluster endosomal targeting motif distal to the dileucine signal.', *Biochem. J.*, 350, pp. 99–107. doi: 10.1042/0264-6021:3500099.

Shewan, A. M. *et al*. (2003) 'GLUT4 Recycles via a trans-Golgi Network (TGN) Subdomain Enriched in Syntaxins 6 and 16 But Not TGN38: Involvement of an Acidic Targeting Motif.', *Molecular Biology of the Cell*, 14(March 2003), pp. 2372–2384. doi: 10.1091/mbc.E02.

Shewan, A. M. *et al*. (2013) 'Endosomal sorting of GLUT4 and Gap1 is conserved between yeast and insulin-sensitive cells.', *Journal of cell science*, 126, pp. 1576–82. doi: 10.1242/jcs.114371.

Shia, M. A. and Pilch, P. F. (1983) 'The β Subunit of the Insulin Receptor Is an Insulin-Activated Protein Kinase', 22(4), pp. 717–721.

Shisheva, A. *et al*. (2001) 'Localization and Insulin-regulated Relocation of Phosphoinositide 5-Kinase PIKfyve in 3T3-L1 Adipocytes', *Journal of Biological Chemistry*, 276(15), pp. 11859–11869. doi: 10.1074/jbc.M008437200.

Shisheva, A. (2008) 'Phosphoinositides in insulin action on GLUT4 dynamics: not just PtdIns(3,4,5)P3', *American Journal of Physiology Endocrinology and Metabolism*, 295(3),

pp. 536–544.

Smith, S. *et al*. (1998) 'Tankyrase, a Poly(ADP-Ribose) Polymerase at Human Telomeres', *Science*, 282(5393), p. 1484 LP-1487. Available at: http://science.sciencemag.org/content/282/5393/1484.abstract.

Smith, S. and Lange, T. De (1999) 'Cell cycle dependent localization of the telomeric PARP , tankyrase , to nuclear pore complexes and centrosomes', 3656, pp. 3649–3656.

Snyder, D. a, Kelly, M. L. and Woodbury, D. J. (2006) 'SNARE complex regulation by phosphorylation.', *Cell biochemistry and biophysics*, 45(1), pp. 111–123. doi: 10.1385/CBB:45:1:111.

Song, G., Ouyang, G. and Bao, S. (2005) 'The activation of Akt/PKB signaling pathway and cell survival', *J Cell Mol Med*, 9(1), pp. 59–71. doi: 10.1111/j.1582-4934.2005.tb00337.x.

Stenkula, K. G. *et al*. (2010) 'Insulin controls the spatial distribution of GLUT4 on the cell surface through regulation of its postfusion dispersal', *Cell Metabolism*. Elsevier Ltd, 12(3), pp. 250–259. doi: 10.1016/j.cmet.2010.08.005.

Stephens, L. *et al*. (1998) 'Protein Kinase B Kinases That Mediate Phosphatidylinositol 3,4,5-Trisphosphate-Dependent Activation of Protein Kinase B', *Science*, 279(5351), p. 710 LP-714. Available at: http://science.sciencemag.org/content/279/5351/710.abstract.

Strahl, T. and Thorner, J. (2007) 'Synthesis and function of membrane phosphoinositides in budding yeast, Saccharomyces cerevisiae', *Biochimica et Biophysica Acta - Molecular and Cell Biology of Lipids*, 1771(3), pp. 353–404. doi: 10.1016/j.bbalip.2007.01.015.

Streb, H. *et al*. (1983) 'Release of Ca2+ from a nonmitochondrial intracellular store in pancreatic acinar cells by inositol-1,4,5-trisphosphate.', *Nature*, 306(5938), pp. 67–69. doi: 10.1038/306067a0.

Sun, X. J. *et al*. (1991) 'Structure of the insulin receptor substrate IRS-1 defines a unique signal transduction protein', *Nature*, 352(6330), pp. 73–77. Available at: http://dx.doi.org/10.1038/352073a0.

Sun, Y. *et al*. (2014) 'Myosin Va mediates Rab8A-regulated GLUT4 vesicle exocytosis in insulin-stimulated muscle cells', 25. doi: 10.1091/mbc.E13-08-0493.

Sutton, R. B. *et al*. (1998) 'Crystal structure of a SNARE complex involved in synaptic exocytosis at 2.4[thinsp]A resolution', *Nature*, 395(6700), pp. 347–353. Available at: http://dx.doi.org/10.1038/26412.

Suzuki, K. *et al*. (2005) 'Rapid hop diffusion of a G-protein-coupled receptor in the plasma membrane as revealed by single-molecule techniques', *Biophysical Journal*, 88(5), pp. 3659–3680. doi: 10.1529/biophysj.104.048538.

Suzuki, K. and Kono, T. (1980) 'Evidence that insulin causes translocation of glucose transport activity to the plasma membrane from an intracellular storage site.', *Proceedings of the National Academy of Sciences of the United States of America*, 77(5), pp. 2542–2545. doi: 10.1073/pnas.77.5.2542.

Suzuki, T. *et al*. (2001) 'The apical localization of SGLT1 glucose transporter is determined by the short amino acid sequence in its N-terminal domain.', *European journal of cell biology*, 80, pp. 765–774. doi: 10.1078/0171-9335-00204.

Takata, K. (1996) 'Glucose transporters in the transepithelial transport of glucose', *Journal of Electron Microscopy*, 45(4), pp. 275–284. doi: 10.1093/oxfordjournals.jmicro.a023443.

Tam, J. and Merino, D. (2015) 'Stochastic optical reconstruction microscopy (STORM) in

comparison with stimulated emission depletion (STED) and other imaging methods', *Journal of Neurochemistry*, 135(4), pp. 643–658. doi: 10.1111/jnc.13257.

Tan, J. and Brill, J. A. (2014) 'Cinderella story: PI4P goes from precursor to key signaling molecule', *Critical Reviews in Biochemistry and Molecular Biology*, 49(1), pp. 33–58. doi: 10.3109/10409238.2013.853024.

Tan, X. *et al.* (2015) 'Emerging roles of PtdIns(4,5)P2 - beyond the plasma membrane', *Journal of Cell Science*, 128(22), pp. 4047–4056. doi: 10.1242/jcs.175208.

Tarassov, K. *et al.* (2008) 'An in Vivo Map of the Yeast Protein Interactome', *Science*, 320(5882), pp. 1465–1470. doi: 10.1126/science.1153878.

The Expert Committee on the Diagnosis and Classification of Diabetes Mellitus (2003) 'Report of the Expert Committee on the DESCRIPTION OF DIABETES CATEGORIES OF GLUCOSE', *Diabetes Care*, 26(suppl 1), pp. 5–20. doi: 10.2337/diacare.25.2007.S5.

Thévenod, F. *et al.* (1986) 'Inositol 1,4,5-trisphosphate releases Ca2+ from a nonmitochondrial store site in permeabilized rat cortical kidney cells.', *Kidney international*, 29, pp. 695–702. doi: 10.1038/ki.1986.54.

Thomas, L. L. and Fromme, J. C. (2016) 'GTPase cross talk regulates TRAPPII activation of Rab11 homologues during vesicle biogenesis.', *The Journal of cell biology*, 215(4), pp. 499–513. doi: 10.1083/jcb.201608123.

Thorens, B. (1993) 'FACILITATED GLUCOSE TRANSPORTERS IN EPITHELIAL CELLS', *Annu Rev Physiol*, 55, pp. 591–608.

Thorens, B. (2001) 'GLUT2 in pancreatic and extra-pancreatic gluco-detection', *Molecular Membrane Biology*. Taylor & Francis, 18(4), pp. 265–273. doi: 10.1080/09687680110100995.

Tirone, T. A. and Brunicardi, F. C. (2001) 'Overview of glucose regulation', *World Journal of Surgery*, 25(4), pp. 461–467. doi: 10.1007/s002680020338.

Toyoda, T. *et al.* (2011) 'Myo1c regulates glucose uptake in mouse skeletal muscle', *Journal of Biological Chemistry*, 286(6), pp. 4133–4140. doi: 10.1074/jbc.M110.174938.

Tups, A. *et al.* (2011) 'Central Regulation of Glucose Homeostasis', in *Comprehensive Physiology*. John Wiley & Sons, Inc. doi: 10.1002/cphy.c160015.

Turner, J. R. *et al.* (1997) 'Physiological regulation of epithelial tight junctions is associated with myosin light-chain phosphorylation.', *The American journal of physiology*, 273(4 Pt 1), pp. C1378-85. Available at: http://eutils.ncbi.nlm.nih.gov/entrez/eutils/elink.fcgi?dbfrom=pubmed&id=9357784&retmode=ref&cmd=prlinks%5Cnpapers3://publication/uuid/3737BC09-59ED-4AC6-8F46-A7DE37E95203.

Uldry, M. *et al.* (2002) 'GLUT2 is a high affinity glucosamine transporter', *FEBS Letters*, 524(1–3), pp. 199–203. doi: 10.1016/S0014-5793(02)03058-2.

Varnai, P. *et al.* (2005) 'Selective cellular effects of overexpressed pleckstrin-homology domains that recognize PtdIns(3,4,5)P3 suggest their interaction with protein binding partners', *Journal of Cell Science*, 118(20), pp. 4879–4888. doi: 10.1242/jcs.02606.

Varnai, P. *et al.* (2006) 'Rapidly inducible changes in phosphatidylinositol 4,5-bisphosphate levels influence multiple regulatory functions of the lipid in intact living cells', *Journal of Cell Biology*, 175(3), pp. 377–382. doi: /10.1083/jcb.200607116.

Várnai, P. and Balla, T. (1998) 'Visualization of phosphoinositides that bind pleckstrin homology domains: calcium-and agonist-induced dynamic changes and relationship to myo-

inositol-', *The Journal of cell biology*, 143(4), pp. 501–510. Available at: http://scholar.google.com/scholar?hl=en&btnG=Search&q=intitle:No+Title#0%5Cnhttp://jcb.rupress.org/content/143/2/501.short.

Del Vecchio, R. L. and Pilch, P. F. (1991) 'Phosphatidylinositol 4-kinase is a component of glucose transporter (GLUT 4)-containing vesicles', *Journal of Biological Chemistry*, 266(20), pp. 13278–13283.

Verhey, K. J. and Birnbaum, M. J. (1994) 'A Leu-Leu sequence is essential for COOH-terminal targeting signal of GLUT4 glucose transporter in fibroblasts', *Journal of Biological Chemistry*, 269(4), pp. 2353–2356.

Vijayakrishnan, N., Phillips, S. E. and Broadie, K. (2010) 'Drosophila Rolling Blackout Displays Lipase Domain-Dependent and Independent Endocytic Functions Downstream of Dynamin', *Trrafic*, 11(12), pp. 1567–1578. doi: 10.1111/j.1600-0854.2010.01117.x.Drosophila.

Voliovitch Hedva *et al.* (1995) 'J. Biol. Chem.-1974-Ciaranello-4528-36', *The Journal of biological chemistry*, pp. 18083–18087. doi: 10.1074/jbc.273.52.34710.

Voss, D. (2005) *Funktionsanalyse des Saccharomyces cerevisiae Proteins Fgy1 und dessen Einfluss auf die heterologe Expression der Glukosetransporter GLUT1 und GLUT4 aus Säugetieren*. Universität Düsseldorf.

Wang, C. *et al.* (2005) 'Binding of PLCdelta1PH-GFP to PtdIns(4,5)P2 prevents inhibition of phospholipase C-mediated hydrolysis of PtdIns(4,5)P2 by neomycin1', *Acta Pharmacologica Sinica*, 26(12), pp. 1485–1491. doi: 10.1111/j.1745-7254.2005.00223.x.

Wang, C. and Liao, J. K. (2012) 'A Mouse Model of Diet-Induced Obesity and Insulin Resistance', *Methods Mol Biol*, 821, pp. 421–433. doi: 10.1007/978-1-61779-430-8.

Wang, J. *et al.* (2007) 'PI4P Promotes the Recruitment of the GGA Adaptor Proteins to the Trans-Golgi Network and Regulates Their Recognition of the Ubiquitin Sorting Signal', *Molecular Biology of the Cell*, 18, pp. 2646–2655. doi: 10.1091/mbc.E06.

Wang, W. *et al.* (2017) 'Impact of different promoters, promoter mutation, and an enhancer on recombinant protein expression in CHO cells', *Scientific Reports*. Springer US, 7(1), pp. 1–10. doi: 10.1038/s41598-017-10966-y.

Wang, Y. J. *et al.* (2003) 'Phosphatidylinositol 4 phosphate regulates targeting of clathrin adaptor AP-1 complexes to the Golgi', *Cell*, 114(3), pp. 299–310. doi: 10.1016/S0092-8674(03)00603-2.

Wasley, A. and J., A. M. (2000) 'Epidemiology of hepatitis C: geographic differences and temporal trends.', *Semin. Liver Dis.*, 20, pp. 1–16.

Weber, T. *et al.* (1998) 'SNAREpins: minimal machinery for membrane fusion', *Cell*. Nature Publishing Group, 92(6), pp. 759–772. doi: 10.1016/S0092-8674(00)81404-X.

Weyer, C. *et al.* (1999) 'The natural history of insulin secretory dysfunction and insulin resistance in the pathogenesis of type 2 diabetes mellitus', *The Journal of clinical investigation*, 104(6), pp. 787–794. doi: 10.1172/jci7231.

White, M. F. (2002) 'IRS proteins and the common path to diabetes.', *American journal of physiology. Endocrinology and metabolism*, 283(3), pp. E413-22. doi: 10.1152/ajpendo.00514.2001.

White, M. F., Maron, R. and Kahn, C. R. (1985) 'Insulin rapidly stimulates tyrosine phosphorylation of a Mr-185,000 protein in intact cells', *Nature*, 318(6042), pp. 183–186. Available at: http://dx.doi.org/10.1038/318183a0.

Wieczorke, R. *et al*. (2003) 'Characterisation of mammalian GLUT glucose transporters in a heterologous yeast expression system', *Cellular Physiology and Biochemistry*, 13(3), pp. 123–134. doi: 10.1159/000071863.

Wiese, R. J. *et al*. (1995) 'Activation of mitogen-activated protein kinase and PI 3-kinase is not sufficient for the hormonal stimulation of glucose uptake, lipogenesis, or glycogen synthesis in 3T3-L1 adipocytes.', *J. Biol. Chem.*, 270, pp. 3442–3446.

Williams, D. and Pessin, J. E. (2008) 'Mapping of R-SNARE function at distinct intracellular GLUT4 traffi cking steps in adipocytes', 180(2), pp. 375–387. doi: 10.1083/jcb.200709108.

Wollert, T. *et al*. (2009) 'The ESCRT machinery at a glance', *Journal of Cell Science*, 122(13), pp. 2163–2166. doi: 10.1242/jcs.029884.

Wong, K., Meyers, R. and Cantley, L. C. (1997) 'Subcellular locations of phosphatidylinositol 4-kinase isoforms', *Journal of Biological Chemistry*, 272(20), pp. 13236–13241. doi: 10.1074/jbc.272.20.13236.

Wu, X. *et al*. (2014) 'Structural Insights into Assembly and Regulation of the Plasma Membrane Phosphatidylinositol 4-Kinase Complex', *Developmental Cell*. Elsevier, 28(1), pp. 19–29. doi: 10.1016/j.devcel.2013.11.012.

Xu, Y. *et al*. (2011) 'Dual-mode of insulin action controls GLUT4 vesicle exocytosis', *Journal of Cell Biology*, 193(4), pp. 643–653. doi: 10.1083/jcb.201008135.

Yang, G. *et al*. (2004) 'Newly Synthesized Hepatitis C Virus Replicon RNA Is Protected from Nuclease Activity by a Protease-Sensitive Factor(s)', *Journal of Virology*. American Society for Microbiology, 78(18), pp. 10202–10205. doi: 10.1128/JVI.78.18.10202-10205.2004.

Ye, J. *et al*. (2012) 'Primer-BLAST: a tool to design target-specific primers for polymerase chain reaction.', *BMC bioinformatics*, 13, p. 134. doi: 10.1186/1471-2105-13-134.

Yeh, T.-Y. J. *et al*. (2007) 'Insulin-stimulated exocytosis of GLUT4 is enhanced by IRAP and its partner tankyrase.', *The Biochemical journal*, 402(2), pp. 279–290. doi: 10.1042/BJ20060793.

Yenush, L. *et al*. (1996) 'The pleckstrin homology domain is the principal link between the insulin receptor and IRS-1.', *The Journal of biological chemistry*, 271(39), pp. 24300–6. doi: 10.1074/JBC.271.39.24300.

Zaid, H. *et al*. (2008) 'Insulin action on glucose transporters through molecular switches, tracks and tethers', *Biochemical Journal*, 413(2), pp. 201–215. doi: 10.1042/BJ20080723.

Zhao, F.-Q. and Keating, A. F. (2007) 'Functional properties and genomics of glucose transporters.', *Current genomics*, 8(2), pp. 113–28. doi: 10.2174/138920207780368187.